

**PERFORMANCE EVALUATION OF SUGARCANE
BAGASSE ASH AS A SUPPLEMENTARY CEMENTITIOUS
MATERIAL FOR CONCRETE**

A THESIS

Submitted by

BAHURUDEEN A

for the award of the degree

of

DOCTOR OF PHILOSOPHY



**DEPARTMENT OF CIVIL ENGINEERING
INDIAN INSTITUTE OF TECHNOLOGY MADRAS**

AUGUST 2014

THESIS CERTIFICATE

This is to certify that the thesis titled "**PERFORMANCE EVALUATION OF SUGARCANE BAGASSE ASH AS A SUPPLEMENTARY CEMENTITIOUS MATERIAL FOR CONCRETE**" submitted by **Bahurudeen A.**, to the Department of Civil Engineering, Indian Institute of Technology, Madras, for the award of the degree of **Doctor of Philosophy** is a bona fide record of research work carried out by him under my supervision. The contents of this thesis, in full or in parts, have not been submitted and will not be submitted to any other Institute or University for the award of any degree or diploma.

Prof. Manu Santhanam

Research Guide

Department of Civil Engineering

IIT Madras, 600 036

Place: Chennai

Date:

ACKNOWLEDGEMENTS

I thank Almighty for this delightful opportunity to study at IIT Madras under the guidance of Dr. Manu Santhanam. I express my deepest sense of gratitude to my research supervisor Dr. Manu Santhanam, for his valuable guidance, constant support, friendly approach, patience for long discussions, thoughtful feedback, encouragement and commitment to this research study. Apart from the research, I have learnt from him, uncompromising standards for quality, brilliant way of teaching, correcting students with encouraging words and motivation which would be helpful for my professional career as a teacher as well as researcher.

I express my sincere thanks to the present Head of Civil Engineering Department, Prof. A. Meher Prasad and the former head Prof. S.R. Gandhi, for providing excellent facilities in the department.

I am also very much grateful to Prof. Ravindra Gettu and Dr. Radhakrishna G. Pillai for their valuable support, comments and suggestions during various stages of this research study. Additionally, I express my gratitude for their tireless efforts and help in BTCM research group meetings. I would like to thank my Doctoral Committee members Dr. Gandham Phanikumar and Dr. S. Sankaran, Associate Professors, Metallurgical and Materials Engineering, IIT Madras for their constant support, refreshing insights and suggestions towards this research study.

I take this opportunity to express my sincere thanks to Prof. M.S. Mathews and Prof. K. Ramamurthy who inspired and encouraged me throughout this research study. I am also extremely thankful to all faculty members of Building Technology and Construction Management division for their intangible support.

I would like to thank Prof. Surendra P. Shah, Prof. Mark Alexander and Prof. Yunus Ballim for their valuable discussions and inputs during their stay at IIT Madras.

I express my sincere thanks to all lab staff especially Mr. Soundarapandian, Ms. Malarvizhi, Mr. Krishnan, Mr. Subramanian, Mr. Murthy, Mr. Dhanasekaran, Mr. Pugazhenthir, Mr. Raagavaiah and Ms. Meena for their help in successful

completion of the experimental work. In addition, I would like to thank to Mr. Krishna, Mr. Kanagathiri, Mr. Prasanth, Mr. Hari, Mr. Chinnaiah for their assistance during processing and casting.

I am pleased to thank Mr. Murali, Department workshop facility for his inestimable help in fabrications of moulds and Mr. Muthusamy, and Mr. Marimuthu, Department Computer Facility for providing a wonderful facility and system support during the course of the study.

I am very delightful to acknowledge the support from all beloved intern students especially Anto Marckson, Anand Kumar, Deepak Kanraj, Vaisakh, Mirza, Kaiser, Arun Kishore, Suren, Rajeswari, Karthiga, Surendar, Gokul for their valuable contributions in this research study.

I have been pleased with a friendly group of fellow research scholars and I owe my sincere thanks to each and every one. I would like to thank Mr. Srinivasan for his timely help in material collection and Mohammed Haneefa, Jayachandran, Dhanya, Hemalatha, Abul, Subair, Vahidur, Azif, Suresh Kumar, Pushbakaran, Ram and Sakthivel for technical support in the research study. My fellow scholars and friends, Praveen, Bala, Senthil, Kavi, Sujatha, Prathap Nair, Vasugi, Fazil, Stephanie, Santhosh, Srinath, Sriram, Vinay, Divya, Sirajudeen, Sanish, Sathya, Priya, Prabha, Priyadharsini, Fathima, Manju, Deepa, Thirumalai, Reesha, Sheetal, Jeevan, Anitha, Ranjitha, Pinky, Venkata, Shobha, Elson, Muthu, Sunitha, Karmugil, Shiva, Mohan, Berlin, Yusuf, Sanoop, Yuvraj, Sooraj, Prabhu, Imran, Vikram, Madhu, Yogesh, Ashams, Aswathy, Ayesha, Ranjith, Aana, Boopathi, Jayashree, Karthick, Deepika, Yamuna, Madhuri, Mohan, Sruthi, Ramya, Arif, Amritha, Marimuthu, Ramaswamy for their kind suggestions, discussions, and intangible help during the course of my research. I am also thankful to all M.Tech students (BTCM and CTAM: 2011- 2014 batches) and Project associates for making my life at IIT memorable.

I would like to thank Ms. Ezhil, Ms. Susmitha, Ms. Aneetha and Mr. Obaiah for their help in BTCM office. Support from Civil engineering office particularly Ms. Rani, Ms. Geetha, Mr. Subramani, Ms. Padmini, Mr. Ramaswamy is gratefully acknowledged.

My heartfelt thanks to my beloved parents, brothers and relatives for their continuous encouragement, love and patience. There are no words to express my appreciation to them.

I am very much grateful to all my friends and well-wishers, for making my stay at IIT Madras most pleasant and memorable. I express my profound thanks to all of them who have supported to complete the research study.

BAHURUDEEN A

ABSTRACT

KEYWORDS: Sugarcane bagasse ash; Pozzolanic activity; Supplementary cementitious material; Cogeneration; Availability; Processing; Superplasticizer; Compatibility; Microstructure; Durability; Heat of hydration; Portland pozzolana cement.

Sugarcane bagasse ash is obtained as a by-product from cogeneration combustion boilers in sugar industries in abundant quantities and is currently disposed as a waste material, leading to severe environmental issues. Sugarcane bagasse ash (SCBA) is mainly composed of amorphous silica and can be used as pozzolanic material in concrete. The utilization of bagasse ash has been constrained because of inadequate understanding of the material and absence of suitable processing methodology. The present study is focused on the proper material characterisation of bagasse ash, assessment of its pozzolanic performance, development of appropriate processing methodology, production of bagasse ash based blended cements and performance evaluation of bagasse ash in concrete.

To achieve the objectives of this research study, a systematic and thorough material characterization (physical, chemical, mineralogical and microstructural characterization) of raw SCBA was performed. Pozzolanic performance of different particles present in raw SCBA was evaluated by five different standard methods to understand their influence on the reactivity of the material. A comprehensive assessment of pozzolanic activity of sugarcane bagasse ash based on different processing methods including burning, grinding, complete removal of fibrous unburnt particles by sieving and combinations of these methods was performed in this study to achieve maximum pozzolanic activity with minimum level of processing energy inputs. This was followed by the production of bagasse ash based cementitious blends with five different levels of cement replacement. Marsh cone and mini-slump test were used to determine the effect of superplasticizer type and water binder ratio on the saturation dosage with these blends. Physical, chemical and mineralogical characteristics of SCBA blended cements and the performance of concrete with these cements in terms of compressive strength, heat of hydration, drying shrinkage were

studied. In addition, durability performance was investigated by six different methods in this study. The accessibility of SCBA to the existing cement plants was also studied and compared with fly ash accessibility using ArcGIS mapping tool and availability maps were developed for major sugarcane producing states.

Results from the study indicate that raw bagasse ash cannot be directly used as a supplementary cementitious material and minimum level of processing is required to define as pozzolanic material as per currently existing specifications. The sample of raw bagasse ash consisted of three different types of particles. Along with fine burnt particles, two different types of fibrous unburnt particles were visually observed – these were extensively characterized through scanning electron microscopy (SEM) investigations. After several trials, complete removal of coarse and fine fibrous unburnt particles from raw bagasse was achieved by sieving through 300 μm sieve. Results from activity tests showed excellent pozzolanic performance (79%) for the fine burnt particles of bagasse ash, and lesser activity for the coarse fibrous particles (44%) and fine fibrous particles (50%). Raw bagasse ash showed lesser pozzolanic activity index (69%) than minimum requirement as per standard (75%) due to the presence of fibrous particles.

The burning temperature was found to affect the pozzolanic performance of bagasse ash. Burnt bagasse ash at 700 °C had maximum pozzolanic activity (86 %). At higher temperatures, crystallization of cristobalite was observed by X-ray diffraction (XRD), and this led to a reduction in pozzolanic activity of the burnt sample. Significant changes in colour and particle size were noticed for the sample burnt at 900 °C. From the results of the grinding study, only the sample of bagasse ash ground to < 53 μm size met the minimum index requirement of 75%. This was because during the grinding process of raw bagasse ash, fibrous unburnt carbon rich particles were ground to a greater degree as compared to the silica particles. Further grinding of sieved and burnt samples (sample burnt at 700 °C) to cement fineness (300 m^2/kg) using ball mill, noticeably increased pozzolanic activity to 106 % and 90 % respectively. In terms of maximum pozzolanic activity and minimum energy inputs, sieving through 300 μm and grinding to cement fineness (300 m^2/kg) was suggested as a suitable processing method for the production of sugarcane bagasse ash based Portland pozzolana cements.

The saturation dosage of polycarboxylic ether (PCE) and sulphonated naphthalene formaldehyde (SNF) types of superplasticizers used in the study was found to be higher for SCBA blended cement as compared to control paste for a constant water to binder ratio. Saturation dosages of PCE admixtures were significantly increased with increase in bagasse ash replacement and a similar trend was observed for SNF based admixture. As a result of low relative density of bagasse ash, the powder volume was considerably increased with an increase in the level of replacement and this caused a reduction in the relative fluidity of the paste. Sugarcane bagasse ash based Portland pozzolana cements were found to be compatible with PCE based superplasticizer and not compatible with SNF based superplasticizer. The irregular structure of the burnt silica rich fine particles (seen in SEM studies) was found to be responsible for the higher saturation dosages.

SCBA blended cement concrete had lower total heat and peak heat rate compared to control concrete. In addition, reduction in heat of hydration was increased with the level of replacement. Compressive strength of SCBA concretes (up to 25% replacement level) were in the same range as control concrete. Drying shrinkage behaviour of SCBA replaced concretes was also similar to that of OPC concrete. Results from durability studies indicated superior performance for bagasse ash blended concrete. Permeability was found to be gradually decreased with an increase in the level of replacement, which is due to pore refinement and improvement in the pore structure caused by the pozzolanic performance of sugarcane bagasse ash.

The comprehensive performance evaluation conducted in this study indicates that sugarcane bagasse ash can be utilized as a supplementary cementitious material to attain high quality concrete.

TABLE OF CONTENTS

ACKNOWLEDGEMENTS	i
ABSTRACT	iv
TABLE OF CONTENTS	vii
LIST OF TABLES	xii
LIST OF FIGURES	xiii
ABBREVIATIONS	xx
NOTATIONS	xxi
CHAPTER 1 INTRODUCTION	
1.1 General.....	1
1.2 Motivation for the present study.....	2
1.3 Objectives, scope and methodology.....	3
1.4 Structure of the thesis.....	7
CHAPTER 2 LITERATURE REVIEW	
2.1 General.....	8
2.2 Cement.....	8
2.2.1 Cement composition.....	9
2.2.2 Hydration of Portland cement.....	10
2.3 Need of cement replacement materials.....	10
2.4 Supplementary cementitious materials.....	12
2.4.1 Pozzolanic reaction.....	13
2.5 Sugarcane bagasse.....	14
2.5.1 Sugarcane bagasse based co-generation.....	15
2.5.2 Sugarcane bagasse ash.....	17
2.6 Potential of sugarcane bagasse ash as supplementary cementitious material in concrete.....	18
2.7 Effect of processing on the pozzolanic activity of supplementary cementitious materials	26
2.7.1 Effect of burning on pozzolanic activity of SCM.....	26
2.7.2 Effect of grinding on pozzolanic activity of SCM.....	27

2.8	Evaluation of pozzolanic activity of SCM.....	29
2.9	Influence of supplementary cementitious materials on binder superplasticizer compatibility	34
2.9.1	Influence of superplasticizer characteristics on compatibility	35
2.9.2	Influence of cement properties on compatibility	37
2.9.3	Influence of supplementary cementitious materials on compatibility	37
2.9.4	Different methods for evaluation of admixture compatibility	38
2.10	Influence of pozzolanic materials on heat of hydration	39
2.10.1	Heat of hydration of cement	39
2.10.2	Influence of pozzolanic materials on heat of hydration	40
2.10.3	Methods for measurement of heat of hydration.....	41
2.11	Influence of pozzolanic materials on durability of concrete.....	42
2.12	Research needs.....	43
2.13	Summary of literature review.....	45

CHAPTER 3 CHARACTERIZATION TECHNIQUES AND MATERIALS USED FOR THE STUDY

3.1	Introduction.....	46
3.2	Characterization techniques	46
3.2.1	Scanning electron microscopy	47
3.2.2	X-Ray diffraction method	49
3.2.3	X-ray fluorescence Spectroscopy	50
3.2.4	Laser particle size analyser	51
3.2.5	Fourier Transform Infrared spectroscopy	52
3.3	Materials used.....	54
3.3.1	Sugarcane bagasse ash	54
3.3.2	Cement.....	58
3.3.3	Aggregates.....	59
3.3.4	Superplasticizers.....	60
3.4	Summary.....	60

CHAPTER 4 EVALUATION OF POZZOLANIC PERFORMANCE AND MICROSTRUCTURE OF SUGARCANE BAGASSE ASH

4.1	Introduction.....	61
4.2	Different particles present in raw bagasse ash	61

4.3	Methods for evaluation of pozzolanic activity.....	65
4.3.1	Strength activity index test	65
4.3.2	Lime reactivity test	67
4.3.3	Frattoni test	68
4.3.4	Electrical conductivity method	70
4.3.5	Lime saturation method	72
4.4	Results and discussion	73
4.4.1	Strength activity index test	73
4.4.2	Lime reactivity test	74
4.4.3	Electrical conductivity method	75
4.4.4	Frattoni test	78
4.4.5	Lime saturation method	79
4.4.6	Discussion of test methods.....	80
4.5	Microstructural characterization of bagasse ash	81
4.5.1	Microstructure of raw bagasse ash	81
4.5.2	Microstructure of coarse fibrous particles	87
4.5.3	Microstructure of fine fibrous particles	92
4.6	Loss on ignition test	97
4.7	Summary	98
 CHAPTER 5 INFLUENCE OF DIFFERENT PROCESSING METHODS ON THE POZZOLANIC PERFORMANCE OF SUGARCANE BAGASSE ASH		
5.1	Introduction.....	99
5.2	Processing methods.....	99
5.2.1	Burning process	100
5.2.2	Grinding process	103
5.2.3	Methods for evaluation of pozzolanic activity of processed samples.....	104
5.3	Results and discussion.....	105
5.3.1	Effect of burning on pozzolanic activity	105
5.3.2	Effect of grinding on pozzolanic activity of raw bagasse ash	115
5.3.3	Effect of grinding on sieved and burnt samples	119
5.3.4	Comparison of processing methods	123
5.4	Summary	125

CHAPTER 6 PRODUCTION OF SUGARCANE BAGASSE ASH BASED PORTLAND POZZOLANA CEMENT AND EVALUATION OF COMPATIBILITY WITH SUPERPLASTICIZERS

6.1	Introduction.....	126
6.2	Production of SCBA based Portland pozzolana cements	126
6.3	Characteristics of SCBA based Portland pozzolana cements	129
6.4	Compatibility of SCBA based Portland pozzolana cement with superplasticizers	132
6.4.1	Method of paste preparation	133
6.4.2	Marsh cone test.....	133
6.4.3	Mini-slump test.....	135
6.5	Results and discussion.....	138
6.6	Summary.....	149

CHAPTER 7 PERFORMANCE EVALUATION OF SUGARCANE BAGASSE ASH BASED PORTLAND POZZOLANA CEMENT IN CONCRETE

7.1	Introduction.....	150
7.2	Materials and methods	151
7.2.1	Heat of hydration.....	151
7.2.2	Specimen preparation for durability testing	154
7.2.3	Chloride based tests	156
7.2.4	Gas based tests	160
7.2.5	Water based tests	163
7.2.6	Electrical resistivity of concrete	167
7.2.7	Drying Shrinkage.....	169
7.3	Results and discussion	170
7.3.1	Heat of hydration.....	170
7.3.2	Compressive strength	172
7.3.3	Chloride based tests	173
7.3.4	Gas based tests	175
7.3.5	Water based tests	177
7.3.6	Electrical resistivity of concrete	180
7.3.7	Drying Shrinkage.....	181
7.4	Summary	182

CHAPTER 8 AVAILABILITY OF SUGARCANE BAGASSE ASH AND POTENTIAL FOR USE IN INDIAN CEMENT PLANTS

8.1	Introduction	183
8.2	Availability of sugarcane bagasse ash	183
8.2.1	Contribution of India in world sugarcane production	184
8.2.2	Availability of sugarcane bagasse in India	187
8.2.3	Availability of sugarcane bagasse ash in India	190
8.3	Availability mapping using ArcGIS	194
8.3.1	Location of plants	194
8.3.2	Availability mapping	198
8.4	Summary	209

CHAPTER 9 CONCLUSIONS AND RECOMMENDATIONS FOR FURTHER STUDY

9.1	Introduction	210
9.2	Specific conclusions.....	210
9.2.1	Characterization of sugarcane bagasse ash	210
9.2.2	Microstructure of sugarcane bagasse ash	212
9.2.3	Influence of processing on pozzolanic performance	212
9.2.4	Admixture compatibility	214
9.2.5	Performance evaluation of SCBA based blended cements	214
9.2.6	Availability mapping of sugarcane bagasse ash	216
9.3	Major contributions from the study	216
9.4	Recommendations for further study	217

REFERENCES.....	219
------------------------	------------

LIST OF PAPERS ON THE BASIS OF THIS THESIS.....	238
--	------------

DOCTORAL COMMITTEE.....	239
--------------------------------	------------

CURRICULUM VITAE	240
-------------------------------	------------

LIST OF TABLES

Table	Title	Page
3.1	Physical properties of raw sugarcane bagasse ash	55
3.2	Oxide composition of raw sugarcane bagasse ash by XRF.....	55
3.3	Oxide composition of cement	58
3.4	Physical properties of cement	58
3.5	Physical properties of aggregates	59
3.6	Characteristics of superplasticizers used for the study.....	60
4.1	Elemental composition (%) by EDS of observed phases from A-I	96
4.2	Loss on ignition for the test samples	97
5.1	Physical characteristics of burnt samples	107
6.1	Physical characteristics of SCBA blended cements	130
6.2	Chemical composition of SCBA blended cements	131
8.1	Bagasse ash generation in sugar mills in states of India	192

LIST OF FIGURES

Fig.	Title	Page
1.1	Methodology for the present research study.....	6
2.1	CaO–Al ₂ O ₃ –SiO ₂ ternary diagram of different pozzolanic materials (Lothenbach et al., 2011)	12
2.2	Illustration of pozzolanic reaction and pore refining (Based on: Newman and Choo, 2003)	13
2.3	Appearance of sugarcane bagasse	14
2.4	Bagasse ash based cogeneration process	16
2.5	Sugarcane bagasse ash.....	17
2.6	Effect of burning temperature on the reactivity of SCBA (Cordeiro et al., 2009)	19
2.7	Relationship between pozzolanic activity and Blaine fineness of SCBA (Cordeiro et al 2009)	20
2.8	Setting time of bagasse ash blended paste (Ganesan et al., 2007).....	21
2.9	Temperature variation of concrete with bagasse ash (Chusilp et al., 2009)..	22
2.10	Relationship between the ratio of water permeability of concrete and replacement level (Chusilp et al., 2009)	23
2.11	Chloride permeability of BRWA blended concretes (Horsakulthai et al., 2009)	24
2.12	Chloride diffusion coefficient at 28 days (Horsakulthai et al., 2009)	24
2.13	Corrosion current in concrete (Horsakulthai et al. 2009)	25
2.14	NMR patterns of rice husk ash burnt at different temperatures (Nair et al., 2008)	27
2.15	Conductivity curve (McCarter and Tran, 1996)	32
2.16	Rate of conductivity (McCarter and Tran, 1996)	33
2.17	Frattini curve (Donatello et al., 2010)	34
2.18	Mechanisms of action of superplasticizers (Jolicoeur and Simard, 1998; Mehta and Monteiro, 2006).....	36
3.1	Scanning electron microscope used for the study	47
3.2	Sample holder used in the study.....	48

3.3	Sputter coating equipment.....	48
3.4	Placing of sample on the sample stage of SEM	49
3.5	XRD instrument used in the study	50
3.6	X-ray fluorescence spectrometer used for the study.....	51
3.7	Laser particle size analyser used for the study	51
3.8	Grinding disk	53
3.9	Pellet preparation chamber	53
3.10	Hand pressure arrangement for pellet preparation.....	53
3.11	X-ray diffraction pattern of raw bagasse ash	56
3.12	FTIR pattern of raw bagasse ash	57
3.13	Particle size distribution of raw bagasse ash	57
3.14	Particle size distribution of aggregates by sieve analysis	59
4.1	Appearance of raw sugarcane bagasse ash (SCBA)	62
4.2	Separation of different particles from raw SCBA by sieving	62
4.3	Coarse fibrous unburnt particles (CFU) present in the bagasse ash sample.	63
4.4	Fine fibrous unburnt particles (FFU) in the bagasse ash sample	63
4.5	Comparison of coarse and fine fibrous particles	64
4.6	Appearance of sieved fine burnt particles (Sieved SCBA)	64
4.7	Casting sequence of control	66
4.8	Casting of SCBA replaced specimens	67
4.9	Lime water curing and testing of specimen	67
4.10	Preparation of filtrate from different samples.....	69
4.11	Determination of $[\text{OH}]^-$ and $[\text{Ca}]^{2+}$ concentration.....	70
4.12	Schematic diagram of perspex cell for electrical conductivity measurement	71
4.13	Preparation of hydrated lime-pozzolan mixture and electrical conductivity measurement	72
4.14	Compressive strength of mortar cubes at 7 days in strength activity index test	73
4.15	Compressive strength of mortar cubes at 28 days in SAI test	74
4.16	Conductivity curve for raw bagasse ash	76
4.17	Derivative curve for raw bagasse ash.....	76
4.18	Conductivity curve for sieved bagasse ash.....	77

4.19	Derivative curve for sieved bagasse ash	77
4.20	Frattini diagram for assessing pozzolanicity	78
4.21	Lime saturation test	79
4.22	Microstructure of raw bagasse ash	82
4.23	Presence of different particles in the micrograph of raw bagasse ash	83
4.24	Presence of fibrous particles (B) and spherical particle (A) in the micrograph of raw bagasse ash	83
4.25	Presence of fine fibrous particle (E) in the micrograph of raw bagasse ash.	84
4.26	High magnification view of spherical particle	84
4.27	Microstructure of fine burnt particles	85
4.28	Irregular structure of fine burnt particles	85
4.29	Microstructure of fine burnt particles along with fibrous particles	86
4.30	Microstructure of fine burnt particles at higher magnification	86
4.31	Microstructure of coarse fibrous particles	88
4.32	Presence of scattered epidermal layer in the coarse fibrous particles	88
4.33	Microstructure of epidermal layer and carbon rich cellular structure.....	89
4.34	Orientation of epidermal layer at higher magnification.....	89
4.35	Presence of dumbbell-shaped particles in the epidermal layer	90
4.36	Microstructure of epidermal layer at high magnification	90
4.37	Presence of pits in the cell walls of coarse fibrous particles	91
4.38	Cellular structure of carbon layer at high magnification	91
4.39	Microstructure of fine fibrous particles	93
4.40	Microstructure of partially burnt fine fibrous particles	93
4.41	Microstructure of intercellular structure	94
4.42	Microstructure of cellular structure at higher magnification.....	94
4.43	Presence of pits in the cell walls at higher magnification	95
4.44	Intercellular channels of fine fibrous particles	95
4.45	Micrograph of cellular channels at higher magnification.....	96
5.1	Burning of bagasse as fuel in cogeneration boiler	100
5.2	Electrical furnace used in the study	101
5.3	Controlled burning of raw bagasse ash in electrical furnace for different durations	101
5.4	Appearance of bagasse ash burnt at 30 min (left) and 75 min (right)	

respectively	102
5.5 Controlled burning of raw bagasse ash at different temperatures for optimized time (90 minutes)	102
5.6 Ball mill used in the study.....	104
5.7 Compressive strength after 7 and 28 days curing for bagasse ash samples burnt at different temperatures.....	106
5.8 Partially burnt fibrous carbon particle in 600 °C burnt sample	108
5.9 Appearance of fibrous carbon particles in 600 °C burnt sample	108
5.10 Presence of fibrous carbon particles in 700 °C burnt sample	109
5.11 Appearance of more number of fibrous carbon particles in 700 °C burnt sample	109
5.12 Appearance of severely burnt particle in 800 °C burnt sample	110
5.13 Appearance of fibrous carbon particles in 800 °C burnt sample	110
5.14 X-Ray diffraction patterns of burnt samples	111
5.15 Raw bagasse ash (left) and white particles at 900 °C (right)	112
5.16 Microstructure of white particles in the 900 °C burnt sample	113
5.17 Microstructure of white particles (900 °C burnt sample) at higher magnification	113
5.18 Microstructure of white particles in the 900 °C burnt sample, sieved through 75 µm sieve	114
5.19 Microstructure of sieved white particles from the 900 °C burnt sample at higher magnification.....	114
5.20 Compressive strength after 7 and 28 days curing.....	116
5.21 Fineness of ground samples of bagasse ash.....	117
5.22 Appearance of more number of carbon particles (I &II) in the ground samples; different parts of ground carbon particles (III-VI)	118
5.23 Compressive strength of mortars with sieved and ground samples of bagasse ash after 7 and 28 days curing	119
5.24 Compressive strength of mortars with burnt and ground samples of bagasse ash after 7 and 28 days curing	120
5.25 SEM Micrograph of BG samples showing the presence of Carbon particles	121

5.26	SEM micrograph of BG samples, with more Carbon particles	121
5.27	Frattoni graph for the various samples	122
5.28	Comparison of strength activity index values for different bagasse ash samples	124
6.1	Production of SCBA based Portland Pozzolana cement	128
6.2	Particle size distribution for the OPC and blended cements in this study....	131
6.3	X-ray diffraction patterns of OPC and blended cements	132
6.4	Schematic diagram of Marsh cone apparatus.....	134
6.5	Marsh cone test being performed	135
6.6	Mini-slump apparatus	136
6.7	Schematic diagram of mini-slump apparatus	136
6.8	Conduct of mini-slump test	137
6.9	Marsh cone test results for control paste (w/b=0.45)	138
6.10	Marsh cone test results for 10 %PPC (w/b=0.45)	139
6.11	Marsh cone test results for 15 %PPC (w/b=0.45)	139
6.12	Marsh cone test results for 20 %PPC (w/b=0.45)	140
6.13	Mini-slump test results for control (w/b=0.45)	141
6.14	Mini-slump test results for 10 % PPC (w/b=0.45)	141
6.15	Mini-slump test results for 15 % PPC (w/b=0.45)	142
6.16	Mini-slump test results for 20 % PPC (w/b=0.45)	142
6.17	Marsh cone test results for control paste (w/b=0.40)	143
6.18	Marsh cone test results for 10 %PPC (w/b=0.40)	144
6.19	Marsh cone test results for 15 %PPC (w/b=0.40)	144
6.20	Marsh cone test results for 20 %PPC (w/b=0.40)	145
6.21	Mini-slump test results for control (w/b=0.40)	146
6.22	Mini-slump test results for 10 % PPC (w/b=0.40)	146
6.23	Mini-slump test results for 15 % PPC (w/b=0.40)	147
6.24	Mini-slump test results for 20 % PPC (w/b=0.40)	147
6.25	SEM micrograph of irregular processed bagasse ash particles	148
7.1	Schematic diagram of adiabatic calorimeter (based on Gibbon et al., 1997;	

Prasath and Santhanam, 2013)	152
7.2 Sequence of heat of hydration test	153
7.3 Specimen preparation for durability tests	154
7.4 Conditioning of specimen as per DI manual (2009)	155
7.5 Vacuum saturation of specimens	156
7.6 Rapid chloride penetration test setup (based on ASTM 1202-12)	157
7.7 Conductivity cell (DI manual, 2009)	158
7.8 Schematic diagram of chloride conductivity test (Based on DI manual, 2009)	158
7.9 Chloride conductivity test setup	159
7.10 Proper positioning of specimen for oxygen permeability test	160
7.11 Schematic diagram of oxygen permeability cell (Based on DI manual, 2009)	161
7.12 Oxygen permeability test setup	161
7.13 Schematic diagram of Torrent air permeability apparatus (Torrent Air permeability test user manual, 2010)	162
7.14 Torrent air permeability test setup	163
7.15 Schematic diagram of water permeability test apparatus	164
7.16 Placing of specimens in water permeability cell	165
7.17 Depth of water penetration	165
7.18 Water sorptivity test: a) Graph for mass gain (Mwt) against the square root of time to determine slope; b) Test set up using support as per DI manual (2003)	166
7.19 Schematic diagram of Wenner resistivity test (Resipod Proceq user manual, 2013)	168
7.20 Wenner resistivity test	168
7.21 Drying shrinkage test set up	169
7.22 Comparison of total heat curves	170
7.23 Comparison of heat of hydration rates for cements	171
7.24 Comparison of maturity heat rates for cements	172
7.25 Compressive strength of concrete after 3, 28 and 56 days of curing	173
7.26 Total charge passed at 28 and 56 days of curing	174
7.27 Chloride conductivity for concrete at 28 and 56 days of curing (qualitative	

classifications for concrete are also indicated)	175
7.28 Oxygen permeability for concrete at 28 and 56 days of curing	176
7.29 Torrent air permeability for concrete at 28 and 56 days of curing	177
7.30 Sorptivity index for concrete at 56 days of curing	178
7.31 Water penetration depth for concrete at 28 and 56 days of curing.....	179
7.32 Resistivity for concrete at 28 and 56 days curing (qualitative classifications indicating corrosion risk based on Feliu et al. (2009) are also marked)	180
7.33 Drying shrinkage behaviour of concretes	181
8.1 World sugarcane production (Based on: http://www.vsisugar.com/india/statistics/international_sugar.html)	184
8.2 World sugarcane production in three consecutive fiscal years	185
8.3 State wise sugarcane production in India (2010-11) (Based on: Annual report on sugarcane cultivation, CACP, 2012)	186
8.4 Trends of sugarcane production and area under cultivation in India (Based on Report of Cooperative sugar, 2011)	187
8.5 Sugarcane crushed and bagasse generated in India over the last 6 decades.	188
8.6 Generation of sugarcane bagasse in Indian states - Mean 2009-10 to 2010.	189
8.7 Total number of sugar mills with cogeneration plants	190
8.8 Trend in bagasse based cogeneration in Tamil Nadu (Based on: Tamil Nadu electricity regulatory commission report, 2012)	193
8.9 Location of cement plants in India	195
8.10 Location of sugar mills in India	196
8.11 Location of thermal power plants in India	197
8.12 Availability of sugarcane bagasse ash in India	199
8.13 Availability of fly ash in India	200
8.14 Location of cement plants on the availability map of SCBA ash	201
8.15 Location of cement plants on the availability map of fly ash	202
8.16 Location of sugar mills, cement and thermal plants in Tamil Nadu.....	204
8.17 Location of sugar mills, cement and thermal plants in Karnataka.....	205
8.18 Location of sugar mills, cement and thermal plants in Uttar Pradesh.....	206
8.19 Location of sugar mills, cement and thermal plants in Maharastra.....	207
8.20 Location of sugar mills, cement and thermal plants in Andra Pradesh.....	208

ABBREVIATIONS

ASTM- American Society for Testing and Materials

BS- British Standard

CFU- Coarse Fibrous Unburnt particles

CH- Calcium Hydroxide

CSH- Calcium Silicate Hydrate

DIN - Deutsches Institut für Normung

EDX- Energy Dispersive X-ray analysis

FFU- Fine Fibrous Unburnt particles

IS- Indian Standard

ITZ- Interfacial Transition Zone

LOI- Loss on Ignition

MT- Million Tonnes

OPC- Ordinary Portland Cement

PCE- Poly-carboxylic Ether

PPC- Portland Pozzolana Cement

SAI- Strength Activity Index

SCBA-Sugarcane Bagasse Ash

SCM-Supplementary cementitious material

SE- Secondary Electrons

SEM- Scanning Electron Microscopy

SNF- Sulphonated Naphthalene Formaldehyde

XRD- X-Ray Diffraction

XRF- X-Ray Fluorescence

NOTATIONS

i	=	electrical current
T	=	Temperature
V	=	Applied potential
k	=	coefficient of permeability
θ	=	X-ray incidence angle (Bragg angle)
w/c	=	water to cement ratio
°C	=	Degree Celsius
K	=	Kelvin
M	=	Molarity
N	=	Normality

CHAPTER 1

INTRODUCTION

1.1 GENERAL

The cost of building materials is increasing rapidly due to high demand of construction materials, their transportation costs, dwindling natural sources and environmental restrictions. The manufacturing process of conventional materials like cement results in the rapid depletion of limited natural resources, consumes a lot of energy and also leads large carbon dioxide emissions to the atmosphere, which causes severe environmental problems. It is thus very important to find alternative materials for use in concrete.

On the other hand, solid waste generation is increasing globally due to population growth, urbanization and changes in lifestyle. In India annually more than 960 million tonnes solid waste is generated due to various activities, including from mining, industrial, and municipal processes (Pappua and Saxenaa, 2007). Disposal of solid waste becomes difficult due to environmental restrictions and land requirement. Due to environmental awareness and technology advancement, utilization of solid waste materials has become an attractive alternative solution to disposal.

Supplementary cementitious materials (SCMs) are widely used in concrete because of the enhancement of fresh and hardened properties, including significant reduction in heat of hydration, additional strength gain as a result of pozzolanic reactions, lower permeability due to pore refinement and better performance against aggressive agents. Incorporation of SCMs helps to achieve durable and sustainable concrete.

Global research has moved towards maximum utilization of alternative cementitious materials in concrete for sustainability in the construction industry. While numerous alternative materials, including several wastes and by-products, are available for use in concrete, their effective utilization has been hampered because of insufficient

understanding of the appropriate selection and characterization techniques that need to be applied for these new materials.

This research is an attempt to use sugarcane bagasse ash (SCBA) as a supplementary cementitious material in concrete. Sugarcane bagasse ash is obtained as a by-product from sugar industries, and previous research has shown that it can be used as a supplementary cementitious material. This study focuses on developing a suitable methodology to utilize sugarcane bagasse ash in a large scale. Production of sugarcane bagasse ash based Portland pozzolana cement and its performance evaluation in cement paste, mortar and concrete is also described in the present study.

1.2 MOTIVATION FOR THE PRESENT STUDY

Only a limited number of studies are available in literature on the evaluation of bagasse ash as supplementary cementitious material in concrete. These studies are seen to be from Brazil, Thailand, and Taiwan (and some from India), which are the countries that produce significant quantities of sugarcane. In spite of these studies, the utilization of bagasse ash has been constrained because of inadequate understanding of the material and lack of suitable methodology for use in a large scale. Proper characterization and processing of bagasse ash were not investigated in earlier research studies. Appropriate processing methods and guidelines need to be developed to achieve maximum possible pozzolanic activity of bagasse ash with minimum energy inputs. Different methods and standards are available to assess pozzolanic activity and it is imperative to study these standard test methods for bagasse ash to find its suitability as cementitious material in concrete.

The significance of the present study in the Indian context can be valued by considering the following points. World cement demand was 2,283 million tones (MT) in 2005, with China being the leading producer at 1,064 MT (47% of total) and India in the second place in the production of cement (Lasserre, 2007). In 2010, the world production of hydraulic cement increased to 3,300 MT (USGS, 2011). India is the second largest cement market in the world, accounting for 7–8 % of global cement production with effective capacity of 234 million tonnes per annum (CMA, 2013). Cement manufacturing process leads to large CO₂ emission and rapid depletion of natural resources. The cement

industry contributes about 5% of global CO₂ emissions. The global potential for CO₂ emission reduction through producing blended cement is estimated to be at least 56 MT of CO₂ (Worrell et al., 2001). On the other hand, the potential for application of blended cements depends on the availability of blending materials. India ranks second in the production of sugarcane in the world. Total production of sugarcane in India in 2003 was reported as 289.6 million tonnes (FAO, 2003). Sugarcane bagasse ash is collected as by-product in enormous quantities (44220 tonnes/day) in India and rapid implementation of new cogeneration plants in Indian sugar mills will considerably increase the availability of bagasse ash in the future. Disposal of bagasse ash is becoming a problematic issue in India due to land requirement and environmental constraints. Bagasse ash has amorphous silica content and can be used in the production of blended cement instead of being disposed in landfills. Utilization of SCBA as a supplementary cementitious material would help to achieve high quality durable concrete and tackle many environmental issues related to disposal of SCBA. The available literature on SCBA only pertains to the use of raw bagasse ash as mineral admixture in concrete. Development of sugarcane bagasse ash based Portland pozzolana cement needs to be addressed to strive for maximum utilization in the construction sector.

1.3 OBJECTIVES, SCOPE AND METHODOLOGY

The main objective of the study is to evaluate the suitability of sugarcane bagasse ash as a supplementary cementitious material in concrete. The following specific sub-objectives are formulated for this purpose:

- To develop a systematic methodology for the chemical, physical, mineralogical and morphological characterization of sugarcane bagasse ash.
- To investigate the influence of burning and grinding on pozzolanic activity of sugarcane bagasse ash.
- To evaluate pozzolanic activity of sugarcane bagasse ash by different standard methods and identify the material with maximum possible pozzolanic activity along with minimum processing of bagasse ash

- To develop SCBA based Portland pozzolana cement and to investigate its performance in cement paste, cement mortar and concrete.

The scope of the study is limited to the following with respect to materials used and the test methods adopted:

- The study is confined to sugarcane bagasse ash from a cogeneration plant (Madras Sugar Limited, Tamil Nadu, India) as a supplementary cementitious material.
- Ordinary Portland cement (53 grade) conforming to IS 12269-1987 is used in this study. Standard hydrated lime as specified by IS 1727-2004 is used for lime reactivity test.
- Burning temperature is limited to the range 600 °C to 900 °C and burning time is optimized based on numerous trials. Grinding of raw bagasse ash is designed to get particle sizes from 210 μm to 45 μm .
- Blending of processed bagasse ash with ordinary Portland cement (OPC) for SCBA based Portland pozzolana cement (PPC) production is limited to five different levels (5 %, 10 %, 15 %, 20 % and 25 %) of replacements.
- PPC with three different replacements of bagasse ash (10 %, 15 %, and 20 %), two different water to cementitious materials ratios (0.40 and 0.45) and two different superplasticizers (SNF and PCE based) are used for admixture compatibility study.

The present study is divided into four phases, specifically, material characterization of sugarcane bagasse ash, influence of processing on the pozzolanic performance, material processing as well as production of SCBA based Portland pozzolana cement and performance evaluation. Figure 1.1 illustrates the methodology followed in the present study. This methodology is developed with inputs from ASTM C1709-11, Standard guide for evaluation of alternative supplementary cementitious materials (2013) and IS 1727-2004, Methods of test for pozzolanic materials for use in concrete. The studies undertaken in each phase are described below.

1st Phase: Characterization of sugarcane bagasse ash

- A systematic and thorough material characterization (physical, chemical mineralogical and microstructural characterization) of raw sugarcane bagasse ash.
- A comprehensive experimental investigation of pozzolanic performance of different particles present in raw sugarcane bagasse ash by five different international standard methods.

2nd Phase: Influence of different processing methods on the pozzolanic performance of sugarcane bagasse ash

- Effect of burning on pozzolanic activity of sugarcane bagasse ash
- Influence of different levels of grinding on pozzolanic activity of sugarcane bagasse ash
- Evaluation of pozzolanic activity of sugarcane bagasse ash after complete removal of coarse fibrous particles by sieving and assessment of combinations of these processing methods on pozzolanic activity.
- Influence of different processing methods on the microstructure of processed sample of bagasse ash

3rd Phase: Material processing and Production of SCBA based PPC

- Selection of suitable processing methods based on maximum pozzolanic activity and minimum level of energy inputs for producing the blending material.
- Production of suitable processed bagasse ash with controlled methods
- Production of bagasse ash based Portland pozzolana cement with five different levels of replacements.

4th Phase: Performance tests on cement paste, mortar and concrete

- Physical, chemical and mineralogical characteristics of SCBA blended cements.
- Interaction of superplasticizers with bagasse ash based Portland pozzolana cements.
- Influence of bagasse ash replacement on compressive strength, heat of hydration and drying shrinkage.

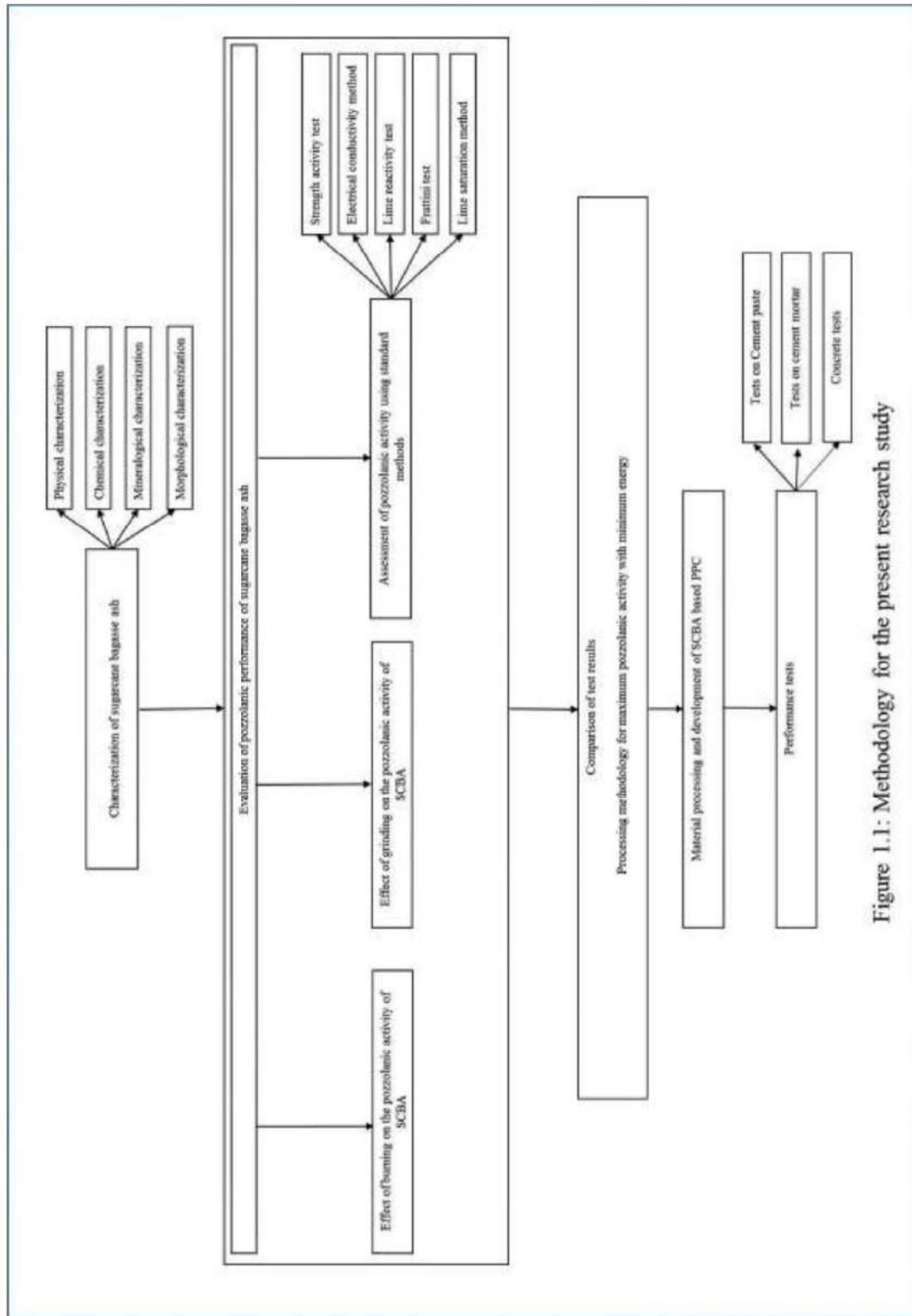


Figure 1.1: Methodology for the present research study

- Experimental investigation on durability performance of bagasse ash based Portland pozzolana cements in concrete by six different test methods.

1.4 STRUCTURE OF THE THESIS

A general introduction along with motivation for the present study as well as objectives, scope and methodology of the study have been described in the preceding section of this chapter. A comprehensive review of literature on the use of bagasse ash as supplementary cementitious material with a special emphasis on material characterization, different processing methods, methods for pozzolanic assessment, and performance evaluation of different pozzolanic materials is presented in Chapter 2. Based on the critical review of literature, needs for the present research study are highlighted in the same chapter. Chapter 3 explains physical and chemical properties of materials and characterization techniques used for the experimental investigations in the study. Chapter 4 describes the assessment of pozzolanic activity of bagasse ash by different methods and comprehensive microstructural characterization of raw bagasse ash. Chapter 5 presents the effects of different processing methods on the pozzolanic activity of bagasse ash and the selection of the best method to produce the processed material. Production and characteristics of bagasse ash based blended cements as well as interaction with superplasticizers are presented in Chapter 6. Chapter 7 provides mechanical and durability performance evaluation of concretes with SCBA based Portland pozzolana cements. Chapter 8 deals with availability mapping of bagasse ash in India and potential for use in Indian cement plants in blended cements. The conclusions drawn from the present study and recommendations for further research are presented in Chapter 9.

CHAPTER 2

LITERATURE REVIEW

2.1. GENERAL

Supplementary cementitious materials are widely used in modern construction to achieve durable and sustainable concrete. A number of alternative materials, including reactive pozzolans and fillers, are available in enormous quantities. Proper understanding of new pozzolanic materials is imperative to attain maximum pozzolanic benefits and high quality concrete using such materials. Most of the pozzolanic materials are obtained from industrial by-products and cannot be directly used in concrete. Minimum level of processing is required to satisfy the standard regulations for pozzolanic materials. As a consequence of the variations in material characteristics, a systematic evaluation study needs to be carried out to find potential use of these materials and to achieve suitable energy-efficient processing methodologies. This review of literature focuses on integrating the available information on the characterization of sugarcane bagasse ash and its performance as supplementary cementitious material in concrete from earlier research studies. In addition to this, the existing information in different standards, methods and guidelines for the evaluation of pozzolanic performance of alternative cementitious materials is also reviewed. Different factors that significantly influence pozzolanic activity are elaborately reviewed in this chapter to get interrelated information for the development of an effective characterization strategy for the evaluation of new supplementary cementitious materials.

2.2. CEMENT

Portland cement is primarily a calcium silicate cement, which is manufactured by firing a uniformly ground mixture of limestone or chalk (calcium carbonate) and an appropriate amount of clay or shale to partial fusion, at a high temperature (1500 °C) in a rotary kiln

(Newman and Choo, 2003). The ASTM C219-13a definition states that —“Portland cement is a hydraulic cement produced by pulverizing clinker, consisting essentially of crystalline hydraulic calcium silicates, and usually containing one or more of the following: calcium sulfate, up to 5 % limestone, and processing additions”. Greeks and Romans produced the first calcium silicate cements. They ground volcanic ash as well as mixed with lime and water to produce superior binder for use in mortar (Newman and Choo, 2003). Later this notion was a basic conception for the development of pozzolanic additions (fly ash, silica fume, blast furnace slag and metakaolin) and for modern blended cement production (Blezard, 1998). Modern Portland cement is credited to Joseph Aspdin who calcined the mixture of limestone and clay at a high temperature in a shaft kiln to produce clinker and further ground to lesser fineness to achieve a better binding material than lime.

2.2.1. Cement composition

Calcium silicates are the most important constituents of Portland cement. Raw materials for cement manufacturing process include calcareous materials and argillaceous materials (Neville, 2011). Generally limestone, chalk, marl, and sea-shell are preferred as source for calcium whereas silica (SiO_2), alumina (Al_2O_3) and iron oxide (Fe_2O_3), are typically obtained from shale or clay. Advancement in technology as well as controlled manufacturing process leads to consistent in modern cement production.

Portland cement consists of four oxides (CaO , SiO_2 , Al_2O_3 and Fe_2O_3) as main constituents. Along with these oxides, MgO , K_2O , Na_2O , Mn_2O_3 , SO_3 , TiO_2 , P_2O_5 , and trace elements (0.01%) are present as minor constituents in Portland cement (Neville, 2011; Newman and Choo, 2003). Portland cement clinker contains four main minerals - two calcium silicate minerals (tricalcium silicate and dicalcium silicate denoted as C_3S and C_2S respectively) and two aluminate minerals (tricalcium aluminates and tetra calcium alumino ferrite denoted as C_3A and C_4AF respectively) (Mehta and Monteiro, 2006). Chemical composition and physical characteristics of cement primarily govern fresh and hardened properties of concrete. Raw materials and production process considerably influence on the chemical composition of cement (Neville, 2011, Gambhir, 2013).

2.2.2. Hydration of Portland cement

Anhydrous calcium silicate and aluminate phases in the Portland cement react with water to form hydrated phases. The reaction of cement with water is generally described as hydration of cement; this leads to formation of different solid hydrated products resulting in a dense hydrated structure which is responsible for the development of compressive strength (Mehta and Monteiro, 2006; Neville, 2011). The hydration process of cement is categorized into four different stages (Ridi et al., 2011; Jolicoeur and Simard, 1998; Taylor, 1997) namely initial hydration stage (0-15 min), dormant period (2-4 hours), acceleration period (4-8 hours) and deceleration period (8-24 hours). In the initial hydration period, wetting of cement grains and dissolution of different easily soluble ions occurs. A layer of amorphous gel is formed around the surface of cement particles. Subsequently, as a result of nucleation process, tricalcium aluminate reacts with dissolved sulfate (SO_4^{2-}) ions and forms calcium sulphoaluminate (denoted as Ettringite) (Mehta and Monteiro, 2006). In addition to this, the initial C-S-H gel formed around the cement grains acts as barrier for further hydration of C_3S . This barrier causes the hydration reactions to slow down after the initial stage, and this period is termed as dormant period (Neville, 2011; Ridi et al., 2011). As a result of diminishing of ionic strength, and increased diffusion, rapid dissolution of C_3S take place after the dormant period, and C-S-H as well as CH are formed as hydrated products. This is denoted as the acceleration period (4-8 hours). During the acceleration period, a stiffer matrix is attained because of hydrated product formation. At the end of the acceleration stage, ettringite to monosulphate conversion generally occurs because of exhaustion of SO_4^{2-} ions for C_3A reactions.

2.3 NEED FOR CEMENT REPLACEMENT MATERIALS

Blended cements are technically superior to ordinary Portland cement, as their use results in improved fresh and hardened properties, in addition to resistance against aggressive agents compared to ordinary Portland cement. Durability performance of concrete with blended cements is significantly improved because of pozzolanic reaction and pore

refinement. Use of blended cements in construction helps to achieve high quality and durable concrete.

World cement demand is significantly increased because of rapid development in the construction sector. Production of cement is an energy intensive process. Energy consumption of cement plants was reported as 5 % of total industrial energy consumption in the world (World Energy council, 1995). Cement production in the world was estimated at 2840 million tonnes in 2008 and substantially increased to 3300 million tonnes in 2010. This figure is expected to reach 4,380 million tonnes in 2050 (Vanoss, 2012; Hasanbeigi et al., 2012). India and china contribute 55 % and 7% of total cement production in the world (USGS, 2012). Due to the high demand and stable increase in the cement production, enormous quantities of raw materials are mined at a high rate from the limited natural resources. Moreover, CO₂ emission from the cement industries contributes 5-6 % of the total CO₂ emission in the world. CO₂ emission from the Indian cement industry is predicted to reach 835 MT by 2050 (510 % increase compared to present CO₂ emissions) (WBCSD/IEA, 2013). It is imperative to use alternative cementitious materials to reach sustainable development in cement production.

Use of supplementary cementitious materials leads to significant reduction in CO₂ emission from the cement industries and lowers the consumption rate of limited natural resources. In India, blended cement production was 37 % of total cement production in 2000, and considerably increased to 67 % in 2011 (WBCSD/IEA, 2013). Fly ash and slag are widely used for the blended cement production. In addition to this, a number of waste and by-products generated from other industries, are abundantly available in the major cement producing countries. Some of these materials have potential for use as supplementary cementitious material. Utilization of these materials as mineral admixture instead of using limited naturally available resources for producing cement will tackle the problem of disposal of waste materials and help to achieve sustainable concrete.

2.4 SUPPLEMENTARY CEMENTITIOUS MATERIALS (SCM)

A number of by products and solid waste materials which have reactive amorphous silica as main constituent in their chemical composition, can be used as supplementary cementitious materials or pozzolanic materials (cement replacement materials). According to ASTM C219-13a, Pozzolan is defined as “a siliceous or siliceous and aluminous material, which in itself possesses little or no cementitious value but will, in finely divided form and in the presence of moisture, chemically react with calcium hydroxide at ordinary temperatures to form cementitious hydrates.” Different materials such as fly ash (FA), ground granulated blast furnace slag (GGBFS), rice husk ash (RHA), metakaolin (MK), silica fume (SF), palm oil fuel ash, and sugarcane bagasse ash (SCBA) are used as pozzolanic materials as well as in blended cement production. The composition of different SCMs can be understood from the ternary diagram shown in Figure 2.1. Silica fume has more than 90 % silica content in its oxide composition and can be used as highly pozzolanic material. GGBFS has around 35 % of silica content with 40 % of CaO. Because of higher CaO content, slag is a cementitious and pozzolanic material. Similarly, Class F fly ash can be termed as pozzolanic material, whereas Class C fly ash can be defined as cementitious and pozzolanic material.

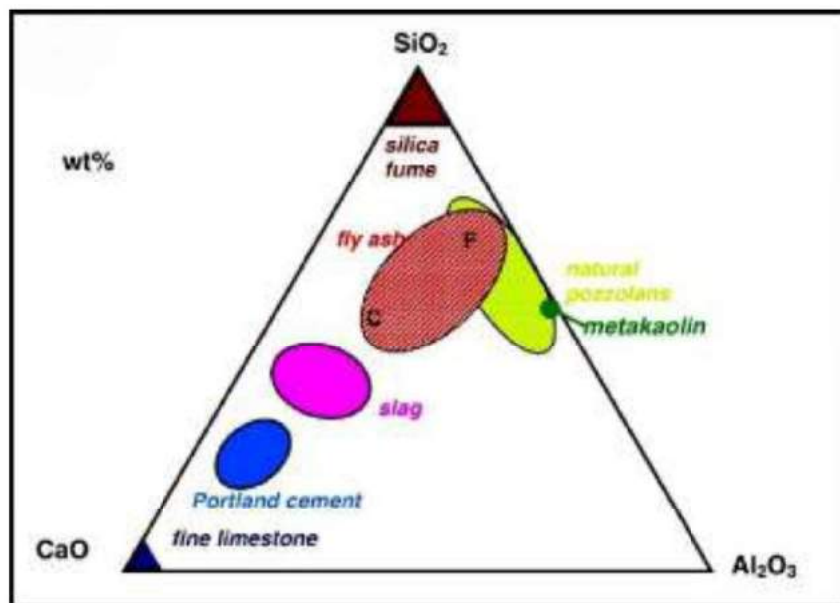


Figure 2.1: CaO–Al₂O₃–SiO₂ ternary diagram of different pozzolanic materials (Lothenbach et al., 2011)

2.4.1. Pozzolanic reaction

Amorphous silica present in the supplementary cementitious materials reacts with available calcium hydroxide in the cementitious system (from cement hydration process) in the presence of water and produces calcium silicate hydrate. Because of the formation of additional calcium silicate hydrate (C-S-H), increase in long-term strength is observed in blended cement concrete compared to ordinary Portland cement concrete.



Large hexagonal calcium hydroxide crystals are consumed in the pozzolanic reaction and converted into C-S-H gel. In addition to higher strength, improvement in the microstructure has been reported as a result of pore refining process caused by pozzolanic reaction (Cabrera and Plowman, 1981; Asbridge et al., 2002; Duan et al., 2013). Pozzolanic reaction of fly ash particles is illustrated in Figure 2.2. From the hydration of C_3S and C_2S , calcium hydroxide is formed as a hydrated product. Fly ash particles react with calcium hydroxide and produce additional C-S-H. As a result of the pozzolanic reaction, the interstitial spaces in the matrix get filled, as illustrated in Figure 2.2.

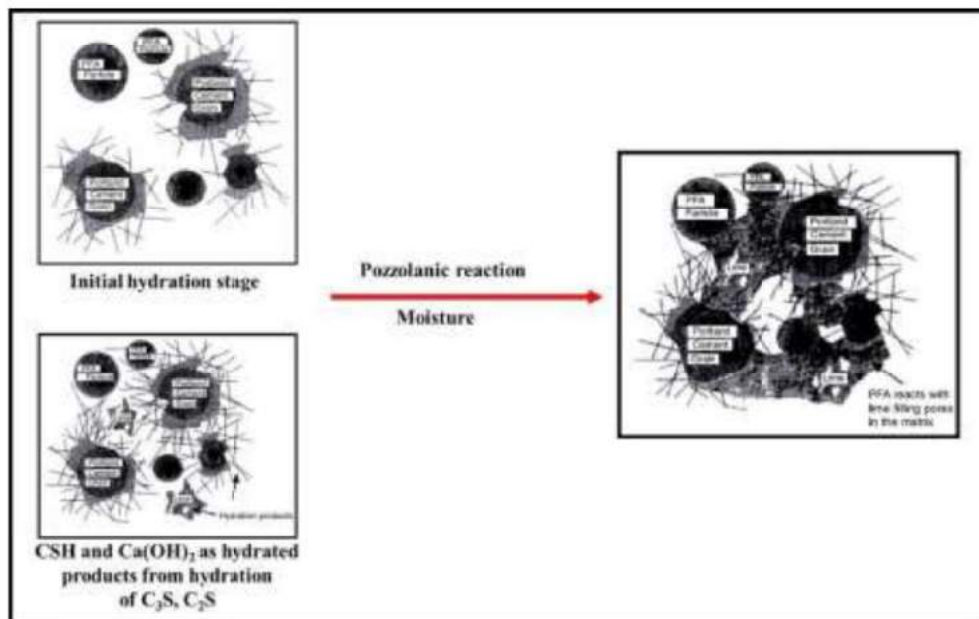


Figure 2.2: Illustration of pozzolanic reaction and pore refining
(Based on: Newman and Choo, 2003)

2.5 SUGARCANE BAGASSE

Sugarcane is used in the production of variety of sugars like white sugar, gur, khandasari etc. Sugar production from sugarcane involves shredding of fresh sugarcane, then mixing with water, and crushing using heavy rollers to extract the juice. The fibrous material left over after the juice extraction is called ‘bagasse’ (shown in Figure 2.3). In the earlier times bagasse was burnt in fields as a method of disposal. Later it was found that it can be used for a variety of purposes such as in production of paper products, cane ethanol, manufacturing of animal feeds etc. (Solomon, 2011). At present, it is mainly used as a fuel in sugar mills for cogeneration. The burning of bagasse in cogeneration boiler produces sufficient heat energy for all the needs of a typical sugar mill, with a quantity of energy to spare. The surplus energy produced in the co-generation process is supplied to local households or factories with collaboration with the state electricity board. It is called as co-generation because bagasse is used as fuel and the steam produced by this heating is used in the production of electricity as well as for heating in juice treatment and clarification processes.



Figure 2.3: Appearance of sugarcane bagasse

The crushing of sugarcane stalks produces 28-30% by weight of bagasse (Xiasun et al., 2003). The moisture content in bagasse is about 50% and therefore it should undergo some drying prior to its use as fuel in the cogeneration process. The constituents of bagasse include hemi-cellulose, cellulose, lignin, wax, ash etc. It has about 40-50% moisture content and 2-3% sugar and the remaining is just fibrous material (WADE Report, 2004).

2.5.1 Sugarcane bagasse based co-generation

The concept of sugarcane based co-generation involves the production of two forms of energy from bagasse. As two forms of energy are derived from single source of fuel, the process is called co-generation. The crushing of sugarcane is followed by the juice treatment and clarification processes. The working principle of the co-generation system is based on the conventional Rankine cycle theory (STAI Report, 2009). Burning of bagasse in controlled cogeneration boiler generates high pressure steam. This high pressure steam is used to rotate turbines which produce electricity. Generally, after the high pressure steam passes through the turbine, the pressure of steam reduces considerably. In most cases like in coal based electricity generation, this low pressure steam is condensed as waste. However, in the sugar production process, the low pressure steam emanating from the turbine exhaust is used as thermal energy for the juice treatment process. Figure 2.4 describes the cogeneration process concisely.

The configuration of cogeneration system includes a back pressure or extraction cum back pressure type steam turbine generator and a fired steam boiler. 1 ton of sugarcane produces approximately 280-300 kg of bagasse, the burning of which produces about 500-600 kg of steam (Solomon, 2011) in the cogeneration process. It is interesting to note that the amount of CO₂ emitted in burning of bagasse from a stalk of sugarcane in the cogeneration process is found to be roughly equal to the quantity of CO₂ taken up by the plant during photosynthesis (Souza et al., 2011). Thus the CO₂ emission in bagasse based cogeneration can be said to be neutral with the CO₂ consumption by the sugarcane plants; therefore the use of bagasse for burning is environment friendly compared to the cogeneration using coal as fuel.

As stated earlier, high pressure steam is directed for electricity production. Low pressure steam is passed to the boiler of sugar production process. If excess steam is available, it is condensed into water and again this water is circulated to production system in the modern cogeneration boilers, to enable a zero waste scenario.

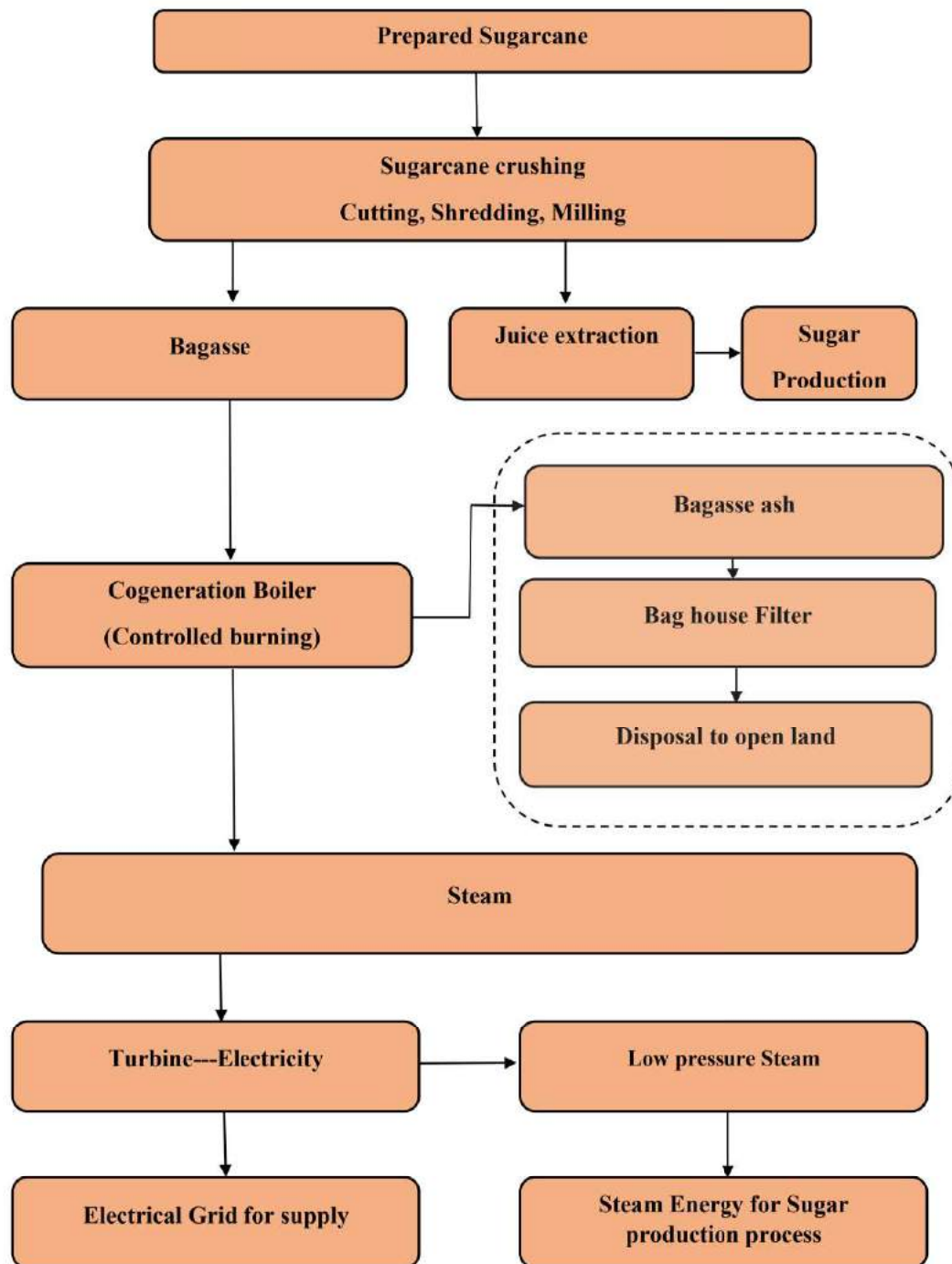


Figure 2.4: Bagasse ash based cogeneration process

2.5.2. Sugarcane bagasse ash

The residue after burning bagasse in the cogeneration boiler, namely bagasse ash (shown in Figure 2.5), is collected using a bag-house filter. The collected bagasse ash is stored in large silos in the cogeneration plant, and periodically mixed with water and disposed to the nearest land. Raw bagasse ash collected from the disposal area needs to be further dried at 105 – 110°C for 24 hours to remove moisture, before its use in concrete. Plants ingest orthosilicic acid from ground water, which is later polymerized as amorphous silica in the plant cells (Kamiya et al., 2000). When bagasse is used as fuel in the combustion boiler of the cogeneration plant under controlled burning, reactive amorphous silica is formed because of combustion process and it is present in the residual ashes (Chusilp et al., 2009).



Figure 2.5: Sugarcane bagasse ash

Raw bagasse ash is composed of mainly silica (60-75 %), CaO, K₂O and other minor oxides including Al₂O₃, Fe₂O₃, and SO₃ (Ganesan et al., 2007; Cordeiro et al., 2009; Morales et al., 2009; Frias et al., 2011; Somna et al., 2012). Amount of silica present in

the residual ashes was directly related to the burning temperature of bagasse in the boiler (Singh et al., 2000; Cordeiro et al., 2009). Due to the presence of unburnt particles, the loss on ignition of raw bagasse ash was found to be higher than the permissible range in the standard for use as pozzolanic material (Batra et al., 2008; Ganesan et al., 2007). Chusilp et al. (2009) reported 20 % loss on ignition for raw bagasse ash. Somna et al. (2012) reported that more than 65 % of particles of raw bagasse ash were retained on a 45 μm sieve. Low specific gravity (1.8-2.1) of raw bagasse ash was reported in the previous studies, as a result of large amount of lightweight unburnt particles (Ganesan et al., 2007; Somna et al., 2012).

2.6 POTENTIAL OF SUGARCANE BAGASSE ASH AS SUPPLEMENTARY CEMENTITIOUS MATERIAL IN CONCRETE

Material characterization and performance evaluation are needed to evaluate new alternative supplementary cementitious materials for use in concrete. This process includes chemical, physical, mineralogical and microstructural characterization. Chemical characterization is imperative to find major, minor, and trace elements in the alternative materials. Special attention is needed for the compounds which influence the hydration of cement or properties of the concrete (ASTM C1709-11). If such compounds are present, then suitable test should be carried out to find the availability of these compounds to participate in the hydration reactions. Characterization and performance evaluation of sugarcane bagasse ash in previous research studies has been reviewed and presented in this section.

In an X-ray diffraction study, the amorphous hump in the diffraction pattern between 20 and 25 $^{\circ}2\theta$ showed clear evidence for the presence of amorphous silica. Quartz (Q) and Crystobalite were also found to be present in the X-ray diffraction pattern (Ganesan et al., 2007). In another study (Cordeiro et al., 2009), to estimate strength gain due to only the pozzolanic reactivity of bagasse ash, SCBA and an inert material (crushed Quartz) were ground to same fineness. Pozzolanic activity index and Chapelle activity were estimated separately for both materials. Filler effect of SCBA and inert crushed quartz was almost balanced because of same fineness. Compressive strength of mortar which had SCBA was higher than mortar that had inert material. This is again solid evidence for

the pozzolanic activity of SCBA. The effect of burning on pozzolanic activity was studied using Chapelle test by Cordeiro et al. (2009) and the results of the study showed that the maximum reactivity of SCBA was found at around 500 °C as shown in Figure 2.6.

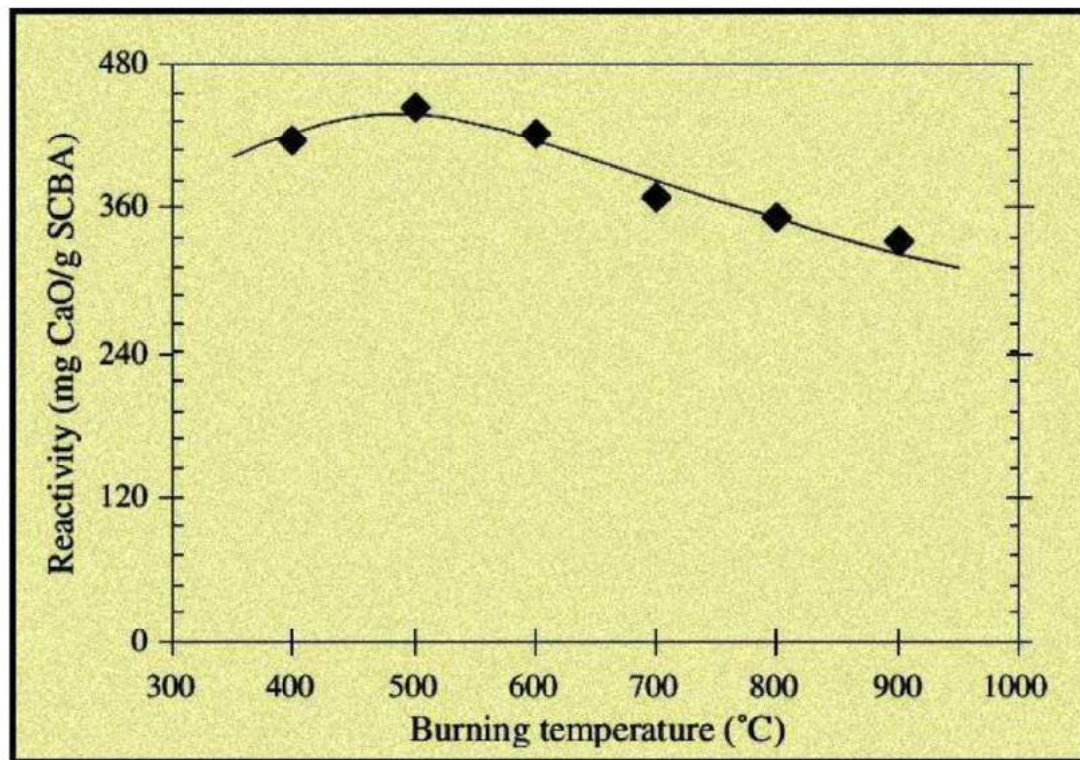


Figure 2.6: Effect of burning temperature on the reactivity of SCBA (Cordeiro et al., 2009)

The effect of different degrees of grinding on pozzolanic activity was investigated in a separate study by Cordeiro et al. (2008) in which pozzolanic activity was found to increase with grinding time; the study also suggested that grinding to values of D80 (80% passing size) below 60 μm and Blaine fineness above 300 m^2/kg resulted in products that could be classified as mineral admixture as per ASTM C618-12a. Modified Chapelle activity test was performed for various ground samples and the results are illustrated in Figure 2.7. In this test, one gram of CaO was dissolved in distilled water and diluted to 250 ml. Initial CaO concentration of the solution was known. One gram of ground bagasse ash sample was added in the solution and thoroughly mixed for more than one minute. The solution was kept in an oven at 90 °C for 16 hours. Afterwards, the filtrate was extracted and titrated with hydrochloric acid using phenolphthalein indicator. From

the titration, CaO concentration of the filtrate was determined. Chapelle activity is expressed as the difference between initial CaO concentration and CaO concentration of the filtrate (determined from the titration). Chapelle activity and Blaine fineness of bagasse ash were increased with grinding duration as shown in Figure 2.7, and results from Chapelle activity test well agreed with strength activity test.

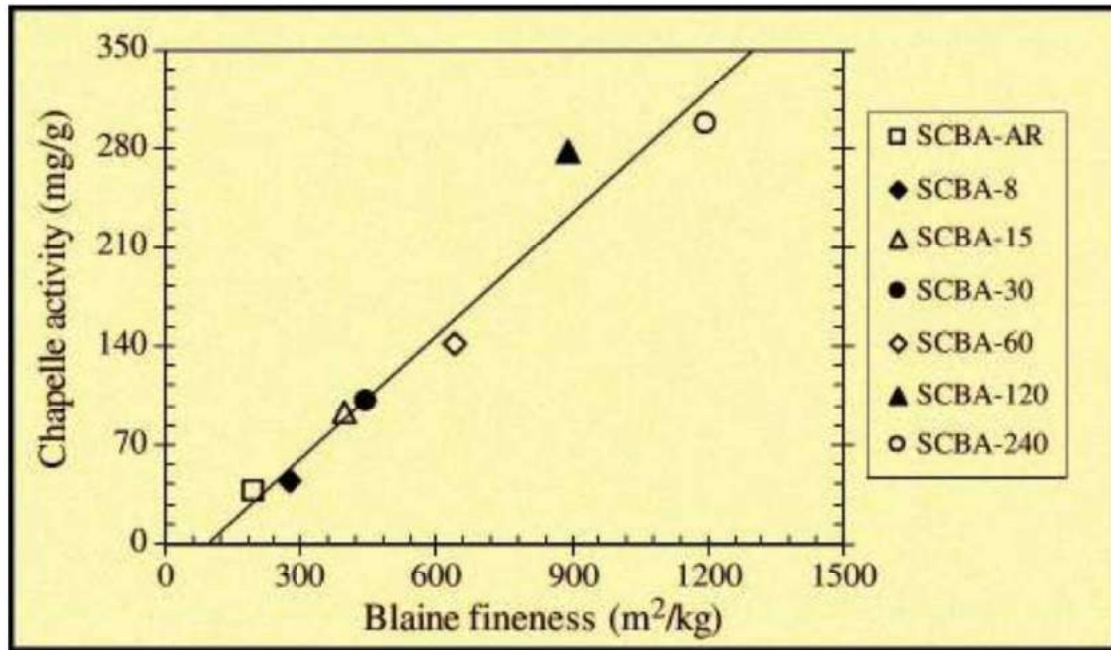


Figure 2.7: Relationship between pozzolanic activity and Blaine fineness of SCBA (Cordeiro et al 2008)

Water consistency and setting time of the blended cements increased with the increase of SCBA because of dilution effect as shown in Figure 2.8. Water requirement of bagasse ash blended mix was more than control mix due to the presence of large fibrous particles (Ganesan et al., 2007).

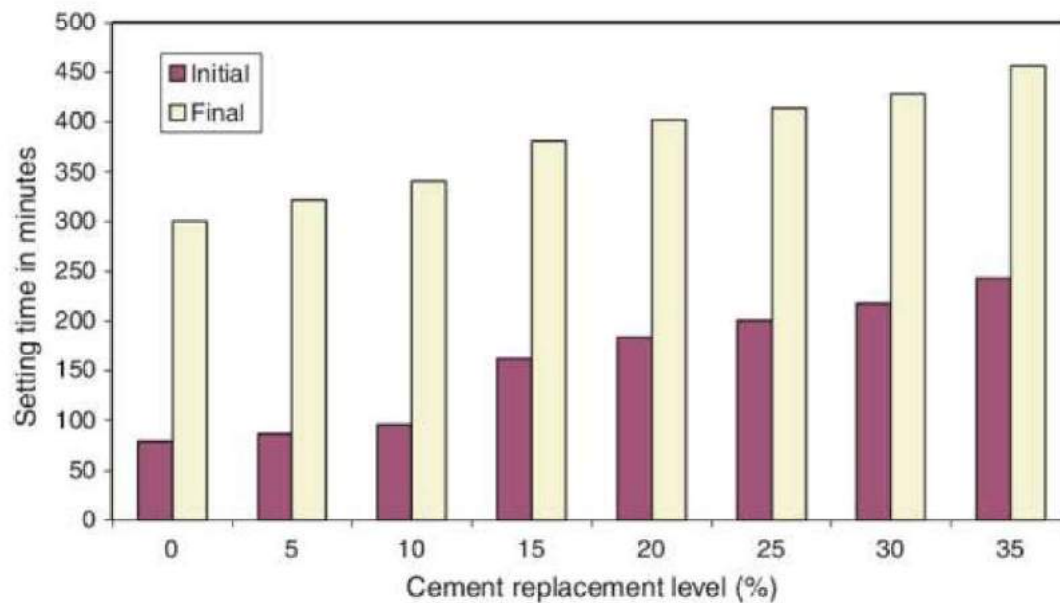


Figure 2.8. Setting time of bagasse ash blended paste (Ganesan et al., 2007)

In some studies, raw bagasse ash has been burnt to higher temperature to reduce coarse fibrous particles as well as to achieve better properties. Burning temperature varies widely from 500 °C - 1000 °C in the past research studies (Frias et al., 2011, Ganesan et al., 2007). In one study, raw bagasse ash was directly burnt to 650 °C for one hour to reduce carbon content from 11.2 % to 4.9 %. Another study involved the evaluation of the performance of bagasse as fuel (Batra et al., 2011). In this study carbon was observed as a main constituent in the floating coarse fraction of bagasse ash. This floating fraction in the bagasse ash was collected and pelletized as gasifier feed material. It is interesting to note that bagasse ash was sieved by using large industrial scale sieves and coarse particles were separated and fed to boiler again as fuel because of high carbon content. High surface area and presence of micropores in the coarse particles help to achieve fuel with activated carbon source. Bagasse ash is rich in silica and insoluble matter is very less. Because of this the separation of coarse particles from bagasse by using floating process was suggested.

In a study by Frias et al. (2011), burnt bagasse ash samples ground to 5.4 μm mean size were used for performance evaluation. Consistency, setting time, compressive strength, water absorption, and chloride diffusion in concrete were investigated. Samples with SCBA showed better performance compared to control specimens. In this study, the

raw bagasse ash performance was not evaluated before processing. Most of the previous research studies directly processed bagasse ash to cement fineness and used as mineral admixture in concrete.

Another study (Chusilp et al., 2009) examined heat evaluation and water permeability of concrete containing SCBA as SCM. In this study, SCBA was ground by using ball mill and sieved through 45 μm sieve. Heat of hydration was measured under semi-adiabatic condition. Concrete cube of 450 mm size was cast and insulated by polystyrene on all sides and the temperature was measured at the centre of the cube for 7 days. Reduction in the heat of hydration was observed in bagasse ash replaced specimens, as depicted in Figure 2.9.

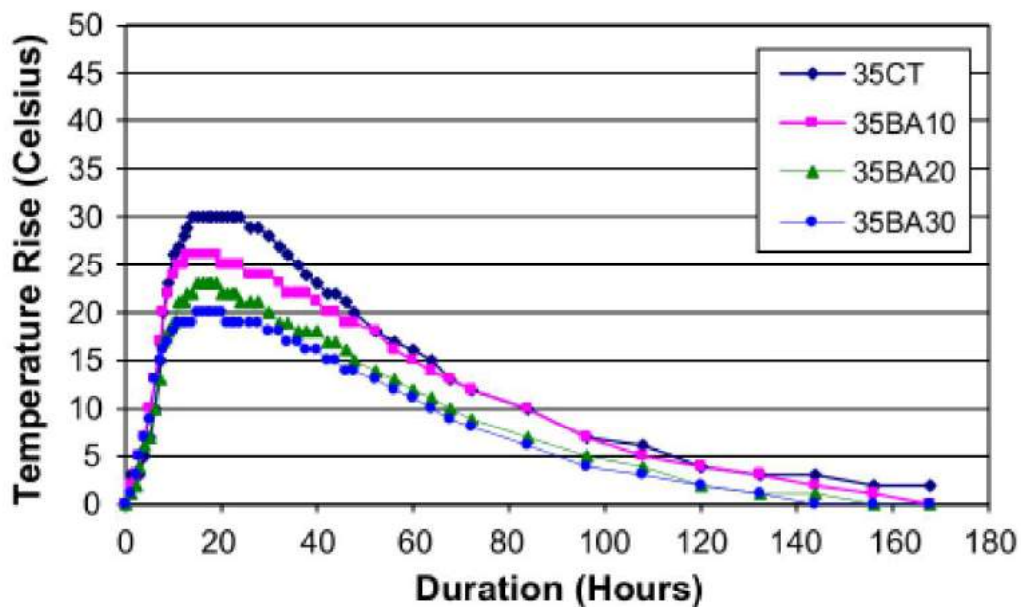


Figure 2.9: Temperature variation of concrete with bagasse ash (Chusilp et al., 2009)

Water permeability of concrete containing ground bagasse ash was investigated in the same study. Specimens were prepared for water permeability test by cutting a 40 mm thick slice from the middle of the cylinder and non-shrinking epoxy resin was applied on the periphery to avoid water leakage and allowed to harden and dry for another 24 hours. The coefficient of water permeability was determined. Concrete with bagasse ash showed less permeability than control concrete due to pozzolanic reaction, as represented in Figure 2.10. The water permeability of concrete decreased with increasing bagasse ash

proportion in concrete. The decrease in permeability was even better after 90 days as compared to 28 days, indicating a delayed additional contribution of the bagasse ash.

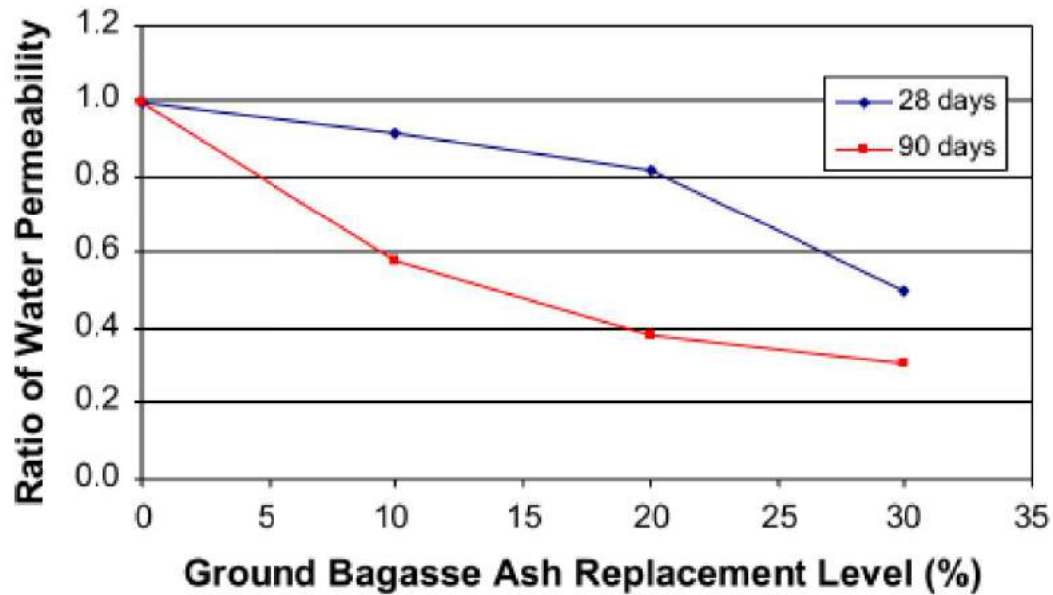


Figure 2.10. Relationship between the ratio of water permeability of concrete and replacement level (Chusilp et al., 2009)

Horsakulthai et al. (2011) investigated the performance of a combination of blending materials (Bagasse ash, Rice husk ash and wood ash – named as BRWA) as supplementary cementitious material in concrete. Compressive strength, chloride penetration depth and chloride diffusion coefficient were measured for different levels of replacement. Reduction in depth of the chloride penetration was observed with increase in BRWA replacement in concrete by using the rapid chloride migration test because of pore refining during pozzolanic reaction. Non-steady state chloride diffusion coefficient was measured for control as well as BRWA replaced concrete specimens by using accelerated salt ponding test (ASPT). Reduction of the chloride diffusion coefficient with the increase in BRWA content was observed. Chloride penetration in control and SCBA replaced concrete are represented in Figure 2.11 and Figure 2.12.

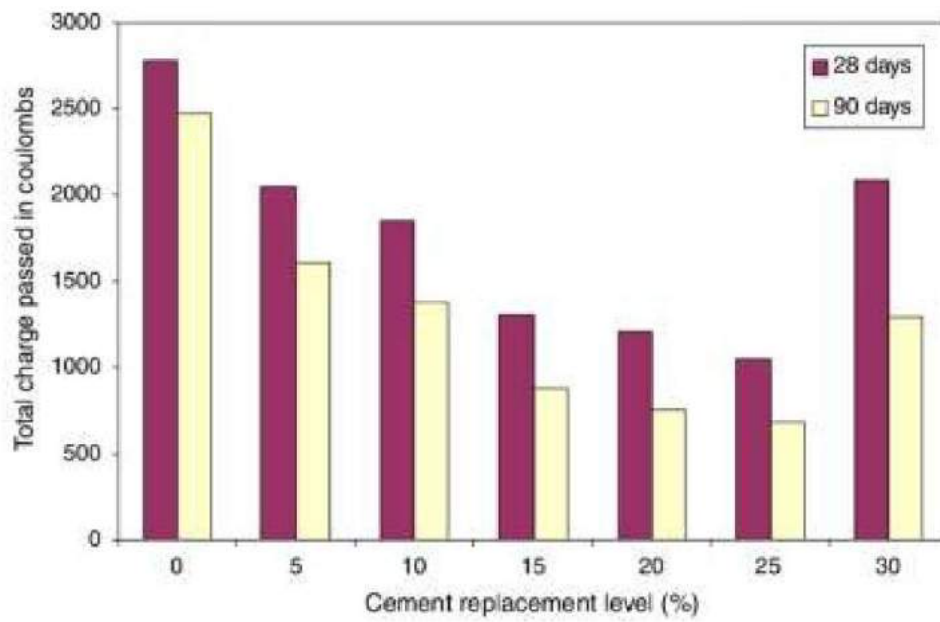


Figure 2.11: Chloride permeability of BRWA blended concretes (Horsakulthai et al., 2009)

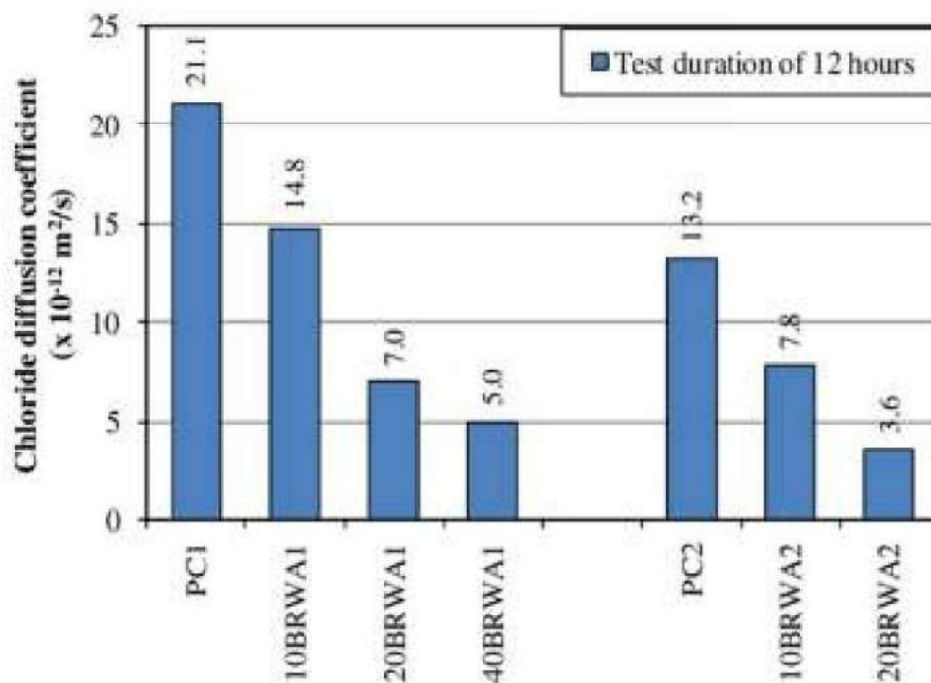


Figure 2.12: Chloride diffusion coefficient at 28 days (Horsakulthai et al., 2009)

Accelerated corrosion test by impressed voltage (ACTIV) as per NT BUILD 356 was used to measure corrosion current in the same study. At the age of 28 days, concrete cylinders with a 12 mm steel diameter round bar partially placed in the center of specimen were immersed in 3% NaCl solution. The steel bar was the anode and a stainless steel sheet was used as cathode. A 5 V DC potential difference was applied across the specimens and the current passed was measured every day. Higher dosage of the BRWA replacement increased the resistivity of concrete as shown in Figure 2.13; these observations agreed with Accelerated salt ponding test (ASPT) and Rapid chloride migration test (RCMT) test.

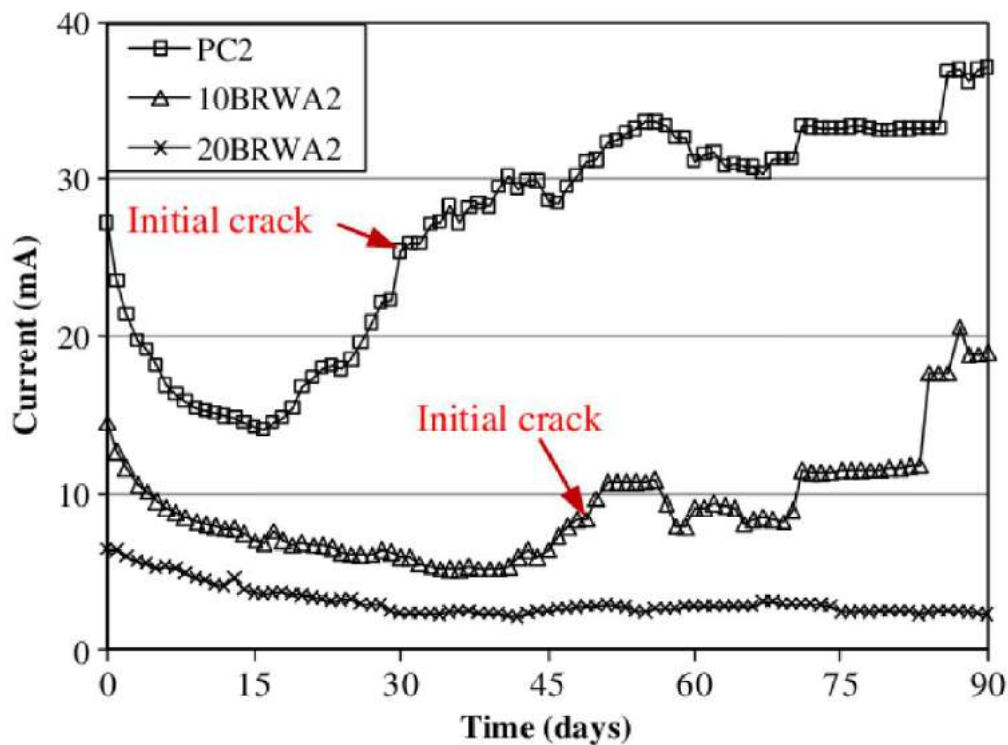


Figure 2.13: Corrosion current in concrete (Horsakulthai et al. 2009)

From the review of available literature on sugarcane bagasse ash presented in this section, it is clear that better performance was observed in strength, heat of hydration, permeability and other durability parameters in bagasse ash blended concretes as compared to plain concrete. From the above discussion, it is evident that bagasse ash has the potential to be used as supplementary cementitious material in concrete. Proper characterization and processing methodology of bagasse ash need to be studied to achieve a high level of utilization in concrete.

2.7 EFFECT OF PROCESSING ON THE POZZOLANIC ACTIVITY OF SUPPLEMENTARY CEMENTITIOUS MATERIALS

Most supplementary cementitious materials including bagasse ash are industrial by-products and cannot be used directly as pozzolanic material in concrete. Minimum level of processing is needed to achieve the status of pozzolanic material as per standards (ASTM C618-12a). Various processing methods have been used in previous research studies to evaluate their effects on the pozzolanic activity of different supplementary cementitious materials including fly ash, silica fume, slag, rice husk ash, and metakaolin. A few notable studies are mentioned here.

2.7.1. Effect of burning on pozzolanic activity of SCM

Burning process significantly influences the pozzolanic activity of supplementary cementitious materials (Brindley and Nakahira, 1958). Chopra et al. (1981) found that the amorphous form of silica was retained in rice husk ash up to 700 °C controlled burning, and further increase in temperature led to crystallization of silica to cristobalite. Nair et al. (2008) studied ^{29}Si MAS NMR spectroscopy patterns for different burnt samples of rice husk ash. A broad peak was observed at -111 ppm along with a small peak at -102 ppm for 500 and 700 °C burnt samples. This was attributed to dense silicate network and reactive silanol groups which were responsible for reactivity of the material. In case of the sample burnt at 900 °C and 1100 °C, narrow peaks were observed at -110 ppm and -112 ppm due to presence of crystalline cristobalite and tridymite as shown in Figure 2.14.

Pozzolanic activity of metakaolin (MK) highly depends on calcination temperature (Bensted and Barnes, 2000). Kaolin is stable at room temperature. Heating to 600-900 °C leads to dehydroxylation of bound hydroxyl ions and breaks down the long range structure of kaolin (Mackenzie, 1970). This results in a highly amorphous transition phase and leads to formation of reactive metakaolin. Heating kaolin at high temperature above 550 °C leads to loss of structural OH groups (Changling et al., 1994). Another study (Sanz et al., 1988) reported that heating above 550 °C caused rearrangement of Si and Al atoms in the kaolin structure and also resulted in the appearance of penta and tetra

coordinated Al. Recrystallization of metakaolin is found to occur at about 900 °C and silicon-spinel is formed at 925 °C. When the temperature is above 1400 °C, mullite is generated (Chao et al., 2010).

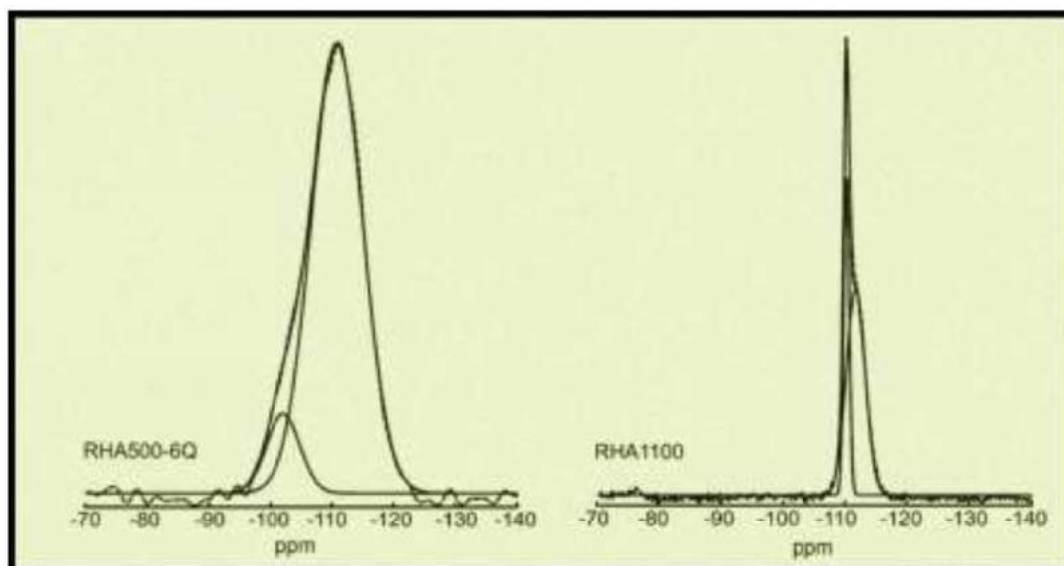


Figure 2.14: NMR patterns of rice husk ash burnt at different temperatures (Nair et al., 2008)

Brindley and Nakahira (1958) investigated the phase transformation of kaolinite by heating to higher temperature and reported the formation of silicon-spinel and mullite. Morat and Comel (1983) suggested 700–800 °C calcination for higher pozzolanic activity. Rashad (2013) reviewed all the calcination research studies of metakaolin and concluded that optimum duration for calcination varies among different researchers. He suggested that the optimum temperature for kaolin calcination to obtain highly reactive MK was 600 °C for 4 hours.

2.7.2 Effect of grinding on pozzolanic activity of SCM

Along with burning temperature, particle size of the supplementary cementing material plays an important role in its reactivity. The influence of the particle size distribution and fineness on the pozzolanic reactivity of a residual rice husk ash (RHA) was studied and good correlation was observed between fineness and reactivity (Cordeiro et al., 2011). In another study, coarse fly ash was ground to various finenesses and effects of grinding on pozzolanic reactivity were investigated. Coarse fly ash showed lower pozzolanic activity

than minimum requirement as per standard and ground fly ash below 9 μm had higher pozzolanic activity of more than 100 % (Kiattikomol et al., 2001). Kroehong et al. (2011) examined the effect of fineness of palm oil fuel ash on the particle packing and pozzolanic reaction. River sand and palm oil fuel ash were ground to the same fineness and used at different replacement levels of cement in this study to find the influence of particle packing as well as reactivity. Pozzolanic activity was increased with fineness of palm oil fuel ash which was attributed to enhancement in pozzolanic performance. Pan et al. (2003) investigated the effect of grinding on pozzolanic activity of sewage sludge ash and observed that pozzolanic activity and compressive strength of concrete significantly improved with increase in fineness.

From the previous research studies, it is clear that processing methods highly influence reactivity of pozzolanic materials. It is imperative to study the effects of different processing methods on the pozzolanic activity of any new supplementary cementitious material. Limited studies have been carried out on the effect of fineness of bagasse ash as supplementary cementitious material. Ganesan et al. (2007) investigated the utilization of bagasse ash as pozzolanic material in concrete. In this study raw bagasse ash was directly burnt to 650 °C for one hour to remove unburnt particles and ground to 5.4 μm mean grain to attain cement fineness. The performance of bagasse ash as mineral admixture was evaluated in concrete. When compared control concrete, significant reduction in permeability, and higher strength were reported for bagasse ash blended concrete. In a study by Chusilp et al. (2009), raw bagasse ash samples was ground using ball mill until the particles retained on a 45- μm sieve were less than 5%. In addition, ground bagasse ash was burnt at 550 °C for 45 minutes to reduce loss on ignition from 20 % to 5% and used for performance evaluation in concrete. Improvement in compressive strength and sulfate resistance were observed for processed bagasse ash compared to raw bagasse ash in this study. The effect of burning and three different types of grinding of sugarcane bagasse ash on pozzolanic activity was studied using Chapelle activity test by Cordeiro et al. (2009) – results have been reported in an earlier section; the results of the study showed that the maximum reactivity of bagasse ash was found in the sample that was burnt at around 500 °C and pozzolanic activity was found to increase with fineness. In previous studies, raw bagasse ash was ground to cement fineness and then burnt to an arbitrarily chosen temperature to reduce carbon content, and directly used in the concrete

for the performance evaluation, without proper characterization as well as adequate understanding of the material. It is important to investigate the effect of various processing methods on the pozzolanic performance of bagasse ash including burning, grinding, removal of fibrous unburnt particles by sieving and combination of different processing methods to achieve its effective use in concrete. In the evaluation strategy, proper investigation of the effect of different processing methods on the pozzolanic activity and microstructure of raw bagasse ash needs to be included, with an objective of suggesting a suitable processing methodology for maximum pozzolanic activity with minimum processing energy inputs.

2.8 EVALUATION OF POZZOLANIC ACTIVITY OF SCMs

Various methods have been used in the previous studies to evaluate pozzolanic activity of different supplementary cementitious materials. A few remarkable studies are reported here. Different standards and guidelines are available for the evaluation of new alternative supplementary cementitious materials. IS 1727-2004 (Indian Standard - Methods of test for Pozzolanic materials) describes different tests including wet chemical analysis, fineness, setting time for material characteristics and lime reactivity method to evaluate the reactivity of pozzolanic materials. The primary disadvantage of this guideline is the method of reactivity assessment. This is because strength gain in the lime reactivity test is very slow even after 8 days of curing at $50\pm 2^{\circ}\text{C}$. Specimens prepared with highly reactive materials such as silica fume and metakaolin are also reported to produce low strength results, and the test seems to be more favourable for SCMs that have a larger lime content (i.e. the ones that show cementitious characteristics). This leads to inappropriate assessment of reactivity of new pozzolanic materials.

ASTM C1709-11 (Standard Guide for evaluation of Alternative Supplementary Cementitious Materials (ASCM) for use in concrete) presents a detailed plan for technical evaluation of new alternative cementitious materials. The five different stages and main features of this evaluation pattern, along with some limitations, are summarized below.

Stage I: Characterization of the material - This section describes only chemical characterization. Detailed material characterization strategy is not specified. For example,

no details are available regarding microstructural characterization of new pozzolanic materials. In reality, microstructure greatly influences fresh and hardened properties of concrete. Mineralogical characterization (for instance, X-ray diffraction) also needs to be recommended to assess amorphous silica content, which is the most important characteristic of any pozzolanic material).

Stage II: Determination of appropriate specific surface of new pozzolanic materials – Suitable fineness of new pozzolanic materials need to be identified based on pozzolanic performance, workability and compressive strength of SCM blended mortar and concrete. This section suggests different degrees of grinding of new SCM. Blaine's air permeability method (ASTM C204), Fineness of 45- μm (No. 325) Sieve method (ASTM 430) and BET (Brunauer, Emmett and Teller) gas absorption method are suggested for fineness determination and laser diffraction particle size analysis is suggested for particle size distribution in the section.

Stage III: Testing with respect to existing specifications - ASTM C618-12a (Standard specification for coal fly ash and raw or calcined natural pozzolan for use in concrete), ASTM C989/C989M-13 (Standard specification for slag cement for use in concrete and mortars), or ASTM C1240 (Standard specification for silica fume used in cementitious mixtures). This is an important feature of this standard because reactivity of new pozzolanic materials is evaluated by different methods based on material characteristics. In case of Indian standard IS1727-2004, the procedure (lime reactivity test) suggested for pozzolanic activity may lead to improper evaluation and lack of understanding of new materials.

Stage IV: Concrete performance tests - A comprehensive investigation on the influence of new supplementary cementitious materials on fresh and hardened properties is suggested to evaluate the suitability of new materials for use in concrete. A number of tests are also included in this stage (concrete mixtures covering different replacement levels of new pozzolanic materials with binder contents ranging from 200 to 400 kg/m^3) to assess the performance in concrete. Fresh concrete testing includes slump, air content, and temperature, fresh density, bleeding and setting time. Compressive and flexural strength, modulus of elasticity, drying shrinkage, alkali-silica reaction, permeability, heat of hydration and sulphate resistance are listed in the recommended hardened testing.

Stage V: Field trials, Long-term performance and Durability - Instead of controlled laboratory testing, performance of new supplementary materials in actual construction applications as well as in aggressive environment are suggested in this phase. The main demerit of these tests is that they are long term evaluations; further, a minimum of three evaluations in different field conditions with minimum of one year duration for each trial are suggested, which would increase the time for evaluation.

While the above-described ASTM C1709 standard provides useful guidelines, it is clear that several additional inputs and accelerated evaluation methods are desired to reduce the time to evaluate new supplementary materials such as bagasse ash. Some alternative methodologies for the reactivity evaluation of different SCMs are described in the subsequent passages.

Paya et al. (2001) measured electrical conductivity of fly ash/lime aqueous suspension. Loss in electrical conductivity was observed due to reaction between calcium hydroxide (in aqueous solution) and pozzolanic material. The loss of conductivity of the suspension varied with time and this variation was directly related to reactivity of the pozzolanic material.

Luxan et al. (1989) proposed a quick and reliable method to determine pozzolanic activity of natural pozzolans by conductivity measurement. Difference in conductivity right after mixing and after 120 seconds with a natural pozzolan in a saturated lime solution was measured. According to this method, adsorption phenomenon is predominant in the initial 2 minutes which represents the reactivity of the pozzolanic material in the solution.

Paya et al. (2002) studied reactivity of SCBA by using thermogravimetric monitoring in lime paste as well as in OPC paste. Pozzolanic activity was evaluated in terms of reacted lime in the control and SCBA replaced mixture. 30 % OPC was replaced with SCBA for OPC/SCBA mix and 3 parts of SCBA and 7 parts of hydrated lime were used for lime/SCBA mixture. Pastes were sealed in airtight bottles and stored at 20 °C for 56 days. After curing, samples were ground by manual grinding and acetone was used to stop the hydration process. The thermogravimetric loss curve and its first derivative curve were obtained for all mixtures. Three main zones were identified and zone corresponding

to 520-580 °C was attributed to dehydroxilation of calcium hydroxide. The amount of calcium hydroxide available in the paste was because of Ca(OH)_2 produced during the hydration of cement minus the consumption due to pozzolanic reaction. The fixed lime was calculated for all mixes to evaluate pozzolanic activity of SCBA. Fixed lime content was higher for SCBA mixes, which was solid evidence for the pozzolanic activity of SCBA.

Kinetic parameter of pozzolanic reaction was measured by using kinetic-diffusive model with non-linear regression techniques and pozzolanic activity of bagasse ash was evaluated from the reaction rate constant, in the study by Frias et al. (2011). Ground bagasse ash, coarse bottom bagasse ash and laboratory burnt ash were used for this study. The absolute loss of lime concentration versus reaction time curve was fitted with a kinetic diffusive model and statistical parameters were calculated. The reaction rate constant was proposed as a direct index for the reactivity of pozzolanic material. The laboratory controlled burnt sample showed a higher reaction rate index value than the other samples, which was clear evidence for better pozzolanic reaction. McCarter and Tran (1996) studied direct activation of pozzolanic materials with calcium hydroxide. Effect of activation in the pozzolanic activity test was examined in two ways – using saturated Ca(OH)_2 solution, and powdered Ca(OH)_2 activation as shown in Figure 2.15.

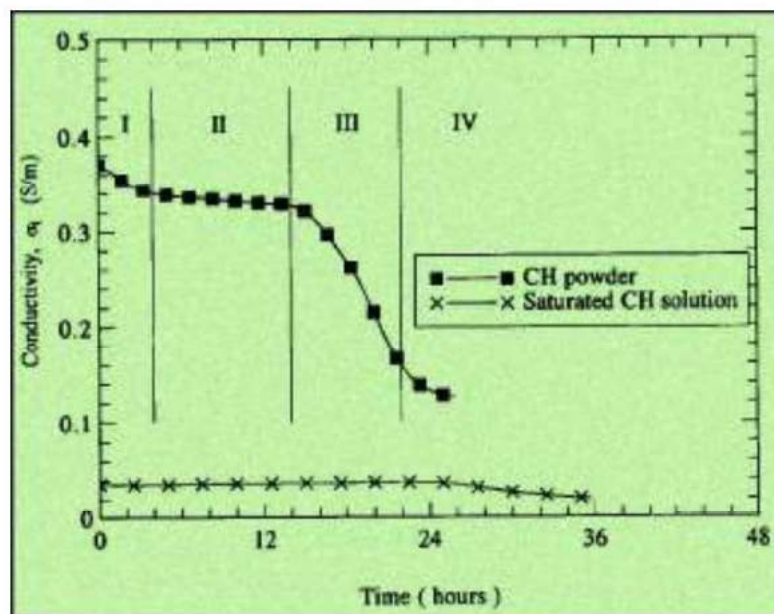


Figure 2.15: Conductivity curve (McCarter and Tran, 1996)

The study suggested that powdered CH activation is more reliable and accurate for conductivity measurement. Pozzolan activity was determined from the first derivative of conductivity measurement as represented in Figure 2.16.

Moropoulou et al. (2004) assessed pozzolan activity by differential thermal and thermo gravimetric analysis. Reacted $\text{Ca}(\text{OH})_2$ was quantified by DTA/TG analysis, and was suggested as an indicative parameter for pozzolan activity evaluation. Donatello et al. (2010) studied suitability of different pozzolan activity test methods. According to this study, reduction of Ca^{2+} in terms of CaO due to pozzolan reaction in the lime saturation method did not correlate with other methods. But significant correlation was observed between strength activity test and Frattini test in terms of reactivity of the different cementitious materials. Reduction in Ca^{2+} (in term of CaO) and OH^- ions concentration was observed in Frattini test due to the consumption of calcium hydroxide in the pozzolan reaction, which is shown in Figure 2.17.

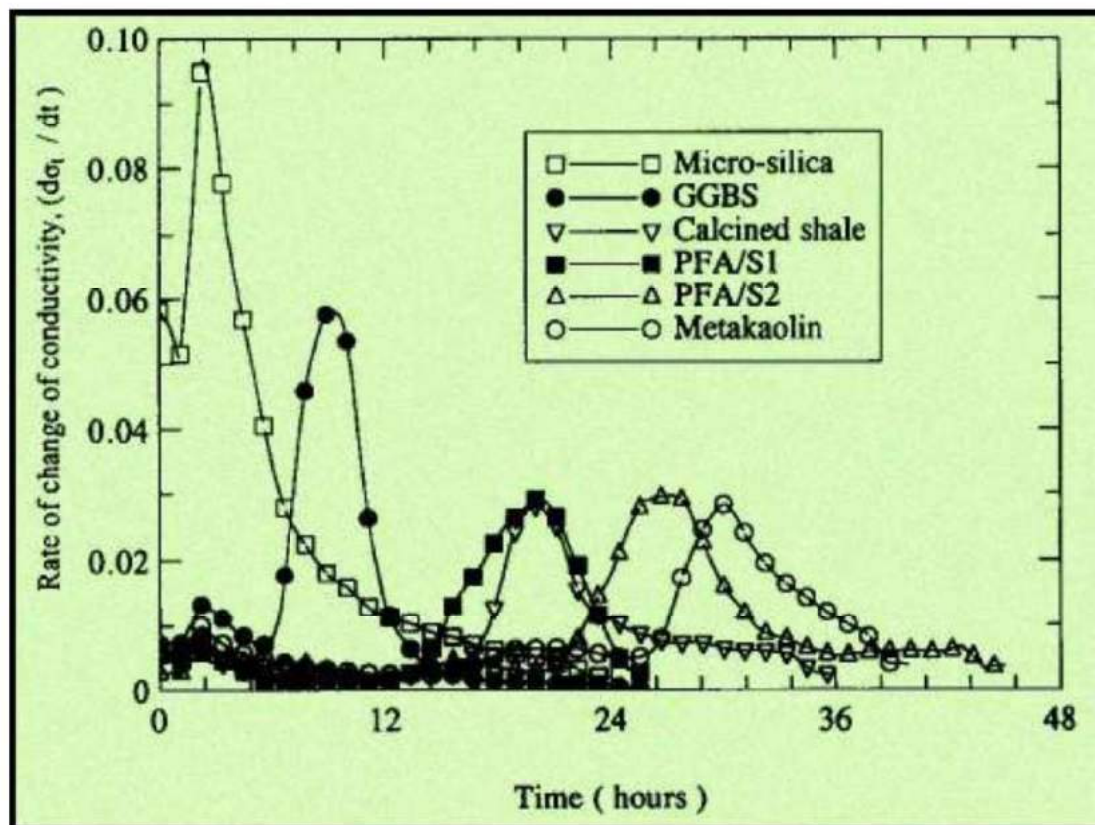


Figure 2.16: Rate of conductivity (McCarter and Tran, 1996)

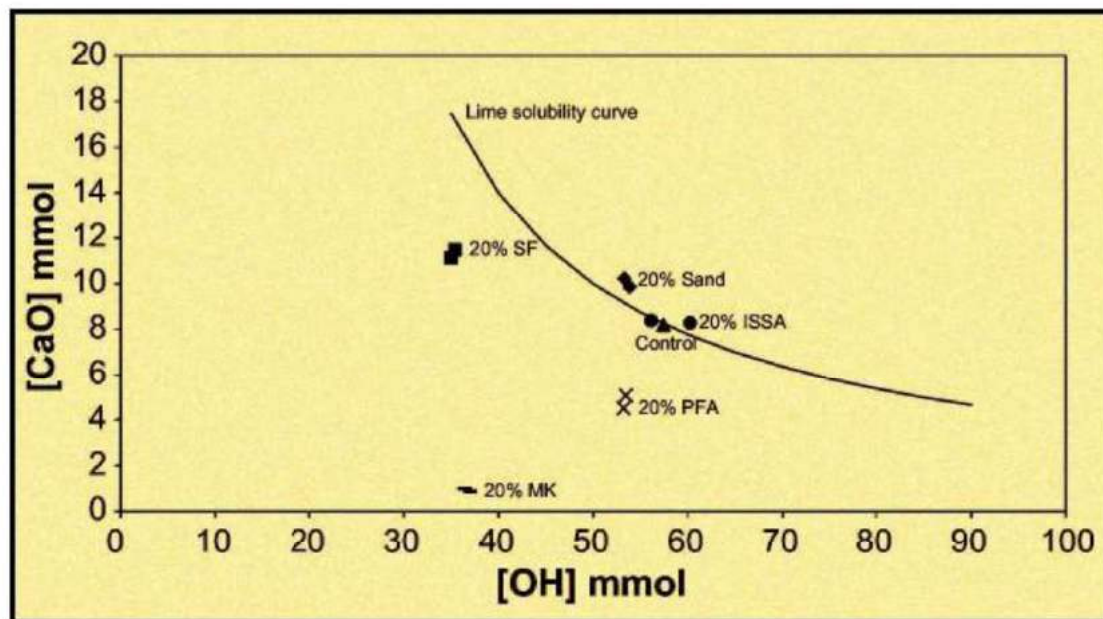


Figure 2.17 Frattini curve (Donatello et al., 2010)

Limited studies have been carried out on evaluation of pozzolanic performance of bagasse ash. It is important to characterize the pozzolanic activity of raw bagasse ash by using various available standard methods to enable its effective use in concrete. Pozzolanic activity of different sets of particles present in bagasse ash, or any new SCM for that matter can enable the creation of suitable processing methodology to produce an effective SCM with minimum additional energy inputs.

2.9 INFLUENCE OF SUPPLEMENTARY CEMENTITIOUS MATERIALS ON BINDER SUPERPLASTICIZER COMPATIBILITY

The addition of chemical admixtures in concrete enhances its fresh and hardened properties (Neville, 2011; Gambhir, 2006). Different chemical families of superplasticizers are used in modern high performance concretes to achieve required fluidity. Since most high performance concretes have binary or ternary combinations of cementitious materials, or use blended cements, proper understanding of the interaction between different superplasticizers and blended cement is essential. Selection of water reducer/superplasticizer should be based on the compatibility criteria because the performance of superplasticizer is noticeably influenced by a number of parameters including temperature, composition and fineness of cement, dosage of water

reducer/superplasticizer, addition of mineral admixtures, time of addition of superplasticizer to the fresh mix and type of superplasticizer (Jayasree and Gettu, 2008). A number of research studies that investigate the compatibility concerns of superplasticizer with blends of cement and different supplementary cementitious materials including fly ash, silica fume, slag, rice husk ash, and metakaolin are mentioned here.

2.9.1 Influence of superplasticizer characteristics on compatibility

Characteristics of the superplasticizer including its structure, presence of functional groups, and its dosage significantly influence the flow properties of cement paste (Sakai et al., 2003). Superplasticizers are categorized into four different families: Sulphonated Naphthalene Formaldehyde (SNF), Sulphonated Melamine Formaldehyde (SMF), Poly-Carboxylic Ether (PCE) based admixtures and Modified Lignosulphonates (LS) (Ramachandran, 2002). Presence of low molecular weight fraction and sugar content in the lignosulphonates leads to excessive retardation (Ramachandran, 2002; Jayasree and Gettu, 2008). Removal of sugar content and low molecular weight fraction can be achieved by fermentation and centrifuging process respectively. Modified lignosulphonates can be used as superplasticizers (Bonen and Sarkar, 1995).

Degree of retardation varies with type of superplasticizer (Zhang et al., 2010). Non-adsorbed superplasticizer adversely influences the fluidity of paste (Kjeldsen et al., 2006). Degree of sulphonation and the presence of sulphonate group at β position (Aitcin, 1998) significantly affect the performance of SNF based superplasticizers. When superplasticizer is added to the cement paste, it is adsorbed on the cement grains. Due to this adsorption of anionic molecules of superplasticizer on the cationic cement grains, electrical double layer is formed (Mollah et al., 1995, Krishna, 1996). Electrostatic repulsion between cement particles leads to effective dispersion as illustrated in Figure 2.18. Higher amount of adsorption of superplasticizer leads to greater repulsion and better workability (Roncero et al., 2002). Better fluidity was observed for high molecular weight SNF than lower molecular weight (Andersen et al., 1987). Because of condensation of SMF at high temperatures, the stability of this admixture is highly affected (Torresan and Khurana, 1998) and leads to incompatibility problems in the

warmer countries. Higher affinity of SMF based superplasticizer with C_3A is also a key factor affecting its compatibility with cement (Mailvaganam, 1999).

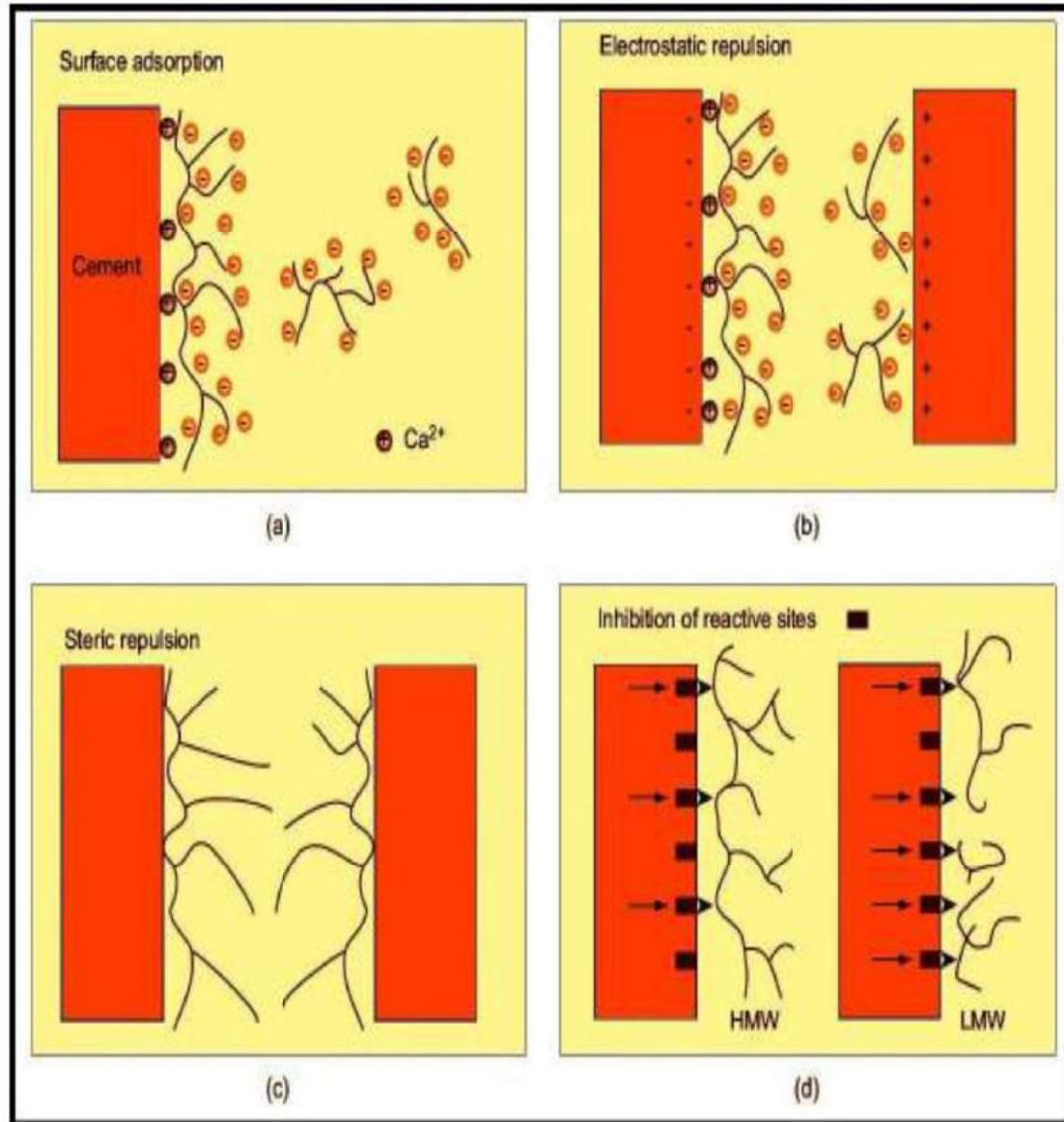


Figure 2.18: Mechanisms of action of superplasticizers (Jolicoeur and Simard, 1998; Mehta and Monteiro, 2006)

Modern superplasticizers are synthetic water soluble polymers with high molecular weight. Poly-carboxylic ether (PCE) based superplasticizers have a primary backbone chain with various functional groups such as carboxyl, polar and ionic groups in the side chain. In case of PCE based superplasticizer, in addition to electrostatic repulsion, steric hindrance is also developed by side chains. Because of the combined effect of

electrostatic repulsion and steric hindrance, effective dispersion can be achieved with low dosage of PCE based admixtures (Collepari, 1998).

2.9.2 Influence of cement properties on compatibility

Chemical composition of cement, fineness, presence of soluble alkali, C_3A content, types of gypsum and addition of supplementary cementitious materials used during cement manufacturing process are important factors which significantly govern the compatibility between superplasticizer and cement (Jolicoeur and Simard, 1998; Jiang et al., 1999; Dodson and Hayden, 1989). Rapid adsorption of melamine and naphthalene sulphonate based superplasticizers on the surface of C_3A adversely affects C_3A hydration (Mailvaganam, 1999). Orthorhombic form of C_3A is more reactive with PCE based superplasticizers than cubic form of C_3A (Magarotto et al., 2003). SNF based superplasticizers interact with C_3A in competition with sulphate ions. This results in retardation of C_3A hydration and also leads to loss of fluidity in the paste (Jolicoeur and Simard, 1998). Duval and Kadri (1998) reported that C_3A and soluble alkali sulphates in the cement highly influenced superplasticizer adsorption. Presence of large amounts of soluble alkali in cement paste enhances the solubility of sulphate ions and causes reduction in fluidity (Nkinamubanzi and Aitcin, 2004). The fineness of cement intensely affects compatibility between superplasticizers and cement. Higher specific surface area leads to an increase in superplasticizer dosage due to more water requirement (Vikan et al., 2007).

2.9.3 Influence of supplementary cementitious materials on compatibility

Compatibility of superplasticizer with fly ash blended cement paste was studied by several researchers. Similar changes on the rheological parameters for control and fly ash blended cement paste were observed for different dosage of PCE based superplasticizers (Alonso et al., 2007; Puertas et al., 2005). Effect of addition of fly ash and limestone powder on flow properties was studied by Sahmaran et al. (2006), who found that flow properties were enhanced for the same dosage of PCE based superplasticizer compared to control paste, up to 30 % of replacement. Similar trends on workability parameters were

observed for slag blended cement paste, where lesser saturation dosage was observed than control paste (Palacios et al., 2009). Another study reported that yield stress and plastic viscosity decreased for samples containing slag than fly ash blended paste (Park et al., 2005). Higher fluidity of fly ash blended cement paste is attributed to the spherical shape of fly ash particles (Nehdi and Rahman, 2007). Addition of metakaolin as pozzolanic material significantly increased saturation dosage and caused reduction in fluidity (Jayashree, 2009). Incorporation of silica fume as mineral admixture increased dosage of admixture and water demand compared to control paste (Agullo et al., 1999). Addition of metakaolin led to increase in saturation dosage due to higher water demand in the mix (Hallal et al., 2010).

2.9.4 Different methods for evaluation of admixture compatibility

Various methods were used in the previous research studies to determine saturation dosage of superplasticizer and rheological parameters. Jayshree and Gettu (2008) studied the flow behavior of cement paste with different superplasticizers to find the optimum dosage by using Marsh cone and mini slump tests. Similar trends were observed in Marsh cone and mini slump test, and the Marsh cone test was suggested as a good representation of relative fluidity of superplasticized cement paste. Saturation dosage of different superplasticizers for cement-silica fume mix was investigated using Marsh cone test by Agullo et al. (1999), who suggested that Marsh cone was a reliable test for the selection of suitable superplasticizers, as well as to find optimum dosage. Viscometer and zeta potential analyzer, and parallel plate rheometer were also suggested in earlier research studies (Alonso et al., 2013; Ferraris et al., 2001; Jayasree and Gettu, 2008).

Improper selection or incompatibility of superplasticizer with cement and pozzolanic materials leads to adverse effects on the fresh and hardened properties (Jolicoeur and Simard, 1998). Segregation, delayed setting, loss of workability, less workability retention are the common problems observed in incompatible superplasticized concrete (Jayasree, 2009). This primarily happens because incorporation of supplementary cementitious materials in modern high strength concrete leads to greater consumption of superplasticizer when compared to conventional concrete (Jayasree and Gettu, 2008; Agullo et al., 1999). Influence of sugarcane bagasse ash and fly ash on the rheological

behavior of cement pastes was studied by Quero et al. (2013) and loss on fluidity was observed with SCBA replacement. Increase in viscosity and yield stress was observed with increase in bagasse ash replacement, but the interaction of different superplasticizers with bagasse ash was not addressed.

Concerning all the discussions mentioned above, it is evident that types of superplasticizer, types of pozzolanic material and water binder ratio significantly affect compatibility of superplasticizer with blended cement. There is still a need to evaluate the effect of the interaction of superplasticizer with cementitious systems with pozzolanic materials, in order to achieve desirable fresh and hardened properties. A comprehensive investigation of compatibility concerns between sugarcane bagasse ash based PPC and superplasticizer is not available in the existing literature. In previous research studies, bagasse ash was only used as mineral admixture without proper characterization of its pozzolanic performance. Interaction of superplasticizer with SCBA based Portland pozzolana cement by using simple methods such as Marsh cone and mini-slump tests need to be investigated to achieve desirable fresh properties.

2.10 INFLUENCE OF POZZOLANIC MATERIALS ON HEAT OF HYDRATION

2.10.1 Heat of hydration of cement

Reaction of cement with water is exothermic. Heat produced in this reaction is called heat of hydration. Heat evolution in the hydration of ordinary Portland cement was studied by several researchers and heat evolution pattern was categorized into five different stages namely initial hydration period, induction period, acceleration and set, deceleration and hardening (Ridi et al., 2011). In the initial stage, wetting of highly hydrophobic cement particles occurs. In addition to this, congruent dissolution of the soluble salts in aqueous phase and correspondingly incongruent dissolution of other chemical species available in the cement takes place in the initial stage of hydration. Because of wetting of cement grains, more heat is evolved (termed as heat of wetting) in this short stage and also precipitation of first hydrated products occurs. After the initial stage, quiescence period or induction stage occurs, where heat liberation is found to be reduced (Gambhir, 2011; Newman and Choo, 2003). In acceleration stage, the rate of heat evolution is increased

considerably due to rapid dissolution and reaction of the cementitious compounds. As a result of rapid hydration of cement particles, more hydrated phases are formed in the acceleration and deceleration stages. In the final hardening stage, water diffuses through hydrated products and leads to hydration of anhydrous cement particles. In this stage, heat liberation is found to be significantly reduced.

2.10.2 Influence of pozzolanic materials on heat of hydration

Heat evolved as a result of hydration of cement grains is reported as 500 J/g of cement (Neville, 2011). Due to low thermal conductivity of concrete as well as rapid cooling of exterior surface of concrete to environment, significant thermal gradient is created between inside and outer surface of concrete (Schindler and McCullough, 2002). Higher amount of heat of hydration in the concrete leads to early age thermal cracking as a result of temperature gradient and thermal stresses. Early age thermal cracking needs to be controlled to achieve enhanced performance as well as durable concrete (Darwin and Browning, 2008). This can be achieved by control of the heat of hydration. Heat evolution of concrete is significantly governed by mineralogical characteristics of the cement, its fineness, use of supplementary cementitious materials and water to binder ratio in concrete (Snelson et al., 2008). Reduction in heat of hydration with the use of different supplementary cementitious materials is reported by several researchers (Mostafa and Brown, 2005).

Rate of heat evolution is noticeably influenced by pozzolanic activity of supplementary cementitious materials. Different heat evolution patterns have been reported for various pozzolanic materials. Zhang et al. (2002) studied the effect of chemical and mineral admixtures on the heat of hydration of cement. Although significant reduction in heat liberation was not observed with the use of superplasticizer, a delay in the exothermic reaction was reported due to retarding effect of superplasticizers. In case of fly ash blended cement, significant heat reduction was clearly observed with increase in the replacement level (Snelson et al., 2008). Similar behavior was reported by Frias et al. (2000) for fly ash blended cement. In contrast, higher heat liberation was observed for 10 % metakaolin replaced mortar in the initial few hours

compared to control mortar. This is attributable to the higher pozzolanic activity of metakaolin. This observation was validated by Bai and Wild (2002). In this study, reduction of heat liberation was reported for fly ash based binary cement. Dilution effect due to the higher level of replacement and lesser pozzolanic reactivity were reported as the reasons for the reduction in heat liberation. Similar observation was also reported for palm oil fuel ash by Awal and Shehu (2013). Lower pozzolanic reactivity of this material led to noticeable reduction in the heat of hydration at initial stages, as well as in the total heat evolution, with an increase in the replacement level. Higher pozzolanic reactivity of silica fume led to an increase in rate of heat evolution at initial stages, similar to metakaolin, as observed by a number of researchers (Snelson et al., 2008; Frias et al., 2000). The above results indicate that pozzolanic reactivity of supplementary cementitious materials is directly related to the rate of heat evolution at initial stages of hydration.

2.10.3 Methods for measurement of heat of hydration

Different methods have been suggested for measurement of heat of hydration. Heat of solution calorimetry, Semi-adiabatic calorimetry, Aadiabatic calorimetry, Isothermal conduction calorimetry, Hot box method, quantification by using X-ray diffraction and Adaptive Neuro-Fuzzy Inference System (ANFIS) have been used for heat of hydration measurement in the previous research studies. Ballim and Graham (2003) proposed maturity approach for the measurement of rate of heat evolution which is independent of the starting temperature by using an adiabatic test. To achieve real time-temperature histories in the actual structures, which is dissimilar from controlled adiabatic test conditions, a combined effect of time and temperature on the extent and rate of hydration is expressed in terms of maturity by using Nurse-Saul and Arrhenius expressions (Wang and Dilger, 1998; Naik, 1985; Breugel, 1998). The maturity of concrete cured at different temperatures is described in terms of the equivalent maturity time (t_{20}) of concrete cured at 20 °C. If concrete is constantly cured at a temperature of 20 °C, the maturity time is similar to the clock time (Ballim and Graham, 2003).

Montakarntiwong et al. (2013) measured the heat of hydration of concrete containing raw bagasse ash using a simple method by inserting a thermocouple at the center of the

concrete specimens in semi-adiabatic condition. Reduction in heat evolution was reported with increase in the replacement level of bagasse ash. This study involved measurement of heat of hydration of raw bagasse ash blended concrete.

A detailed investigation of the rate of heat evolution of bagasse ash is not available in the present literature. Suitable assessment of the influence of bagasse ash as well as processed bagasse ash on the heat of hydration with respect to wide range of replacement levels needs to be performed. In addition to this, it is imperative to measure the heat of hydration of raw bagasse ash in adiabatic condition without exchange of heat, and also to represent the heat evolution in terms maturity to simulate real field conditions (Ballim and Graham, 2003; Graham et al., 2011).

2.11 INFLUENCE OF POZZOLANIC MATERIALS ON DURABILITY OF CONCRETE

Supplementary cementitious materials densify the microstructure of concrete and help to achieve low permeability concrete. Pore structure, pore connectivity and interfacial transition zone (ITZ) of concrete significantly influence the mechanical and durability properties of concrete (Gambhir, 2013; Newman and Choo, 2003; Mehta and Monteiro, 2006). The interfacial transition zone (approximately 30-50 microns around aggregate) that is more porous and rich in calcium hydroxide deposits as opposed to the bulk paste (Mehta and Monteiro, 2006) serves to increase the permeability of concrete. When pozzolanic materials are used, reactive silica present in the materials reacts with calcium hydroxide to produce additional C-S-H gel. Permeability of concrete is significantly reduced because of pore refinement as well as additional CSH formation from the pozzolanic reaction.

A number of research studies have been conducted on the influence of fly ash, slag, metakaolin, rice husk ash and silica fume on the durability performance of concrete. Resistance of concrete containing mineral admixtures against chlorides and other deteriorating agents is reported to be significantly enhanced when compared to control concrete (Githachuri and Alexander, 2013; Otieno et al., 2014). Duan et al. (2013) studied the effect of slag and metakaolin on the microstructure, compressive strength,

carbonation and freeze-thaw resistance, and permeability of concrete. Considerable reduction in permeability and improvement in ITZ were observed when slag or metakaolin were used. Performance of volcanic tuff blended cements against alkali-silica reaction and sulphate resistance was investigated by Turanli et al. (2005) and greater reduction in expansion was observed compared to control specimens. Shekarchi et al. (2010) investigated permeability of 15 % metakaolin blended concrete and reduction in water penetration (50%), gas permeability (37%), water absorption (28%) and ionic diffusion (47%) were reported. Similar observations for metakaolin have been reported by several researchers (Khatib and Clay, 2003; Zhang and Malhotra, 1996; Coleman, 1996; Aquino et al., 2001; Walters and Jones, 1991; Badogiannis and Tsivilis, 2009).

Durability performance of new SCMs against aggressive deteriorating agents like chlorides, sulphates, oxygen, carbon dioxide and moisture need to be systematically evaluated. A detailed investigation of durability performance of bagasse ash is not available from previous research studies. As stated earlier, Chusilp et al. (2009) studied the performance of concrete containing bagasse ash against water permeability with different replacement levels and reduction in the water penetration depth was reported. Instead of a single test, there is a need still to look at the durability performance of bagasse ash by different test methods, because ingress of aggressive chemicals is based on different transport mechanisms including permeation, adsorption, diffusion, migration, convection, absorption, sorption and combination of these above mechanisms (Alexander et al., 1999). A systematic and thorough investigation of durability performance needs to be undertaken in the performance evaluation for bagasse ash or any new pozzolanic material to enable its potential use in concrete.

2.12. RESEARCH NEEDS

Characterisation and suitability of bagasse ash as a supplementary cementitious material were investigated in a limited number of previous research studies. Proper characterization strategy of bagasse ash and suitable processing methodology for use in a large scale are not reported in the existing literature.

ASTM C1709-11 is used as a standard for evaluation of new alternative supplementary cementitious materials for use in concrete, but suitable processing methods for new alternative materials are not well-defined in this standard. Appropriate processing methods and guidelines need to be developed to achieve better performance in concrete. Different methods and standards are available to evaluate pozzolanic activity of supplementary cementitious materials and to characterize these materials towards effective use in concrete (Donatello et al., 2010). It is imperative to study these standard test methods for bagasse ash to find its suitability as cementitious material in concrete.

Availability of pozzolanic materials is an important aspect to be addressed, in order to plan efficient utilization of such materials. Availability of sugarcane bagasse ash is increasing rapidly because of rapid implementation of number of new cogeneration plants especially in India. Information on availability of bagasse ash is not available in the current literature. Proper quantification of availability and accessibility of sugarcane bagasse ash to cement plants needs to be addressed.

Use of chemical admixtures is common in modern concrete applications, especially in high strength concrete. Compatibility of binders with SCBA or any new supplementary cementitious materials with chemical admixtures needs to be investigated in detail to achieve desirable fresh properties.

Supplementary cementitious materials are widely used because of their desirable properties such as additional strength gain, enhancement in durability as a result of pore refinement, lower heat of hydration etc. Improvement in the fresh and hardened properties of concrete due to addition of SCBA needs to be addressed through a systematic investigation.

Only raw bagasse ash was used as mineral admixture in the previous research studies. Development of sugarcane bagasse ash based Portland pozzolana cement based on maximum pozzolanic performance with minimum processing energy needs to be addressed to achieve its effective utilization in concrete. A comprehensive performance evaluation of bagasse ash based blended cements in cement paste, mortar and concrete with different levels of replacement needs to be performed.

2.13. SUMMARY OF LITERATURE REVIEW

The available information on characterization of sugarcane bagasse ash as supplementary cementitious material and its applications in concrete have been reviewed in this chapter. In addition, influence of various processing methods on pozzolanic performance of SCMs, different methods suggested in the standards for the evaluation of pozzolanic activity and need of performance evaluation of new SCMs in concrete have been reported. Irrespective of available information, there is still a need to investigate the proper characterization strategy for sugarcane bagasse ash. Proper assessment of pozzolanic performance of bagasse ash and performance evaluation in concrete will throw light on an improved understanding of bagasse ash and lead to achieve its effective utilization in concrete.

CHAPTER 3

CHARACTERIZATION TECHNIQUES AND MATERIALS USED FOR THE STUDY

3.1 INTRODUCTION

Various characterization techniques and materials used for the present study are presented in this chapter. The working principle of characterization tools such as Scanning Electron Microscopy (SEM) with energy dispersive X-ray analysis (EDS), X-Ray Diffraction (XRD), X-Ray Fluorescence spectroscopy (XRF), laser particle size analyzer and Fourier transform infrared spectroscopy (FTIR) and sample preparation for these techniques are summarized in the following sections. Material properties of raw sugarcane bagasse ash, ordinary Portland cement, fine aggregates, coarse aggregates, and superplasticizers are also reported in the chapter.

3.2 CHARACTERIZATION TECHNIQUES

Scanning electron microscopy was used to investigate the microstructure of bagasse ash and different processed samples in the study. In addition, EDS analysis was used along with SEM to obtain the elemental compositions of all the observed phases. Oxide compositions of bagasse ash, different processed bagasse ash samples and blended cements were determined using X-ray fluorescence spectroscopy. FTIR was used to identify the bond types in different molecules present in the bagasse ash and their corresponding characteristic bands. X-ray diffraction was used to find the crystalline phases present in the materials used for the study. The particle size distribution of materials was obtained by laser particle size analyzer.

3.2.1 Scanning electron microscopy (SEM)

Scanning electron microscopy is widely used to determine morphological characteristics, composition and surface features (texture and topography) of cementitious materials with enhanced resolution. The electron beam generated from a tungsten filament (by heating the filament to high temperature) is directed along the SEM column towards the sample for interaction. The incident electron beam interacts with the sample and generates different types of signals (secondary electrons, backscattered electrons, Auger electrons, X-rays). Topographic contrast (surface texture and roughness) can be obtained by secondary electrons whereas compositional contrast is observed by backscattered electrons. Because of the electronic transitions and emission of X-rays, different elements present in the sample can be determined by energy dispersive X-ray (EDX) analysis. Scanning electron microscope used in the study is shown in Figure 3.1.



Figure 3.1: Scanning electron microscope used for the study

Microstructure of raw sugarcane bagasse ash and changes in the microstructure upon application of different processing methods were comprehensively investigated by secondary electron imaging. Variations in the elemental composition due to different processing was obtained by EDS analysis in the present study. Raw bagasse ash was dried at 105 °C for 24 hours to remove moisture and the dried raw bagasse ash was used

for SEM analysis. The sample was spread on a sample disk with sticky carbon tape as shown in Figure 3.2 and further coated with a layer of gold-palladium by sputter coating (see Figure 3.3) to achieve better sample-electron beam interaction and to avoid surface charging.



Figure 3.2: Sample holder used in the study



Figure 3.3: Sputter coating equipment

After coating, the sample was placed on the sample stage as shown in Figure 3.4 and morphology of bagasse ash particles was observed using secondary electron (SE) mode.



Figure 3.4: Placing of sample on the sample stage of SEM

3.2.2 X-ray diffraction method (XRD)

X-ray diffraction technique is an effective tool to study the crystallography of materials and phase compositions of a polycrystalline sample. The quantitative determination of phase composition in the cement clinker by referencing the relative peak intensities, state of crystallinity of different phases, determination of polymorphic changes, and other salient features of individual phases can be studied by X-ray powder diffraction technique (Bensted and Barnes, 2002). XRD instrument used in the study is shown in Figure 3.5.

The X-ray beam is generated and allowed to pass through slits to collimate the beam. This X-ray beam interacts with specimen and gets diffracted. The diffracted rays are passed through monochromators to eliminate the wavelengths other than the principal $K\alpha$ radiation, and collected by a detector. A spectrum of diffraction is plotted with intensity versus deviation angle 2θ to get a diffraction pattern of the tested sample. Identification of peaks in the bagasse ash spectrum was achieved by comparing the X-ray diffraction pattern with an international standard database like JCPDS (International Joint Committee on Powder Diffraction Standards) with the help of a software tool 'X'Pert Highscore Plus' in this study.



Figure 3.5 XRD instrument used in the study

The powder diffraction method is an appropriate method for the characterization and identification of polycrystalline phases in cementitious systems. Dried bagasse ash sample was ground and then sieved through 75 μm sieve and used for XRD analysis. Mineralogical characteristics of raw sugarcane bagasse ash, different burnt samples of bagasse ash, ordinary Portland cement and SCBA based Portland pozzolana cements were determined by using XRD in the present study.

3.2.3 X-ray Fluorescence Spectroscopy (XRF)

X-ray fluorescence analysis is a reliable and rapid method that uses characteristic X-ray (fluorescent X-ray) to find the elemental composition of the materials. The incident X-rays from the X-ray tube are focused towards the sample. These high energy X-rays generate electronic transitions in the sample atoms, resulting in the emission (fluorescence) of X-rays from the sample atoms. Thus, the sample emits fluorescent X-rays, which are characteristic of the elements present in the sample.

Dried bagasse ash sample and other cementitious samples were pelletized with high purity boric acid and the pellets were used for testing. The emitted X-rays can be detected by an energy dispersive (or wave length dispersive) detector. Elemental composition can be found from the net intensity of energy peaks. From the elemental composition, oxide

compositions of bagasse ash and cements were determined by stoichiometric adjustments. X-ray fluorescence spectrometer used in the present study is shown in Figure 3.6.



Figure 3.6: X-ray fluorescence spectrometer used for the study

3.2.4 Laser Particle size analyser

Laser diffraction method is a commonly used technique to determine the particle size distribution of SCMs due to its ability to work over a wide range from submicrons to millimeter sizes. Laser particle size analyser used for the study is shown in the Figure 3.7.



Figure 3.7: Laser particle size analyser used for the study

The laser diffraction method is rapid as well as reliable and presents easy repeatability. In this method, a fluid stream with the sample intercepts a laser beam. The beam, based on the particle size, is scattered with different angles. Large particles present in the sample scatter the incident light at small angles compared to small particles. By using laser diffraction method, particle size distribution of the material is directly measured from the halo of the scattered pattern.

In the present study, particle size distributions of the sugarcane bagasse ash and different blended cements were determined by using this method. Because of wide range of particles present in the bagasse ash, this method was adopted in the material characterisation. In most cases, the sample can be directly used for particle size analysis without any preparation. If the sample has very fine particulates like silica fume, a wet analysis method is adopted. In this method, particles are dispersed in a suitable non-reactive liquid medium and the particle size of the sample is analyzed. In the current study, the dried raw bagasse ash, and blended cements were directly used for particle size analysis.

3.2.5 Fourier Transform Infrared (FTIR) spectroscopy

For FTIR, the dried bagasse ash was ground with potassium bromide (KBr) powder using a small grinding disk and a pellet was prepared using hand pressure equipment. The grinding disk, pellet preparation chamber and the hand pressure tool are shown in the Figures 3.8-3.10. In this technique, the light from an infrared source is passed through an interferometer and directed towards the prepared sample. Different functional groups, which are present in the sample absorb characteristic frequencies of infrared radiation; as a result, an interference pattern is obtained. With the help of a Fourier transform, the interference pattern is converted into a spectrum. The peaks in this spectrum denote the absorption of infrared energy towards molecular bond vibrations and stretching/bending. This enables the determination of molecular structure. Self calibration is possible by using laser He-Ne standard calibrator.



Figure 3.8: Grinding disk



Figure 3.9: Pellet preparation chamber



Figure 3.10: Hand pressure arrangement for pellet preparation

3.3 MATERIALS USED

3.3.1 Sugarcane bagasse ash

Sugarcane bagasse ash was collected from Madras Sugar Limited, Tamil Nadu, India for this study. In sugar industries, the bagasse ash is collected by using bag-house filter. The collected bagasse ash is mixed with water and transported to the nearest disposal area. Raw bagasse ash collected from such a disposal site was dried at 105 – 110 °C for 24 hours to remove evaporable moisture content, and the dried sample was used for all investigations.

Determination of material properties of dried raw bagasse ash was carried out as per IS 1727-2004 and the results are given in Table 3.1. The determination of standard consistency, initial and final setting time were performed in accordance with IS: 4031-2005 using the mixture of bagasse ash and ordinary Portland cement (53 grade) in the proportion of 0.2N:0.8 where N is the ratio of specific gravity of bagasse ash to specific gravity of cement, as indicated in IS 1727-2004. The normal consistency of the control cement paste was 30 % and for the raw bagasse ash replaced paste was 50 %. The presence of coarse fibrous particles in the raw bagasse ash increased the water requirement for the same workability. Initial and final setting times were higher than control paste; similar results were also reported in a previous study (Ganesan et al., 2007). Soundness test was performed as per guidelines and a small expansion, less than the permissible limit, was observed in all the specimens. The specific gravity of raw bagasse ash was determined by using Standard Le Chatelier flask and kerosene (density 0.73 g/cc) as per IS 1727-2004. The specific surface area of raw bagasse ash was found using Blaine air permeability test as per ASTM C204-11. Raw bagasse ash has low specific surface area (145 m²/kg) as well as low specific gravity (1.91) because of the presence of lightweight coarse fibrous carbon particles.

Oxide composition of raw bagasse ash was determined by X-ray fluorescence (XRF) and the results (typical only; not average) are given in Table 3.2. Raw bagasse ash had more than 70 % SiO₂ and 7 % CaO.

Table 3.1: Physical properties of raw sugarcane bagasse ash

CHARACTERISTICS	RAW SCBA
Specific Gravity	1.91
Specific surface area (Blaine)	145 m ² /kg
Moisture content	46 %
Loss on ignition	21 %
Bulk Density	294 kg/m ³
Soundness test (Expansion)	0.8 mm
Consistency	50 %
Initial setting time	195 minutes
Final setting time	330 minutes

Table 3.2: Oxide composition of raw sugarcane bagasse ash by XRF

OXIDE	AMOUNT (%)
CaO	7.77
SiO ₂	72.95
Al ₂ O ₃	1.68
Fe ₂ O ₃	1.89
MgO	1.98
K ₂ O	9.28
SO ₃	4.45

X-ray diffraction technique (using Cu K α radiation) was used for mineralogical analysis. The dried bagasse ash sample was ground and sieved through 75 μ m sieve. The diffraction pattern of bagasse ash clearly shows the amorphous hump between 20 and 25

$^{\circ}2\theta$ which is attributed to the presence of reactive silica. Quartz (Q) and Crystobalite (C) were also observed to be present, as presented in the diffraction pattern in Figure 3.11.

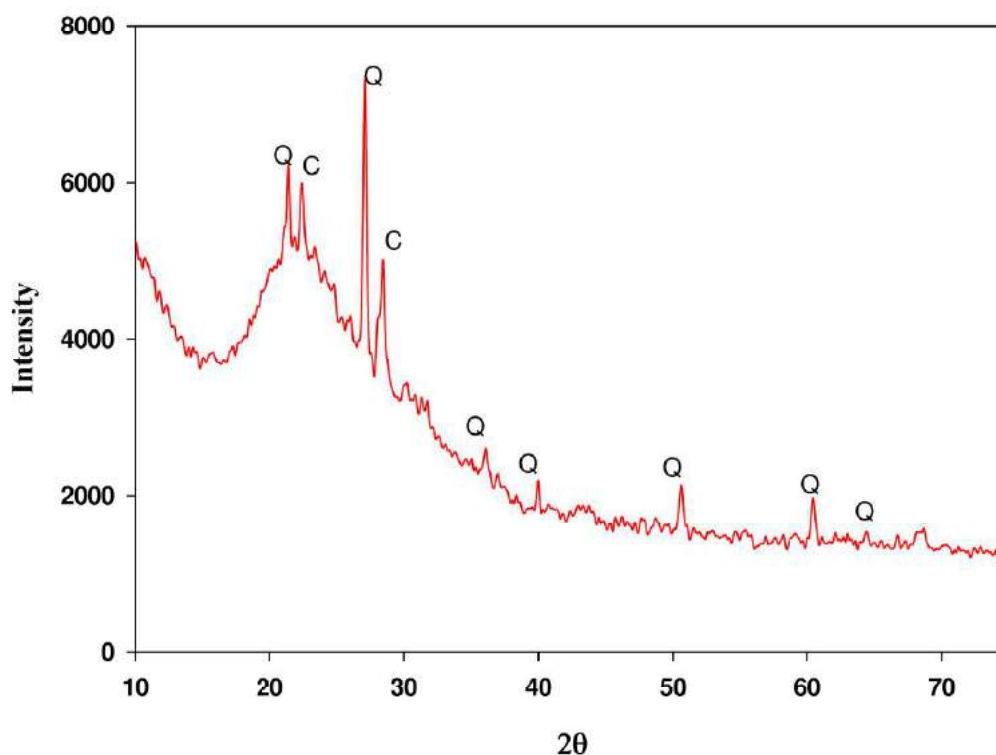


Figure 3.11: X-ray diffraction pattern of raw bagasse ash

Fourier Transform Infrared (FT-IR) spectrometry analysis was performed for dried bagasse ash. The bagasse ash was mixed with a powder of KBr crystal. As mentioned earlier, by using micro-disk and hand pressure arrangement, pellets was prepared for testing. Wide characteristic bands were observed at 472, 798 and 1092 cm^{-1} which represent finger print of the vibration of Si-O bonds. Observed bands at 2884 cm^{-1} and 2992 cm^{-1} as shown in Figure 3.12 are attributed to the presence of carbon particles in the raw bagasse ash.

Although limitation on the measurement of widest range of particles present in the sample, laser diffraction was used for particle size analysis. Particle size distribution of raw bagasse ash by laser diffraction is presented in Figure 3.13. Raw bagasse ash has different sized particles and it is evident from this distribution that the raw bagasse ash sample had around 13% particles greater than $300\text{ }\mu\text{m}$.

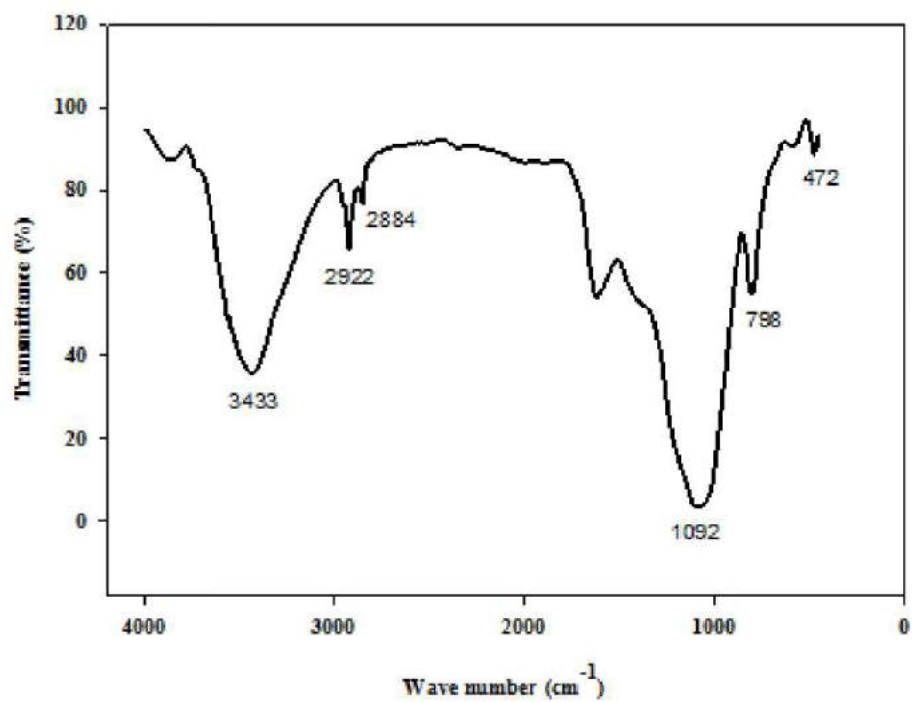


Figure 3.12: FTIR pattern of raw bagasse ash

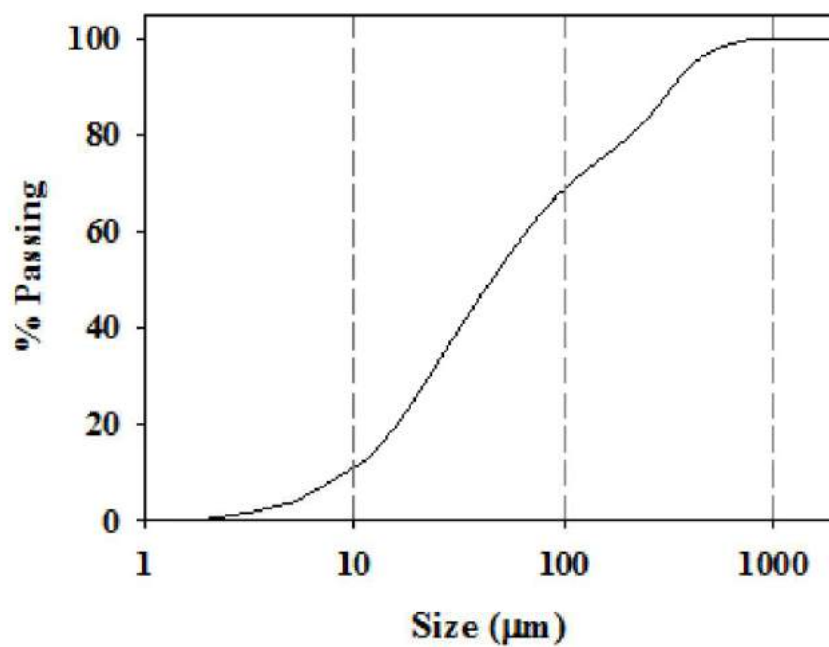


Figure 3.13: Particle size distribution of raw bagasse ash

3.3.2 Cement

In the present study, ordinary Portland cement (53 grade confirming the requirements of IS 12269-2008) was used. Oxide composition of cement was determined by XRF and is presented in Table 3.3. Physical characteristics of cement were found as per IS 4031-2005 and fineness was determined as per ASTM C204-11. Results are given in Table 3.4.

Table 3.3: Oxide composition of cement

Oxide composition	OPC
SiO ₂	20.68
Al ₂ O ₃	4.12
Fe ₂ O ₃	5.44
CaO	60.36
MgO	0.83
K ₂ O	0.27
Na ₂ O	0.23
SO ₃	2.46

Table 3.4: Physical properties of cement

Characteristics	OPC	Relevant standard
Specific gravity	3.16	IS 4031-Part 11-2005
Fineness (m ² /kg)	310	ASTM C204-11
Soundness, Expansion (mm)	1.61	IS 4031-Part 3-2005
Consistency (%)	30	IS 4031-Part 4-2005
Initial setting time(min)	125	IS 4031-Part 5-2005
Final setting time (min)	165	IS 4031-Part 5-2005

3.3.3 Aggregates

River sand was used as fine aggregate and two different sizes of crushed granite (maximum size of 10 mm and 20 mm respectively) were used as coarse aggregates in the present study. Physical properties of fine and coarse aggregates were determined as per IS 2386-2007 and the results are given in Table 3.5. Particle size distribution of fine and coarse aggregates was found by sieve analysis as per IS 2386-2007, and is presented in Figure 3.14.

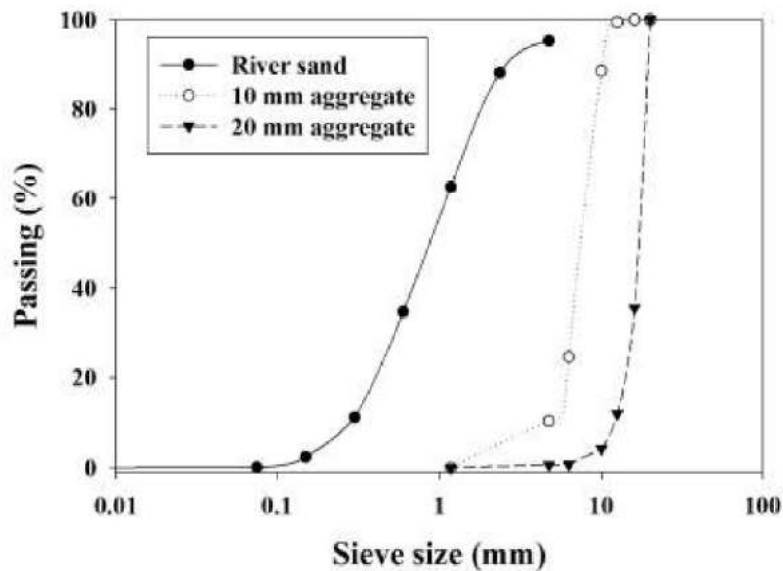


Figure 3.14: Particle size distribution of aggregates by sieve analysis

Table 3.5: Physical properties of aggregates

Characteristics	Fine aggregates (River sand)	Coarse aggregates (10 mm)	Coarse aggregates (20 mm)
Specific gravity	2.58	2.88	2.84
Water absorption (%)	1.07	0.33	0.35
Bulk density (kg/m ³)	1710	1580	1520

3.3.4 Superplasticizers

To understand the interaction between superplasticizers and sugarcane bagasse ash based Portland pozzolana cement, two different superplasticizers were used in this study - a sulphonated naphthalene formaldehyde based admixture (denoted as DC), and a polycarboxylic ether based admixture (specified as GL). Characteristics of superplasticizers, as reported by the manufacturers, are given in Table 3.6. Water content in the superplasticizer was adjusted in the water used for mixing process.

Table 3.6: Characteristics of superplasticizers used for the study

Characteristics	PCE (GL)	SNF (DC)
Specific Gravity	1.10	1.21
pH	6	6.64
Appearance	Dark Brown liquid	Light Brown liquid
Solids content (%)	32	41
Chloride (%)	< 0.2	0.025
Shelf life	12 months	12 months

3.4 SUMMARY

Characterization tools used for the present study were described in the chapter. In addition, methods of sample preparation adopted for different techniques were summarized. Physical, chemical and mineralogical characteristics of raw sugarcane bagasse ash was presented in detail. Moreover, material characteristics of aggregates, superplasticizer and ordinary Portland cement used in the study were determined as per relevant standards and results have been presented in the later part of the chapter.

CHAPTER 4

EVALUATION OF POZZOLANIC PERFORMANCE AND MICROSTRUCTURE OF SUGARCANE BAGASSE ASH

4.1 INTRODUCTION

A clear evaluation of pozzolanic activity of sugarcane bagasse ash is imperative to achieve its effective utilization in concrete. In all previous research studies, raw bagasse ash was ground to cement fineness and directly used in the concrete for the performance evaluation, without adequate characterization. It is important to characterize the pozzolanic activity of raw bagasse ash by using various available standard methods to enable its effective use in concrete. Pozzolanic activity of different sets of particles present in bagasse ash needs to be investigated to attain maximum possible pozzolanic activity. Various methods have been used in previous studies to evaluate pozzolanic activity of different supplementary cementitious materials. A comprehensive evaluation of pozzolanic performance of raw sugarcane bagasse ash (SCBA) as well as different particles present in bagasse ash using five standard methods is described in this chapter. In addition, microstructural analysis of different particles of raw SCBA is also reported in this chapter.

4.2 DIFFERENT PARTICLES PRESENT IN RAW BAGASSE ASH

The sample of sugarcane bagasse ash was found to consist of several types of particles of different sizes, as seen in Figure 4.1. Apart from fine burnt particles, there were several fibrous particles too, which looked to be unburnt. Complete removal of the coarse fibrous particles from raw bagasse ash was achieved by sieving. By numerous trials, it was found that material passing through 300 μm sieve had mostly fine burnt particles. Thus, the oven dried bagasse ash was sieved through 300 μm to remove the fibrous particles, as shown in Figure 4.2. The particle size analysis for raw bagasse ash was carried out by

laser diffraction method. The raw bagasse ash sample had around 13% particles greater than 300 μm , primarily from the fibrous particles (See Figure 3.16). Two different types of fibrous unburnt particles – coarse fibrous particles (CFU) and fine fibrous particles (FFU) – were observed in the raw bagasse ash, as shown in Figures 4.3 and 4.4. These fibrous particles looked entirely different from fine burnt particles and could be visually differentiated because of their dissimilar structures and size. Coarse and fine unburnt fibrous particles are compared side-by-side in Figure 4.5, while the appearance of the sieved SCBA is shown in Figure 4.6.



Figure 4.1: Appearance of raw sugarcane bagasse ash (SCBA)



Figure 4.2: Separation of different particles from raw SCBA by sieving



Figure 4.3: Coarse fibrous unburnt particles (CFU) present in the bagasse ash sample



Figure 4.4: Fine fibrous unburnt particles (FFU) in the bagasse ash sample



Figure 4.5: Comparison of coarse and fine fibrous particles



Figure 4.6: Appearance of sieved fine burnt particles (Sieved SCBA)

4.3 METHODS FOR EVALUATION OF POZZOLANIC ACTIVITY

Pozzolanic activity of raw bagasse ash was determined by five different methods (strength activity index test, lime reactivity test, Frattini test, electrical conductivity test, and lime saturation test). While all five tests were conducted on the raw and sieved SCBA samples, the ASTM strength activity test and Frattini test were conducted additionally on the fibrous particles (CFU and FFU). The methods are described in detail in the subsequent sections.

4.3.1 Strength activity index test

Pozzolanic performance of bagasse ash was evaluated by strength activity test as per ASTM C311-11b. 500 g of ordinary Portland cement (conforming to 53 grade as per IS 12269), 1375 g of Indian standard graded sand (as per IS 383), and 242 ml water were used to cast six numbers of 50 mm control mortar cubes without replacement. Specimen molds preparation, molding of test specimens and tamping were done as per ASTM C109/C109M-12. The flow value of control mortar was measured as per ASTM C1437-07. 20 % mass replacement of cement with bagasse ash as supplementary cementitious material was used as per guidelines. The water content for the bagasse ash replaced mortar was found by trial and error method to get same flow value as the control with $\pm 5\%$ tolerance. In a similar method, specimens were cast with sieved sample, coarse fibrous particles and fine fibrous particles. The casting sequence followed is depicted in Figures 4.7 and 4.8. Specimens were demoulded after 24 hours and cured in saturated lime water at 25 °C (see Figure 4.9). Compressive strength of specimens was determined after 7 days and 28 days of curing. Strength activity index is calculated as the % ratio of strength of bagasse ash replaced mix to the control mix. For fly ash and natural pozzolanic materials, 75% pozzolanic activity index is recommended as minimum requirement to define as supplementary cementitious material as per ASTM C618-12a.



Prepared molds



Addition of graded sand



Mixing



Flow table test



Flow of control mortar



Control specimens

Figure 4.7: Casting sequence of control specimens



Figure 4.8: Casting of SCBA replaced specimens



Figure 4.9: Lime water curing and testing of specimen

4.3.2 Lime reactivity test

Standard 50 mm mortar cubes were prepared and tested as specified in IS 1727 – 2004. Mortar cubes were prepared with hydrated lime: cementitious material: standard sand in

the ratio 1:2M: 9 by weight, where M is the ratio of specific gravity of the supplementary cementitious material to that of hydrated lime. Standard hydrated lime from National Council of Cement and Building Materials (NCCBM) was used in this study as specified in the standard. The amount of water was determined as that required to achieve a flow of $70\pm 5\%$ with the flow table dropped for 10 times in 6 seconds. After casting, the specimens were covered with greased glass plates and kept under wet gunny bags for 48 hours. After demoulding, specimens were cured at $50\text{ }^{\circ}\text{C}$ for eight days, after which the compressive strength was determined. During the compression test, the load was applied at the rate of $35\text{ kg/cm}^2/\text{min}$ as per guidelines. Lime reactivity is represented as the strength of lime and pozzolana mixture.

4.3.3 Frattini test

Frattini test method is based on BS EN 196(5)-2005 standard for pozzolanicity. 2 g of each test sample (raw bagasse ash, FFU, CFU, sieved bagasse ash) was blended with 18 g of ordinary Portland cement. 100 ml of boiled water was pipetted into sealed air-tight polyethylene container and allowed to reach room temperature. 20 g blended sample was poured into container by using stem funnel and kept in an oven at $40\text{ }^{\circ}\text{C}$ for 8 days. After 8 days, samples were taken from controlled temperature and immediately vacuum filtered through $2.7\text{ }\mu\text{m}$ nominal pore size filter paper using sealed Buchner funnel. Duration of vacuum filtration should be less than 30 seconds to avoid carbon-dioxide absorption from the atmosphere. After filtration, the filtrate was cooled down to room temperature. The process of filtrate preparation is shown in Figure 4.10.

50 ml filtrate was then pipetted into a 250 ml beaker and five drops of methyl orange were added as indicator to the sample for $[\text{OH}]^-$ determination. This filtrate was titrated against 0.1 mol/l HCl to determine $[\text{OH}]^-$ concentration. The end point of the titration was indicated by a change of colour from yellow to orange. To determine $[\text{Ca}]^{2+}$ concentration, pH of titrated sample was adjusted to 12.5 ± 0.2 by adding sodium hydroxide solution. The sample was titrated against 0.03 mol/l EDTA solution. Patton and Reeders indicator was used in this titration. The end point was indicated by a change in colour from purple to clear blue, as seen in Figure 4.11.

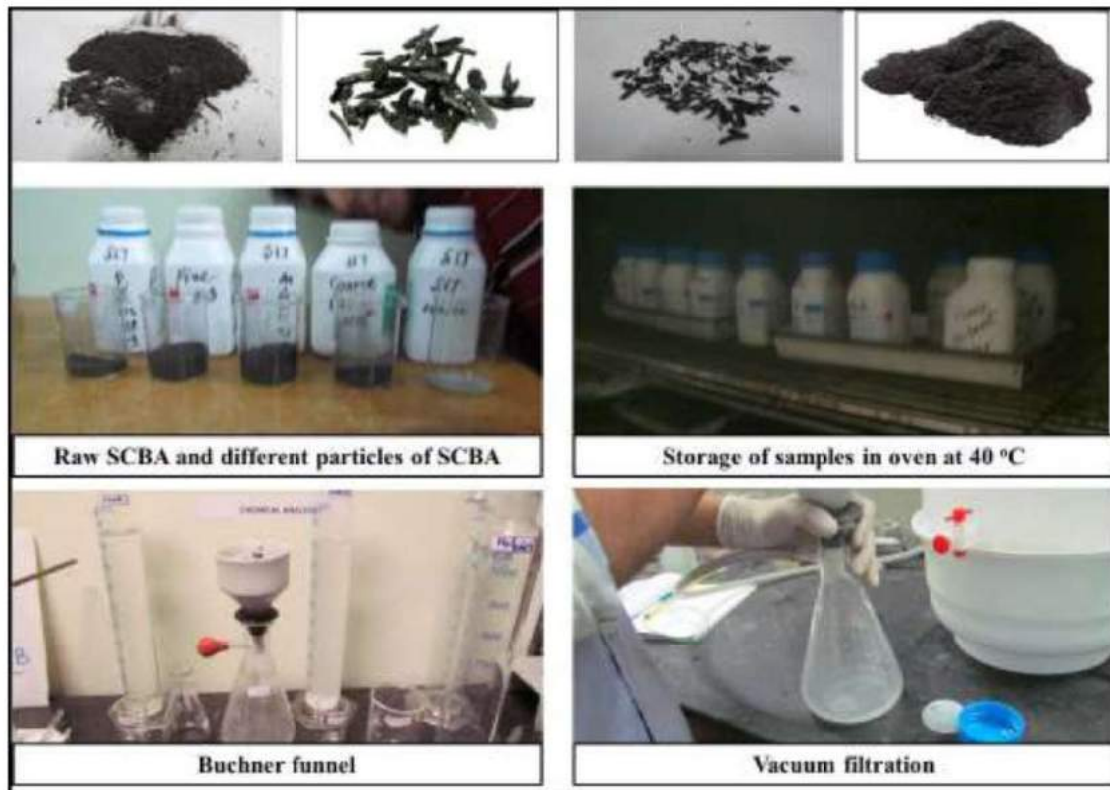


Figure 4.10: Preparation of filtrate from different samples

The results were plotted on a solubility curve, which is a representation of $\text{Ca}(\text{OH})_2$ in ordinary Portland cement and shows $[\text{OH}]^-$ concentration on X-axis in mmol/l and $[\text{Ca}]^{2+}$ concentration, expressed as equivalent CaO, in mmol/l on the Y axis. Concentration of hydroxyl ions and Calcium ions from the test were plotted on the standard solubility curve of calcium hydroxide (illustrated in BS EN 196(5)-2005). Calcium hydroxide is consumed in the pozzolanic reaction and leads to the reduction of $[\text{OH}]^-$ concentration and $[\text{Ca}]^{2+}$ concentration (as equivalent CaO). For reactive supplementary cementitious material, results are below the saturation curve. If results are on the saturation curve or above the curve, tested sample is deemed to represent no (or insufficient) pozzolanic activity.

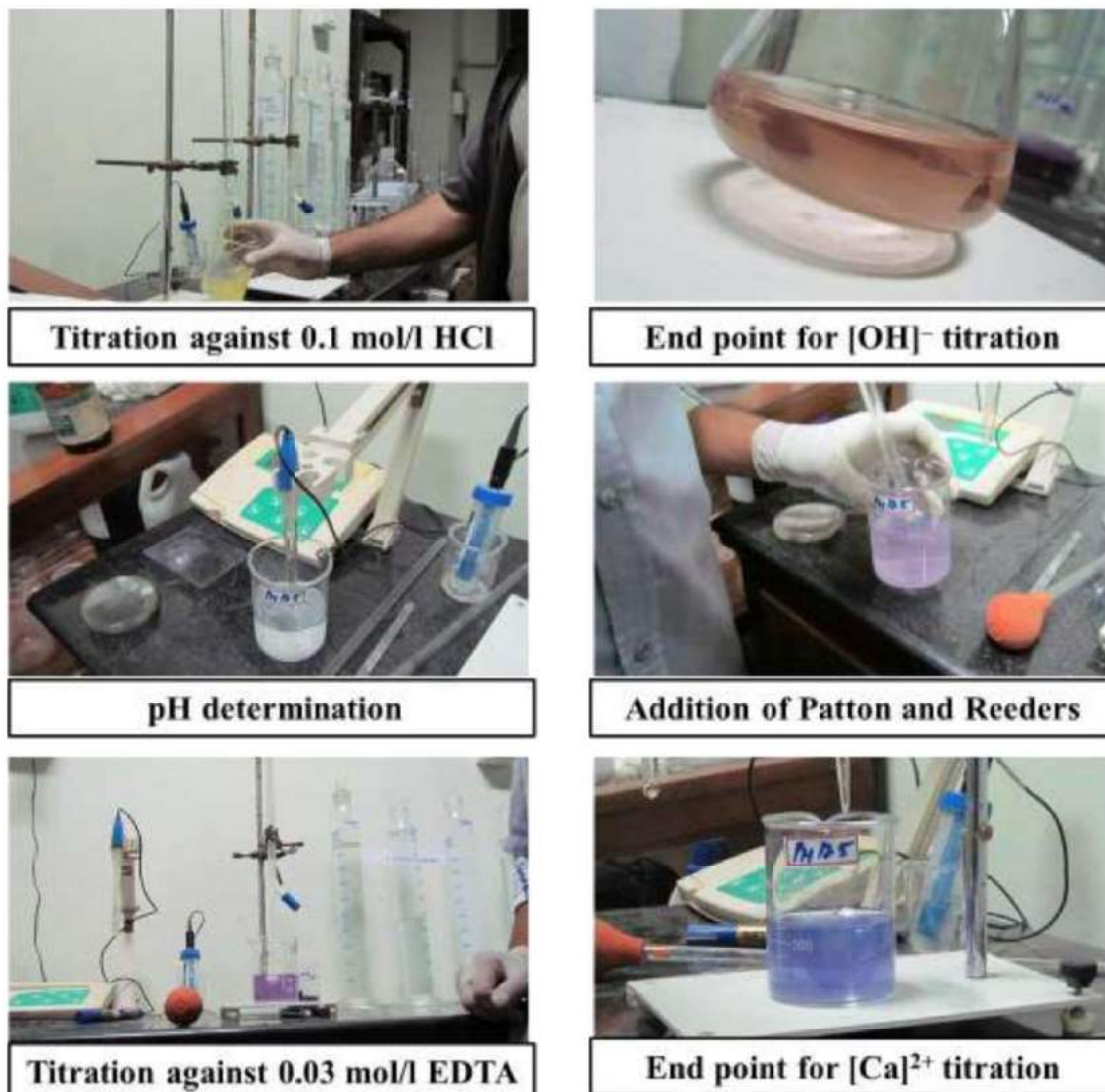


Figure 4.11: Determination of $[\text{OH}]^-$ and $[\text{Ca}]^{2+}$ concentration

4.3.4 Electrical conductivity method

The electrical conductivity method employs the rate of change of conductivity as a parameter to quantify pozzolanicity. In this method, raw bagasse ash was mixed with powdered $\text{Ca}(\text{OH})_2$ in the ratio of 8:2. Water/solid ratio was kept 1.2 as suggested by McCarter and Tran (1998). The mixture was cast in perspex cells of internal dimension 100 x 100 x 100 mm. This sample size is considered as sufficient to get representative bulk electrical measurements. Two opposite walls of the cell had 100 x 100 mm stainless steel electrodes as shown in Figure 4.12 to measure conductivity.

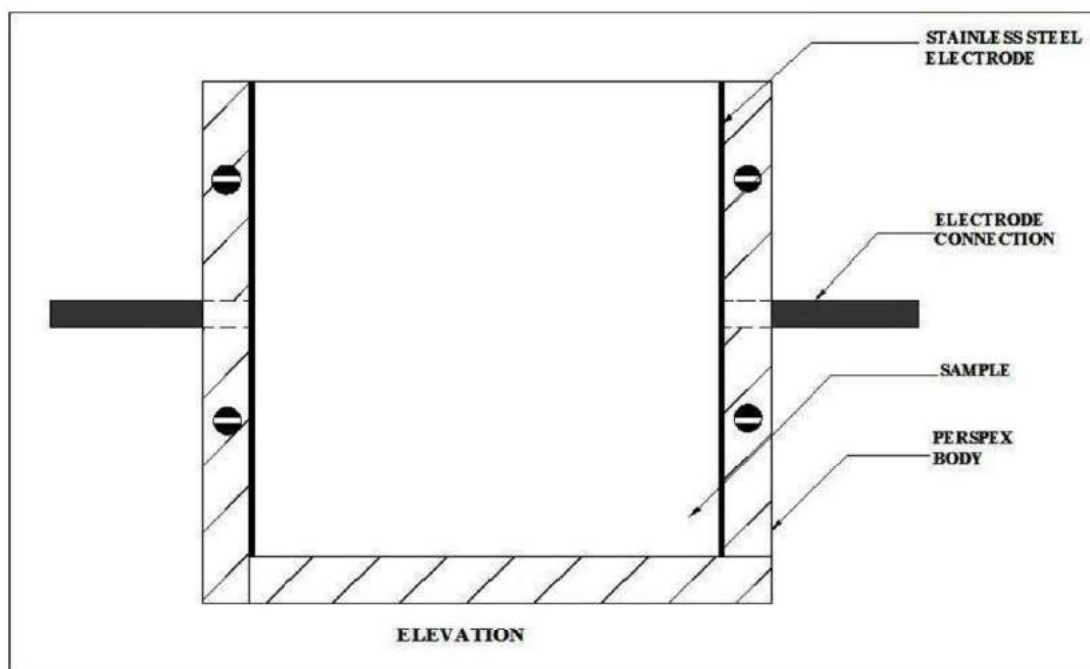


Figure 4.12: Schematic diagram of perspex cell for electrical conductivity measurement

The electric conductance was measured using LCR meter operated at 10 kHz. Data was recorded at 10 min interval over a period extending for 24 to 48 hours, as shown in Figure 4.13. The experiment was performed at controlled temperature of 25 °C, in order to avoid any errors due to temperature variation.



Figure 4.13: Preparation of hydrated lime-pozzolan mixture and electrical conductivity measurement

4.3.5 Lime saturation method

In this method, a controlled quantity of lime is added at the beginning of the test and the residual lime in solution is measured at the end to quantify pozzolanic activity of the cementitious material (Donatello et al., 2010). In Frattini test, the supplementary cementitious material reacts with calcium hydroxide which is formed from the hydration of ordinary Portland cement. In this method, a small amount of pozzolanic material is added in the saturated lime solution to facilitate a direct reaction between pozzolanic materials and calcium hydroxide. Samples were prepared with 1 g of bagasse ash added to 75 ml of saturated lime solution. The lime solution was prepared by dissolving 2 g of lime in 1 litre of distilled water. The containers were sealed and placed in an oven at 40 °C for 3 and 7 days. After this period, the sample was filtered, and the filtrate was titrated to determine $[\text{OH}]^-$ and $[\text{Ca}]^{2+}$ concentration using the same procedure as described in the Frattini test (BS EN 196(5)-2005).

4.4 RESULTS AND DISCUSSION

4.4.1 Strength activity Index

The compressive strengths observed in strength activity index test for raw bagasse ash, CFU, FFU and sieved bagasse ash samples at 7 days and 28 days are shown in Figures 4.14 and Figure 4.15 respectively. From the test result, it is observed that the mix with raw bagasse ash had strength activity index (SAI) of 69% and 72% at 7 days and 28 days respectively. Although the compressive strength increased from 7 to 28 days because of the additional pozzolanic reaction, the associated pozzolanic activity index value was below the minimum requirement of 75 % required to be classified as pozzolanic material as per guidelines (ASTM C618-12a).

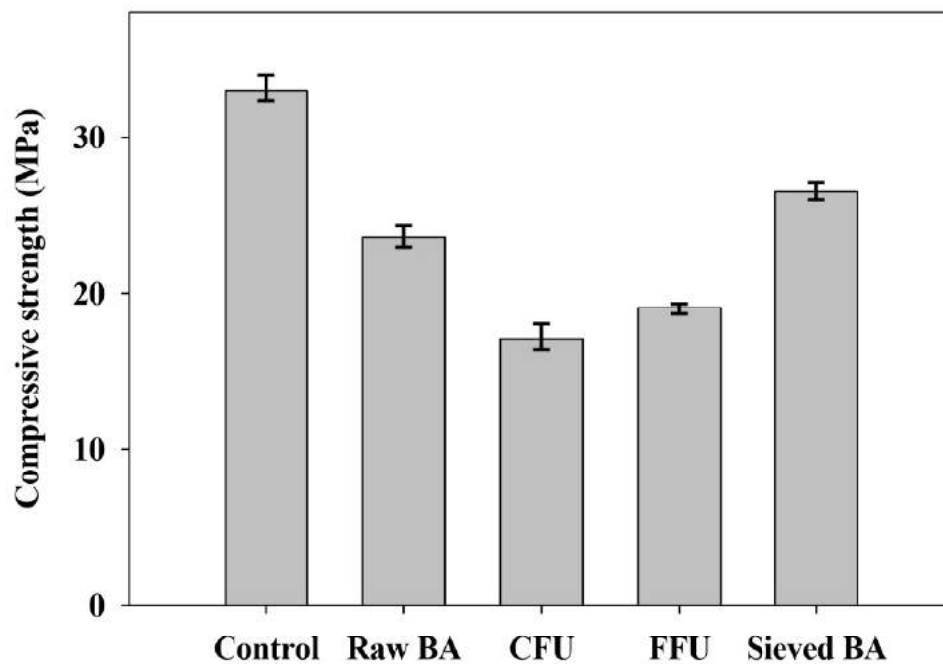


Figure 4.14: Compressive strength of mortar cubes at 7 days in strength activity index test

This may have been due to presence of the unburnt fibrous particles. Pozzolanic activity index of sieved sample was 79% at 28 days, which is higher than the raw bagasse sample and well above the minimum requirement mentioned in the standard. Pozzolanic activity

of coarse fibrous unburnt particles and fine fibrous particles was 45 % and 51 % respectively.

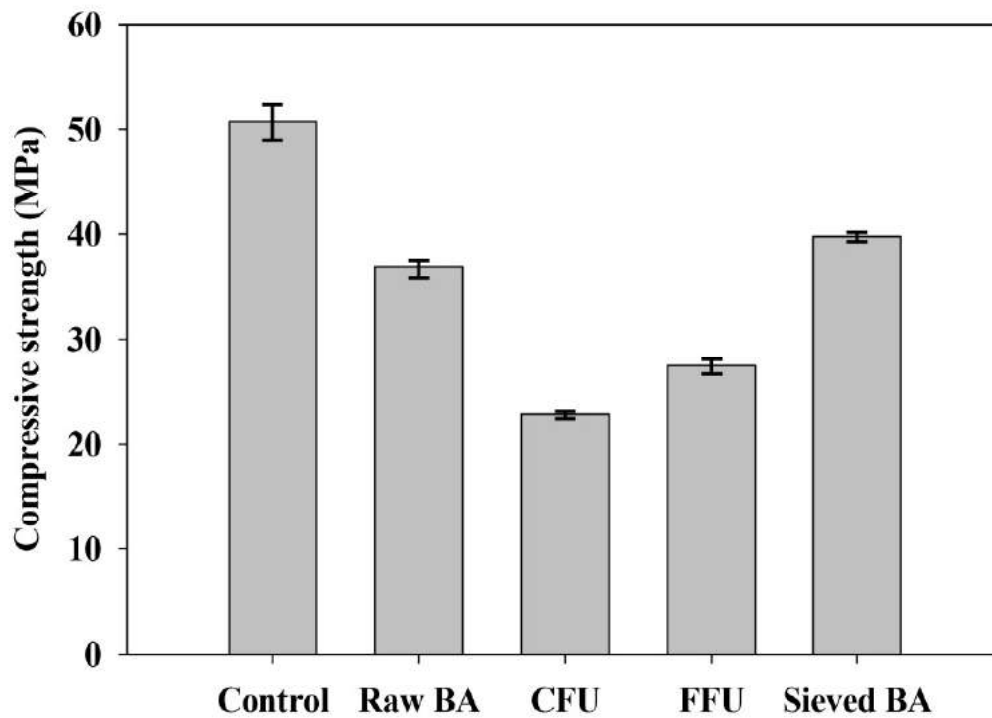


Figure 4.15: Compressive strength of mortar cubes at 28 days in the strength activity index test

In the strength activity test, based on ASTM C 109-11b guidelines, 242 ml water was added to control mortar and flow value was measured as per ASTM C1437-07. Water requirement of raw bagasse sample was increased to 320 ml to achieve the same control flow value. But water requirement of sieved sample was 260 ml, which is lesser than water requirement of raw bagasse ash sample and higher than control sample. From this observation, it is clear that presence of fibrous particles in raw bagasse ash increases the water demand. Removal of these particles not only improves the pozzolanic activity, but also enhances the workability at a given water content.

4.4.2 Lime reactivity test

Lime reactivity of the material is represented as strength of lime and pozzolan mortar mixture. Strength of the mixture is attained purely from pozzolanic activity between

hydrated lime and mineral admixture. In contrast, in the case of strength activity index test discussed in the previous section, a major part of strength is from cement hydration and only a small part is associated with pozzolanic activity. After eight days curing in controlled temperature and humidity, compressive strengths of mortar specimens for the mixes with raw and sieved bagasse ash were found to be 0.86 and 2.21 MPa respectively. Lime reactivity of raw bagasse ash was lesser than the sieved bagasse ash sample, because of higher reactivity of sieved bagasse ash sample. Water requirement to achieve flow of $70\pm 5\%$ as per the standard (IS 1727-2004) for raw bagasse ash mix was 330 ml. For sieved bagasse ash sample, water demand to achieve the same flow was 260 ml due to removal of coarse fibrous fraction in the sieved bagasse ash sample. Observations from lime reactivity test agreed with strength activity test results.

4.4.3 Electrical conductivity test

According to McCarter and Tran (1996), conductivity curve for powdered activation method can be categorized into four different regions namely initial activity stage, dormant period, sudden conductivity drop region and final set region. For the current study, in the initial stage, a small drop in conductivity was observed due to initial chemical activity of the bagasse ash with lime. McCarter and Tran (1996) had suggested that a greater drop in conductivity during initial stage represents better reactivity of cementitious material. For raw bagasse ash, as shown in Figure 4.16, drop in conductivity in the initial stage was observed up to 5 hours. There was a negligible change in conductivity from 5 to 30 hours due to the low reactivity of raw bagasse ash. This period can be denoted as dormant period. For sieved bagasse mix, a gradual drop in conductivity was observed from initial stage up to 20 hours and the second slow reactivity region (akin to dormant period) was not observed as shown in Figure 4.18. This is associated with higher pozzolanic activity of the sieved bagasse sample. Pozzolanic activity was calculated as the ratio of maximum rate of change of conductivity to the time at which this maximum was attained, as suggested by McCarter and Tran.

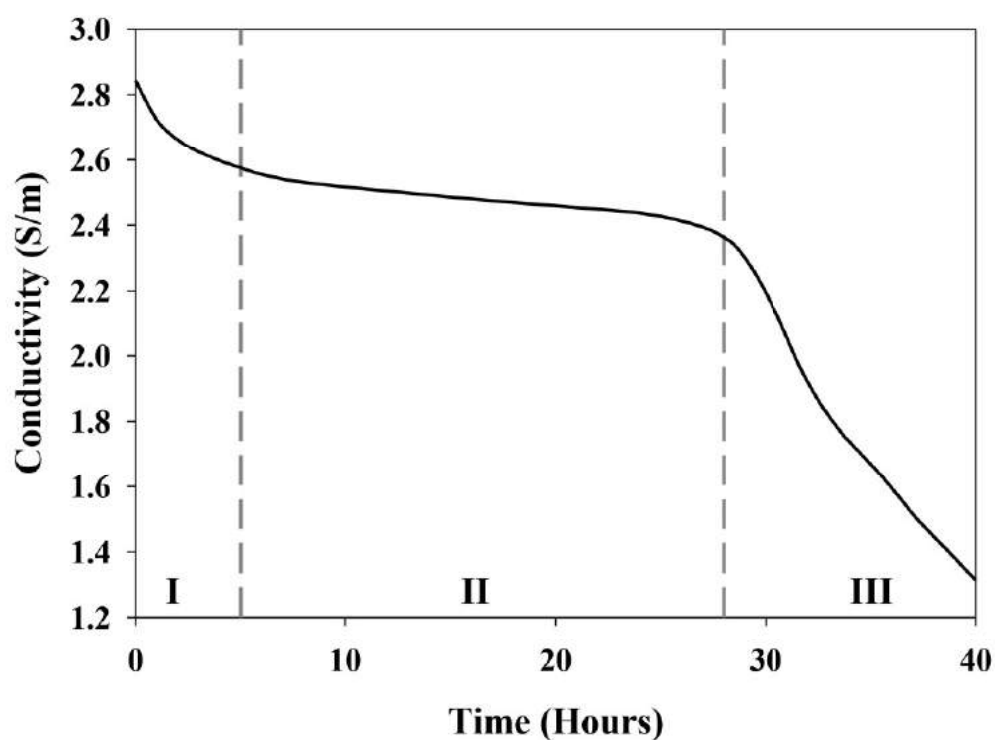


Figure 4.16: Conductivity curve for raw bagasse ash

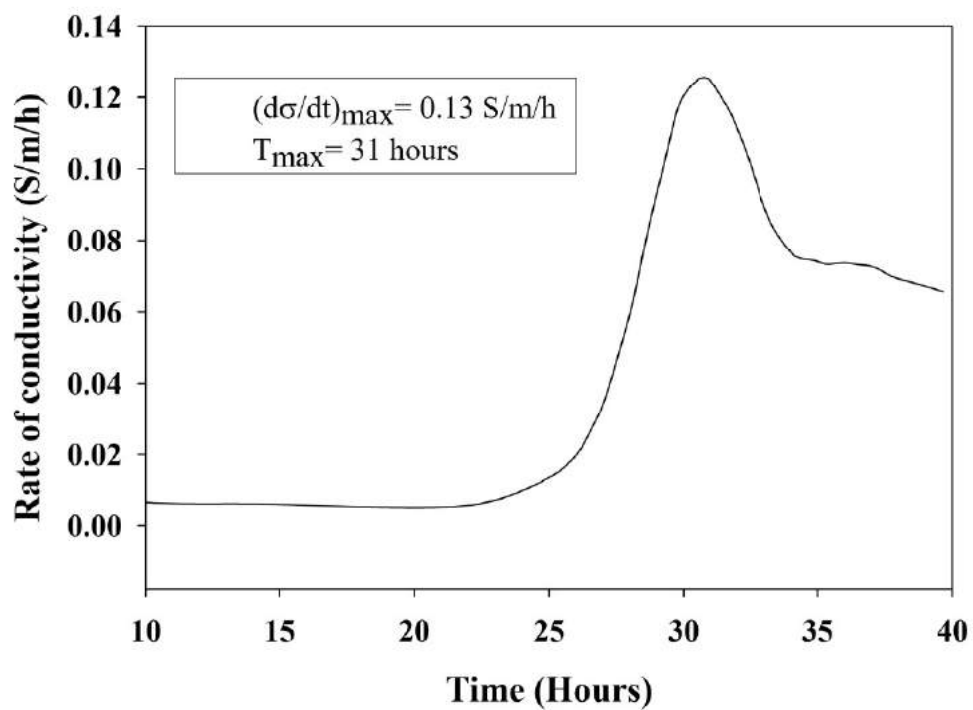


Figure 4.17: Derivative curve for raw bagasse ash

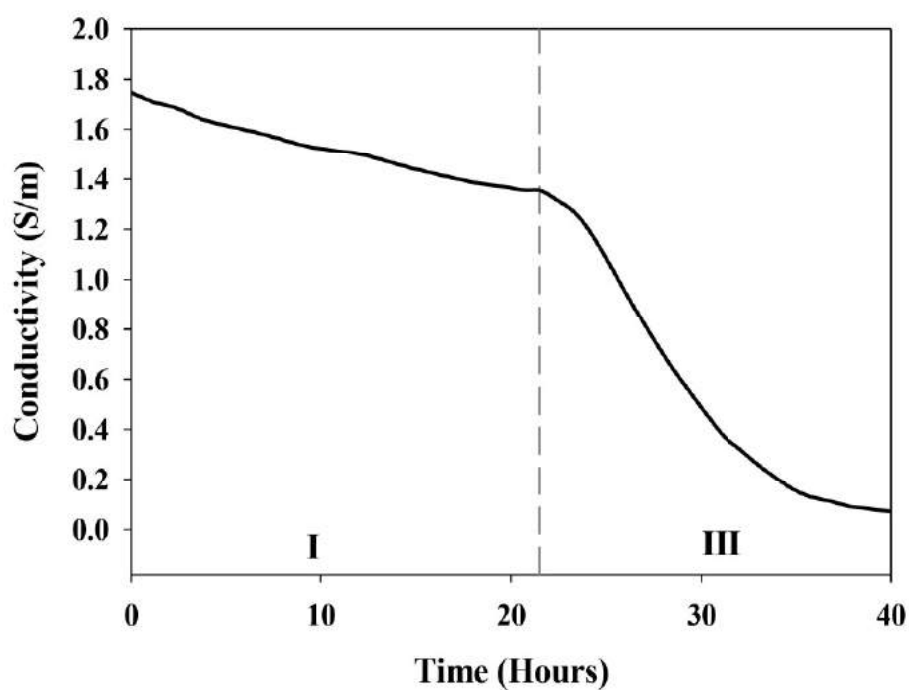


Figure 4.18: Conductivity curve for sieved bagasse ash

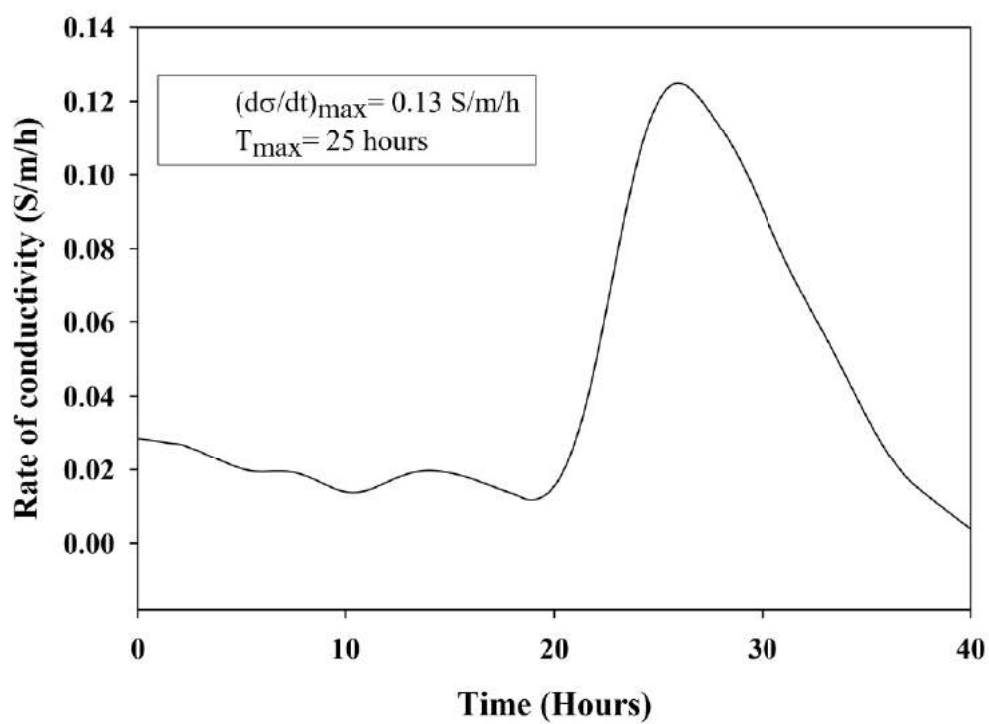


Figure 4.19: Derivative curve for sieved bagasse ash

According to this method, faster attainment of maximum rate of change of conductivity indicates higher pozzolanic activity. The time of attainment of maximum rate of change of conductivity for raw bagasse ash and sieved sample was estimated as 31 hours and 25 hours respectively, as shown in the third region in Figures 4.17 and 4.19. Pozzolanic activity of raw and sieved bagasse ash samples was determined as 45 and 52 % respectively.

4.4.4 Frattini test

Based on the results of the Frattini test, concentrations of $[\text{OH}]^-$ and $[\text{CaO}]$ were plotted on the saturation curve as described in BS EN 196(5)-2005. For sieved bagasse ash, $[\text{CaO}]$ and $[\text{OH}]^-$ concentrations after 8 days were 21.70 and 29.12 mmol/l respectively. For the raw bagasse ash, the corresponding values were 44.07 mmol/l for $[\text{CaO}]$ and 52 mmol/l for $[\text{OH}]^-$. Results of sieved bagasse sample fall well below saturation curve in the Frattini graph, as shown in Figure 4.20. This is a clear evidence of greater consumption of calcium hydroxide in the pozzolanic reaction.

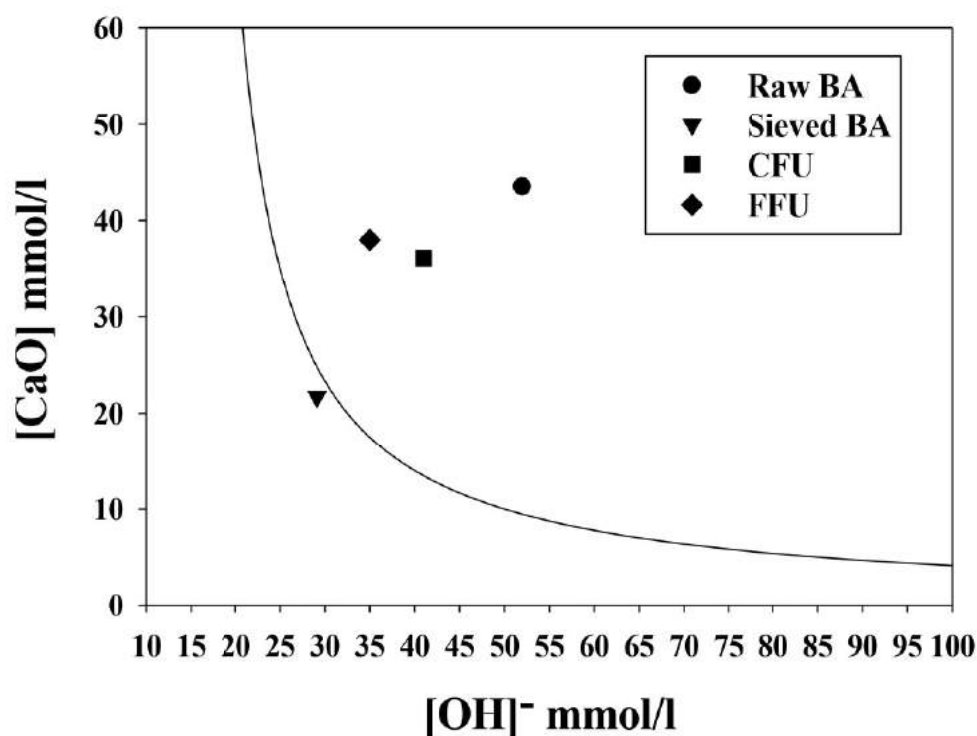


Figure 4.20: Frattini diagram for assessing pozzolancity

Raw bagasse ash sample results were above the curve in the region that represents no pozzolanic activity. Raw bagasse ash sample showed 72 % pozzolanic activity index in strength activity index test but no pozzolanic activity in Frattini test. This may be due to the presence of greater amounts of coarse fibrous carbon particles in the small quantity of raw bagasse ash sample used in the Frattini test. In other words, homogeneity of the sample cannot be guaranteed when only 2 g of the sample is taken for the test.

4.4.5 Lime saturation test

In lime saturation test, percentage of CaO removed was calculated for sieved bagasse ash and raw bagasse ash at 3 days and 7 days. The initial known concentration of CaO in the solution was decreased due to consumption of Ca(OH)_2 in the pozzolanic reaction. Higher percentage of CaO reduction (53% at 3 days and 76% at 7 days) was observed for sieved sample compared to raw bagasse sample at both ages, as shown in Figure 4.21. Higher CaO reduction is due to greater pozzolanic activity of sieved sample than raw bagasse ash. These observations directly agree with other test results.

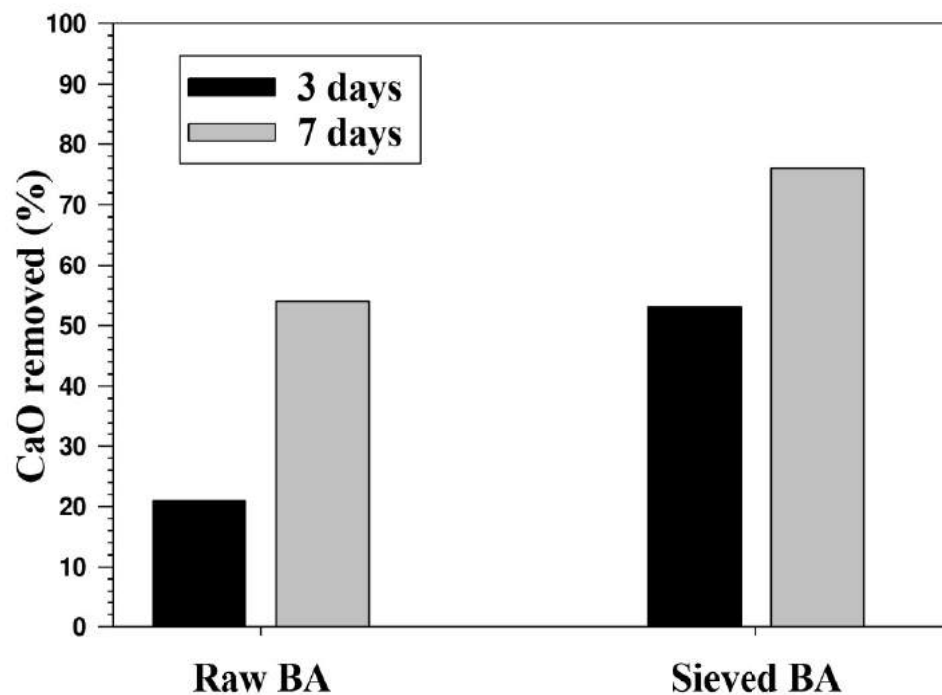


Figure 4.21: Lime saturation test

4.4.6 Discussion of test methods

Different standard tests were carried out for the evaluation of pozzolanic activity of bagasse ash. In the strength activity method, water contents in the control mix and pozzolana mix were not same. As per ASTM 311-11b guidelines, 242 ml water was added to control mix, whereas in the pozzolana mix, extra water was added to obtain 100 ± 5 % flow of the control mix. Supplementary cementitious materials with low specific gravity like natural pozzolans need more water to achieve control flow, because of the resultant increase in powder volume. Different water content in the control mix and pozzolana mix for the strength evaluation is a demerit of the method. However, as a compensation, ASTM 311-11b recommends only 75 % of strength of control as minimum requirement to define sufficient pozzolanicity.

The strength activity test showed higher pozzolanic activity for raw bagasse ash compared to the fibrous particles that were separated from this sample. But in the Frattini test, raw bagasse ash results were found to be in the non-pozzolanic region. This is possibly due to presence of disproportionate amounts of fibrous unburnt particles in the 2 g of raw bagasse ash sample that was taken for the test. This method presents a clear evidence for consumption of calcium hydroxide produced during cement hydration in the pozzolanic reaction. In the strength activity test, a major part of strength is contributed from the hydration of cement. In Frattini method, consumption of calcium hydroxide in the pozzolanic reaction is directly compared with solubility curve of Ca(OH)_2 produced during hydration of ordinary Portland cement to evaluate the pozzolanic reactivity of the material.

Lime saturation test results correlated well with those of Frattini test. The primary advantage of this method is that the ratio of calcium hydroxide to pozzolanic material is higher compared to Frattini test. Because of the larger calcium hydroxide content, the complete reactivity of pozzolanic material can be attained.

The results from the electrical conductivity method also agreed with other test methods. Controlled temperature and the use of deionized water for mixing are recommended (Whittington et al., 1981; McCarter and Tran, 1996), in order to avoid error in the conductivity measurement. From all test results, it is evident that removal of

fibrous particles in bagasse ash enhances its pozzolanic activity and reduces water demand.

4.5 MICROSTRUCTURAL CHARACTERIZATION OF BAGASSE ASH

As mentioned earlier, the sample of sugarcane bagasse ash was found to have completely burnt fine particles and fibrous unburnt particles. Two different types of fibrous unburnt particles were observed in the raw bagasse ash. Results from pozzolanic tests showed good pozzolanic activity for fine burnt particles, whereas little or no pozzolanic activity was observed for fibrous particles. To attain clear scientific insight on the pozzolanic performance of different particles, the structure of the bagasse ash particles was further examined by scanning electron microscopy (SEM) in the secondary electron mode. The micrographs of different particles provide a descriptive qualitative analysis of the phases observed in bagasse ash. Energy dispersive X-ray analysis was also used in conjunction with SEM to obtain the elemental composition of the observed phases.

4.5.1 Microstructure of raw bagasse ash

The micrograph of raw bagasse ash is shown in Figure 4.22. In the raw bagasse ash, particles were found to exhibit a variety of shapes. Four different types of particles (irregular, prismatic, spherical and fibrous) were clearly observed in the micrograph of raw bagasse ash as shown in Figure 4.23. Elemental composition (%) of the observed phases by EDS is presented in Table 4.1. Most of the observed particles in the micrograph of raw bagasse ash were irregular particles (denoted as D in Figures 4.23 and 4.25). Irregular structures of different fine burnt particles are shown in Figures 4.27-4.30. Higher amount of Si (50 %) was found to be present in the observed phases of all irregular particles by EDS analysis. Because of controlled burning at high temperature (500-550 °C) in the cogeneration boiler, fibrous particles were burnt partially and disintegrated parts of fibrous particles were found to be present in the micrograph. As a result, several partially burnt fibrous particles were observed along with irregular particles in the micrograph of raw bagasse ash (marked as B) as shown in Figure 4.24. Carbon was observed as major element in the elemental composition of fibrous particles

by EDS analysis. Individual fine fibrous particle (without breaking) was clearly identified in the micrograph of raw bagasse ash (denoted as E) due to its larger size when compared to irregular, spherical and prismatic particles (see Figure 4.25). Similarly, coarse fibrous particles were also observed in the micrograph. Microstructure of fine fibrous and coarse fibrous particles as well as their elemental compositions of all observed phases are elaborately presented in sections 4.5.2 and 4.5.3. In addition to this, spherical particles were infrequently found in the micrograph of raw bagasse ash (represented as A in Figures 4.23 and 4.24) and a high magnification view of the spherical particle is shown in Figure 4.26. Spherical particles are formed because of melting at high temperature. These spherical particles were found to contain oxides of Mg, P, K, and Si. Elemental compositions of spherical particles are entirely different from other particles (see Table 4.1). Similar spherical shape particles were reported in an earlier research study (Batra et al., 2008). Prismatic particles had well-defined structures (marked as C in Figure 4.23). Similar to irregular particles, prismatic particle also had higher amount of Si (47 %) in their elemental composition.

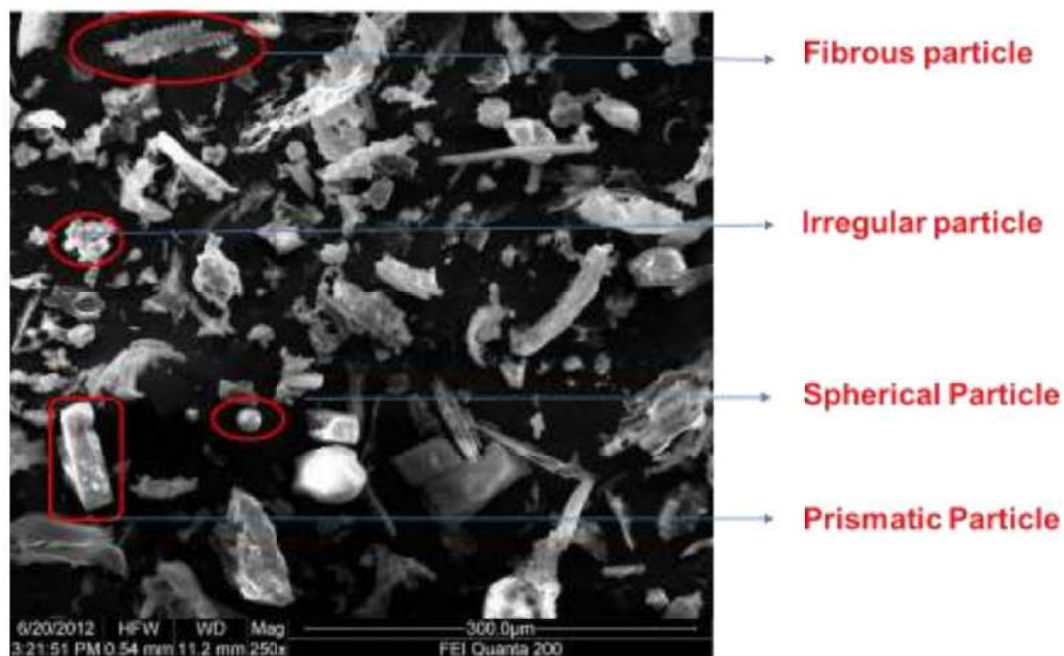


Figure 4.22: Microstructure of raw bagasse ash

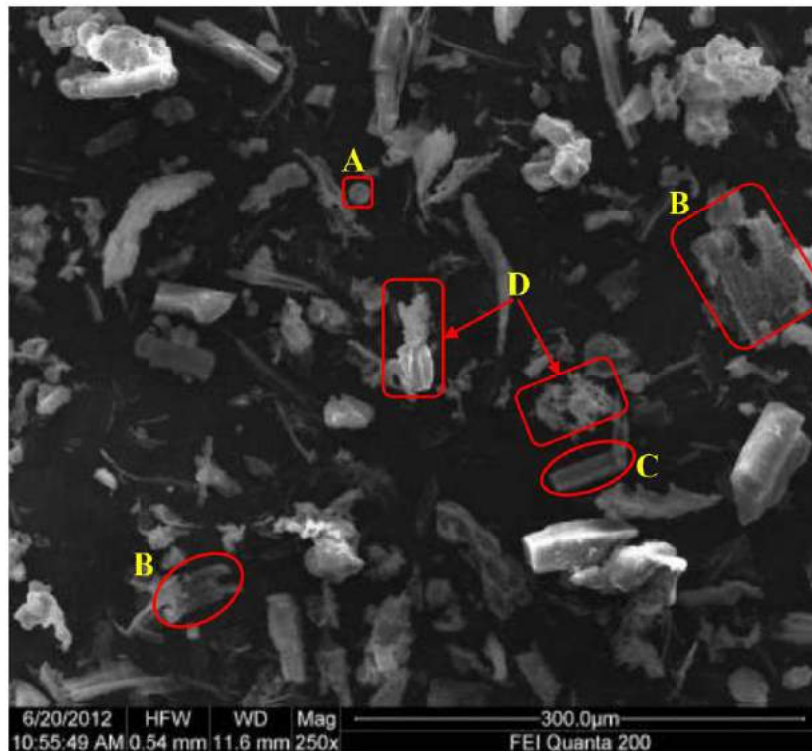


Figure 4.23: Presence of different particles in the micrograph of raw bagasse ash

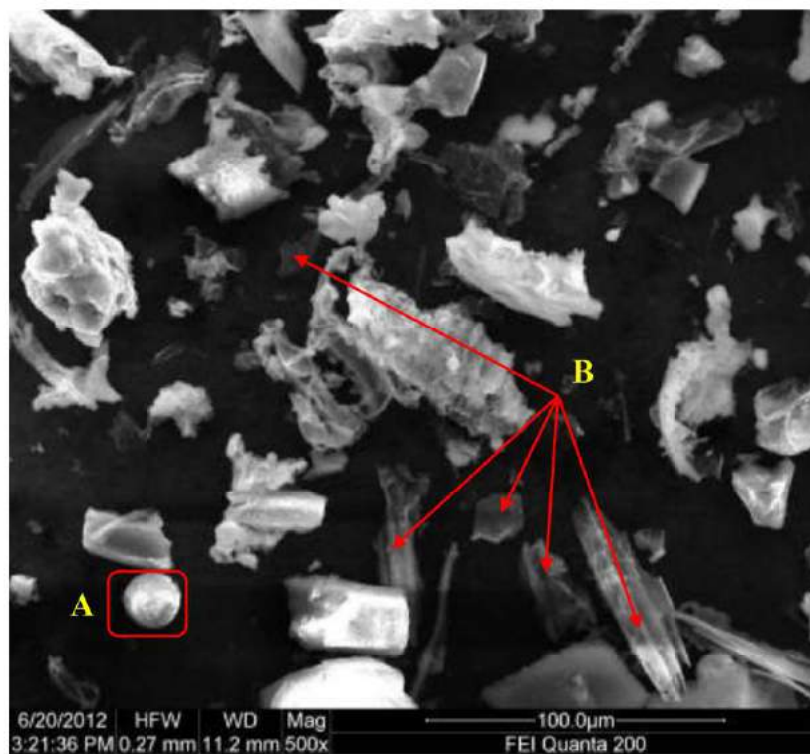


Figure 4.24: Presence of fibrous particles (B) and spherical particle (A) in the micrograph of raw bagasse ash

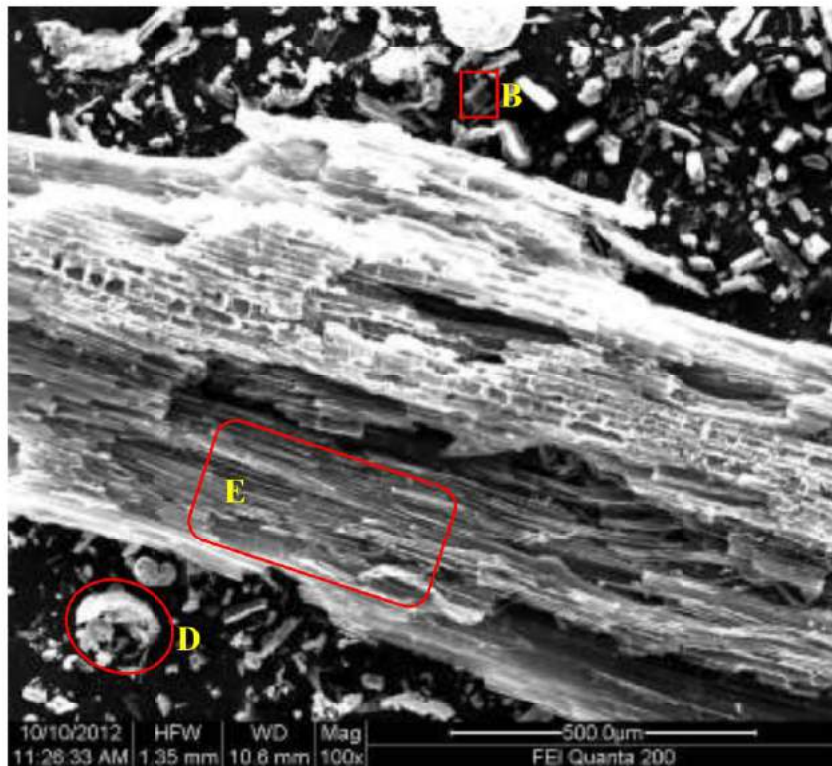


Figure 4.25: Presence of fine fibrous particle (E) in the micrograph of raw bagasse ash

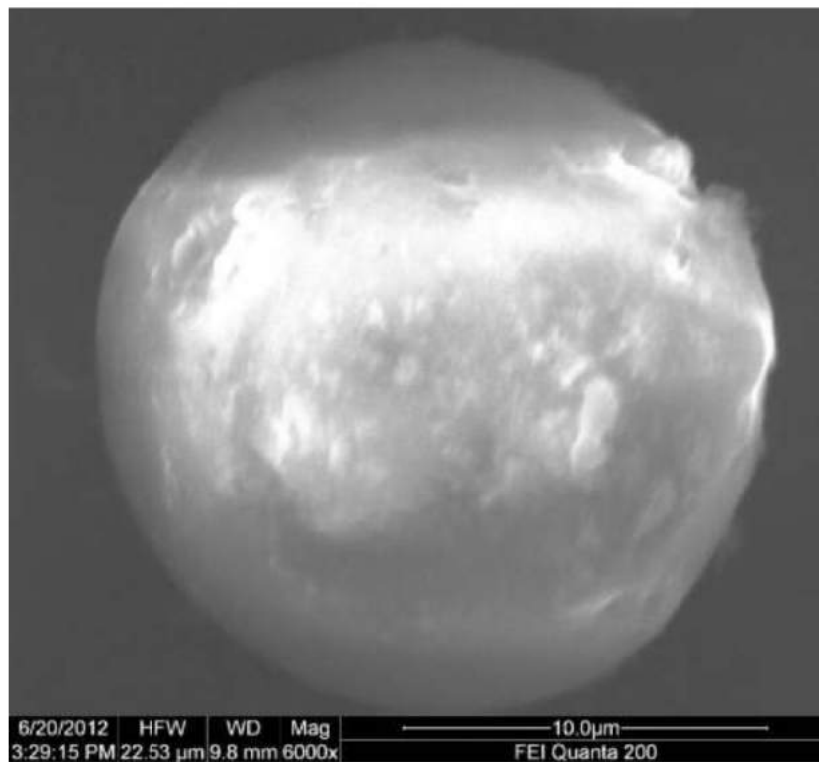


Figure 4.26: High magnification view of spherical particle



Figure 4.27: Microstructure of fine burnt particles

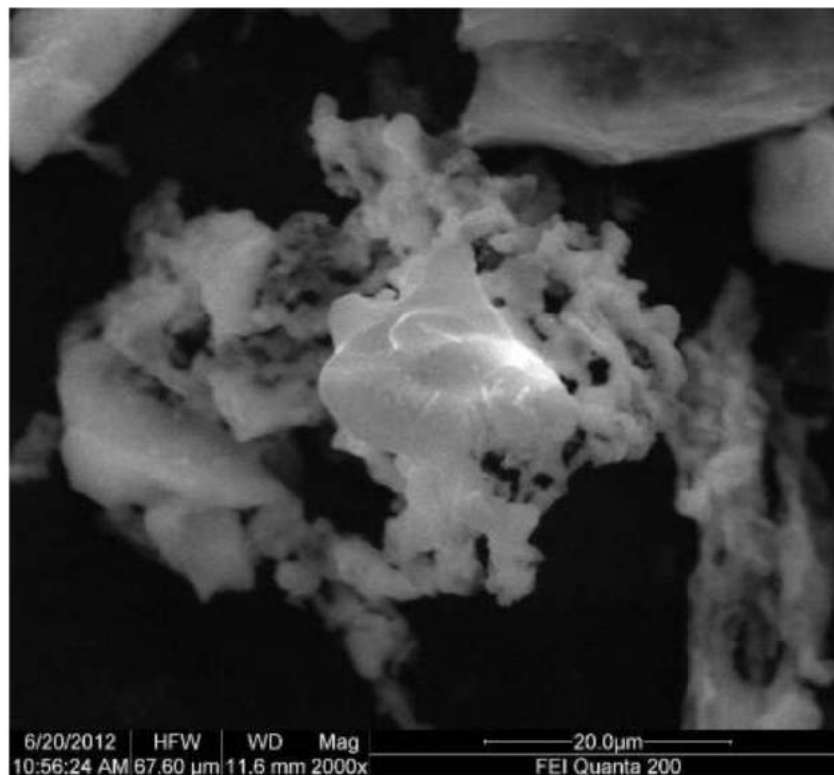


Figure 4.28: Irregular structure of fine burnt particles

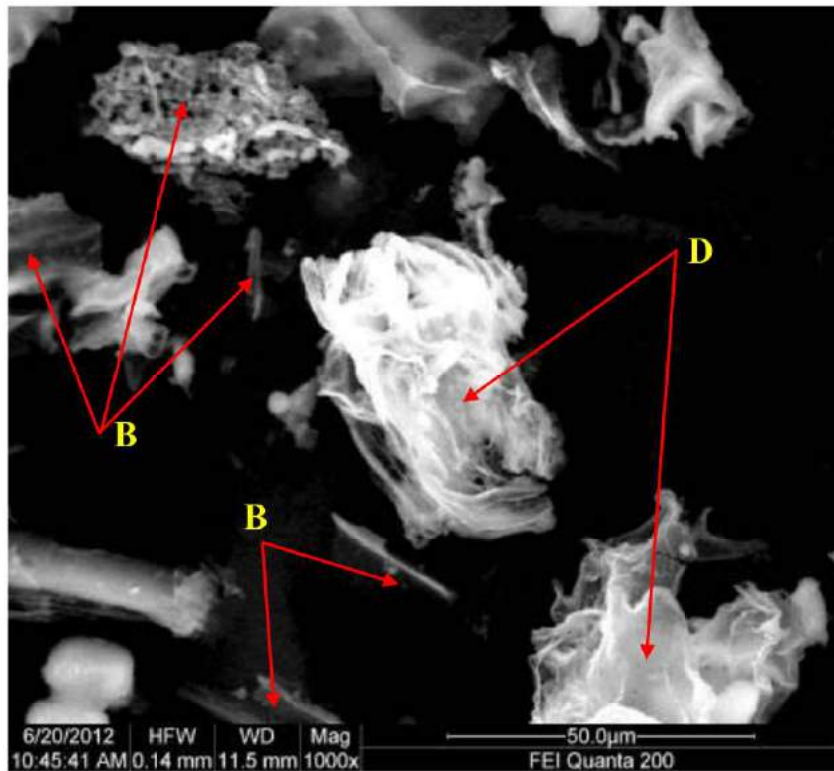


Figure 4.29: Microstructure of fine burnt particles along with fibrous particles

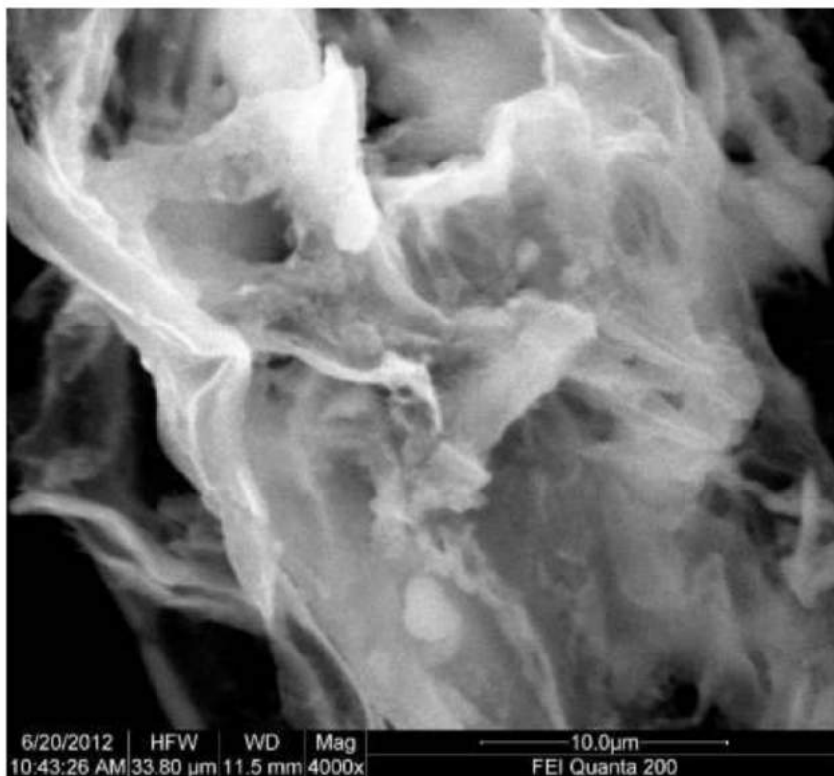


Figure 4.30: Microstructure of fine burnt particles at higher magnification

4.5.2 Microstructure of coarse fibrous particles

As pointed out earlier, fibrous particles were clearly observed in the microstructure of raw bagasse ash. It was interesting to note that these fibrous particles had two completely different types of microstructure. To elucidate microstructure of fibrous particles, these particles were separated from raw bagasse ash by sieving and examined by scanning electron microscopy in the secondary electron mode. Microstructure of coarse fibrous particles is described in this section. Coarse fibrous particles had unique microstructure as depicted in Figure 4.31 and a major part of coarse fibrous particles was cellular structure, which is marked as F in Figures 4.32 and 4.34. Presence of scattered epidermal layers was found on the faces of layered cellular structure in the micrograph of coarse fibrous particles as shown in Figure 4.33. Epidermal layers (represented as G) were found to be randomly distributed on the surface of coarse fibrous particles as depicted in Figure 4.32. Presence and orientation of epidermal layer on the cellular structure at higher magnifications are shown in Figures 4.34 and 4.36. Dumbbell-shaped particles were observed in the epidermal layer (see Figure 4.35) and had a distinct structure. The elemental compositions of layered cellular structure, epidermal layer and dumbbell shaped particles were determined to get a thorough understanding of these particles. Epidermal layer had Si (18 %), O (28 %), C (49 %) and minor elements (K, Mg, Na, Fe, Al). Higher amount of carbon (78.29 %) was detected in the elemental composition of all the observed phases of the layered cellular structure. Dumbbell particles had Si, O, and C as major elements which contributed more than 98 % of its elemental composition as illustrated in Table 4.1. Several pits in the cell wall were observed in the microstructure of fibrous particles as a result of burning in the cogeneration boiler, and these are denoted as I in Figure 4.37. The major part of elemental composition of cell wall pits was Carbon (87 %). From the microstructural observations, it is clearly observed that coarse fibrous particles are composed of higher amount of carbon and not silica. These particles are unburnt fibrous carbon particles and have no pozzolanic value. Higher carbon content is responsible for the observation of lesser pozzolanic index value in the strength activity index and no pozzolanic activity in the Frattini test.



Figure 4.31: Microstructure of coarse fibrous particles

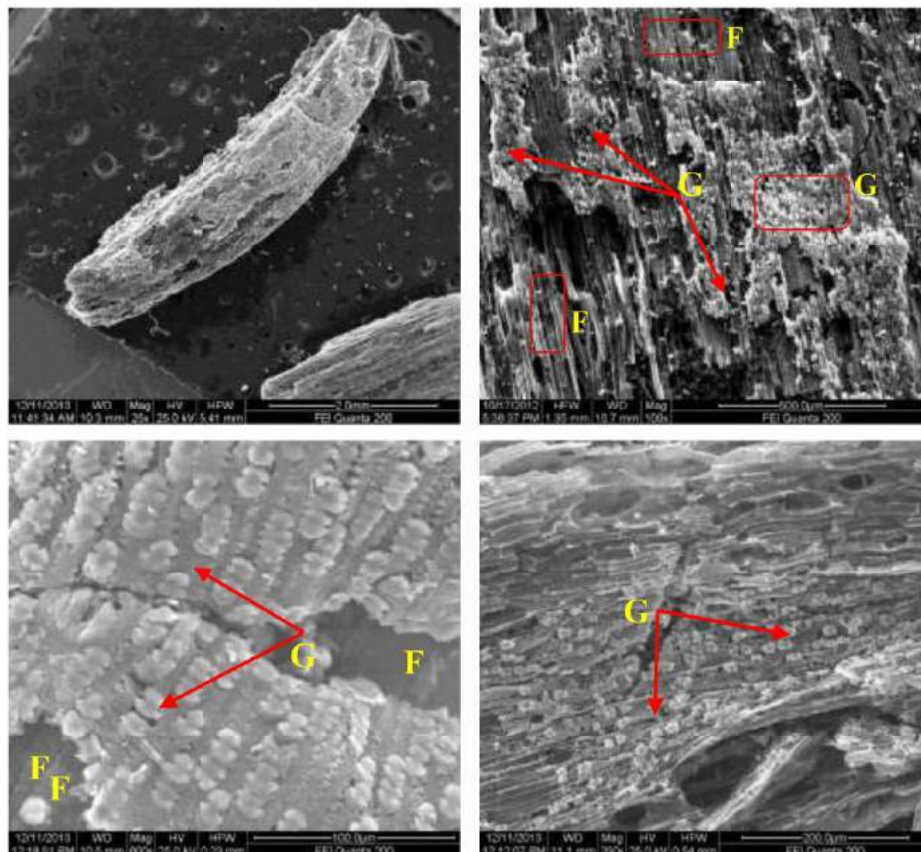


Figure 4.32: Presence of scattered epidermal layer in the coarse fibrous particles

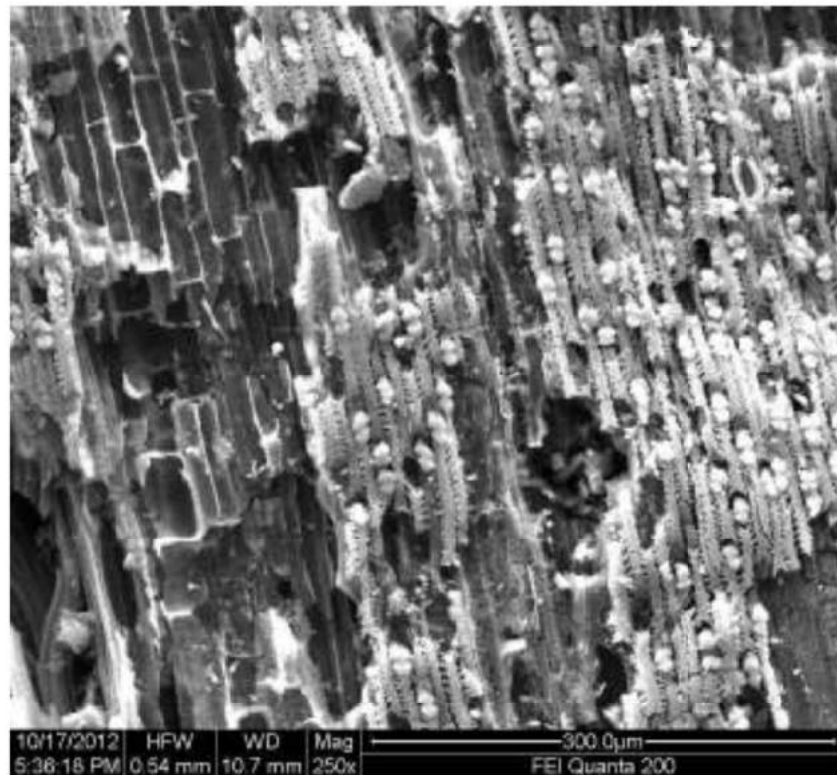


Figure 4.33: Microstructure of epidermal layer and carbon rich cellular structure

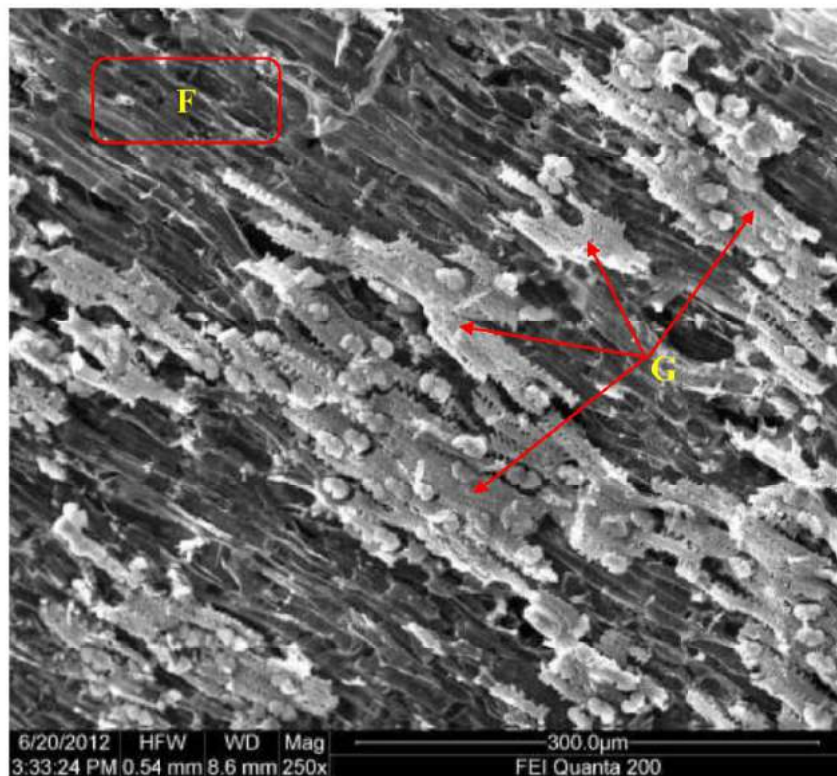


Figure 4.34: Orientation of epidermal layer at higher magnification

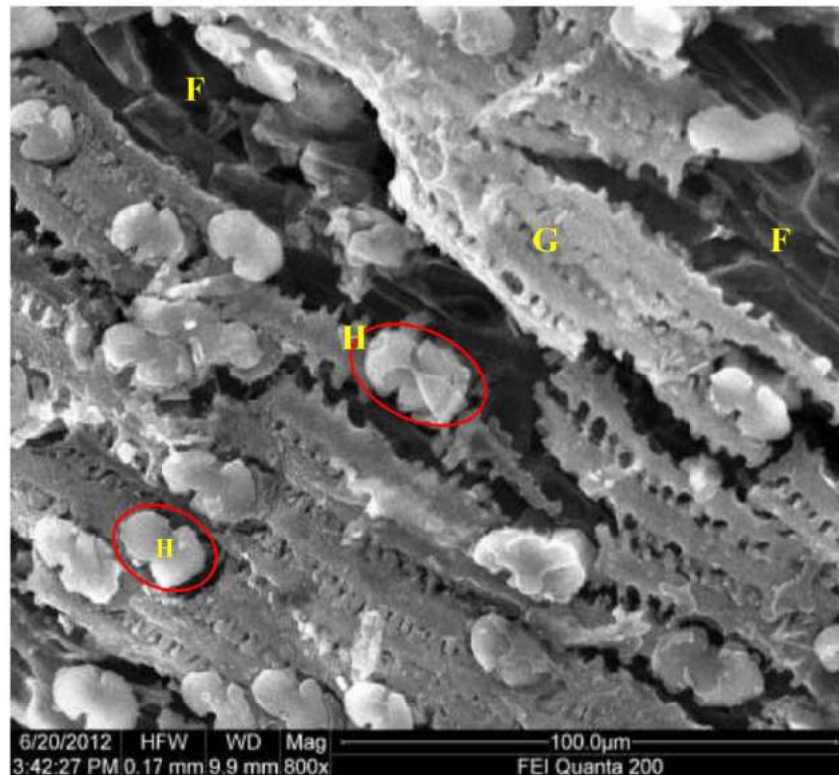


Figure 4.35: Presence of dumbbell-shaped particles in the epidermal layer

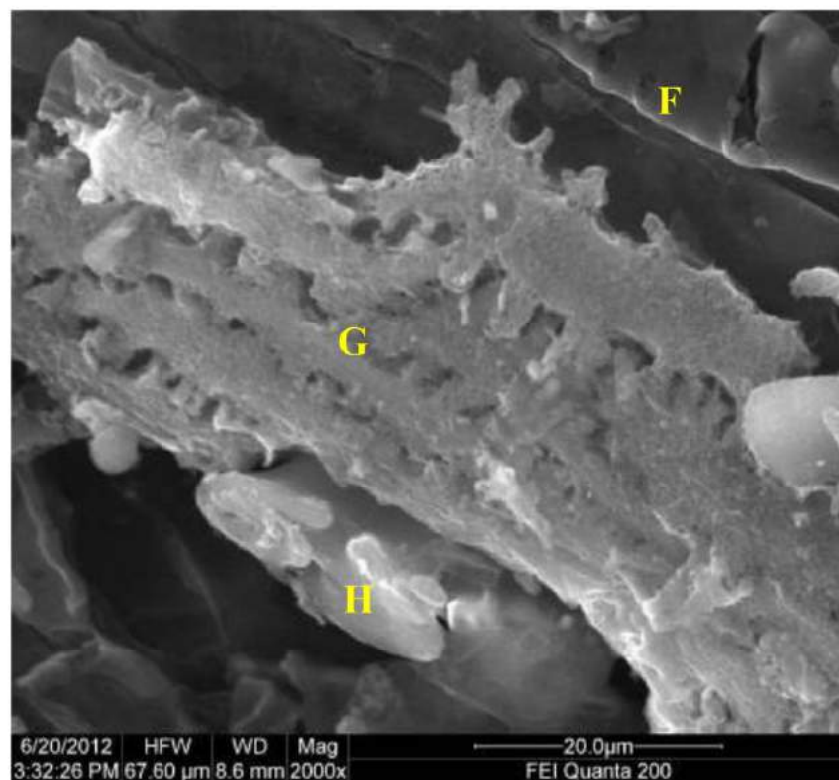


Figure 4.36: Microstructure of epidermal layer at high magnification

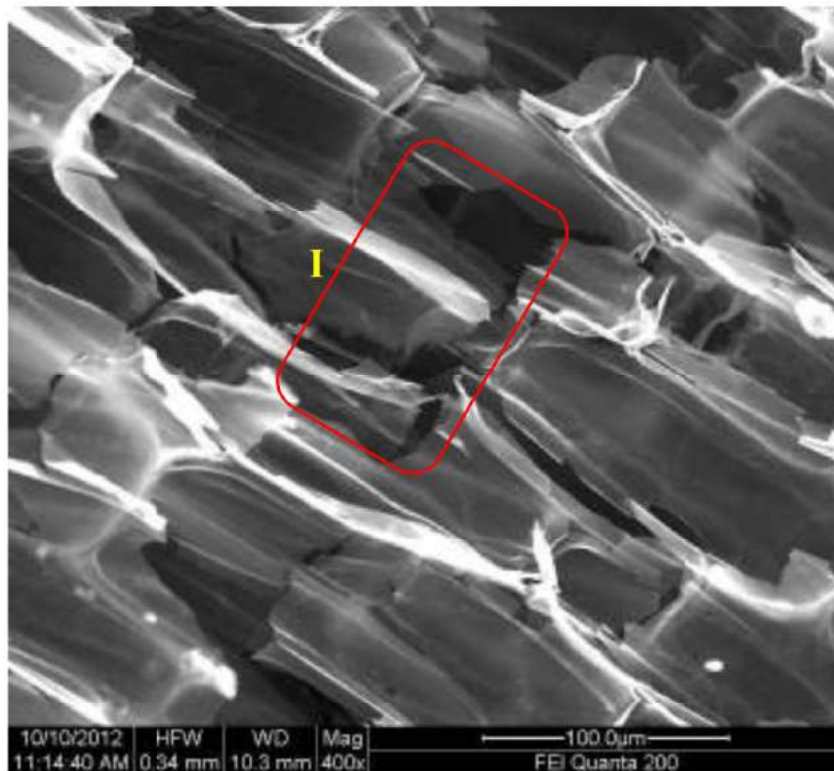


Figure 4.37: Presence of pits in the cell walls of coarse fibrous particles

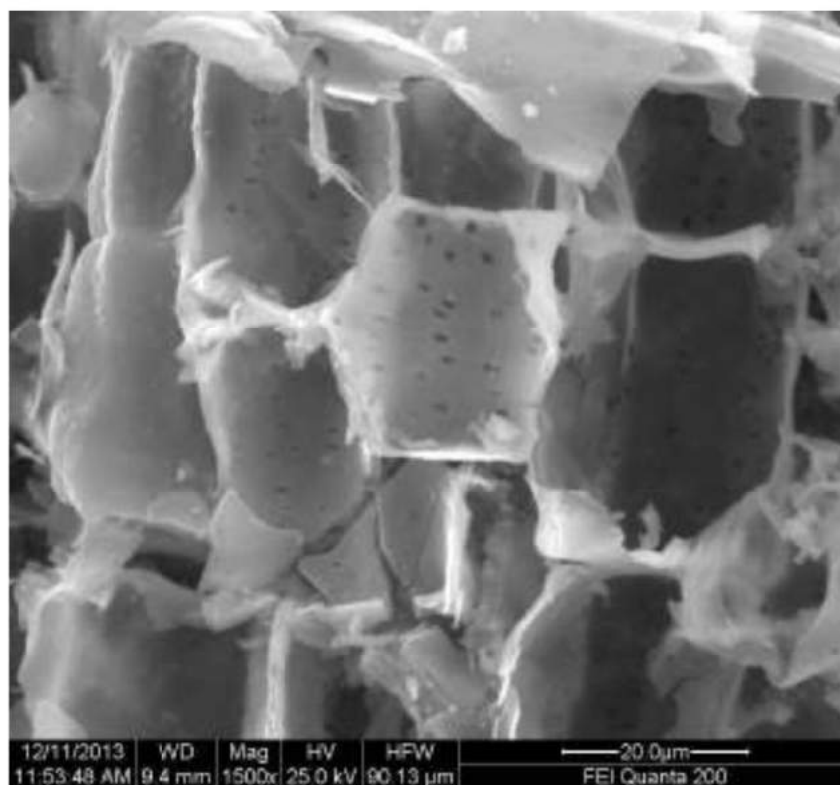


Figure 4.38: Cellular structure of carbon layer at high magnification

4.5.3 Microstructure of fine fibrous particles

In the same manner as coarse fibrous particles, fine fibrous particles were also separated from raw bagasse ash by sieving and their microstructure was investigated. Figures 4.39 – 4.45 show the microscopic features of the fine unburnt (FFU) fibrous particles. Fine fibrous unburnt particles had different cellular structure in the cell wall (see Figure 4.41) compared to coarse fibrous unburnt particles (CFU). The cell wall of these fibrous particles had ordered intercellular structure (denoted as E) as depicted in Figure 4.40. By reason of burning at high temperature in the cogeneration boiler, a number of pits were observed on the cell walls and a higher magnification view of these pits is presented in Figure 4.43. In the microstructure of fine unburnt fibrous particle, in between the intercellular structure, a carbon-rich well defined portion (J) was observed at higher magnifications as shown in Figure 4.42. Intercellular channels in the cell walls were clearly observed in the higher magnification images of fine unburnt fibrous particles as illustrated in Figures 4.44 and 4.45. The observed microstructure of FFU was entirely different from CFU and fine burnt particles. In the previous research studies, fibrous particles were generally categorized as unburnt particles. However, observations from the microstructural analysis directly indicates the different nature of coarse (CFU) and fine (FFU) fibrous particles. To acquire more scientific insight, the elemental compositions of the intercellular structure, the well-defined (Carbon rich) portion and intercellular channels were determined. Intercellular structures had more than 89 % carbon and minor amounts of other elements (Ca, K, Mg, Si). Greater amount of Carbon (83 %) was observed as major constituent along with small amount of Si (1 %) in all the observed phases of the well-defined portion (J). Carbon was detected to be more than 80 % in the elemental composition on the observed phases of all the intercellular channels of cell walls (see Table 4.1). The fine fibrous particles had higher Carbon content along with very less amount of silica (lesser than 2 %) and it was clearly confirmed from the elemental composition of different parts of fine fibrous particles. From microstructural analysis and EDS observations, it can be concluded that fine fibrous particles are carbon rich unburnt particles without reactive silica. As a result, these had no pozzolanic activity in Frattini test and lesser strength than minimum requirement in the strength activity test to define as pozzolanic material.

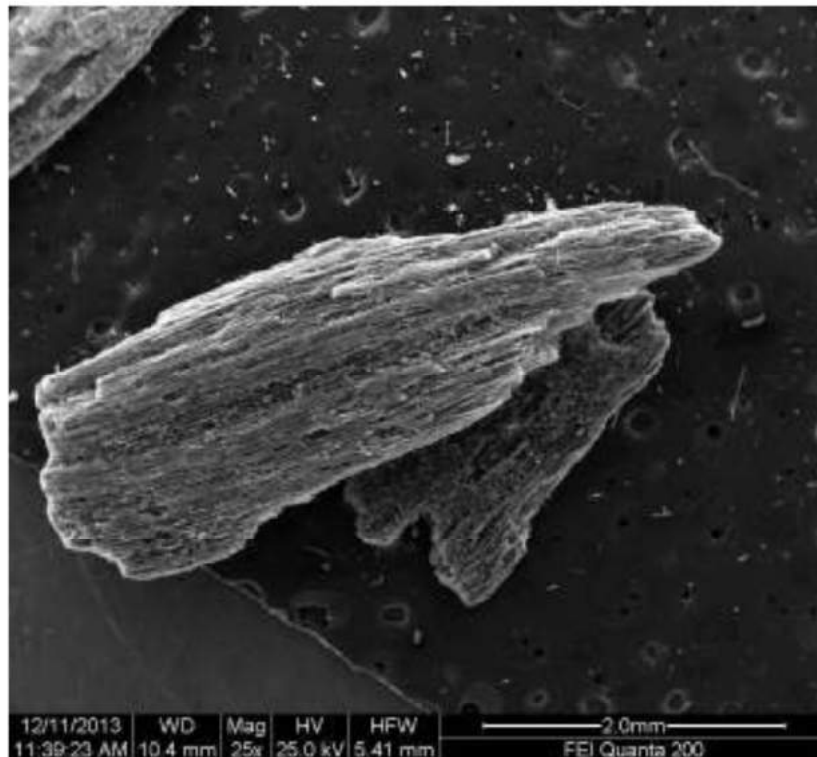


Figure 4.39: Microstructure of fine fibrous particles

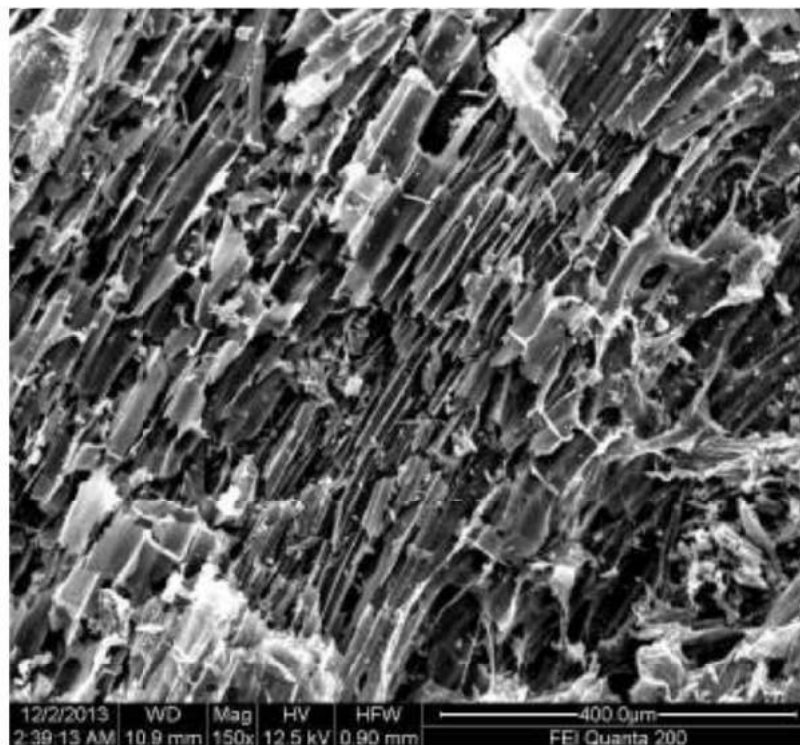


Figure 4.40: Microstructure of partially burnt fine fibrous particles

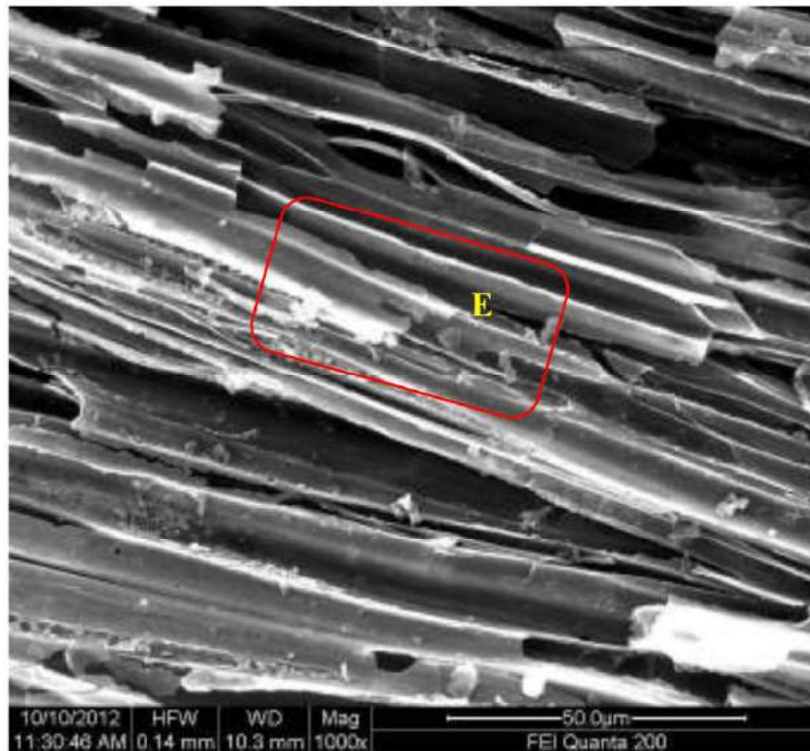


Figure 4.41: Microstructure of intercellular structure

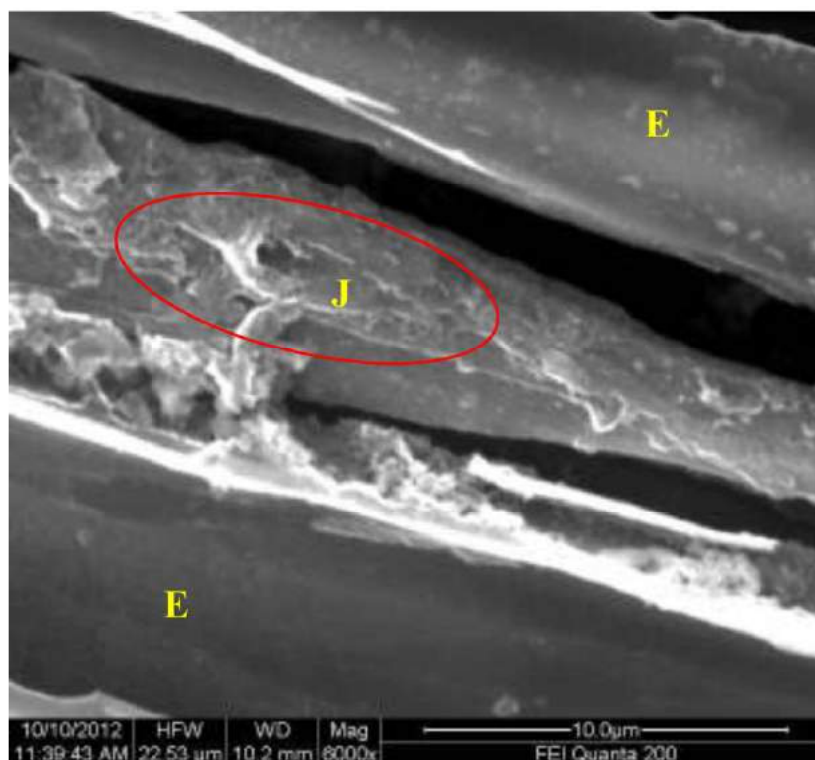


Figure 4.42: Microstructure of cellular structure at higher magnification

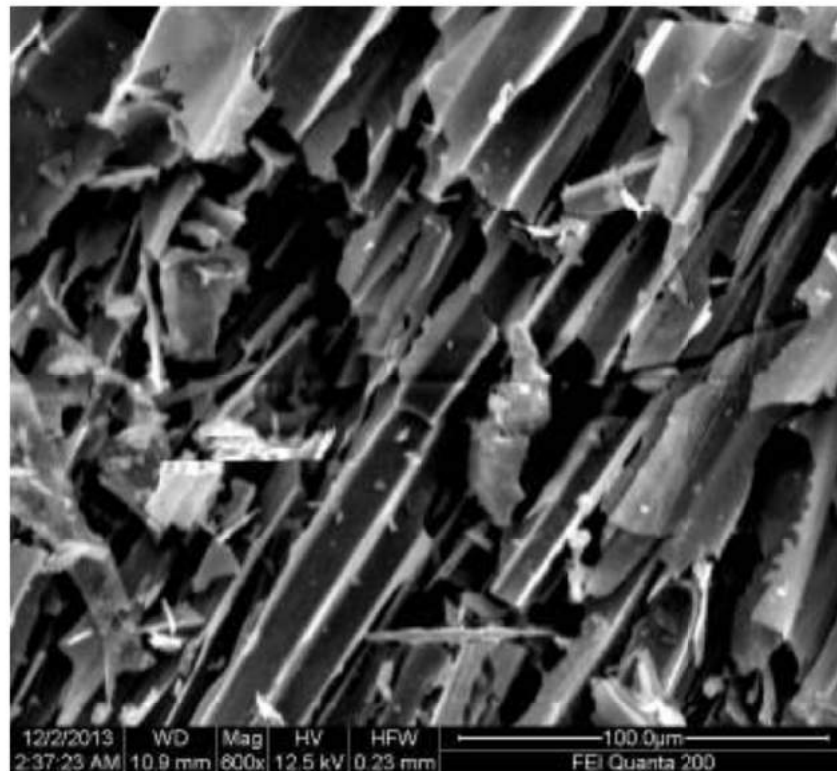


Figure 4.43: Presence of pits in the cell walls at higher magnification

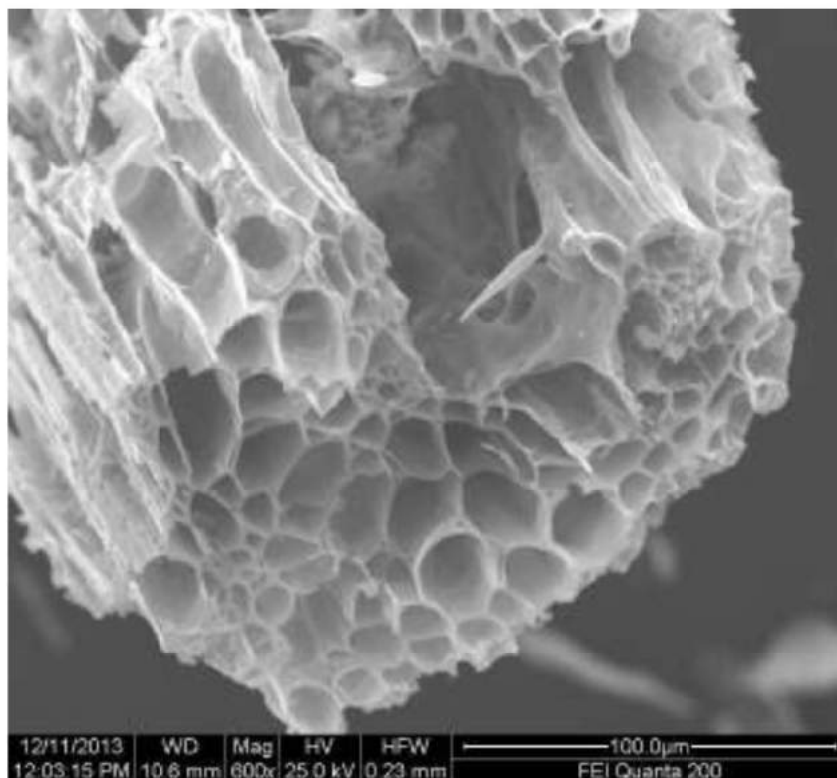


Figure 4.44: Intercellular channels of fine fibrous particles

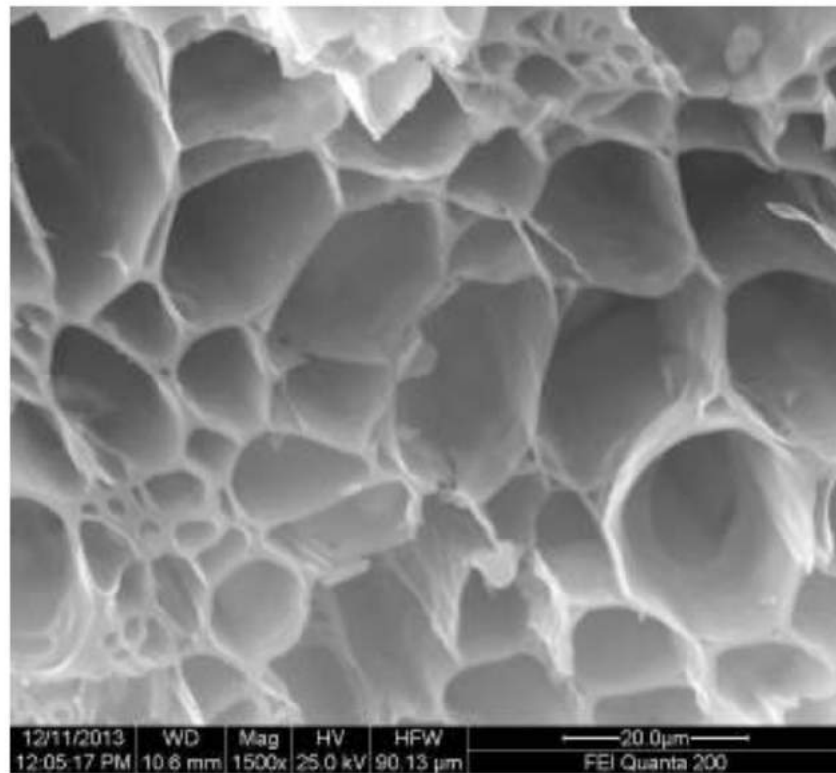


Figure 4.45: Micrograph of cellular channels at higher magnification

Table 4.1: Elemental composition (%) by EDS of observed phases from A-I

Elements	A	B	C	D	E	F	G	H	I	J
Si	15.75	9.51	47.87	50.07	0.71	3.87	18.91	29.32	1.34	1.28
O	38.08	8.36	49.72	46.40	7.20	12.68	28.17	35.37	7.71	10.84
C	-	80.06	-	-	89.03	78.29	49.09	34.20	87.02	83.74
Ca	10.77	0.23	0.30	0.39	0.47	1.09	0.29	0.06	0.55	0.89
Al	-	-	1.12	1.23	0.06	0.21	0.25	0.29	0.09	0.08
Fe	0.90	-	0.27	0.39	0.08	-	0.17	0.07	0.08	0.13
Mg	13.94	0.19	0.31	0.67	0.98	1.13	1.45	0.30	1.12	1.27
Na	-	0.05	0.11	-	0.23	0.12	0.06	0.09	0.20	0.14
P	14.74		-	-	-	-	-	-	-	-
K	5.18	1.15	0.33	0.85	1.05	2.31	1.53	0.31	1.30	1.42

4.6 LOSS ON IGNITION TEST

A large amount of carbon was observed in the elemental composition of fibrous particles. In addition to the SEM analysis, loss on ignition test was carried out as per IS 1727-2004 to find the unburnt carbon content. Raw bagasse ash, coarse fibrous particles and fine fibrous particles were kept in an oven at 105 – 110 °C to remove evaporable water content. 1 g of each dried sample was taken in the porcelain crucible. All the samples were ignited at 1000±25 °C for about 30 minutes in the electrical furnace. Loss in weight due to ignition was measured. Losses on ignition of coarse fibrous particles and fine fibrous particles were found to be 74 % and 72 % respectively. Raw bagasse ash had 21 % of unburnt carbon content due to presence of fibrous particles. Very large unburnt Carbon contents in the fibrous particles were earlier reported in the elemental composition of features E and F (Table 4.1). From these results, it can be concluded that removal of the Carbon rich fibrous particles can significantly reduce loss on ignition of bagasse ash. Utilization of unburnt fibrous particle as fuel for industrial boilers was addressed in an earlier research study (Cetin et al., 2004). In industries, large size industrial sieve shaker is used to separate all fibrous particles from fine particles before disposal. These coarse fibrous particles are used to make fuel pellets or gasifier feed material due to their high carbon content (Batra et al., 2008). Floating process is also used to separate fibrous unburnt carbon material. Floating process is preferred because bagasse ash has negligible amount of soluble content. Due to this, separation process by using water is ideal. These fibrous particles are also used for the manufacturing of activated carbon (Krishnan and Anirudhan, 2002). Loss on ignition of raw bagasse ash, CFU, FFU and sieved bagasse ash is presented in Table 4.2.

Table 4.2: Loss on ignition for the test samples

SAMPLE	LOI (%)
Raw bagasse ash	19.0
Coarse fibrous unburnt particle	74.4
Fine fibrous unburnt particle	71.5
Sieved bagasse ash	3-6

Results from loss on ignition test agree well with elemental composition of fibrous particles by EDS. It is clear that fibrous particles are rich in Carbon and cannot be used as pozzolanic material. Presence of these fibrous particles is responsible for lower pozzolanic activity of raw bagasse ash than minimum requirement as well as higher loss on ignition. As stated earlier, complete removal of carbon rich fibrous particles (CFU and FFU) was achieved by sieving raw bagasse ash through 300 μm sieve. The sieved material had only 3-6 % loss on ignition which is well below the permissible limit for natural pozzolan as per ASTM C618-12a. It is clear that removal of fibrous unburnt particles effectively reduces loss on ignition and considerably improves its pozzolanic activity to 79% which is well above the minimum requirement.

4.7 SUMMARY

Five different test methods were used to evaluate pozzolanic activity of bagasse ash. Results from all test methods indicate superior pozzolanic activity for the sieved bagasse ash. Raw bagasse ash has lesser value of pozzolanic activity than the minimum requirement in the standards due to presence of fibrous carbon particles. Different shapes of particles including prismatic, spherical, irregular, and fibrous were observed in the microstructure of raw bagasse ash. High Carbon content was observed for fibrous particles in the elemental composition by EDS analysis, which was further confirmed by the loss on ignition test. Removal of these fibrous particles reduces loss on ignition and improves its pozzolanic activity. Sieved bagasse ash can thus be used as pozzolanic material.

In terms of the activity characterization methods, Frattini test and electrical conductivity method are more reliable for the evaluation of pozzolanic activity of supplementary cementitious materials, because of the issues associated with the strength based tests.

CHAPTER 5

INFLUENCE OF DIFFERENT PROCESSING METHODS ON THE POZZOLANIC PERFORMANCE OF SUGARCANE BAGASSE ASH

5.1 INTRODUCTION

Most of the supplementary cementitious materials including bagasse ash are industrial by-products. A minimum level of processing is essential to achieve superior pozzolanic performance in concrete, instead of direct addition as a cement replacement material. The utilization of bagasse ash has been constrained due to lack of suitable processing methodology for use in a large scale. Processing methods significantly influence the pozzolanic activity of any supplementary cementitious material. Proper investigation of the effect of various processing methods such as burning, grinding and combination of these methods on the pozzolanic performance of bagasse ash is explained in this chapter. In addition, the effect of processing on the microstructure of bagasse was investigated in this study to attain a clear scientific insight on the pozzolanic performance of processed materials. The selection of a suitable processing methodology to attain maximum pozzolanic activity of sugarcane bagasse ash with minimum level of processing is described in this chapter.

5.2 PROCESSING METHODS

Different processing methods including burning, grinding and chemical activation were suggested to enhance pozzolanic activity of other pozzolanic materials. Because of the presence of coarse unburnt particles in raw bagasse ash and higher value of loss on ignition (more than 20%), burning and grinding were selected in this study. Effects of removal of these fibrous particles from raw bagasse by sieving and combination of above mentioned methods were also investigated to obtain maximum possible pozzolanic activity of bagasse ash.

5.2.1 Burning process

Bagasse is generally burnt in the cogeneration boiler at 500 – 550 °C to utilize maximum fuel value as depicted in Figure 5.1. The resultant bagasse ash is collected from bag-house filter of cogeneration boiler. As described previously, this bagasse ash is disposed to the nearest landfill in a slurry form. For the current study, the wet bagasse ash slurry was further burnt to higher temperature to attain better pozzolanic performance with minimum unburnt matter. As the raw bagasse ash was already burnt at 500 – 550 °C, the following higher temperatures 600 °C, 700 °C, 800 °C and 900 °C were selected to evaluate the influence of burning on the pozzolanic performance of bagasse ash.

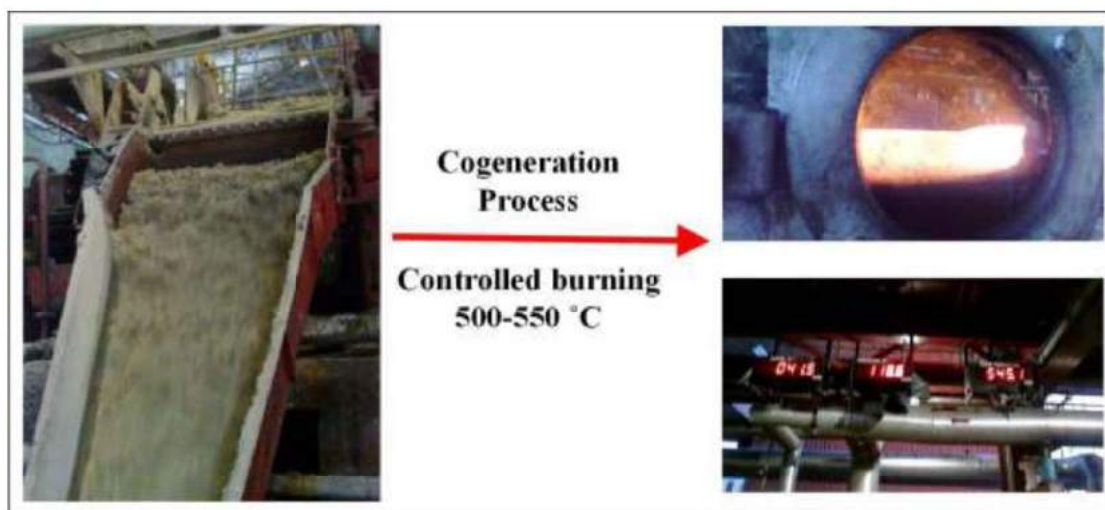


Figure 5.1: Burning of bagasse as fuel in cogeneration boiler

Electrical furnace used in the study is shown in Figure 5.2. A fixed quantity of bagasse ash (2 kg) was taken for burning in the electrical furnace (see Figure 5.3). The burning time was optimized at 90 minutes after numerous trials to achieve uniform burning of the sample at the corresponding temperature. Non-uniform burning of bagasse ash particles was clearly observed in the burnt samples at lesser durations (30 minutes and 75 minutes) as shown in Figure 5.4.

The collected bagasse ash from the boiler was further burnt to 600 °C, 700 °C, 800 °C, and 900 °C for 90 minutes in this study. After burning to particular temperatures, the burnt bagasse ash was suddenly cooled to room temperature to increase the reactivity of

the sample. The burnt sample was stored in air-tight drums (shown in Figure 5.5) until further testing



Figure 5.2: Electrical furnace used in the study

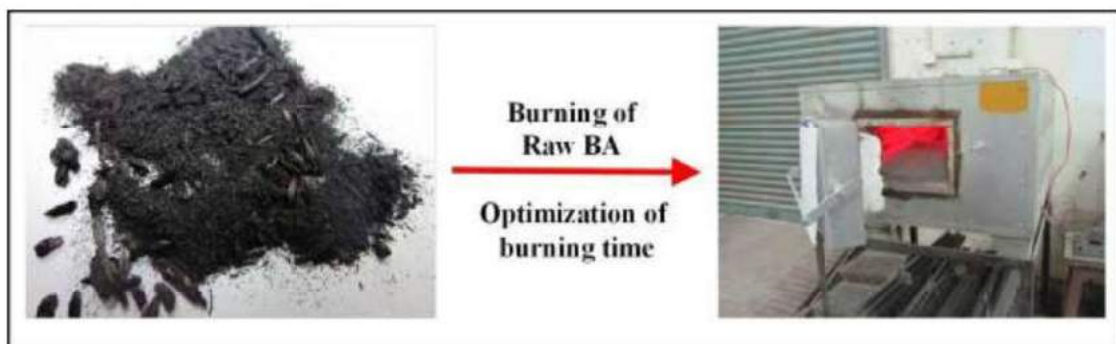


Figure 5.3: Controlled burning of raw bagasse ash in electrical furnace for different durations



Figure 5.4: Appearance of bagasse ash burnt at 30 min (left) and 75 min (right) respectively

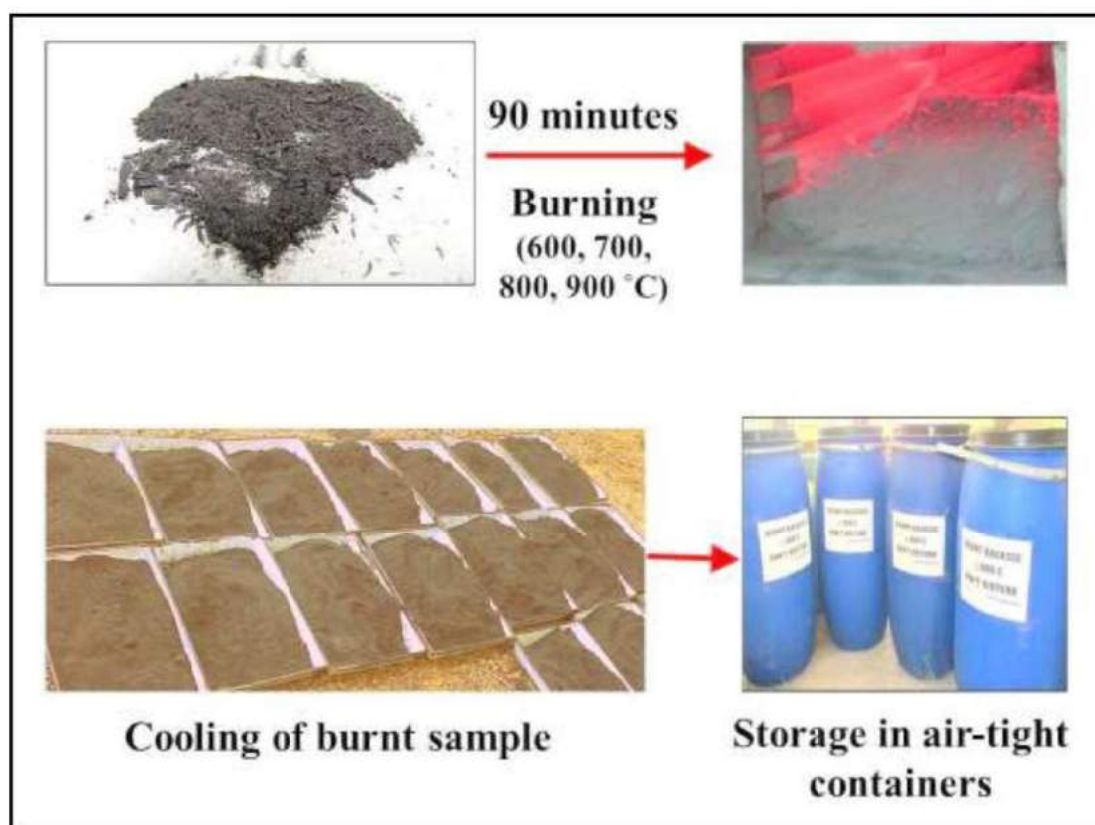


Figure 5.5: Controlled burning of raw bagasse ash at different temperatures for optimized time (90 minutes)

5.2.2 Grinding process

Fineness plays an important role in the performance of alternative cementitious materials in concrete. Two methods of grinding were used to evaluate the effect of grinding on the pozzolanic activity of bagasse ash.

- 1) Raw bagasse ash was ground to different sizes from 210 μm to 45 μm and the effect of grinding on pozzolanic activity was studied by strength activity test. In this method, dried raw bagasse ash was ground by mechanical grinding to obtain different sizes. After grinding of raw bagasse ash, the particular size of ground material was obtained by using the respective size sieve. Raw bagasse ash was ground to 210, 180, 150, 125, 105, 75, 53, 45 μm fineness, and the ground material was stored in air tight containers. For example, for 150 μm ground sample, the ground material passing through 180 μm sieve and retained on 150 μm sieve was used, and for the 53 μm ground sample, the ground material passing 75 μm sieve and retained on 53 μm sieve was used. This scheme was designed to understand the effect of particle sizes in a narrow range on the pozzolanic activity.
- 2) The combined effect of burning and grinding was also investigated to get the maximum possible pozzolanic activity of bagasse ash. The burnt material (as described in 5.2.1) showing highest pozzolanic activity from the burning study was ground to cement fineness (300 m^2/kg). A fixed quantity of burnt bagasse ash, of around 1.5 kg was taken in a ball mill, with 18 mm diameter steel balls. The ball mill used in the study is shown in Figure 5.6. The ball mill was allowed to rotate at a speed of 40 rpm for different durations – 30 min, 60 min, 90 min, and 120 min – and the sample from each grinding duration was collected for measurement of fineness by using Blaine air permeability test as per ASTM C204-11. The material ground for 120 min was found to have required fineness. Blaine air permeability test is suitable to determine specific surface area of solid particles such as cement and not suitable for porous or irregular-shaped materials. Due to the presence of porous and irregular-shaped particles in bagasse ash, for a similar fineness value, bagasse ash particles may be coarser than cement particles. In this study, the burnt sample was ground to cement fineness (300 m^2/kg) in a similar way as cement by using ball mill. However, fineness of ground materials was again measured by Blaine air permeability test for

convenience to compare with cement. After grinding, the material was stored in air tight containers for further testing. In a similar way, the sieved material (described in Section 4.2, Chapter 4) was also ground and pozzolanic activity of both materials was tested.



Figure 5.6: Ball mill used in the study

5.2.3 Methods for evaluation of pozzolanic activity of processed samples

Pozzolanic performance of different classes of burnt bagasse ash and ground bagasse ash was evaluated by strength activity test as per ASTM C311-11b. A detailed methodology has been described earlier in Section 4.4.1 (Chapter 4). Six numbers of 50 mm control mortar cubes were cast without replacement. 20 % mass replacement of cement with burnt samples (600, 700, 800 and 900 °C bagasse ash) and ground samples (210, 180, 150, 125, 105, 75, 53, 45 μm) as supplementary cementitious material was used as per guidelines. In a similar method, specimens were cast with burnt and ground sample (BG) as well as sieved and ground sample (SG) to evaluate the effect of combined processing on pozzolanic performance. As mentioned earlier, strength activity index is calculated as the % ratio of strength of the processed bagasse ash replaced mix to the control mix. Due

to time consumption and variation of water content in the control and processed specimens for strength comparison, Frattini test (EN 196-5) was also carried out to evaluate the pozzolanic activity of burnt and ground sample (BG) as well as sieved and ground sample (SG). The detailed procedure has already been described in Section 4.4.4 (Chapter 4).

5.3 RESULTS AND DISCUSSION

5.3.1 Effect of burning on pozzolanic activity

Compressive strength and strength activity index were determined for raw bagasse ash and different burnt samples. From the test results, it was observed that raw sugarcane bagasse ash had strength activity index (SAI) of 71 % and 72 % at 7 days and 28 days respectively as shown in Figure 5.7. Pozzolanic activity value of raw bagasse ash was below the minimum requirement of 75 % to define as a supplementary cementitious material as per guidelines – this is attributed to the presence of unburnt coarse fibrous particles.

Burning significantly influenced pozzolanic activity of the raw bagasse sample. Pozzolanic activity index of the burnt samples was found to be higher than the raw bagasse sample. While the index increased up to 700 °C, subsequent higher temperature burning was seen to reduce the index value. The sample burnt at 700 °C had maximum pozzolanic activity index value of 84% and 86% at 7 days and 28 days respectively. The compressive strength increased from 7 to 28 days because of the additional pozzolanic reaction of burnt samples. After 700 °C, pozzolanic activity was reduced with an increase in temperature. The sample burnt at 900 °C showed lesser pozzolanic activity and lesser specific surface area compared to raw bagasse ash. Changes in particle size were visually observed in the sample burnt at 900 °C. Although the fineness of burnt samples (600, 700 and 800 °C) was lesser than the raw bagasse ash, pozzolanic activity of these particles was considerably higher than the raw bagasse ash (see Table 5.1). From this observation, it is clear that burning of bagasse ash significantly influences pozzolanic reactivity of bagasse ash.

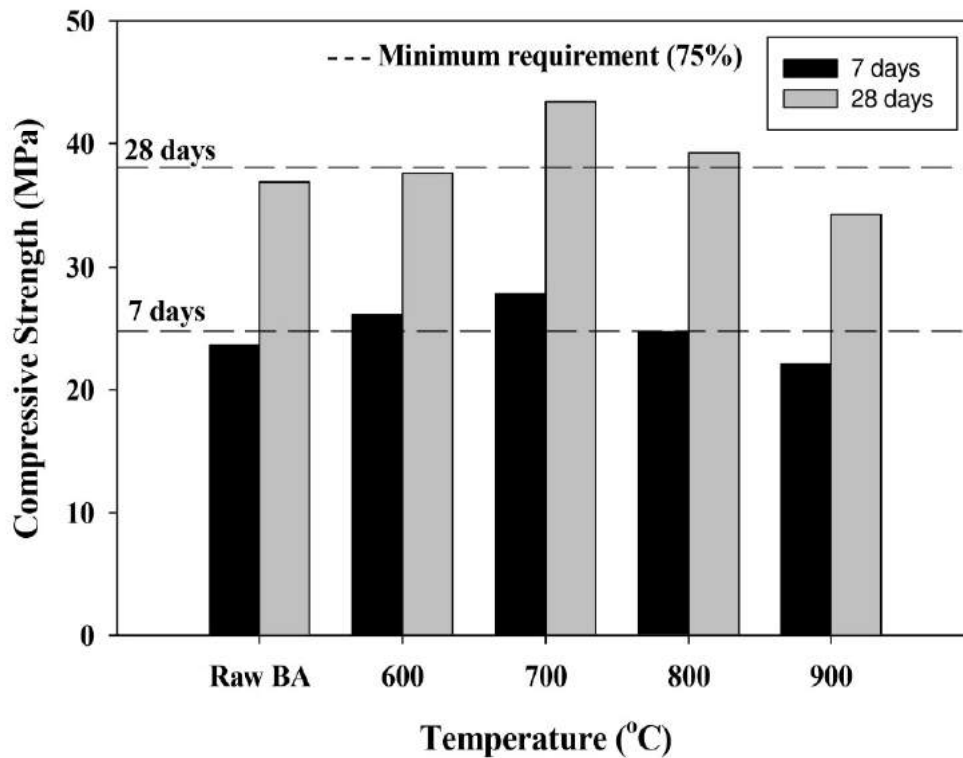


Figure 5.7: Compressive strength after 7 and 28 days curing for bagasse ash samples burnt at different temperatures

The structure of the burnt bagasse ash particles at different temperatures was investigated by scanning electron microscopy (SEM) in the secondary mode with Energy dispersive X-ray analysis. Different levels of burning of fibrous particles were clearly observed in the SEM micrographs of burnt samples, which are presented in Figures 5.8-5.13. Burning of these fibrous particles present in the raw bagasse ash was increased with temperature. Microstructure of the sample burnt at 600 °C is presented in Figures 5.8 and 5.9. Presence of more number of fibrous particles is seen in the micrographs of the sample burnt at 700 °C (see Figures 5.10 and 5.11). Micrographs of burnt sample at 800 °C clearly showed severely burnt fibrous particles as depicted in Figures 5.12 and 5.13. This observation was supported by the results from loss on ignition test of different burnt samples. Loss on ignition of raw bagasse sample was 21 % and it was reduced to 14 % at 700 °C. Presence of fibrous particles leads to higher loss on ignition value than permissible limits and more water requirement in the mix. Specific gravity of burnt

samples was higher than raw bagasse sample due to burning of lightweight fibrous unburnt carbon particles. A small amount of decrease in specific surface was observed up to 700 °C. Coarse particles were found to be present in the samples burnt at 800 °C and 900 °C because of phase transition of amorphous silica to crystalline form. Due to crystallization, the specific surface area of 800 and 900 °C burnt samples was decreased to 118 and 110 m²/kg respectively. Physical properties of different burnt samples are presented in Table 5.1.

Table 5.1: Physical characteristics of burnt samples

Characteristics	Raw SCBA	600 °C	700 °C	800 °C	900 °C
Specific Gravity	1.91	2.07	2.05	2.03	1.93
Specific Surface area (Blaine) m ² /kg	145	136	131	118	110
Strength activity index (SAI) at 7 days (%)	71	79	84	74	66
Strength activity index (SAI) at 28 days (%)	73	74	86	77	67
Loss on ignition (%)	21.0	16.0	14.0	12.8	8.0

An earlier study investigated the effect of burning (Cordeiro et al., 2009) on pozzolanic activity of bagasse ash. In that study, after burning, bagasse ash was further ground to cement fineness and the observed pozzolanic activity also included the effect of additional grinding. In this present study, the burnt sample was directly used without grinding to estimate the effect of calcination temperature on the pozzolanic activity, which is not available in the existing literature.

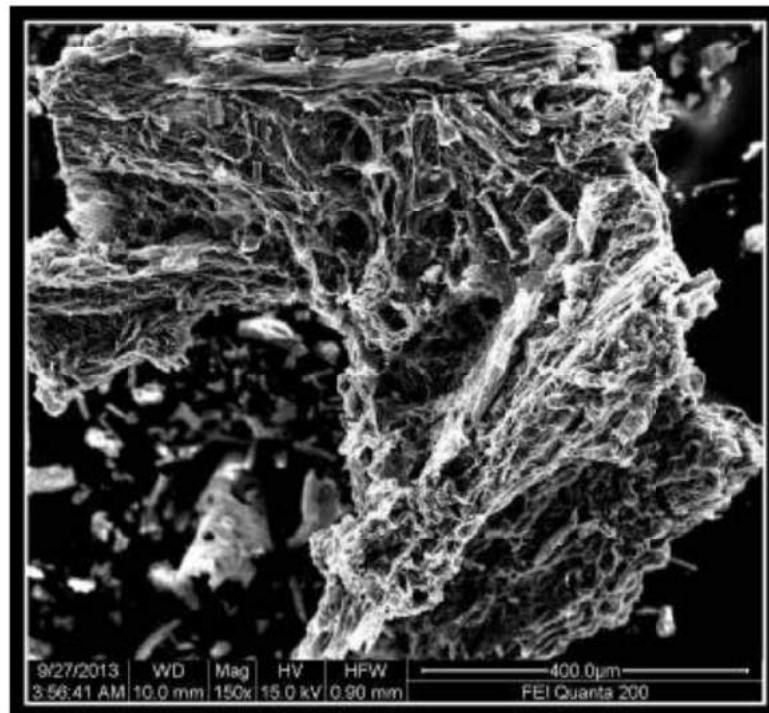


Figure 5.8: Partially burnt fibrous carbon particle in 600 °C burnt sample

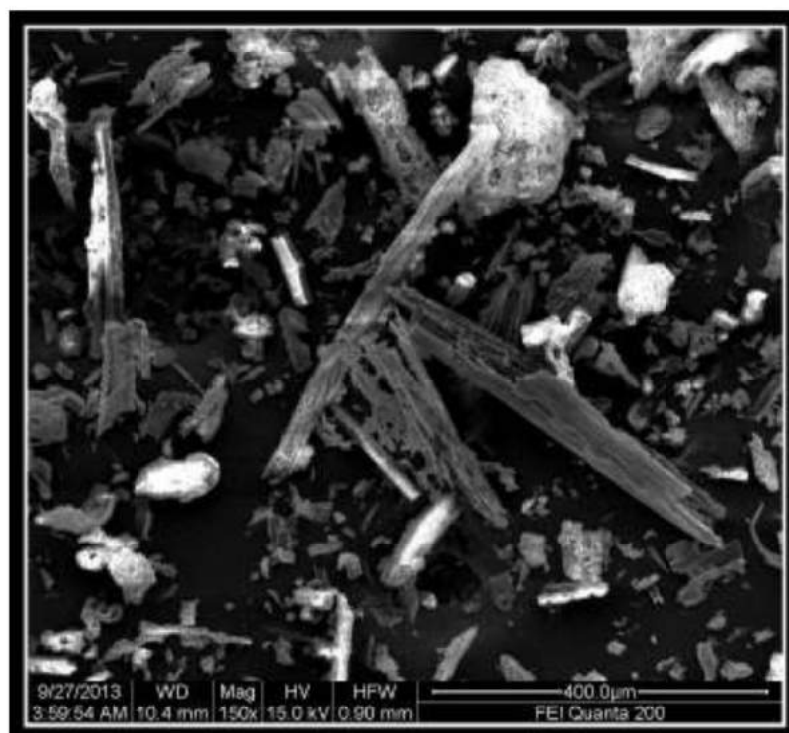


Figure 5.9: Appearance of fibrous carbon particles in 600 °C burnt sample

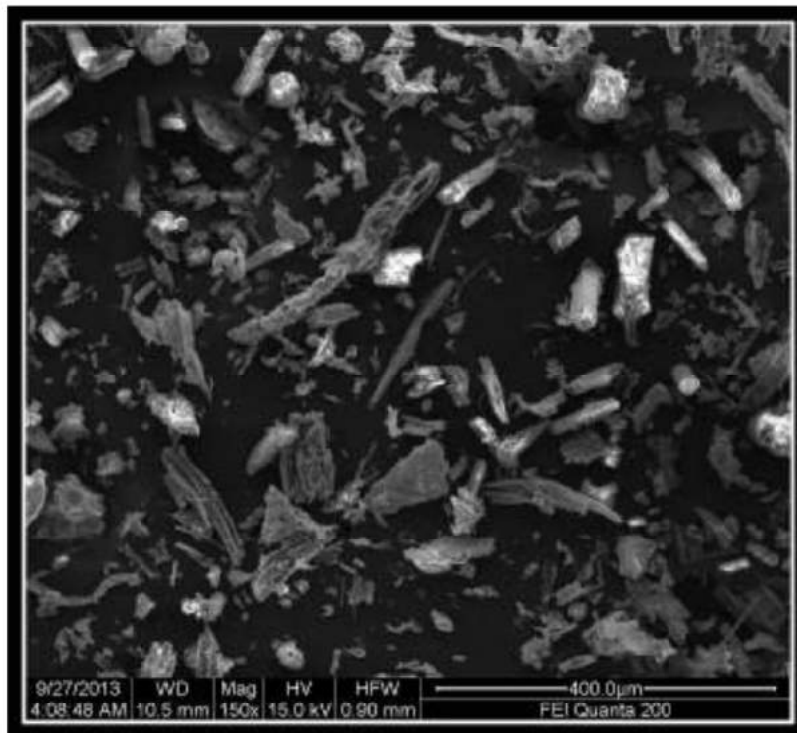


Figure 5.10: Presence of fibrous carbon particles in 700 °C burnt sample



Figure 5.11: Appearance of more number of fibrous carbon particles in 700 °C burnt sample

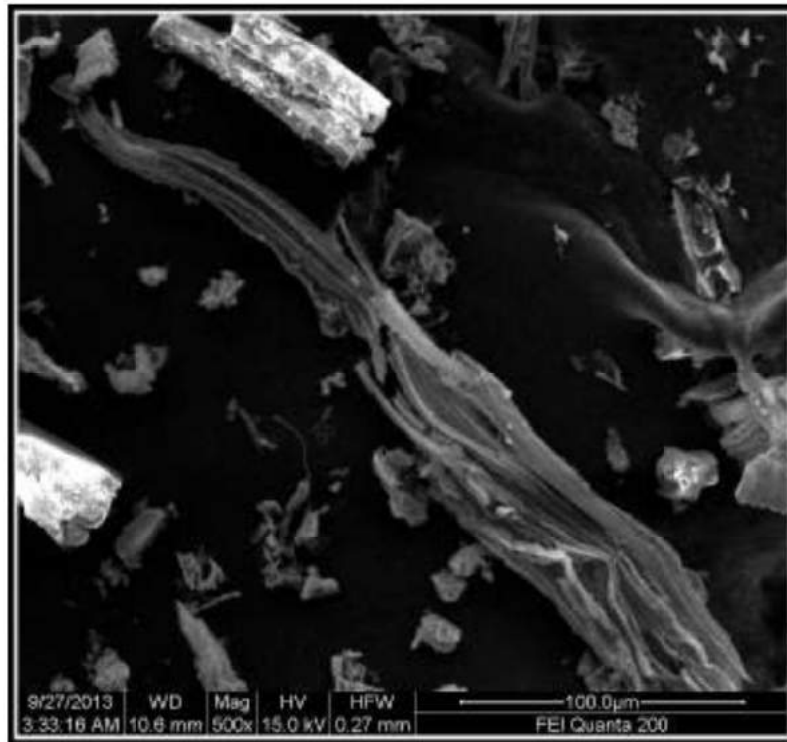


Figure 5.12: Appearance of severely burnt particle in 800 °C burnt sample

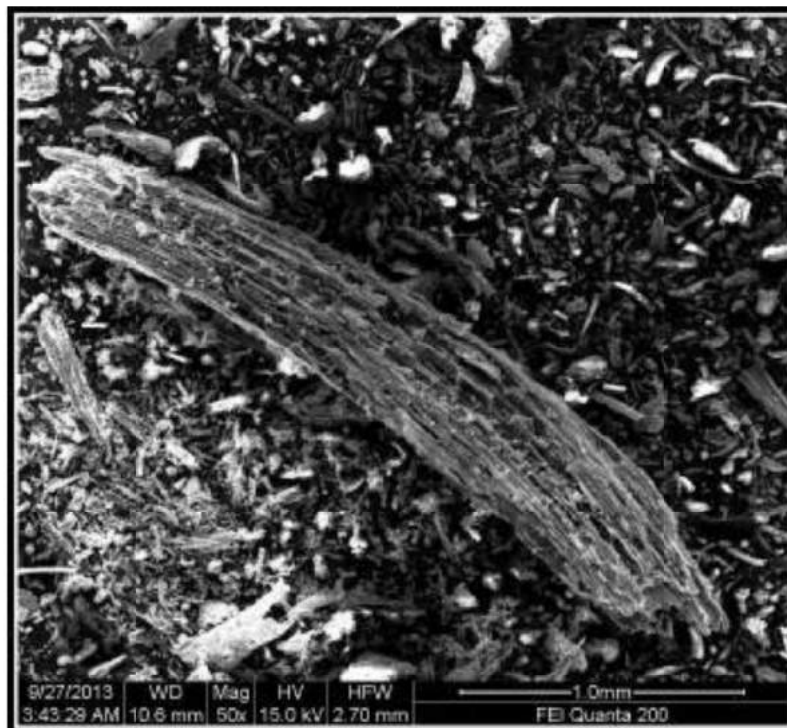


Figure 5.13: Appearance of fibrous carbon particles in 800 °C burnt sample

X-diffraction was performed for all burnt samples. Results are presented in Figure 5.14. Because of controlled combustion of bagasse in the cogeneration plant, amorphous silica was formed, which is characterized by the broad hump between 18 and 25 °2θ. All the XRD patterns also show peaks for quartz (Q). Amorphous silica was retained up to 700 °C and further burning to higher temperature increased crystallization. X-ray diffraction patterns in Figure 5.14 clearly show crystallization of silica to cristobalite (marked as C) after 700 °C. Reduction in the pozzolanic activity after 700 °C is attributed to the crystallization of amorphous silica content to cristobalite. Similar behaviour in the pozzolanic activity was observed in the earlier research studies for rice husk ash and metakaolin (Chopra et al., 1981; Rashad, 2013). Hamad and Khattab (1981) studied reactivity of silica in the rice husk ash and reported that up to 700 °C, the silica present in the rice husk ash was mainly in an amorphous form. Amorphous silica started to crystallize at higher temperature and converted to cristobalite at 800 °C. Cristobalite and tridymite were detected in the samples burnt at 1150 °C.

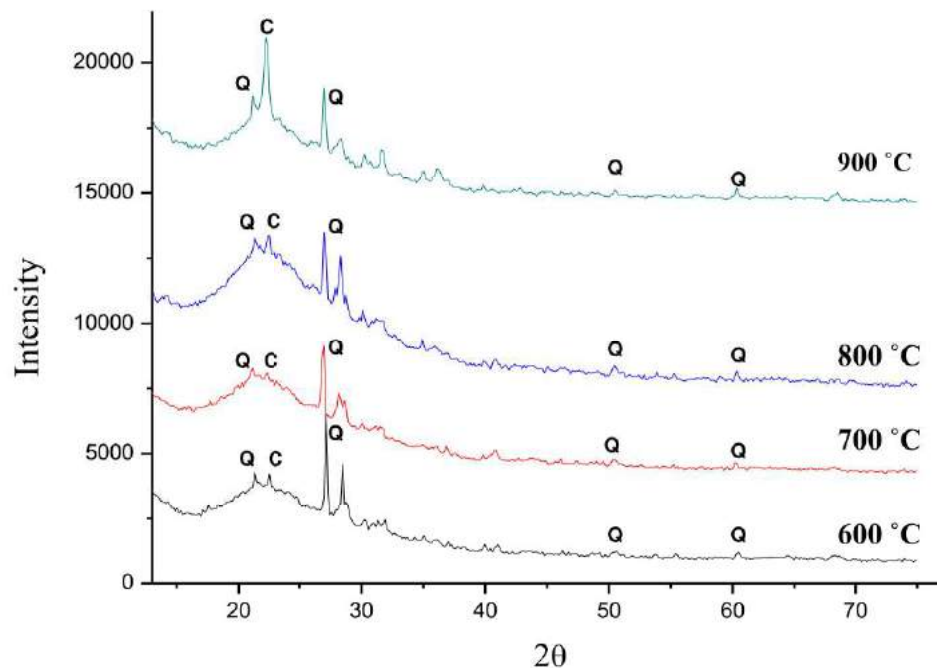


Figure 5.14: X-Ray diffraction patterns of burnt samples

After 900 °C burning, changes in colour and particle size were observed visually. Burnt samples at 800 °C and above showed the presence of some white particles. The samples burnt above 900 °C had completely white particles due to crystallization as well as thermal decomposition of bagasse ash at higher temperature. It is interesting to note the colour change from extreme black of raw bagasse ash to completely white particles as shown in Figure 5.15.



Figure 5.15: Raw bagasse ash (left) and white particles at 900 °C (right)

More number of prismatic particles (which were Si based as seen in EDS) were clearly observed in the SEM micrographs of white particles, as shown in Figures 5.16 to 5.19. The microstructure of raw bagasse ash, described earlier (Chapter 4; section 4.5.1), showed more fibrous carbon particles and irregular particles. Spherical and prismatic particles were rarely observed in the microstructure of raw bagasse ash. Presence of the prismatic particles in the microstructure of raw bagasse ash is attributed to burning of those particular particles to higher temperature.

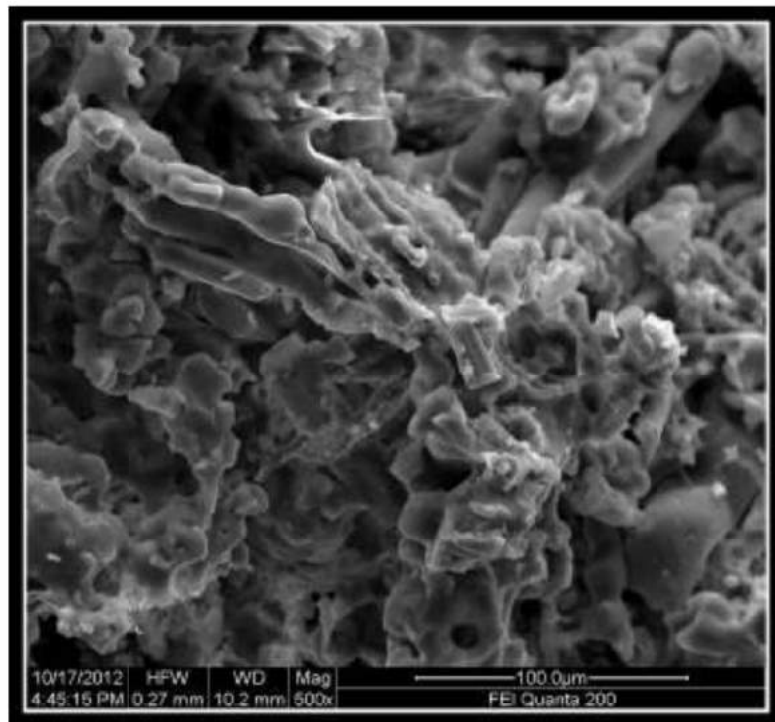


Figure 5.16: Microstructure of white particles in the 900 °C burnt sample

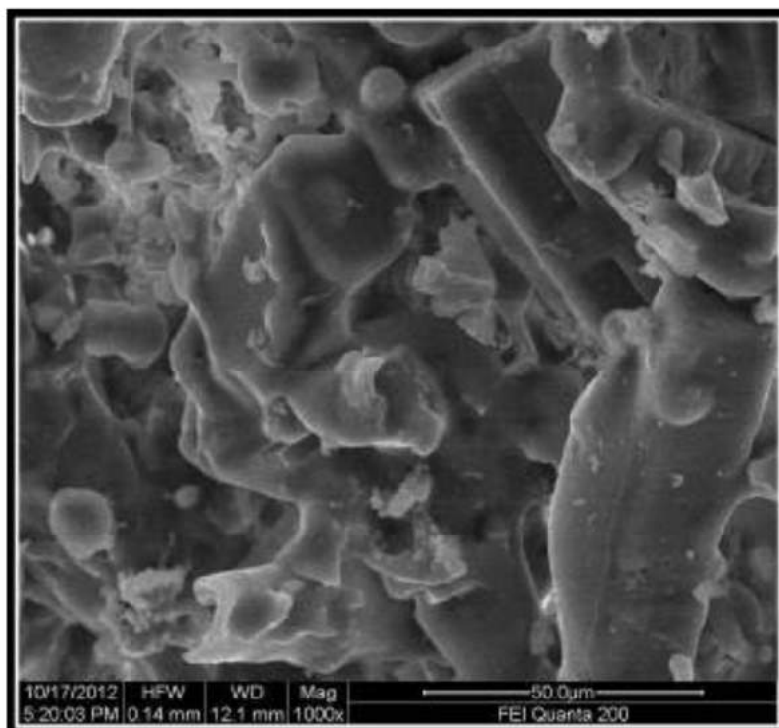


Figure 5.17: Microstructure of white particles (900 °C burnt sample) at higher magnification

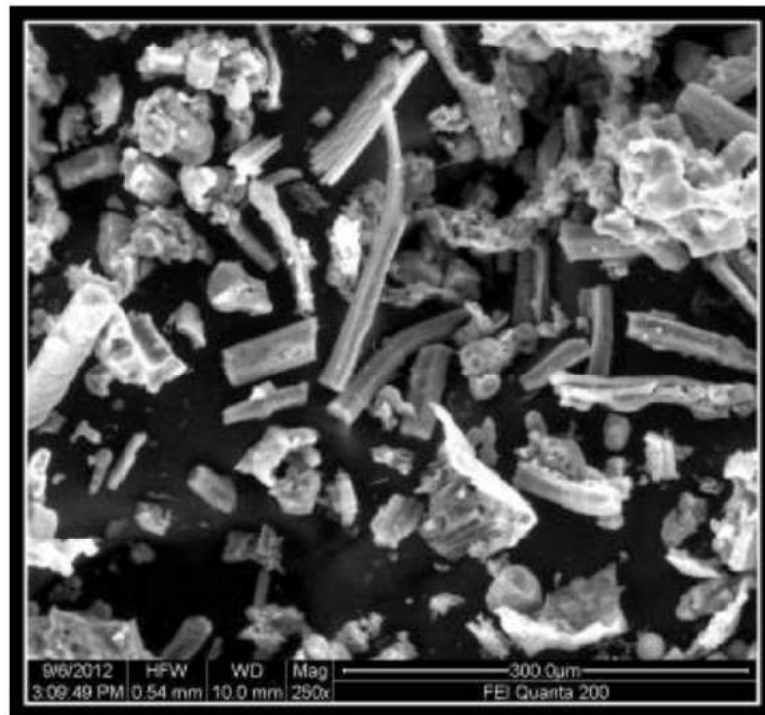


Figure 5.18: Microstructure of white particles in the 900 °C burnt sample, sieved through 75 µm sieve

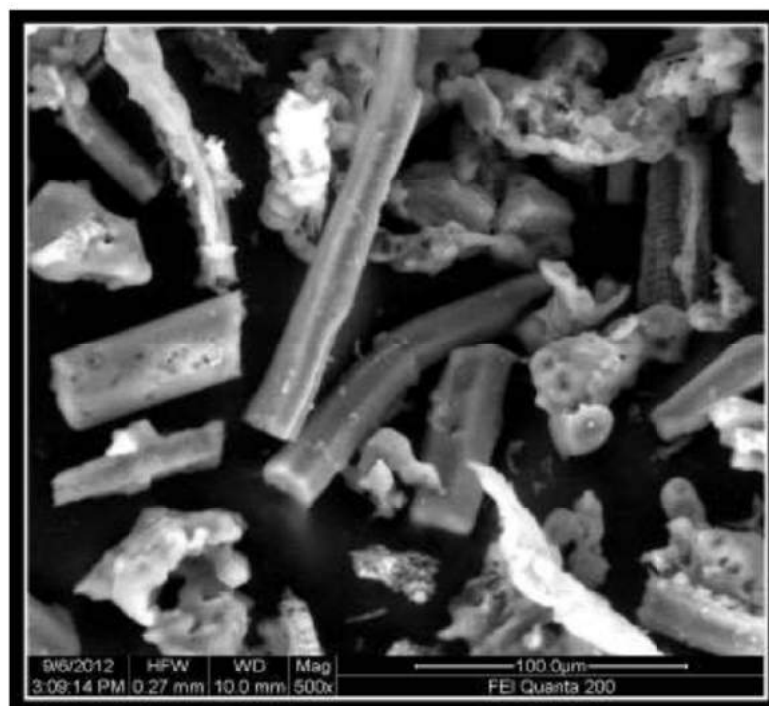


Figure 5.19: Microstructure of sieved white particles from the 900 °C burnt sample at higher magnification

Although raw bagasse is burnt at 500 – 550 °C in the cogeneration process, particles which are near to the funnel opening in the boiler experience greater temperature than the controlled boiler temperature. The white particles shown in Figure 5.15 had a similar structure to the prismatic particles observed in the microstructure of raw bagasse ash; lot of prismatic particles were seen in the microstructure without any fibrous carbon particles. This clearly reveals crystallization at higher temperatures, which is bound to influence the pozzolanic activity of sugarcane bagasse ash adversely.

Based on ASTM C 109-11b guidelines, 242 ml water was added to control mortar and flow value was measured as per ASTM C1437-07. Water requirement of raw bagasse sample increased to 320 ml to achieve the same control flow value. But water requirement of burnt samples was 265 ml, which was lesser than raw bagasse ash sample and higher than the control sample. Thus, it can be concluded that the presence of fibrous particles in the raw bagasse is responsible for higher water requirement.

5.3.2 Effect of grinding on pozzolanic activity of raw bagasse ash

Reactivity of any supplementary material is influenced by its fineness. Raw bagasse ash was ground to different sizes ranging from (finer than) 210 µm to 45 µm. The effect of grinding on pozzolanic activity was studied by strength activity test at 7 days and 28 days.

Results are shown in Figure 5.20. Interestingly, most ground bagasse ash samples had pozzolanic activity lesser than raw bagasse ash sample. This is not in agreement with studies for other supplementary cementing materials. In case of rice-husk ash, pozzolanic activity index was reported to increase with an increase in fineness (Cordeiro et al., 2011). Higher value of pozzolanic activity index was observed for ground coal fly ash than raw fly ash sample in another study (Kiattikomol et al., 2001). In the current study, the samples ground up to > 75 µm size had lesser pozzolanic activity index value at 28 days than raw bagasse ash sample, and well below the minimum requirement to define as pozzolanic material as per ASTM C618-12a. The sample ground to 45 µm size had pozzolanic activity higher than minimum required index value at 7 days, while both samples below 53 µm size showed sufficient reactivity at 28 days. Thus, to achieve the

minimum requirement (75% pozzolanic activity index), the raw bagasse ash sample needs to be ground to a material finer than 53 μm .

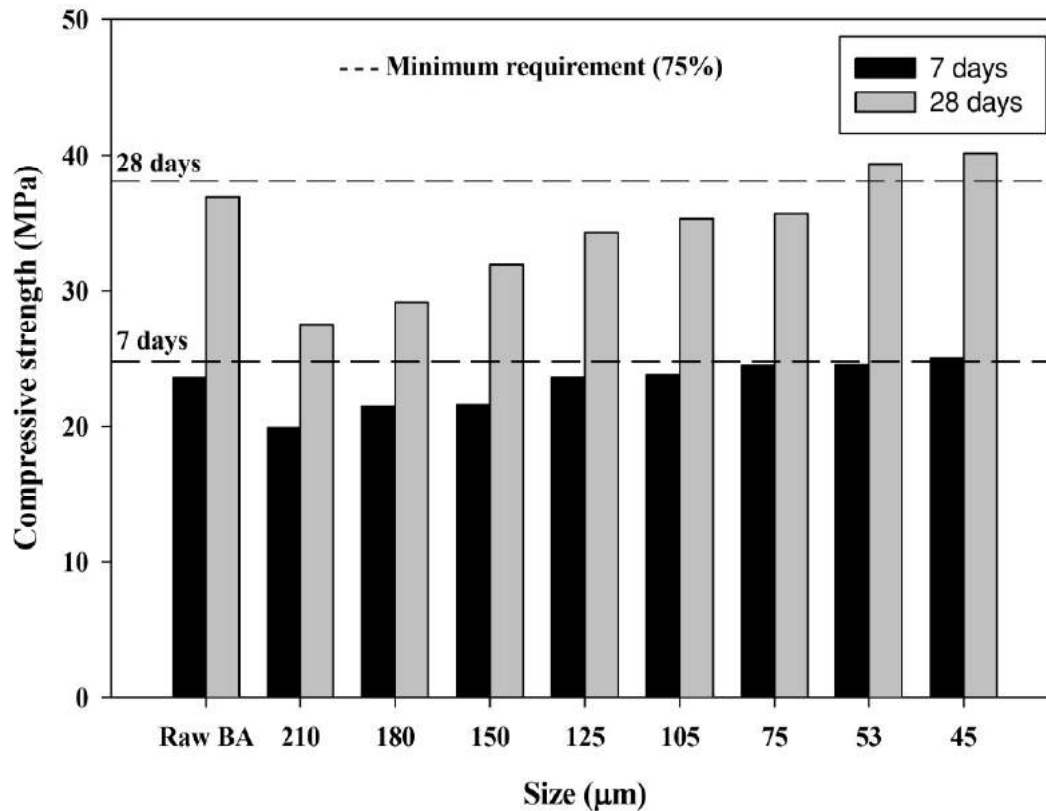


Figure 5.20: Compressive strength after 7 and 28 days curing

Specific surface areas of different ground samples were determined by Blaine air permeability test. Results are shown in Figure 5.21. The pozzolanic activity index and fineness were increased with increase in the degree of grinding. The fineness gradually increased from 130 m^2/kg (210 μm) to 320 m^2/kg (45 μm) with different level of grinding. Although the pozzolanic activity of ground samples was increased marginally from 210 μm to 53 μm , the observed pozzolanic activity was lesser than the minimum requirement (75%). The strength activity indices are also plotted in the same graph as shown in Figure 5.21.

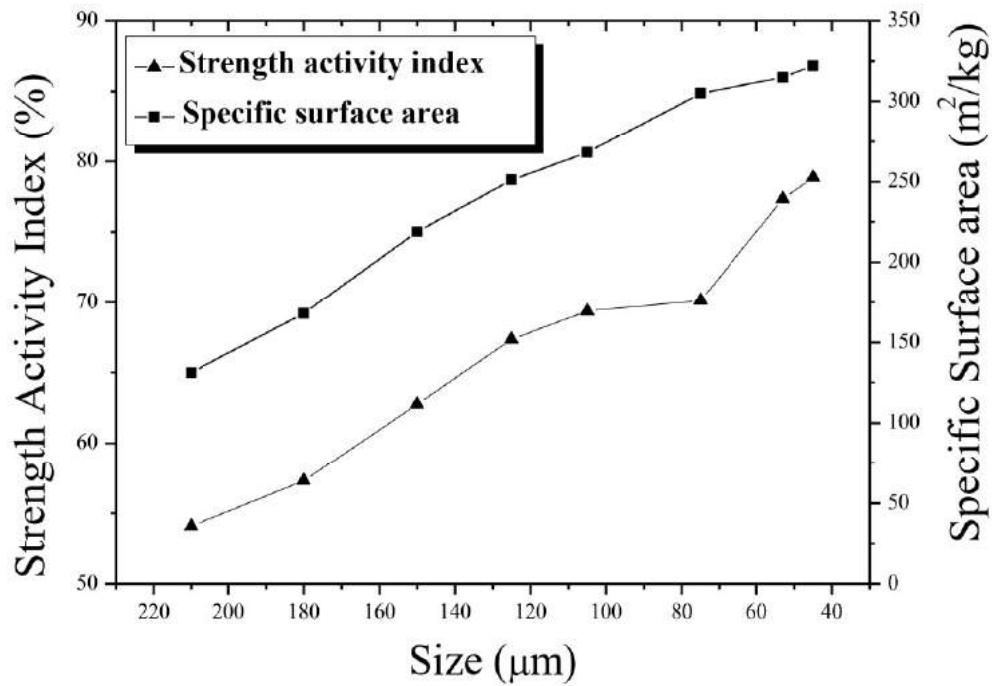


Figure 5.21: Fineness of ground samples of bagasse ash

Scanning electron microscopy (SEM) in the secondary mode with Energy dispersive X-ray analysis was used to observe the effect of grinding on the microstructure of ground bagasse ash samples. As reported earlier, raw bagasse ash had coarse fibrous particles and fine particles. Coarse carbon particles were ground along with fine burnt particles during the grinding process. When the raw sample was ground to a particular size, because of lightweight cellular structure and presence of intercellular channels, fibrous particles were ground faster than fine silica particles for the same time of grinding. More number of fibrous particles were clearly observed in the microstructure of all ground samples, as seen in the SEM micrographs in Figure 5.22. Thus, grinding of the bagasse ash did not significantly influence the pozzolanic activity due to presence of more fibrous unburnt carbon particles in the ground samples (these are marked as 'c' in the micrographs).

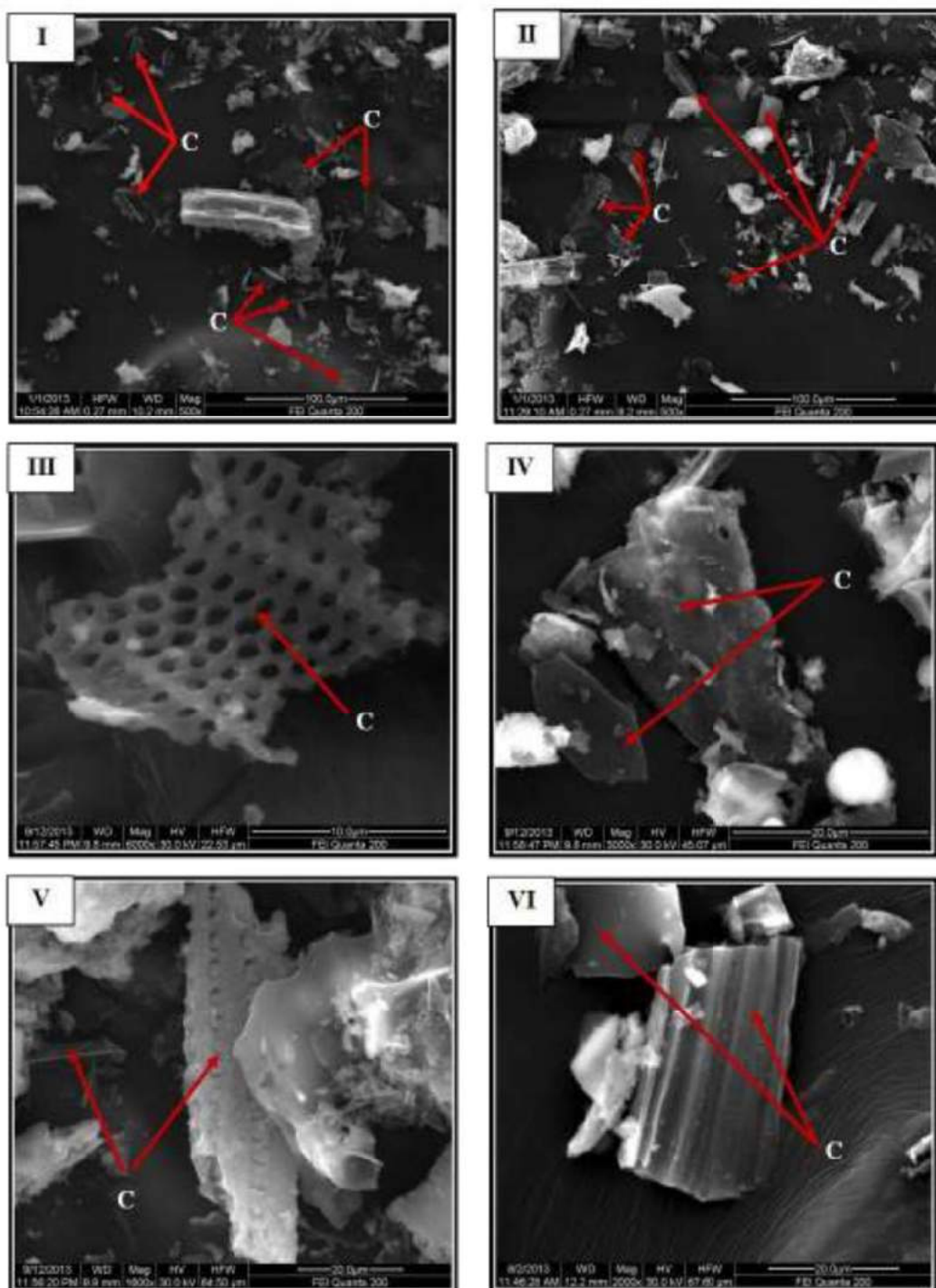


Figure 5.22: Appearance of more number of carbon particles (I & II) in the ground samples; different parts of ground carbon particles (III-VI)

5.3.3 Effect of grinding on sieved and burnt samples

The complete removal of coarse and fine fibrous particles from raw bagasse ash was achieved by the sieving process (through 300 μm sieve) described earlier in Chapter 4. The strength activity index of the sieved material was determined to be 79%, which is higher than raw bagasse ash and well above the minimum required pozzolanic index value as per standard. To investigate the combined effect of burning and grinding and to achieve maximum possible pozzolanic activity, the sieved sample and burnt sample which showed high pozzolanic activity index (i.e. the sample burnt at 700 $^{\circ}\text{C}$) were further ground to cement fineness (300 m^2/kg). The results of strength activity index tests are shown in Figures 5.23 and 5.24.

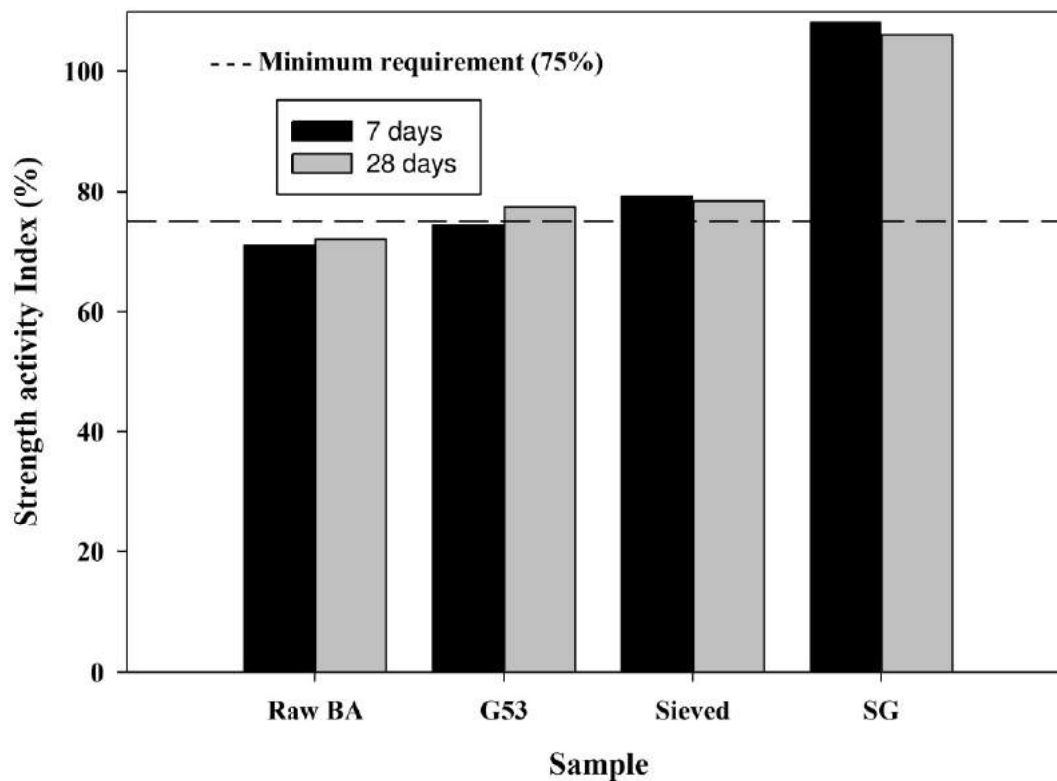


Figure 5.23: Compressive strength of mortars with sieved and ground samples of bagasse ash after 7 and 28 days curing

The pozzolanic activity of Sieved and Ground sample (SG) was 106 % which was higher than control sample as shown in Figure 5.23. 700 °C Burnt and Ground sample (BG) showed 90 % pozzolanic activity which was significantly higher than minimum requirement (75%), as seen in Figure 5.24. Although pozzolanic activity index value of the burnt and ground (BG) sample was increased from 86 % to 90 % by the process of grinding, it showed lesser index value than the SG sample, possibly due to continued presence of fibrous carbon particles. Greater amounts of fibrous particles were observed (marked as C) in the SEM micrograph of the BG sample, as shown in Figures 5.25 and 5.26. The grinding of sieved sample significantly increased its reactivity because of removal of coarse fibrous carbon particles (in the sieving process itself) before grinding.

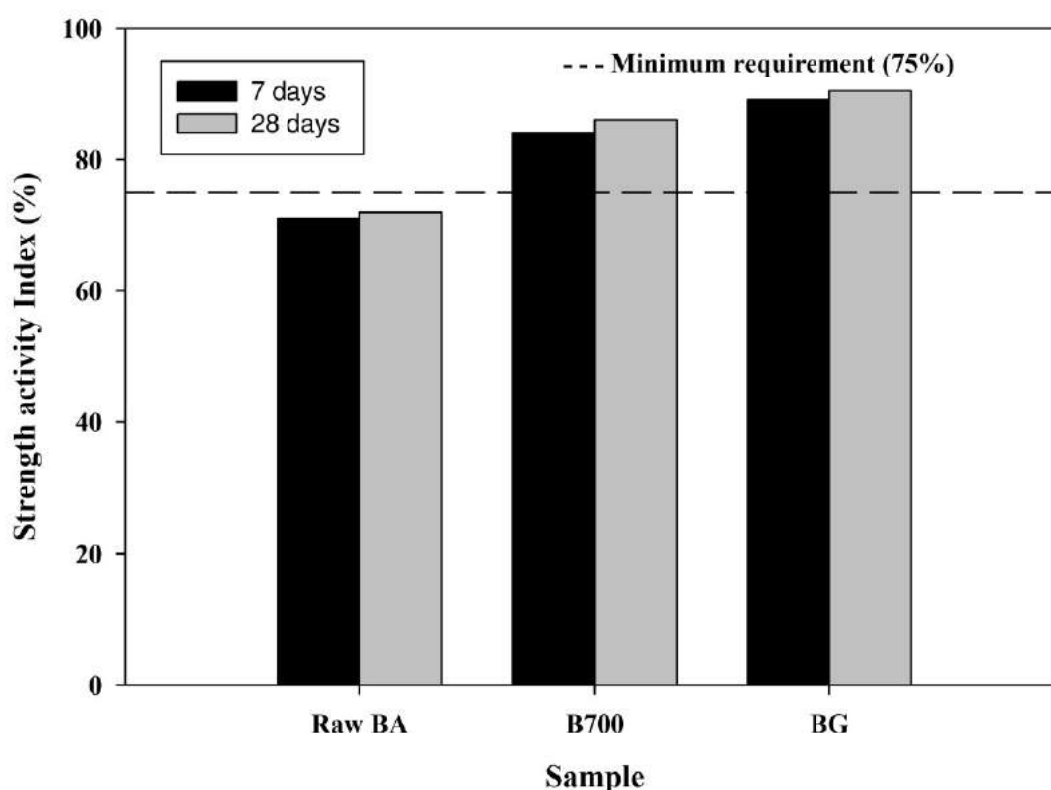


Figure 5.24: Compressive strength of mortars with burnt and ground samples of bagasse ash after 7 and 28 days curing

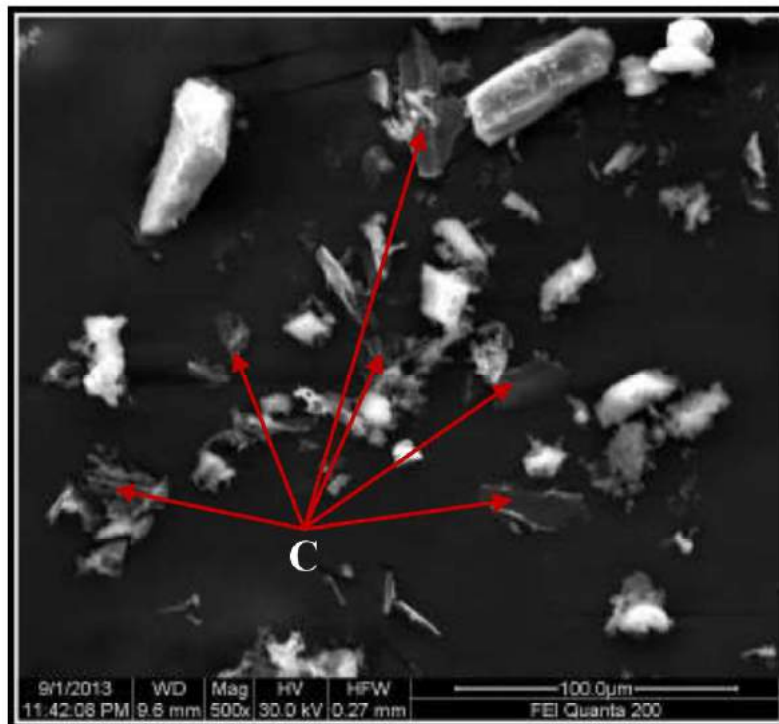


Figure 5.25: SEM Micrograph of BG samples showing the presence of Carbon particles

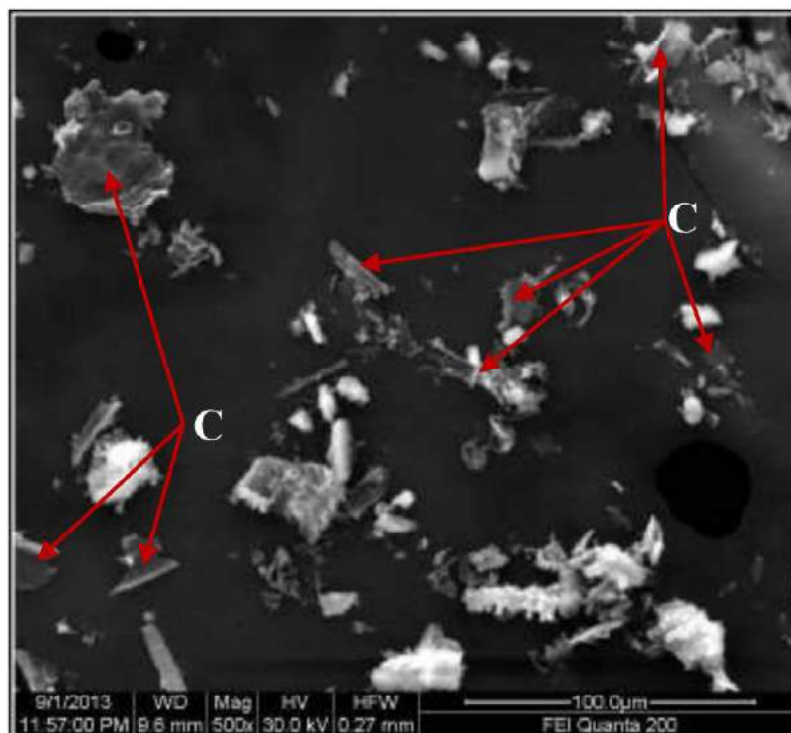


Figure 5.26: SEM micrograph of BG samples, with more Carbon particles

The Frattini test was used to validate strength activity test results and also to find the pozzolanic reactivity of sieved sample, fibrous particles, white particles and SG sample. Concentrations of $[\text{OH}]^-$ and $[\text{Ca}]^{2+}$ were determined for the samples after 8 days and plotted on the saturation curve as described in BS EN 196(5)-2005. For sieved bagasse ash, $[\text{CaO}]$ and $[\text{OH}]^-$ concentrations after 8 days were 21.70 and 29.12 mmol/l respectively. Results for white particles, fibrous particles and raw bagasse ash were above the saturation curve, as shown in Figure 5.27, that represented no (or insufficient) pozzolanic activity as per standard. Raw bagasse ash showed around 70 % of pozzolanic activity in strength activity test, but insufficient pozzolanic activity in Frattini test.

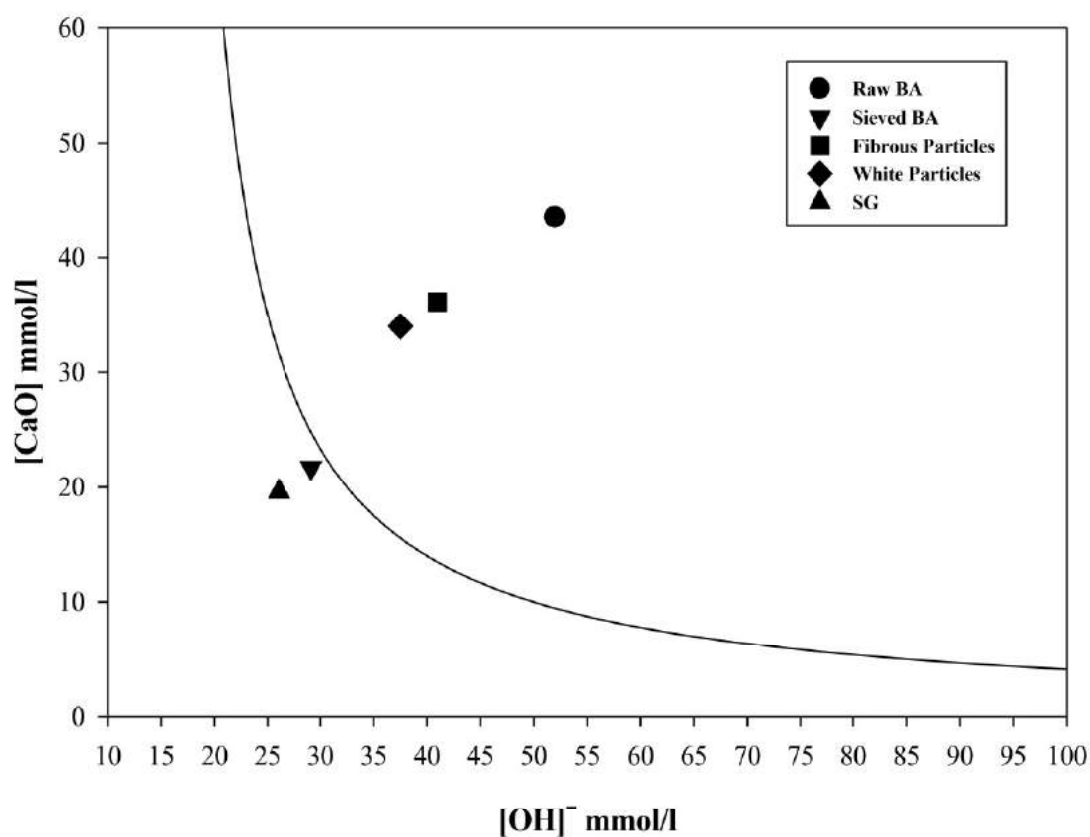


Figure 5.27: Frattini graph for the various samples

This is attributed to the possibility of presence of more number of coarse carbon particles in the small quantity of (2 g) test sample used in the Frattini test. Results of sieved bagasse ash and SG samples were well below the Frattini saturation curve due to higher consumption of calcium hydroxide associated with additional pozzolanic reaction.

Thus, sieved sample and SG sample can be defined as good pozzolanic materials as per Frattini test. Lower reactivity of burnt samples above 700 °C due to formation of white particles was validated with Frattini test. Results from Frattini test agreed well with the strength activity test results.

5.3.4 Comparison of processing methods

It is evident from the results presented in this chapter that the pozzolanic performance of raw bagasse ash significantly varied with respect to processing method. For the purpose of an overall comparison, the pozzolanic activity of bagasse ash prepared with various processing methods is shown in Figure 5.28. The performance of 8 samples is shown here: Raw bagasse ash (Raw BA), Coarse fibrous unburnt (CFU), Fine fibrous unburnt (FFU), Bagasse ash burnt to 700 °C (B700), Bagasse ash ground to finer than 53 µm (G53), Bagasse ash sieved through 300 µm sieve (Sieved), Bagasse ash burnt at 700 °C and then ground to cement fineness, i.e. 300 m²/kg (BG), Bagasse ash sieved through 300 µm sieve and then ground to cement fineness (SG).

The results clearly indicate that raw bagasse ash needs to be processed for use as a supplementary cementitious material. Burning at 700 °C improved pozzolanic activity of raw bagasse ash from 72 % to 86 % at 28 days. Additional grinding of burnt material (700 °C) to cement fineness by using ball mill enhanced pozzolanic activity to an additional extent (90 %).

However, a simple sieving process (passing through 300 µm sieve) increased pozzolanic activity well above the minimum requirement (75%). Further grinding of sieved material improved pozzolanic activity index from 79 % to 106 %, which was the maximum possible pozzolanic index value obtained in this study. Strength activity index of sieved and ground sample (SG) was 108 % and 106 % at 7 and 28 days respectively – only marginally different. However, the absolute value of the strength was greater at 28 days as compared to 7 days.

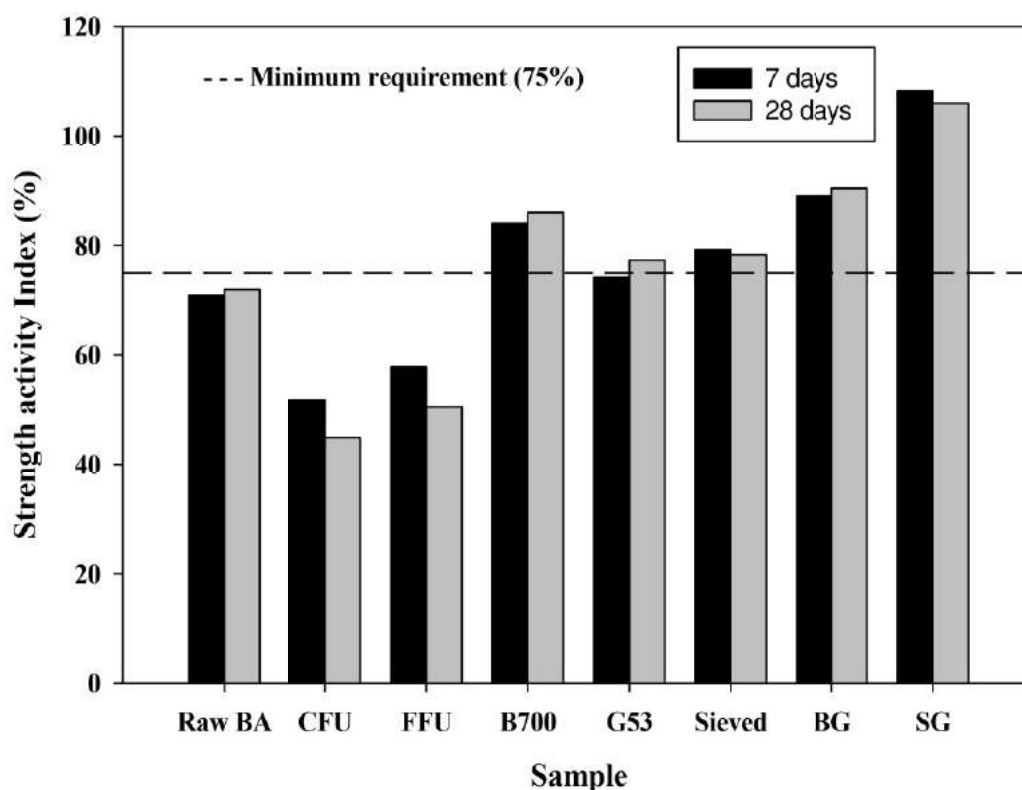


Figure 5.28: Comparison of strength activity index values for different bagasse ash samples

It is essential to select suitable processing methodology for maximum pozzolanic activity with minimum processing energy to reduce the environmental impacts. Although controlled burning at 700 °C showed sufficient pozzolanic activity, it requires additional energy for burning of raw bagasse ash and skilled supervision and strict control on the process, because increase in temperature directly affects pozzolanic activity of the sample. The loss on ignition of the burnt sample at 700 °C was 14% higher than the permissible limit as per standard. Presence of fibrous particles in the burnt sample leads to more water requirement for the same workability. Complete removal of fibrous particles is needed to achieve maximum pozzolanic performance, lower the value of loss on ignition and provide better workability. This study indicates that raw bagasse ash can be sieved by using industrial sieve shaker in cement plant and directly ground with cement and gypsum in the ball mill (or alternative grinding facility), similar to the process of fly ash based Portland pozzolana cement production. Based on the requirement

of minimum processing with maximum pozzolanic activity, sieving and further grinding to cement fineness (SG) is highly recommended from this study.

5.4 SUMMARY

The influence of different processing methods on the pozzolanic performance of bagasse ash was comprehensively investigated in this study. Controlled burning of raw bagasse ash was found to significantly influence the pozzolanic activity. At higher burning temperatures (greater than 700 °C), a reduction in the pozzolanic reactivity was observed as a result of crystallization of cristobalite from the amorphous silica. The study on the effect of grinding of the raw bagasse ash to different sizes on the pozzolanic performance showed that direct grinding of the bagasse ash is not advisable because of the preferential grinding of fibrous carbon particles in the process. In addition to this, further grinding of burnt and sieved samples (to cement fineness) was studied to understand the combined effects on the pozzolanic performance of bagasse ash. After a thorough assessment of the performance, sieving of the material through 300 µm sieve and further grinding to cement fineness (300 m²/kg) was suggested as the desirable processing methodology for bagasse ash for maximum pozzolanic activity, low value of loss on ignition, and minimum processing energy inputs.

CHAPTER 6

PRODUCTION OF SUGARCANE BAGASSE ASH BASED PORTLAND POZZOLANA CEMENT AND EVALUATION OF COMPATIBILITY WITH SUPERPLASTICIZERS

6.1 INTRODUCTION

Production and characteristics of new cementitious blends with processed sample of sugarcane bagasse ash are described in this chapter. Utilization of various supplementary cementitious materials significantly influences fresh and hardened properties of concrete. Interaction of pozzolanic material with cement and chemical admixtures, especially superplasticizers, produces diverse effects on the fresh properties of blended cement concrete. This chapter aims to ascertain the effect of different bagasse ash replacements of cement on the compatibility with superplasticizers in cement paste. Sugarcane bagasse ash based Portland pozzolana cements were produced with five different levels of replacement – 5, 10, 15, 20 and 25 %. Marsh cone and mini-slump test were used to determine the effect of superplasticizer types and water binder ratio on the saturation dosage.

6.2 PRODUCTION OF SCBA BASED PORTLAND POZZOLANA CEMENTS

In this study, instead of direct addition of bagasse ash as a pozzolanic material to the concrete, SCBA based Portland pozzolana cements were produced with different replacement levels. A systematic methodology for the production of blended cements was developed based on proper characterization and suitable processing method. Production of SCBA based PPC is summarized as follows.

- Raw bagasse ash has high moisture content because water is mixed during disposal. Raw bagasse ash was dried at 105 – 110 °C for 24 hours to remove evaporable moisture content, and the dried sample was used for further processing.

- A detailed material characterization (Physical, chemical, mineralogical and microstructural characterization) was conducted for raw bagasse ash (described elaborately in Chapter 4). The sample of sugarcane bagasse ash was found to have completely burnt silica-rich fine particles and two different types of carbon-rich fibrous unburnt particles. It is imperative to characterize the different particles in the raw bagasse ash and obtain maximum reactive components for blended cement production. In addition, a comprehensive investigation of pozzolanic performance of different particles present in the raw sugarcane was performed by using five different methods (described in Chapter 4). From the test results, it was found that fine burnt particles had higher pozzolanic activity than minimum requirement as per standard (ASTM 618-12a) and carbon rich fibrous particles had no pozzolanic activity. Based on these observations, removal of fibrous unburnt carbon particles was adopted in the production of SCBA blended cements.
- The effect of different processing methods (burning, grinding, chemical activation, sieving and combination of above methods) on the pozzolanic performance of dried raw bagasse ash was investigated (explained comprehensively in Chapter 5). Based on the comparison of pozzolanic performance of different processed materials, complete removal of carbon rich fibrous unburnt particles by sieving through 300 μm sieve and further grinding to cement fineness (300 m^2/kg) using ball mill was recommended as the best strategy for producing the blending material for production of SCBA based Portland pozzolana cements. Production of SCBA based Portland Pozzolana cement is illustrated in Figure 6.1.
- The selection of suitable processed material is based on maximum pozzolanic activity as well as desirable material characteristics (lower loss on ignition, improved workability and better performance in concrete). Loss on ignition of raw bagasse ash was 21% due to presence of unburnt carbon particles (LOI of FFU and CFU particles were 72% and 74% respectively). Complete removal of fibrous particles in the sieved material results in the reduction of loss on ignition to 3-6 % which is well below the allowable limit as per ASTM C618-12a. Water requirement for raw bagasse ash and processed sample was determined for the same control flow. The removal of fibrous particles and further grinding to cement fineness led to a reduction in the water requirement from 320 ml to 255 ml.

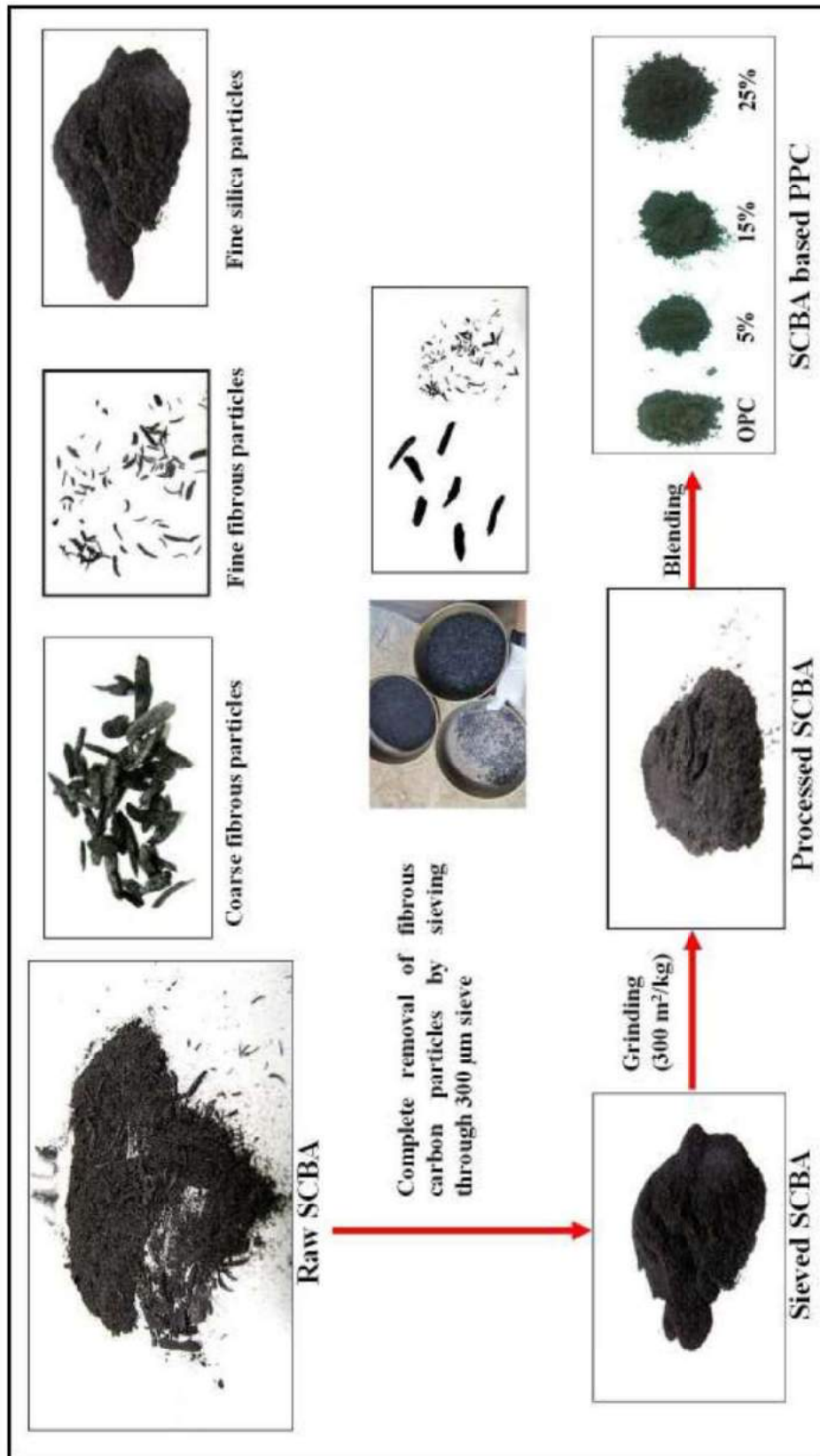


Figure 6.1: Production of SCBA based Portland Pozzolana cement

- From the above discussion, it is clear that removal of fibrous unburnt particles from raw bagasse ash not only increases pozzolanic reactivity but also reduces water demand and loss on ignition. Processed bagasse ash was used for the production of SCBA based PPC.
- The sieved and ground material was then used as replacement for ordinary Portland cement (OPC 53 grade conforming to IS 12269-2008) in different proportions (5, 10, 15, 20 and 25 % mass replacements) by blending to produce the SCBA based Portland pozzolana cements. A kitchen blender was used to achieve uniform blending. The choice of 5% replacement can be justified by the fact that the Indian OPC specifications (IS 12269-2008; IS 8112-2005) permit the inclusion of up to 5% ground mineral additives. On the other hand, 25% can be considered to be a typical replacement level of fly ash in the Portland pozzolan cement produced commonly in India (IS 1489-2005). After the blending process, the materials were stored in individual air tight containers.

6.3 CHARACTERISTICS OF SCBA BASED PORTLAND POZZOLANA CEMENTS

Physical characteristics of SCBA blended cements were determined as per IS 4031-2005 and the results are presented in Table 6.1. Specific gravity was decreased with increase in replacement of bagasse ash due to low relative density of processed bagasse ash. Expansions of all blended cements in the soundness test (using Le Chatelier apparatus) were observed to be lesser than the permissible limit. Specific surface area of all blended cements was determined by Blaine's air permeability test as per ASTM C204-11. Fineness was in a narrow range for all cements (300 - 320 m²/kg). This is as a result of controlled grinding of sieved bagasse ash to similar fineness as ordinary Portland cement (310 m²/kg), which was used in this study for blending. This was further confirmed by particle size distribution of blended cements by using laser particle size analyzer. Ordinary Portland cement and blended cements had similar particle size distributions as shown in Figure 6.2. Because of low specific gravity of processed bagasse ash, the powder volume was increased compared to control paste and led to more water requirement for the same workability, which is clearly reflected in the consistency value

of the blended cement paste. In addition to that, a reduction in the specific gravity of blended cements was observed with increase in the replacement. Although the initial and final setting times were increased with increase in replacement, the observed values were well within the permissible limits described in the standard (IS 1489 Part 1-2005).

Table 6.1: Physical characteristics of SCBA blended cements

Characteristics	OPC	5% PPC	10 % PPC	15 % PPC	20 % PPC	25% PPC	Relevant standard
Specific gravity	3.16	3.13	3.02	2.97	2.86	2.83	IS 4031 (11)-2005
Fineness (m ² /kg)	310	308	306	313	317	308	Min: 300 m ² /kg ASTM C204-11
Soundness, Expansion (mm)	1.61	1.14	1.30	1.10	1.36	1.18	Max: 10 mm IS 4031 (3)-2005
Consistency (%)	30	30	35	40	40	44	IS 4031 (4)-2005
Initial setting time(min)	125	135	135	180	190	225	Min: 30 min IS 4031 (5)-2005
Final setting time (min)	165	165	205	280	285	295	Max: 600 min IS 4031 (5)-2005

The elemental composition of blended cements was determined by X-ray fluorescence and the results are presented in Table 6.2. As expected, the silica content in the blended cement increased with increase in replacement. As a result of higher K₂O content present in the processed bagasse ash, increase in K₂O was perceived for blended cements. Mineralogical characteristics of ordinary Portland cement and blended cements were determined by X-ray diffraction technique. No significant differences were observed in the diffraction patterns of blended cements, as shown in Figure 6.3.

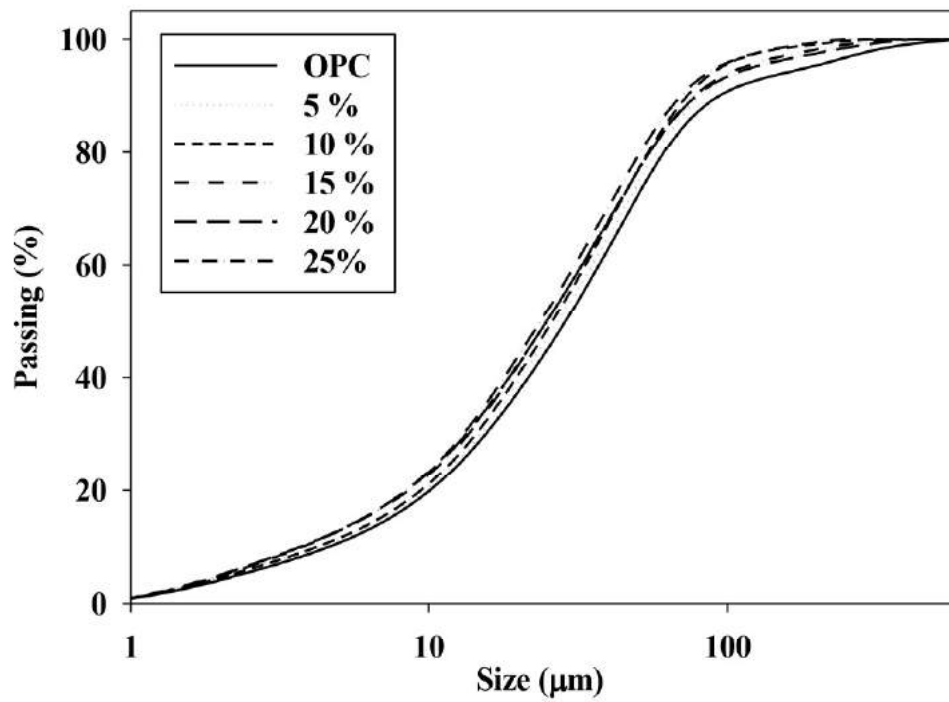


Figure 6.2: Particle size distribution for the OPC and blended cements in this study

Table 6.2: Chemical composition of SCBA blended cements

Oxide composition	OPC	SCBA	5 % PPC	10 % PPC	15 % PPC	20 % PPC	25 % PPC
SiO ₂	20.68	75.67	21.11	25.82	31.16	36.41	40.53
Al ₂ O ₃	4.12	1.52	5.57	5.52	5.44	5.42	5.36
Fe ₂ O ₃	5.44	2.29	4.10	4.10	4.08	4.07	4.06
CaO	60.36	6.62	58.92	55.84	52.46	49.04	46.03
MgO	0.83	1.87	0.92	0.95	0.98	1.01	1.04
K ₂ O	0.27	9.59	0.31	0.31	0.64	1.01	1.25
Na ₂ O	0.23	0.12	0.20	0.20	0.20	0.20	0.20

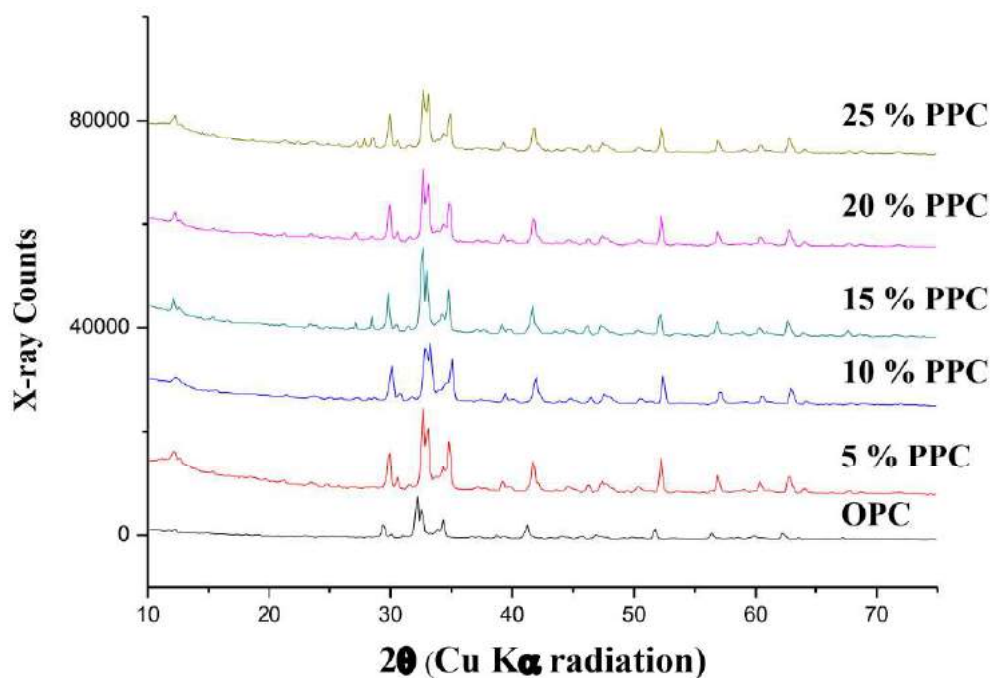


Figure 6.3: X-ray diffraction patterns of OPC and blended cements

6.4 COMPATIBILITY OF SCBA BASED PORTLAND POZZOLANA CEMENT WITH SUPERPLASTICIZERS

The method of preparation of paste, type of mixer, time of addition of superplasticizer etc. are governing factors affecting the cement superplasticizer interaction (Jayashree, 2009). To avoid a negative influence of these parameters, similar methods of mixing and preparation of paste were adopted for all the combinations of cement and superplasticizers. Various methods are available to evaluate rheological parameters and relative fluidity. However, most of the methods including rheometry need specialized equipment, controlled environment and skilled operators. Simple methods such as Marsh cone test and mini-slump test were selected in this study. Three different replacements of bagasse ash (10 %, 15 %, and 20 %), two different water to cementitious materials ratios (0.40 and 0.45) and two different superplasticizers (GL and DC) were used in this study. GL was polycarboxylic ether (PCE) based, while DC was sulphonated naphthalene

formaldehyde based (PCE); their characteristic properties are presented in Table 3.6 (Chapter 3).

6.4.1 Method of paste preparation

Mixing methods significantly influence the fluidity of paste for a given dosage of superplasticizer (Ramachandran, 2002; Atcin, 1998). Jayashree and Gettu (2008) studied the effect of different mixing methods on saturation dosage and mixing, and the Hobart mixer with B-flat beater was suggested for uniform and thorough mixing. In this study, cement and 70 % of water was mixed for one minute in Hobart mixer at lower shaft speed of 139 rpm. Then the superplasticizer was mixed with remaining 30 % of water and added to the paste to achieve better adsorption of superplasticizer and effective repulsion of cement particles. After the addition of superplasticizer, the paste was thoroughly mixed at low speed for two minutes. Afterwards the mixer was stopped and sides of mixer bowl were scraped with a spatula within 15 seconds. Again the paste was mixed for an additional two minutes at medium shaft speed of 285 rpm. In a similar way, the paste was prepared for all the combinations of cement and superplasticizer. Materials were conditioned at 25 °C before 24 hours of mixing in a temperature controlled environmental chamber. Preparation and fresh testing of all pastes was done inside the chamber to eliminate influence of temperature on the cement superplasticizer interaction. Marsh cone flow time and mini-slump spread were measured just after mixing and denoted as 5 minutes reading. The paste was then kept within the mixing bowl and covered with a thin plastic sheet at the controlled temperature for 60 minutes. After 60 minutes, the paste was mixed for 15 seconds at low speed before testing for the 60 minutes reading.

6.4.2 Marsh cone test

Marsh cone is a simple metallic funnel type cone with long neck and small orifice of 8 mm diameter based on EN 445 standard (Camoës, 2005; Jayashree and Gettu, 2008). A schematic diagram of Marsh cone apparatus is presented in Figure 6.4 and all dimensions are marked in mm. The relative fluidity of paste is measured by the flow time of a given

cement-superplasticizer combination. 1000 ml of paste was prepared. The Marsh cone was attached on the stand and a graduated glass cylinder was kept at the bottom of the orifice. 1000 ml of prepared paste was poured into the truncated cone portion. While pouring the paste, the orifice was closed with the index finger and after complete pouring, the paste was allowed to flow through the small orifice as depicted in Figure 6.5. The time taken for 500 ml paste flow was noted. This flow time is directly related to the fluidity of the cement paste as well as effective dispersion of cement particles by superplasticizers.

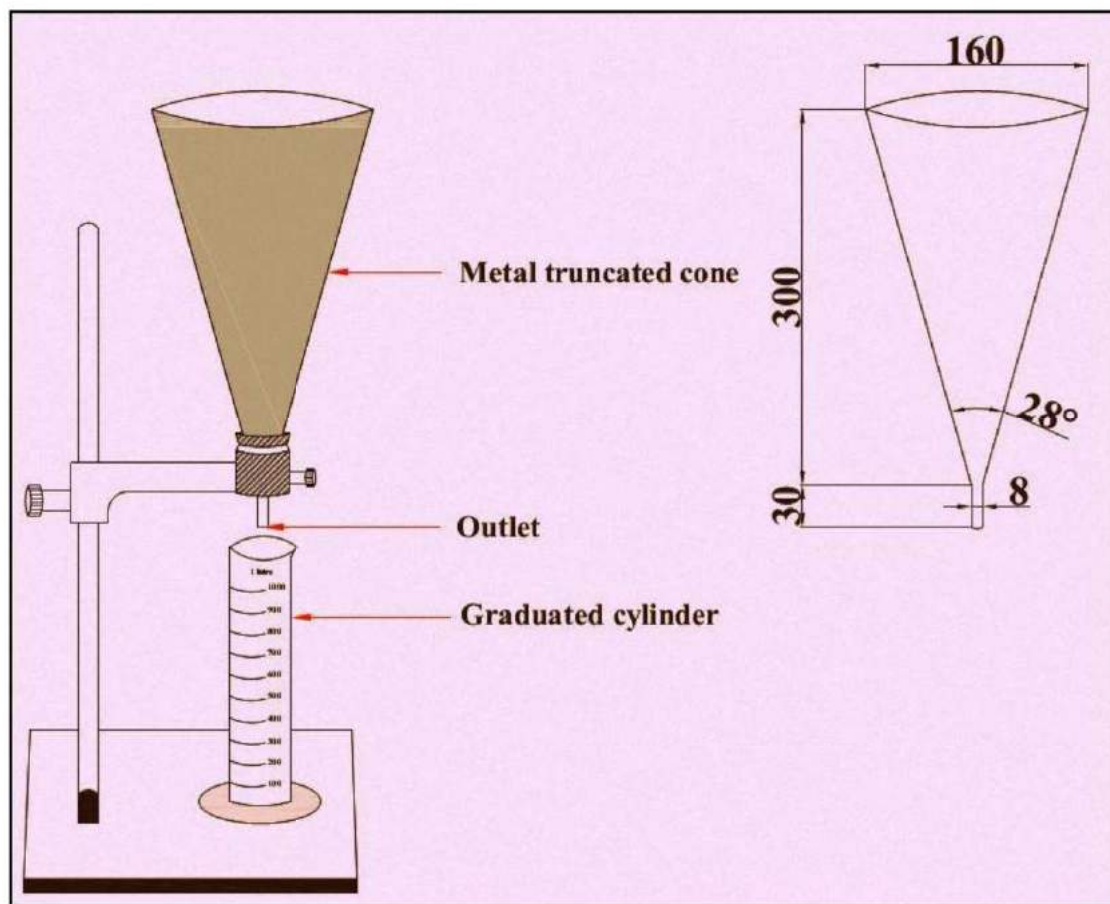


Figure 6.4: Schematic diagram of Marsh cone apparatus

For constant water binder ratio and replacement, different dosages of superplasticizer were used and the corresponding flow time was measured just after mixing (5 minutes) and at 60 minutes. For an increase in the dosage of superplasticizer, dispersion of cement particles was increased and relative fluidity also improved until saturation dosage. Because of increase in relative fluidity, a significant drop in flow time was observed up to

saturation dosage. At saturation dosage, the maximum adsorption of superplasticizer is reached and further increase in dosage cannot alter fluidity of the paste (Hallal et al., 2010). Therefore, saturation dosage can be taken as the dosage at which further increases in superplasticizer dosage cannot notably alter the flow time.

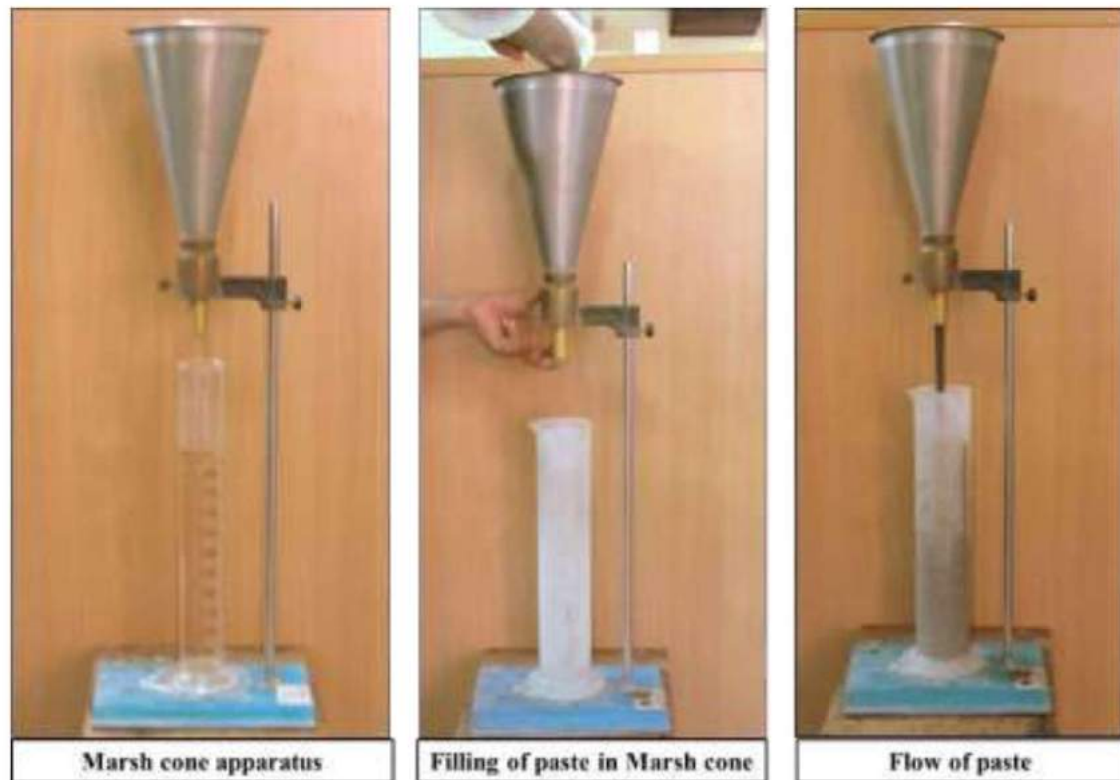


Figure 6.5: Marsh cone test being performed

6.4.3 Mini-slump test

Mini-slump cone is a small size truncated cone type mould (see Figure 6.6) similar in relative dimensions to Abram's slump cone used for concrete slump test. It was developed by Kantro (1980) and is used by many researchers for paste study. A schematic diagram of mini-slump apparatus is shown in Figure 6.7 (all dimensions are in mm). A mini slump cone with 19 mm upper diameter and 37 mm bottom diameter with 57 mm height was used in this study.



Figure 6.6: Mini-slump apparatus

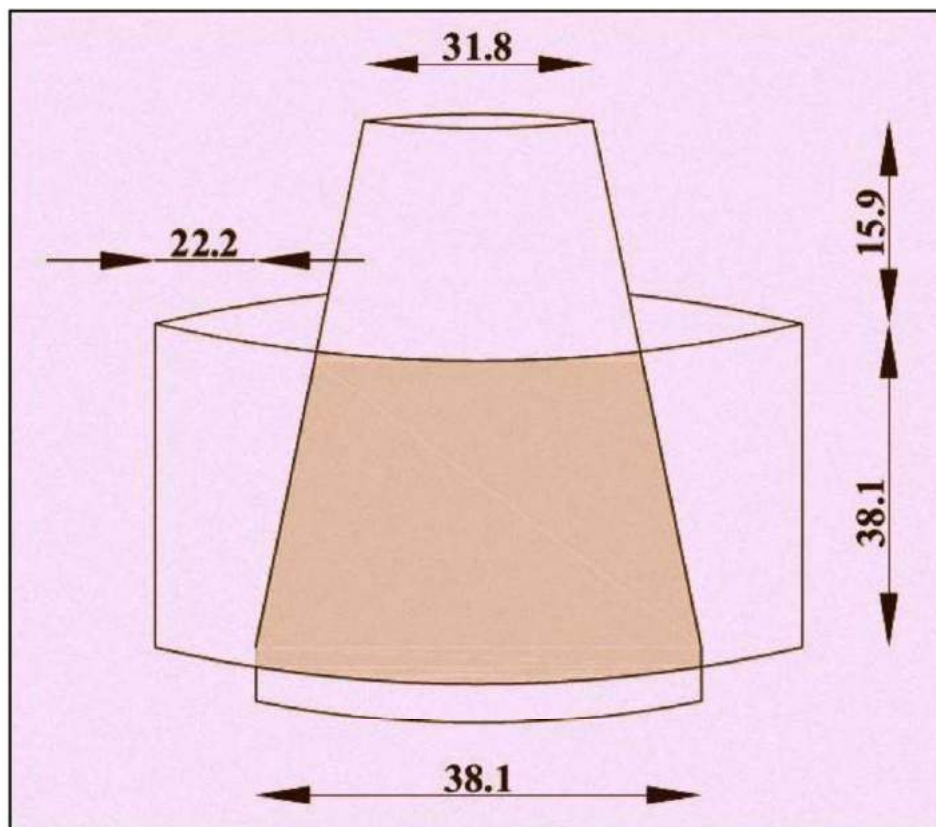


Figure 6.7: Schematic diagram of mini-slump apparatus

A square shaped glass plate was used as the base for testing. The paste was prepared with the required combination of cement and superplasticizer. The mini slump cone was placed at the centre of the glass plate as shown in Figure 6.8, and then filled with the paste. After complete filling, the cone was lifted slowly and the paste was allowed to spread on the glass plate. The diameter of paste spread was measured and the average spread was reported as mini-slump spread in this study. Mini slump spread was measured just after mixing of paste (denoted as 5 min spread) and after 60 minutes to check the loss of fluidity of paste.

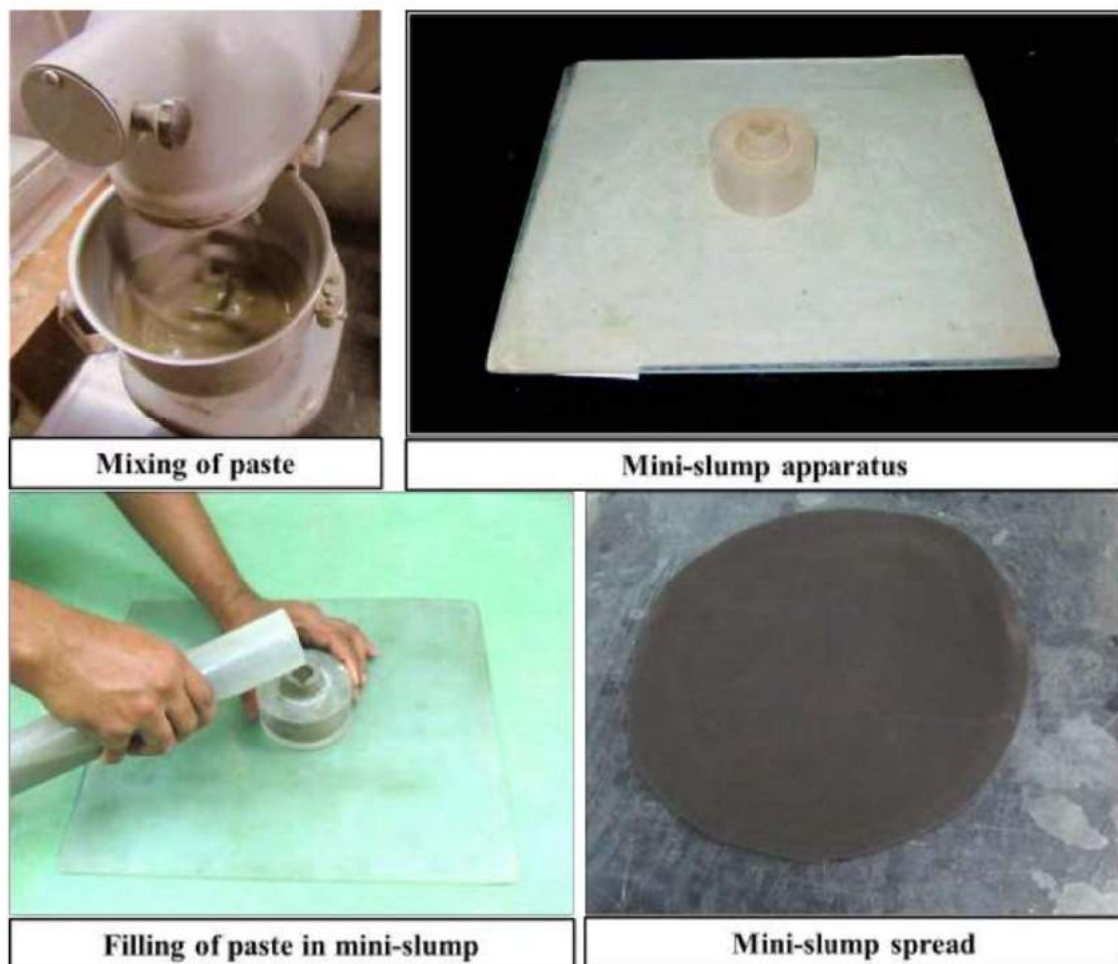


Figure 6.8: Conduct of mini-slump test

6.5 RESULTS AND DISCUSSION

The Marsh cone test results for pastes with w/b of 0.45 are presented in Figures 6.9 - 6.12. From the Marsh cone flow curves, it is clearly observed that incorporation of SCBA highly influenced the saturation dosage of superplasticizer. The control paste without SCBA replacement had low saturation dosages of 0.05 % and 0.1 % for GL and DC admixtures respectively (See Figure 6.9). For a particular dosage of superplasticizer and water binder ratio, the measured Marsh cone flow time of SCBA based pastes was higher than the control paste. In other words, the saturation dosage was increased with increase in SCBA replacement. The saturation dosage of GL was increased from 0.1 % to 0.4 % for increase in replacement from 10 % to 20 % as shown in Figures 6.10 to 6.12.

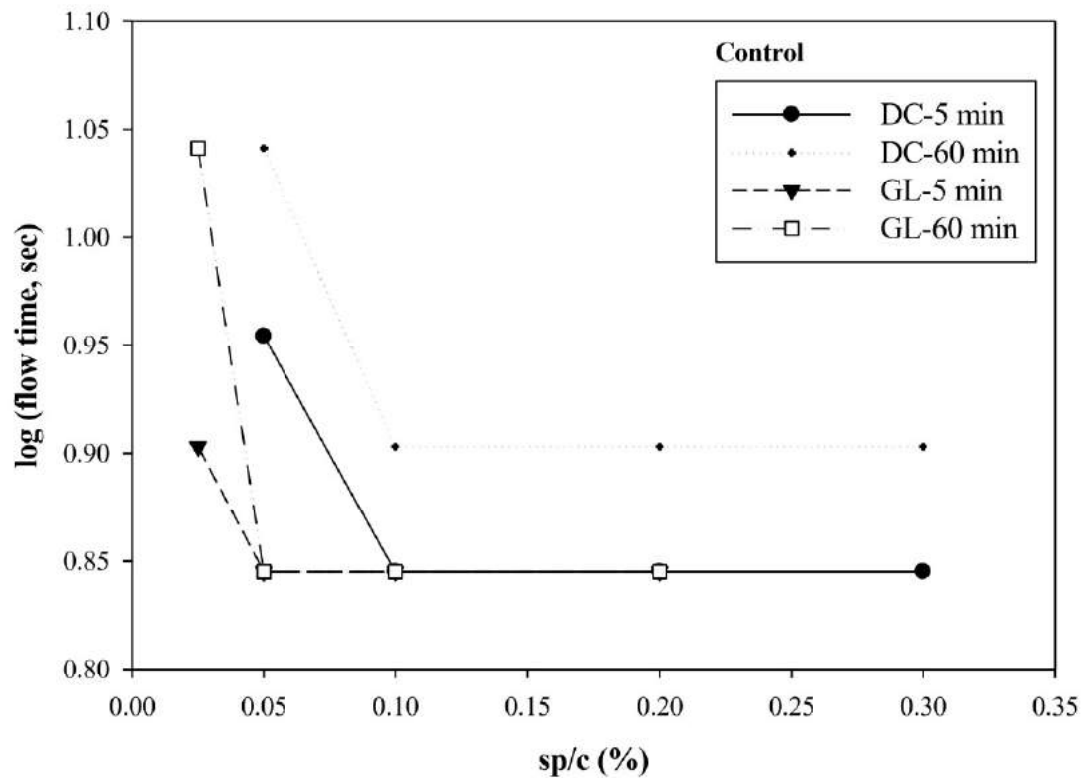


Figure 6.9: Marsh cone test results for control paste (w/b=0.45)

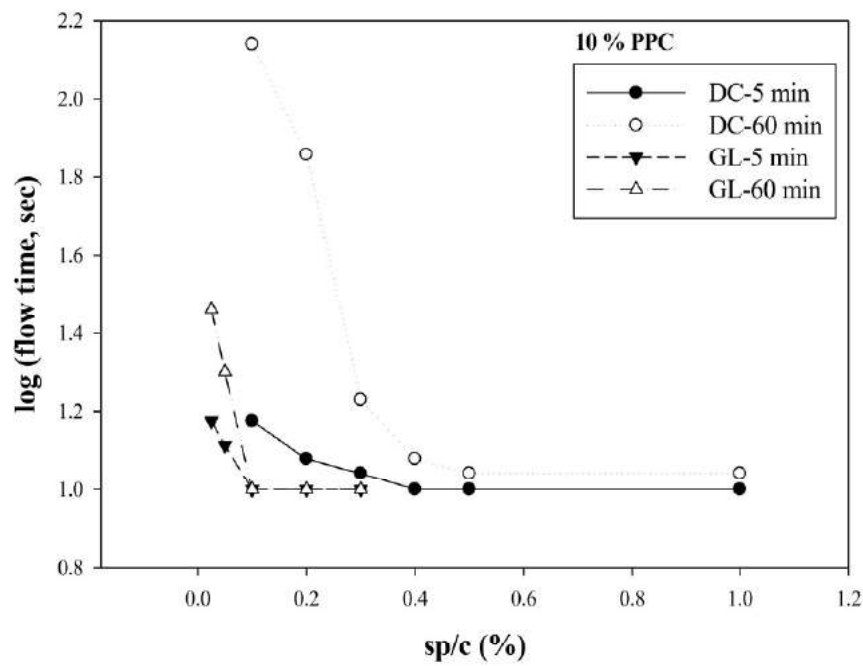


Figure 6.10: Marsh cone test results for 10 %PPC (w/b=0.45)

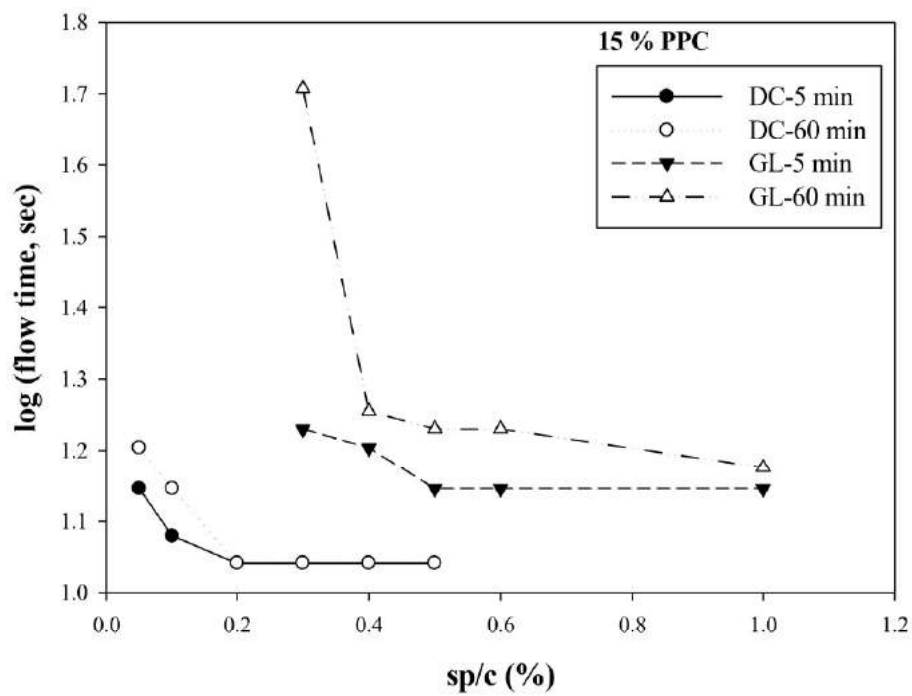


Figure 6.11: Marsh cone test results for 15 %PPC (w/b=0.45)

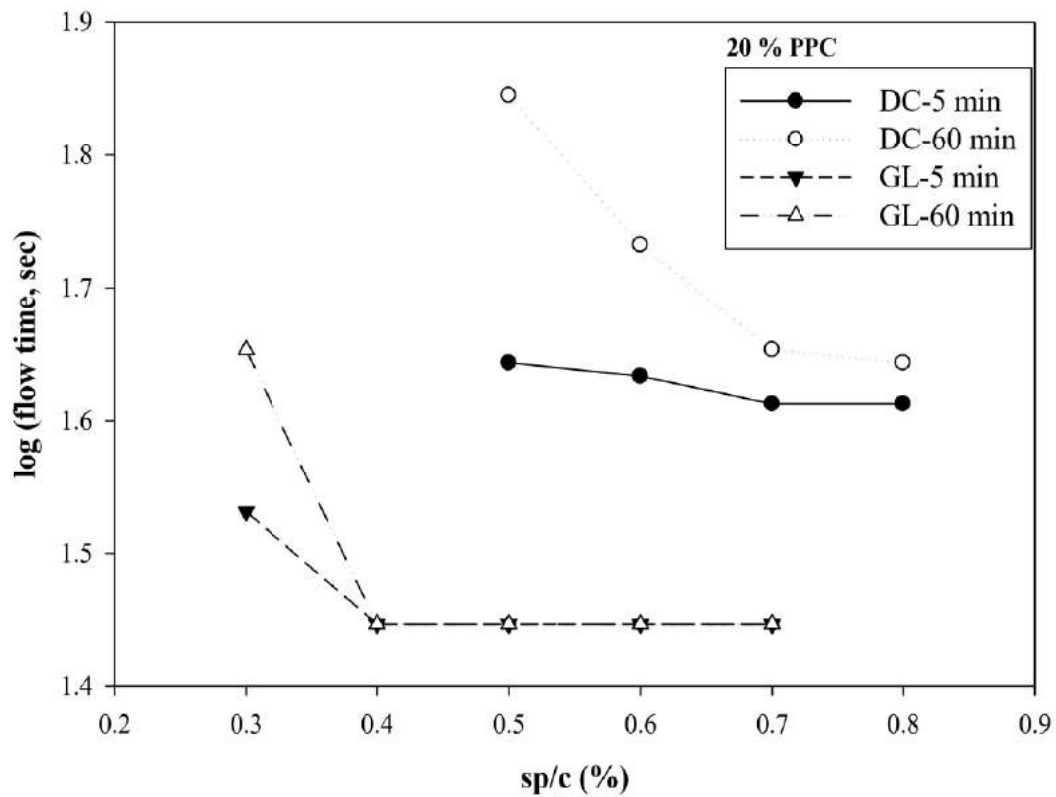


Figure 6.12: Marsh cone test results for 20 %PPC (w/b=0.45)

The performance of SCBA based cements with superplasticizers significantly changed with the type of superplasticizer. This was clearly noticed from the observed value of saturation dosages. Saturation dosage of DC (suphonated naphthalene based admixture) was 0.4 % for 10 % replacement whereas polycarboxylic based GL admixture had only 0.1 % dosage as optimum dosage (see Figure 6.10) for the same replacement and water binder ratio. A similar trend was observed for other SCBA replacements as depicted in Figures 6.11 and 6.12. Effective dispersion of cement particles can be achieved by GL compared to DC admixture because of combined effect of electrostatic repulsion and steric hindrance. Similar results were observed in the previous research studies for metakaolin and silica fume (Agullo et al., 1999; Jayashree, 2009). Mini-slump test was carried out for the same SCBA based cements and superplasticizer combinations to check relative fluidity and results are shown in Figures 6.13-6.16. Mini-slump results strongly agreed with Marsh cone test results.

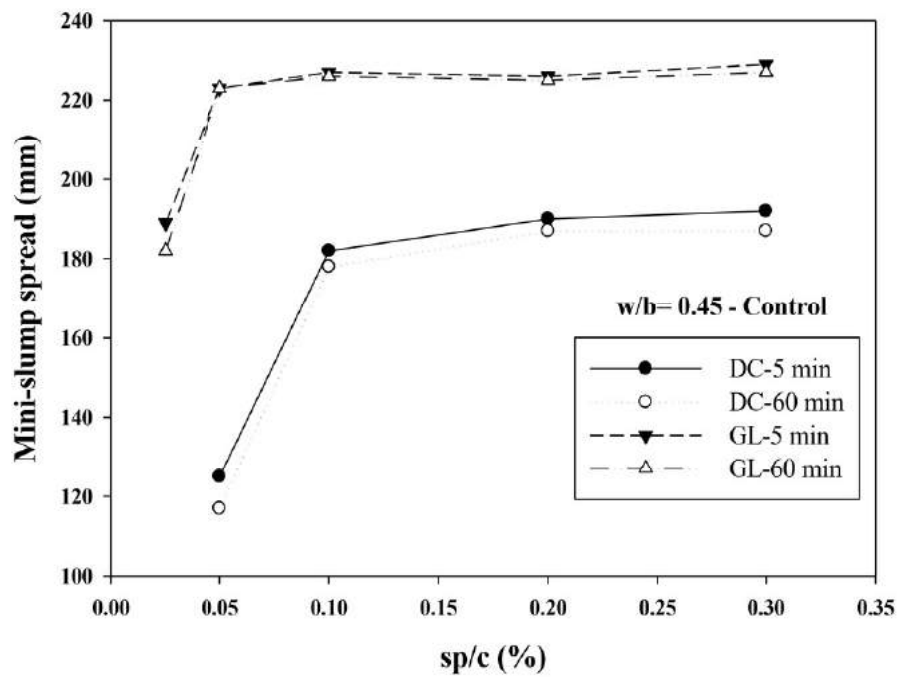


Figure 6.13: Mini-slump test results for control (w/b=0.45)

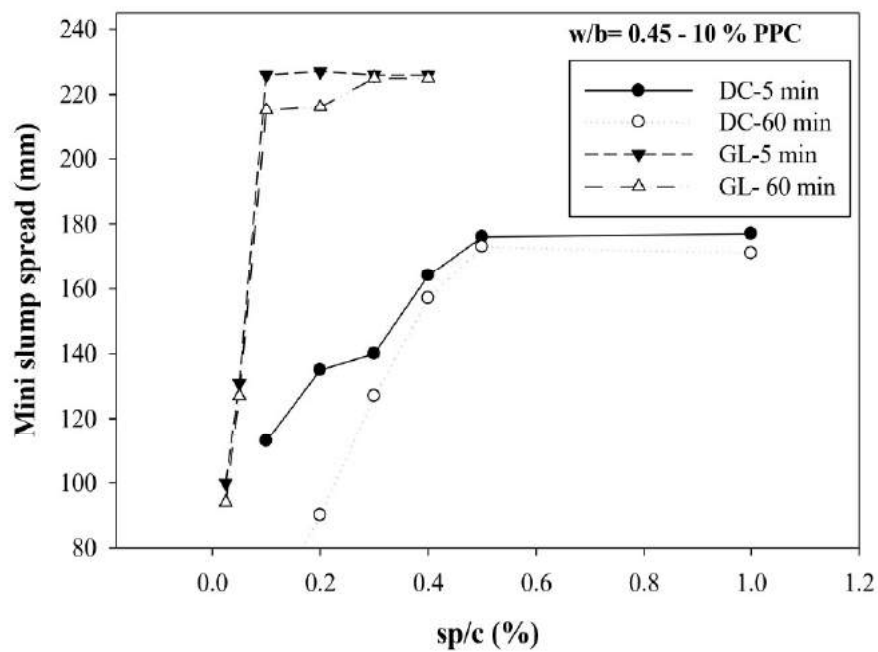


Figure 6.14: Mini-slump test results for 10 % PPC (w/b=0.45)

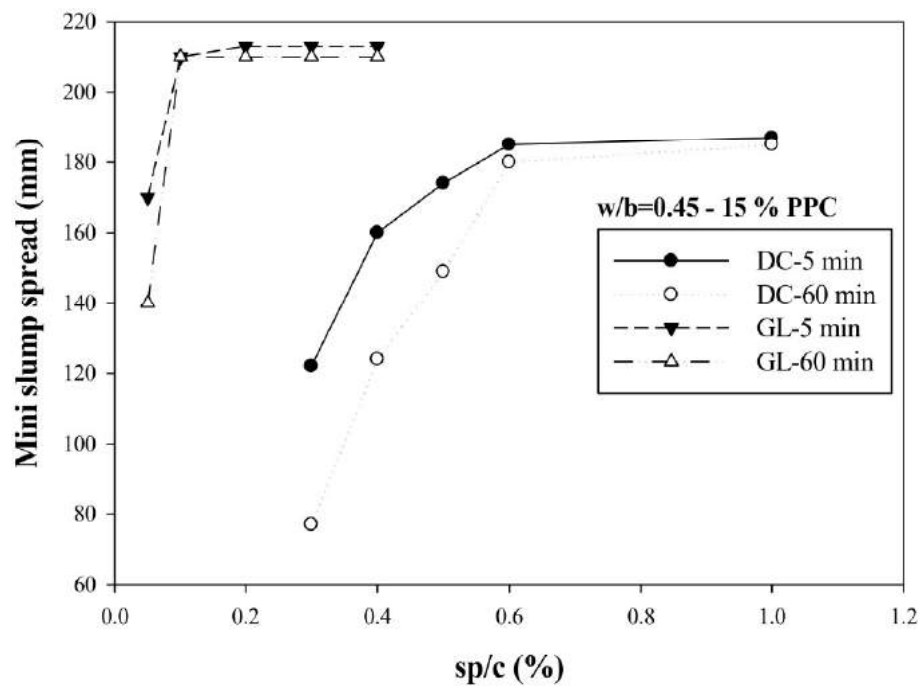


Figure 6.15: Mini-slump test results for 15 % PPC (w/b=0.45)

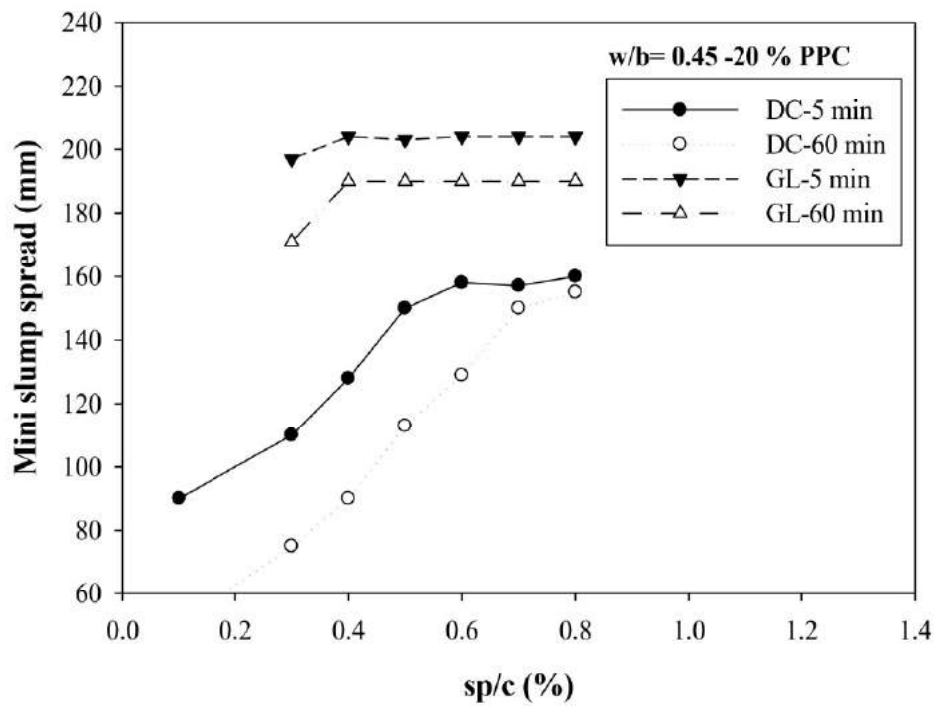


Figure 6.16: Mini-slump test results for 20 % PPC (w/b=0.45)

The mini-slump spread was increased with increase in superplasticizer dosage. However, after saturation dosage only slight change in the spread was observed as shown in Figures 6.13-6.15. In the case of Marsh cone test, saturation dosage was clearly detectable in the flow curve due to significant drop in flow time at all dosages before saturation dosage. After optimum dosage, both admixtures showed no significant changes in the flow curve as shown in Figures 6.9-6.12.

Marsh cone test results for w/b of 0.40 are shown in Figures 6.17-6.20. From the Marsh cone flow curves, it was clearly seen that reduction in water-binder ratio increased the saturation dosage of superplasticizer. For example, the saturation dosage of GL admixture with 15 % PPC was found to be 0.2 % and 0.3 % for water binder ratio of 0.45 and 0.40 respectively as shown in Figures 6.11 and 6.19. A similar trend was clearly observed for the other replacements. Because of lesser amount of water present in the paste, the relative fluidity of paste was decreased, and this led to an increase in the flow time for the same replacement and same superplasticizer dosage. For 0.40 water binder ratio, lesser value of mini-slump spread was observed for all the combinations of cement and superplasticizer dosage compared to 0.45 water-binder ratio.

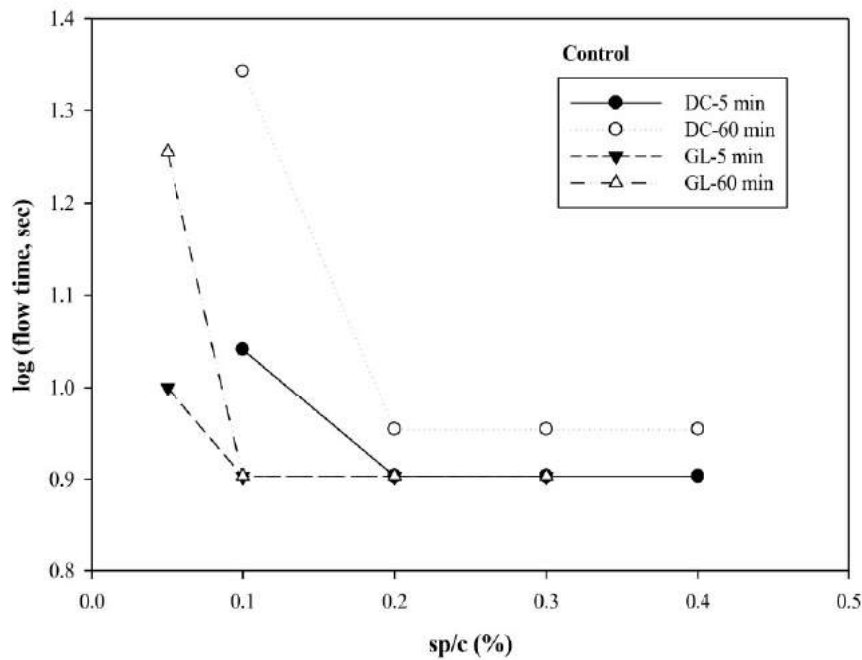


Figure 6.17: Marsh cone test results for control paste (w/b=0.40)

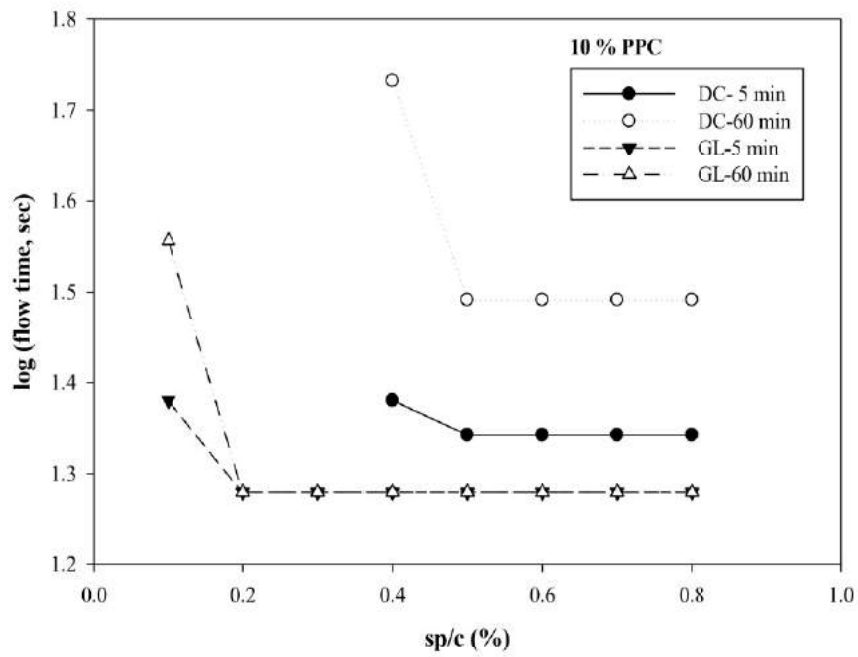


Figure 6.18: Marsh cone test results for 10 % PPC (w/b=0.40)

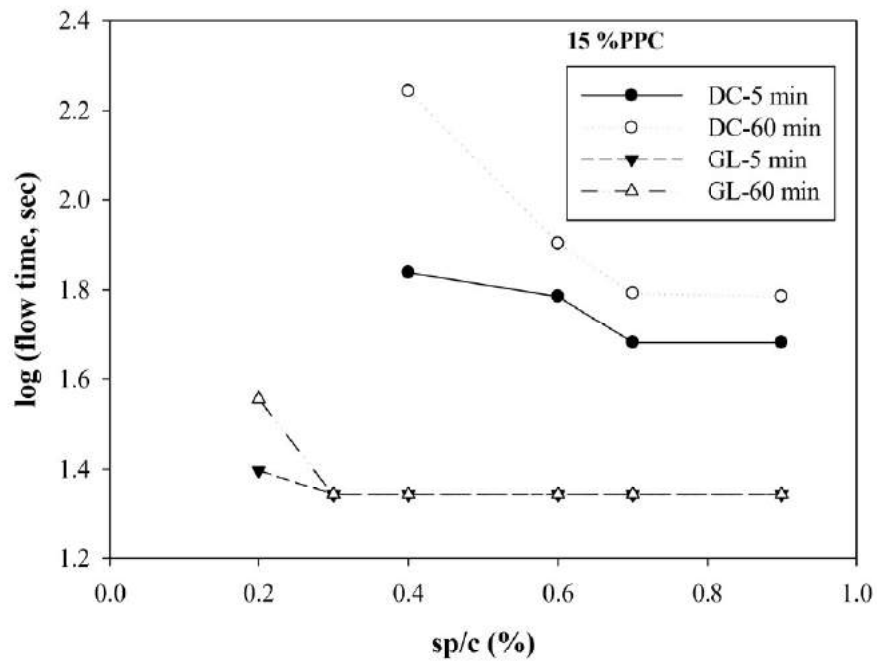


Figure 6.19: Marsh cone test results for 15 % PPC (w/b=0.40)

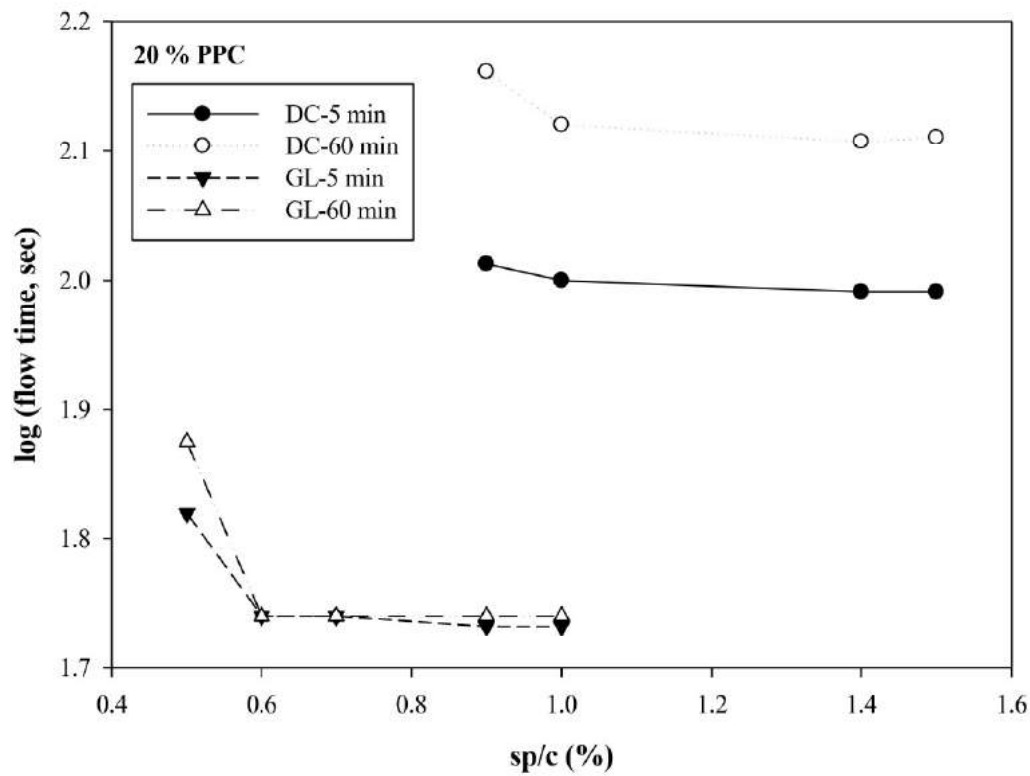


Figure 6.20: Marsh cone test results for 20 % PPC (w/b=0.40)

The lower specific gravity of processed bagasse ash increased the paste volume compared to the control paste. For the same cementitious content and water binder ratio, the volume of bagasse ash blended cement paste was higher and subsequently, the paste volume was increased with replacement. The higher volume of powder at the same water-binder ratio led to a sticky paste and reduction in the relative fluidity compared to control paste. This caused the increase in flow time at higher replacement levels. Mini slump test results for the water binder ratio of 0.40 are shown in Figures 6.21-6.24.

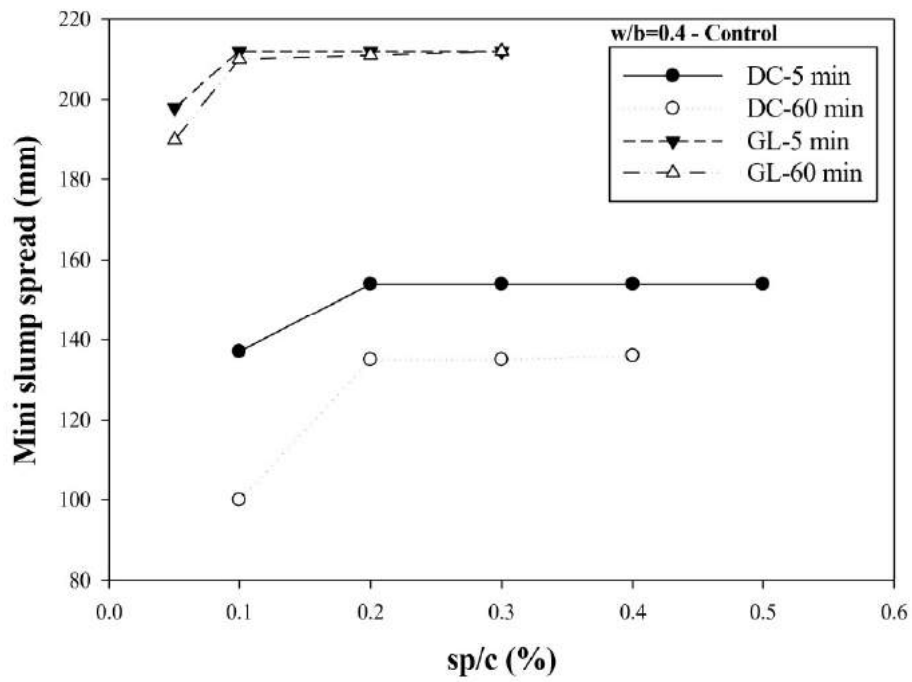


Figure 6.21: Mini-slump test results for control (w/b=0.40)

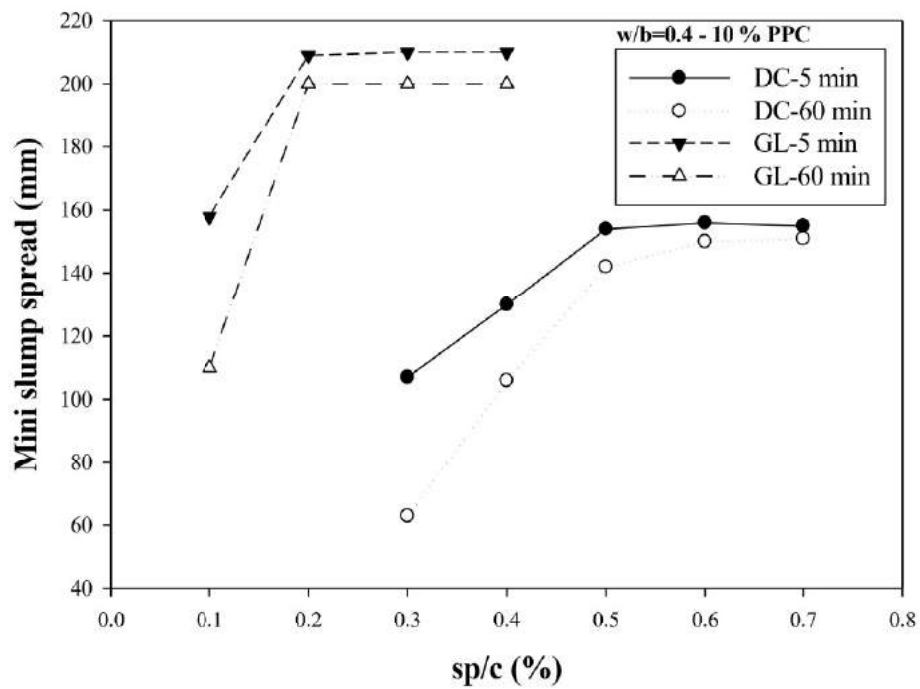


Figure 6.22: Mini-slump test results for 10 % PPC (w/b=0.40)

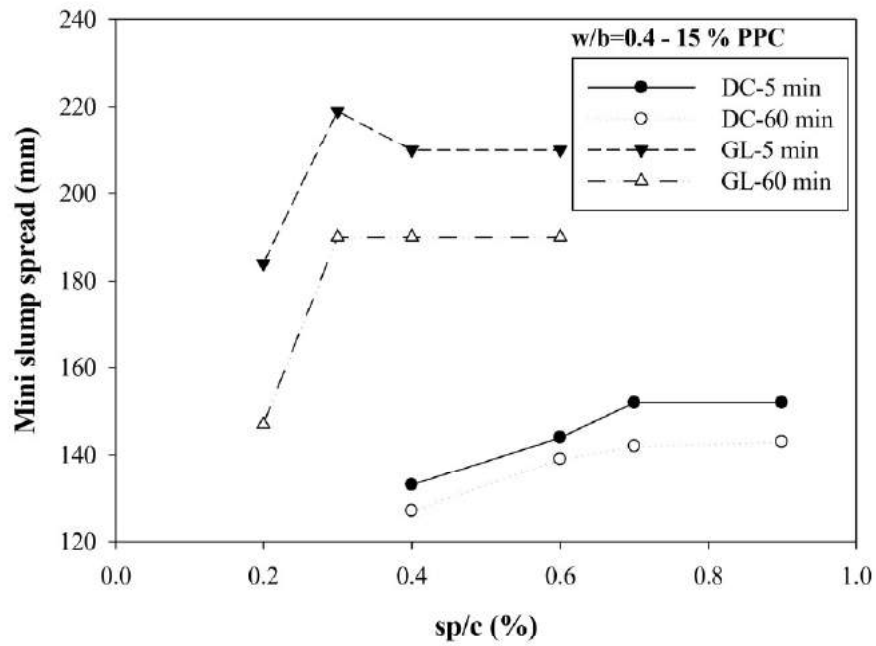


Figure 6.23: Mini-slump test results for 15 % PPC (w/b=0.40)

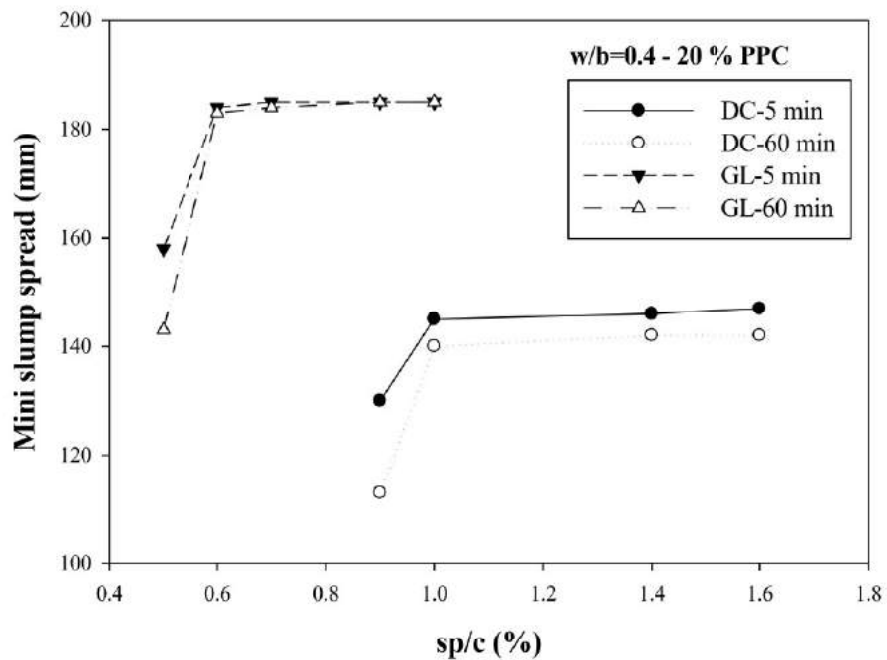


Figure 6.24: Mini-slump test results for 20 % PPC (w/b=0.40)

Increase in water requirement and superplasticizer dosage was clearly observed with increase in SCBA replacement. This is a consequence of the irregular structure of the fine burnt silica particles in bagasse ash. Scanning electron microscopy (SEM) in the SE mode was used to observe microstructure of processed bagasse ash. Irregular structures of fine burnt silica particles were clearly detected in the SEM micrograph of bagasse ash, as shown in Figure 6.25.

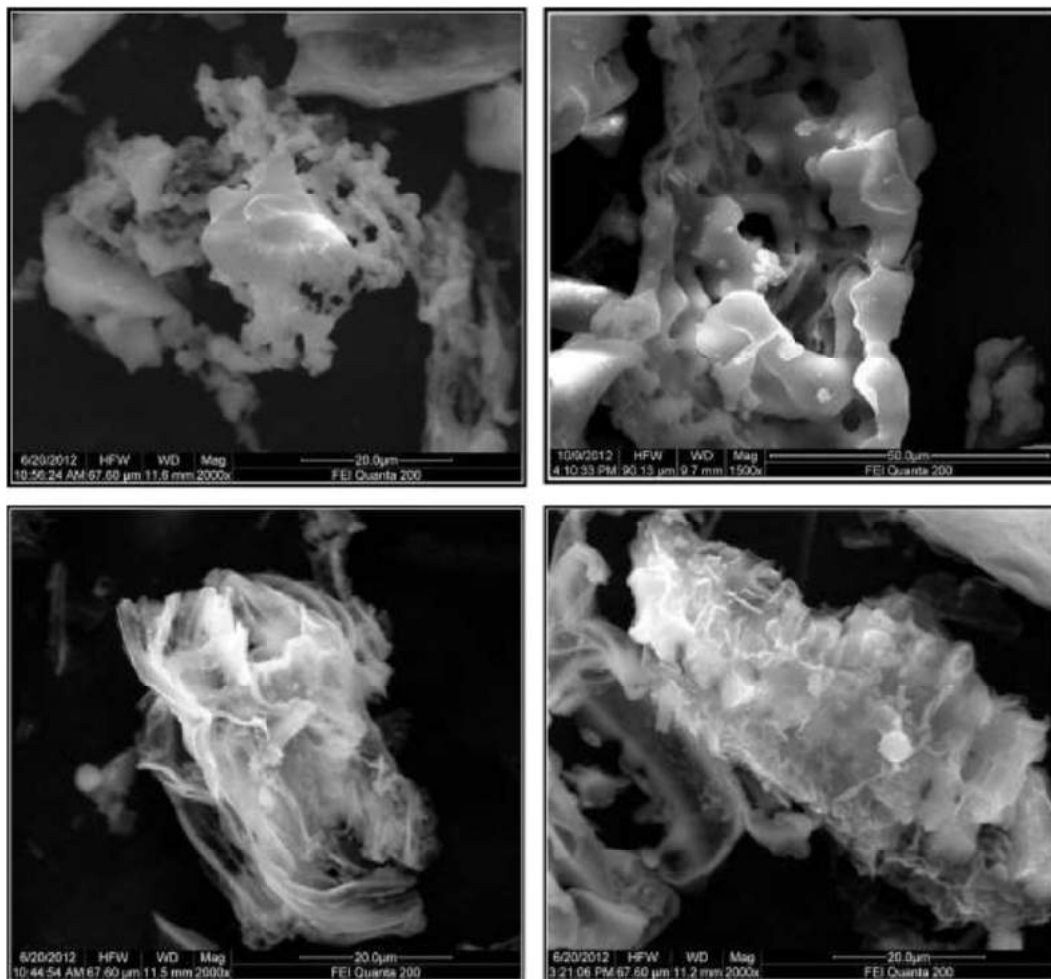


Figure 6.25 SEM micrograph of irregular processed bagasse ash particles

Although coarse fibrous particles were removed from raw SCBA, which was then further ground to cement fineness, the water requirement and superplasticizer dosage were found to be more for same relative fluidity compared to control paste. The highly irregular structure of burnt silica particles led to lesser fluidity. In previous research studies on fly ash, the spherical shape of fly ash particles was clearly observed in the microstructure and was explained as the reason for better workability of fly ash based

cement paste than control paste (Nehdi and Rahman, 2007). Lesser flow time value was observed than control even at higher replacement levels of fly ash (Quero et al., 2013; Camoes, 2005; Hallal et al., 2010). In case of silica fume and metakaolin, reduction in fluidity was observed (Agullo et al., 1999; Jayashree, 2009) because of their fineness.

Aitcin (1998) suggested a method for evaluation of the compatibility of cement-superplasticizer combination based on the comparison of Marsh cone flow curves just after mixing and after 60 min of mixing. He recommended that for compatible combination of cement-superplasticizer, the flow curves at 5 min and 60 min nearly coincide after the saturation dosage. In the present study, a loss in fluidity was clearly noticed between the 5 min and 60 min flow curves for all combinations of SCBA based cements and DC admixture, even after the saturation dosage as shown in Figures 6.9-6.12. However, for the mixes with GL, which was PCE based, the flow curves almost coincided beyond the saturation dosage. Similar trend was observed for all blended cements in this study. Even though increase in bagasse ash replacement led to more consumption of GL and DC superplasticizers, the same flow time between 5 min and 60 min after saturation dosage was only observed for GL admixtures. Hence, based on the methodology of Aitcin (1998), SCBA based cements are deemed to be compatible with polycarboxylic ether based GL admixture, but not with DC (sulphonated naphthalene based) admixture. This is due to effective dispersion of cement grains as a result of combined effect of electrostatic repulsion and steric hindrance.

6.6 SUMMARY

Portland pozzolana cements were prepared by blending OPC with processed bagasse ash at five different replacement levels. Influence of different levels of replacement on the physical, chemical and mineralogical characteristics of blended cements was addressed in detail in this chapter. Compatibility of superplasticizers with processed bagasse ash blended cements was investigated by two simple methods. The saturation dosage of superplasticizer was found to be increased with increase in bagasse ash replacement for both types of admixtures (PCE based superplasticizer and sulphonated naphthalene based superplasticizer) due to higher paste volume of blended cement paste compared to control paste as well as highly irregular nature of processed bagasse ash particles.

CHAPTER 7

PERFORMANCE EVALUATION OF SUGARCANE BAGASSE ASH BASED PORTLAND POZZOLANA CEMENT IN CONCRETE

7.1 INTRODUCTION

In earlier research studies, raw sugarcane bagasse ash was directly burnt to different approximate temperatures to remove or reduce the amount of unburnt particles as well as ground to cement size and used as mineral admixture in the concrete for the performance evaluation. It is essential to evaluate the performance of bagasse ash to facilitate its effective use in concrete after sufficient understanding of the material by suitable characterization and proper processing. In this study, SCBA based Portland pozzolana cements were used for the performance evaluation instead of direct replacement of cement with raw bagasse ash in concrete. These cements were produced through a well-defined methodology of processing of SCBA and blending with OPC. Influence of SCBA blended cements on the compressive strength, heat of hydration, drying shrinkage, and durability was investigated to understand the potential of the sugarcane bagasse ash for use as SCM. Durability performance was investigated by six different methods in this study, namely Oxygen permeability test, Rapid chloride penetration test, Chloride conductivity test, Water sorptivity test, DIN water permeability test and Torrent air permeability test. In addition, Wenner four-probe resistivity meter was used to measure the influence of bagasse ash blended cements on the electrical resistivity of concrete. Mechanical and durability performance of bagasse ash based Portland pozzolana cements in concrete is described in this chapter.

7.2 MATERIALS AND METHODS

In this study, SCBA based Portland pozzolana cements were produced with five different replacement levels (5%, 10 %, 15 %, 20 % and 25 %) and used for concrete casting. Graded river sand was used as fine aggregate and crushed granite was used as coarse aggregate (conforming to IS 383-1970) in the concrete mixes. Polycarboxylic ether (PCE) based high-performance superplasticizer (meeting the requirements of ASTM C494 Type-F) with specific gravity of 1.09 and solids content 30% was used (dosage of 0.5 % by weight of cement).

Six concrete mixes, with binder content of 360 kg/m^3 and w/b of 0.45, were prepared for the performance evaluation. Control mix, and 5 %, 15 %, 25 % replacement mixes were cast for durability testing. In addition to this, 10 % and 20 % replacement mixes were cast for heat of hydration measurement with constant water to binder ratio of 0.45. With the use of a PCE based superplasticizer, all concrete mixes had good workability (85-100 mm slump) and no segregation was observed in any mix. After casting, the specimens were stored in the laboratory environment (29 °C temperature and 71% relative humidity) for 24 hours. Specimens were then demoulded and cured in the moist room until the specified testing duration.

7.2.1 Heat of hydration

Heat of hydration can be substantially reduced with increase in pozzolanic material replacement. Several methods have been reported to measure the heat of hydration. In this study, an adiabatic calorimeter (based on Gibbon et al. (1997), and further modified as described in Prasath and Santhanam (2013)) was used to determine the total heat of hydration in addition to rate of heat evolved for control concrete and two different SCBA replaced concretes. The adiabatic calorimeter consists of a sample chamber, water bath with heater, stirrer, thermal probes to continuously monitor and record the temperatures in the concrete and water bath, and a digital controller system, as shown in Figure 7.1. The materials used for casting were stored at 25 °C before 24 hours of the experiment.

One litre of concrete sample was prepared and taken in a plastic container as shown in Figure 7.2. The thermal probe was placed at the centre of the concrete sample to measure its temperature. The plastic container was kept in the sample chamber as shown in Figure 7.2. The sample chamber was completely lined on the inside with thermally insulated material to avoid the exchange of heat between sample and water bath. In addition to that, a 40 mm thick circumferential air space was provided in between the plastic container with the concrete sample and the outer wall of the sample chamber to prevent heat exchange or any other harmonic responses between the sample and the water bath, which is imperative to ensure an accurate heat of hydration measurement. The temperature of the sample was measured by a thermal probe and the changes in temperature were monitored by a digital controller system. Another thermal probe was placed in the water bath and a heater element was used to maintain the adiabatic condition. The test was continued until no significant increase in the temperature was observed, and this occurred within a 5 day period. Total heat and rate of heat were determined. Moreover, the rate of heat evolution was measured in terms of maturity to normalise the effect of the starting temperature (Ballim and Graham, 2003).

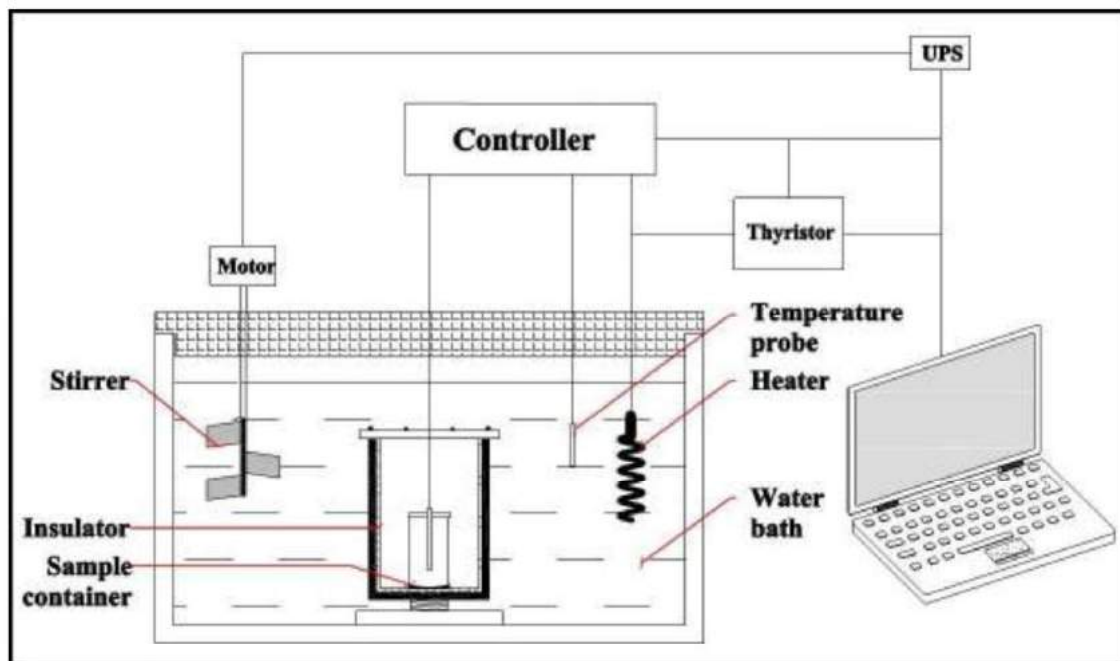


Figure 7.1: Schematic diagram of adiabatic calorimeter (based on Gibbon et al., 1997; Prasath and Santhanam, 2013)



Sample



Insulated sample chamber



Placing of sample chamber in water bath



Adiabatic calorimeter

Figure 7.2: Sequence of heat of hydration test

7.2.2 Specimen preparation for durability testing

Concrete specimens (150 mm cubes) from the different mixes were cast and cured in the moist room. After 28 days and 56 days of curing, 75 mm (outer) diameter cores were extracted from the cubes and coated with epoxy as shown in Figure 7.3. Four test specimens of 70 ± 2 mm diameter with thickness of 30 ± 2 mm were prepared as per Durability index testing manual (2009), for the oxygen permeability, chloride conductivity and water sorptivity tests.

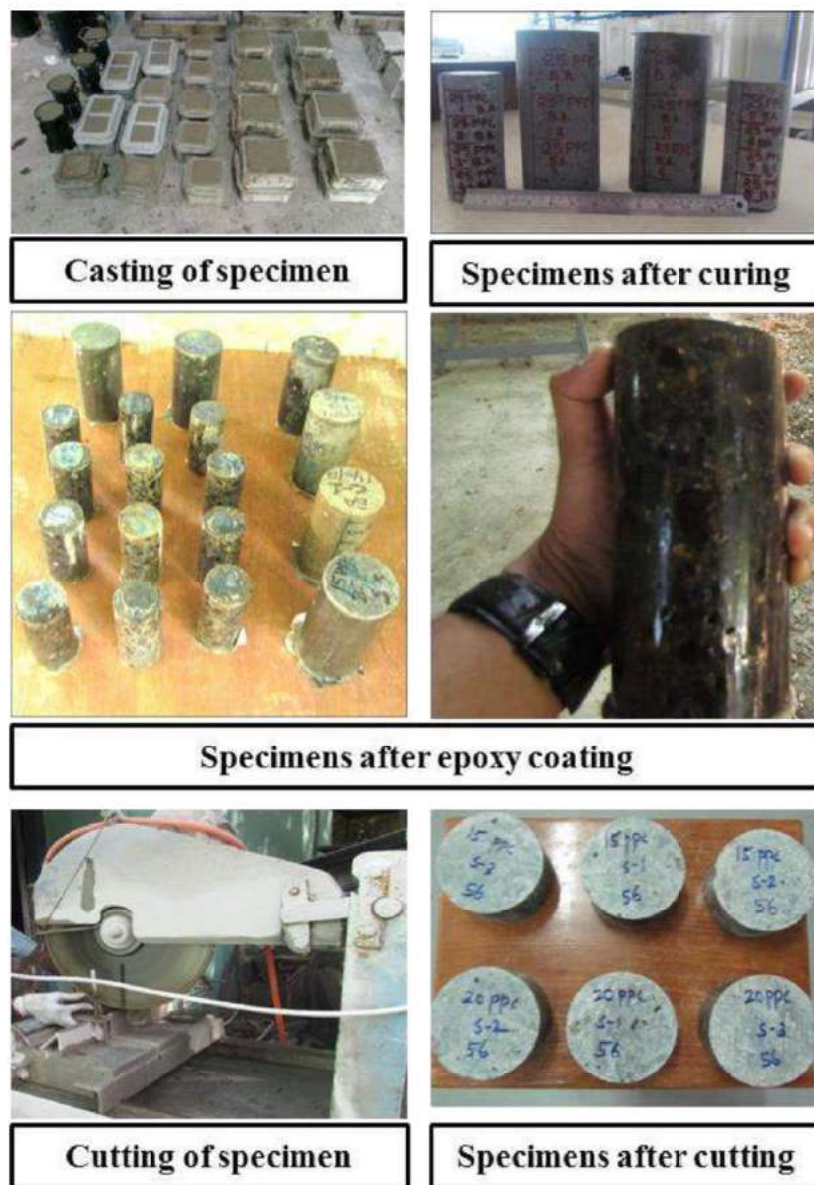


Figure 7.3: Specimen preparation for durability tests

These were kept in an oven at 50 ± 2 °C for seven days to remove moisture without significant alterations in the microstructure. After oven drying, specimens were allowed to cool at 23 ± 2 °C for 2-4 hours as depicted in Figure 7.4. The dry mass, average diameter and thickness of each specimen were measured. For the Torrent test, the 150 mm cube specimen was directly used after conditioning in an oven at 50 ± 2 °C for seven days.



Oven drying of specimens (50 °C for 7 days)



Conditioning of specimens (23 ± 2 °C for 2-4 hours)

Figure 7.4: Conditioning of specimen as per DI manual (2009)

Three specimens of 100 mm diameter and 50 mm thickness were used for RCPT as per ASTM-C1202-12. In RCPT, the specimens were placed vertically (see Figure 7.5) and subjected to dry vacuum in a desiccator for 180 minutes to expel air present in the pores. After dry vacuum, specimens were submerged in distilled water (that was flooded into the chamber) for an additional 60 minutes and vacuum was continued during this period.



Figure 7.5: Vacuum saturation of specimens

After removing the vacuum, the specimens were immersed in the water for a further 18 ± 2 hours. For chloride conductivity test, the specimens were vacuum saturated with 5.0 M sodium chloride solution (procedure similar to that described earlier for RCPT) to ensure that the pore solution conductivity did not affect the conductivity measurement.

7.2.3 Chloride based tests

Accelerated test methods based on migration are commonly used to find the resistance of concrete against chloride ion penetration. In this study, two accelerated methods – the ASTM 1202 Rapid Chloride Penetration Test (RCPT) and the South African Chloride conductivity test were used (DI manual, 2009). For RCPT, after vacuum saturation, the specimens were placed in RCPT migration cells with 3.0 % NaCl solution (catholyte) and 0.3 N NaOH solution (anolyte). A constant potential of 60 ± 0.1 V was applied across the concrete, which accelerates the penetration of chloride ions from catholyte to anolyte through the concrete specimen. The current readings were recorded at 30 minute intervals for 6 hours. The rapid chloride penetration test set up is shown in Figure 7.6. The total

charge passed over the test period was calculated from current readings, to provide a representation of the concrete resistance to chloride ion penetration.

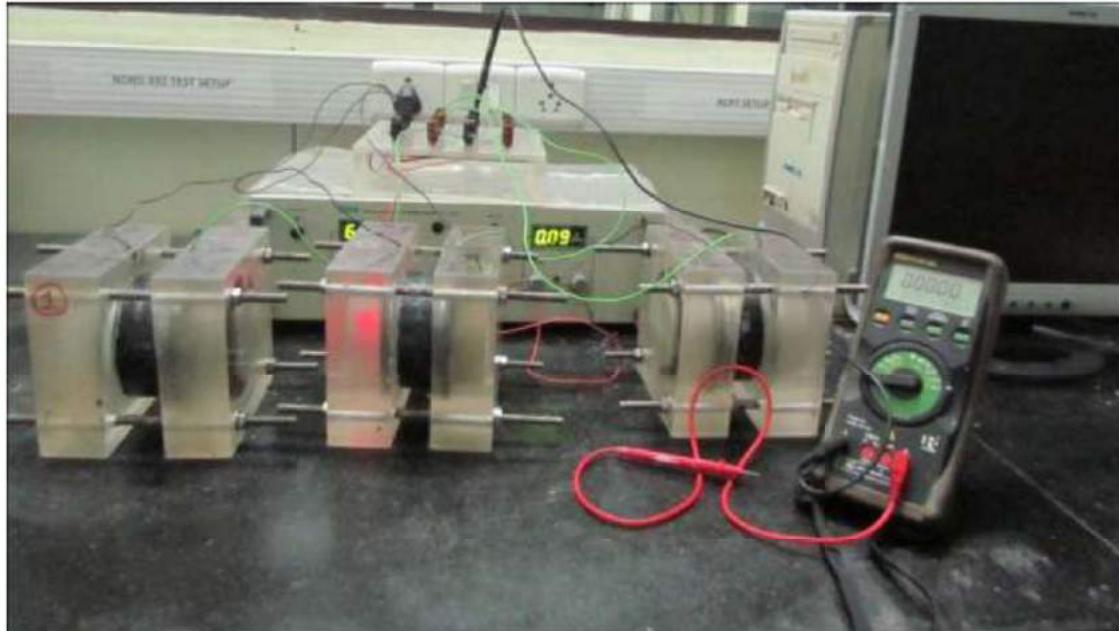


Figure 7.6: Rapid chloride penetration test setup (based on ASTM 1202-12)

In the chloride conductivity test, after vacuum saturation, the specimens were removed from salt solution; the saturated mass of the specimen was measured. The specimen was then placed in the central part of the flexible rubber collar. 5.0 M NaCl was filled in the conductivity cell, which is shown in Figure 7.7. A threaded perspex luggin probe with rubber washer was used to avoid leakage of solution in the conductivity cell as shown in Figure 7.8. Ammeter and voltmeter were connected with the conductivity cell. The applied voltage across the concrete specimen was adjusted to 10 V from a DC power supply and the corresponding current was noted as shown in Figure 7.9.

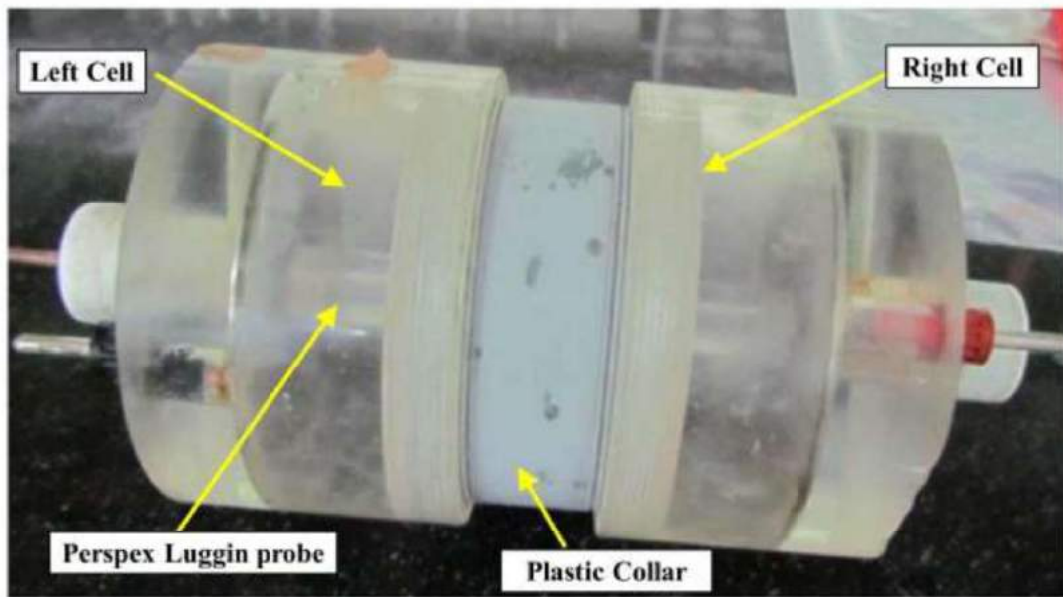


Figure 7.7: Conductivity cell (DI manual, 2009)

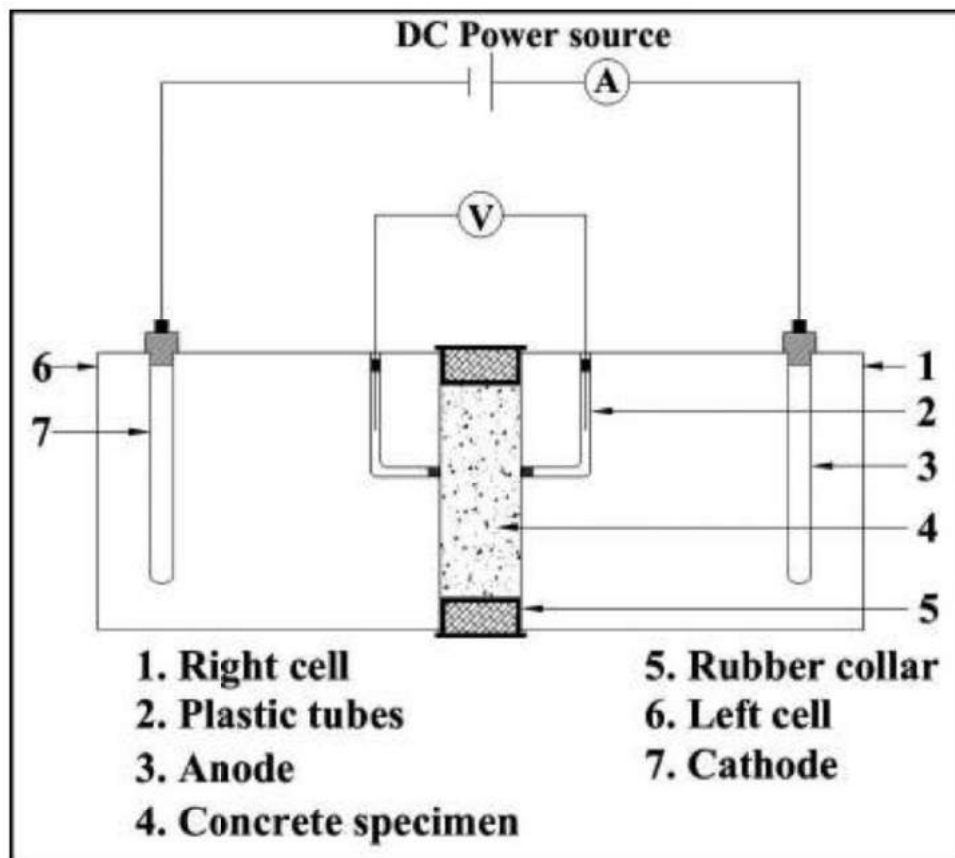


Figure 7.8: Schematic diagram of chloride conductivity test (Based on DI manual, 2009)

The conductivity was then calculated as per equation 7.1. The chloride conductivity index was calculated as the average of the chloride conductivity (obtained using Eqn. (7.1)) of three individual test specimens.

$$\sigma = (id/VA) \quad (7.1)$$

Where

σ = chloride conductivity of the specimen (mS/cm),

i = electric current (mA)

d = average thickness of specimen (mm)

V = potential difference

A = cross-sectional area of the specimen (mm²)

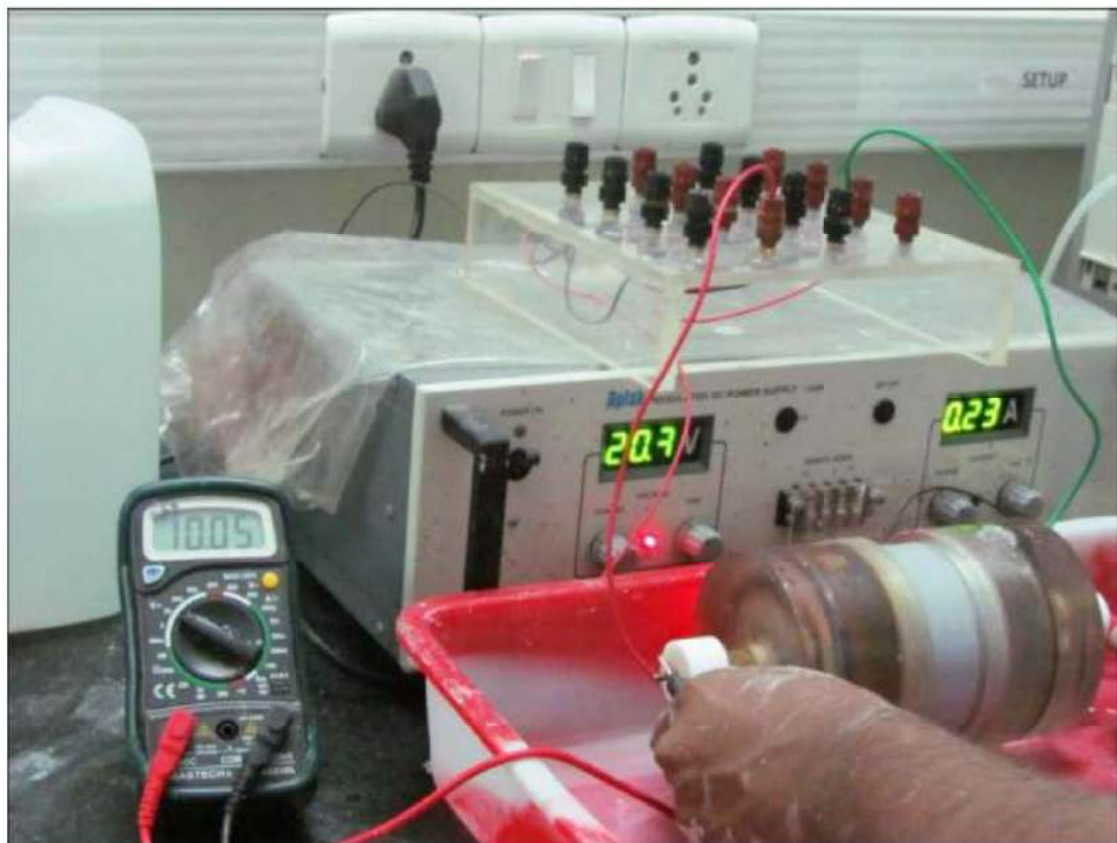


Figure 7.9: Chloride conductivity test setup

7.2.4 Gas based tests

Different accelerated methods are used to estimate gas permeation/diffusion into the concrete in the field as well as in laboratory conditions. In this study, the South African Oxygen permeability test and Torrent air permeability test (Swiss Standard SIA 162/1-2003) were used. In the oxygen permeability test, the conditioned specimen was placed inside a compressible rubber collar, which was then fitted inside a steel sleeve and placed in the permeability cell as illustrated in Figure 7.10. Oxygen was filled inside the pressure vessel and the outlet of the vessel was opened for five seconds to expel the gases present other than oxygen. The pressure was adjusted to 100 ± 5 kPa. A schematic diagram of the oxygen permeability cell is shown in Figure 7.11 and the setup is shown in Figure 7.12. The pressure was measured using a digital pressure gauge every 30 min until 6 hours. The test was stopped after 6 hours.

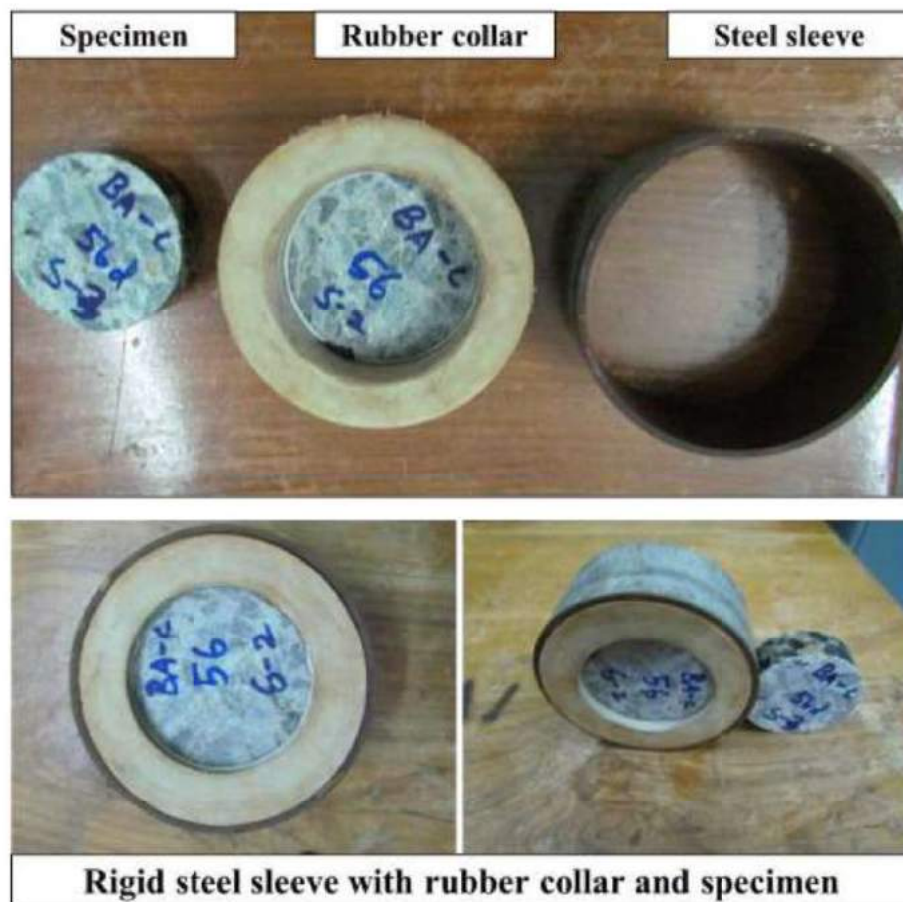


Figure 7.10: Proper positioning of specimen for oxygen permeability test

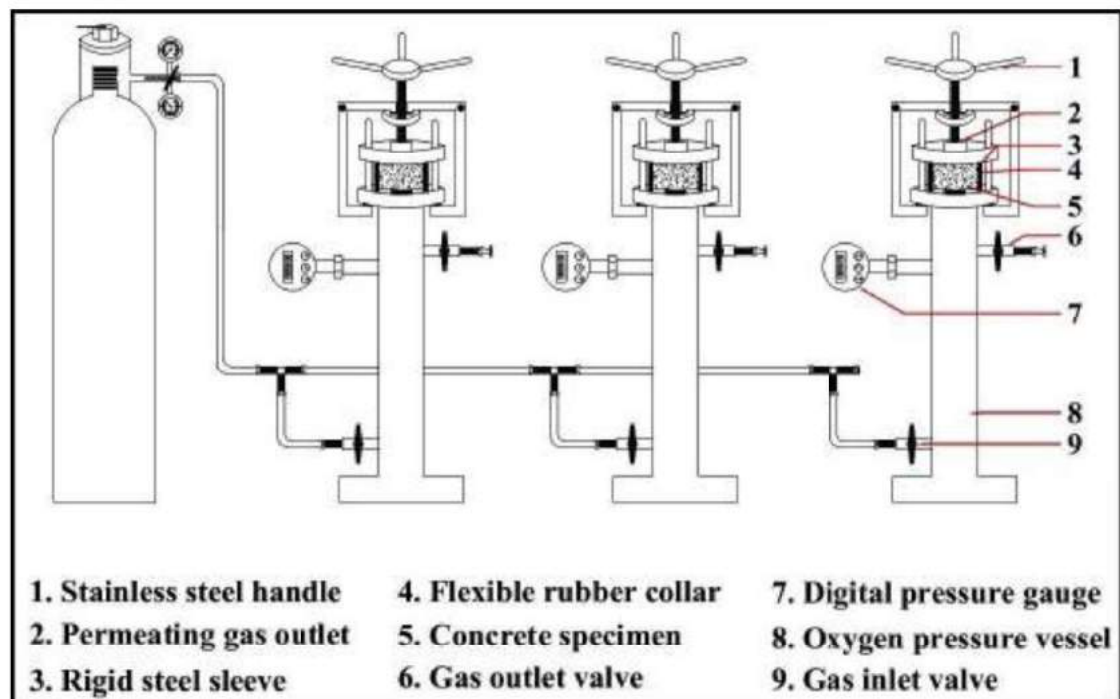


Figure 7.11: Schematic diagram of oxygen permeability cell (Based on DI manual, 2009)



Figure 7.12: Oxygen permeability test setup

The coefficient of permeability was then determined as per the methodology suggested in the South African Durability Index Manual (2009). The oxygen permeability index (OPI) was calculated as the negative log of the average of the coefficients of permeability of the three tested specimens (Alexander et al., 1999). In the Torrent test, the vacuum cell was placed on the cleaned surface of concrete specimen, as shown in Figures 7.13 and 7.14, and the vacuum was created using a pump. When the pressure in the inner chamber reached 30 mbar, the secondary valve was automatically closed to achieve uniform pressure in the inner chamber. A schematic diagram of Torrent air permeability apparatus is presented in Figure 7.13. The air in the pores of the cover concrete, which is initially at atmospheric pressure, starts to flow into the inner chamber of the vacuum cell.

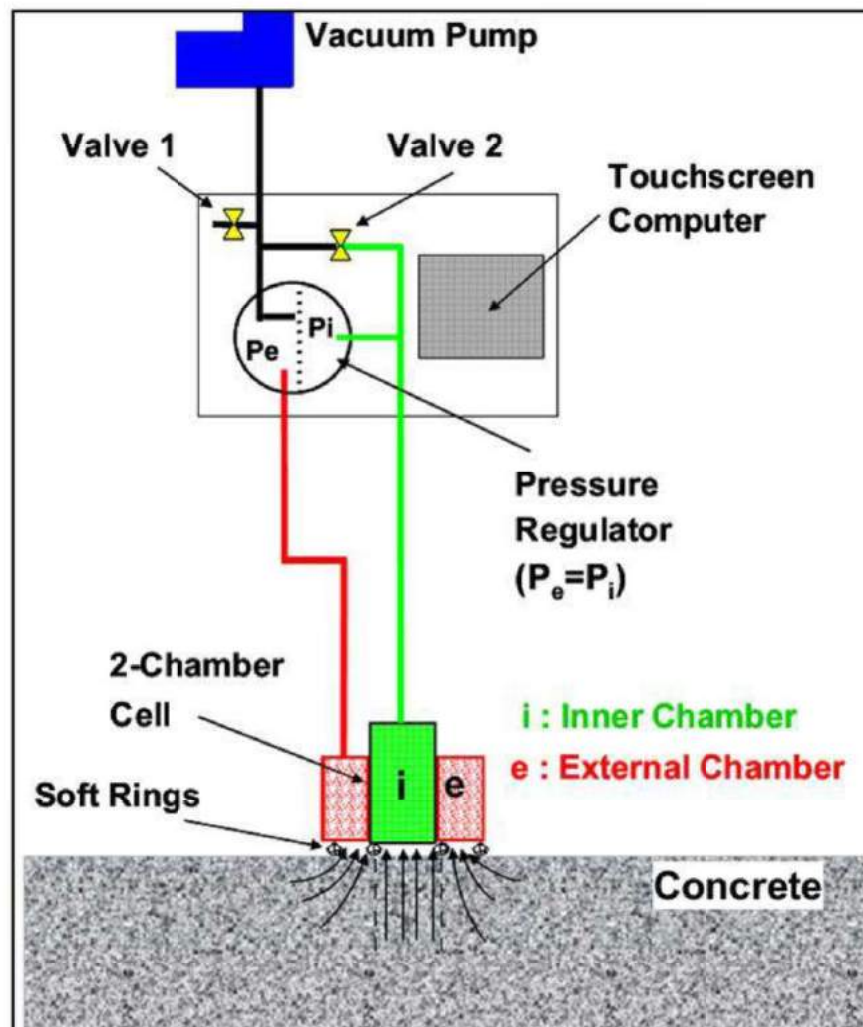


Figure 7.13: Schematic diagram of Torrent air permeability apparatus (Torrent Air permeability test user manual, 2010)

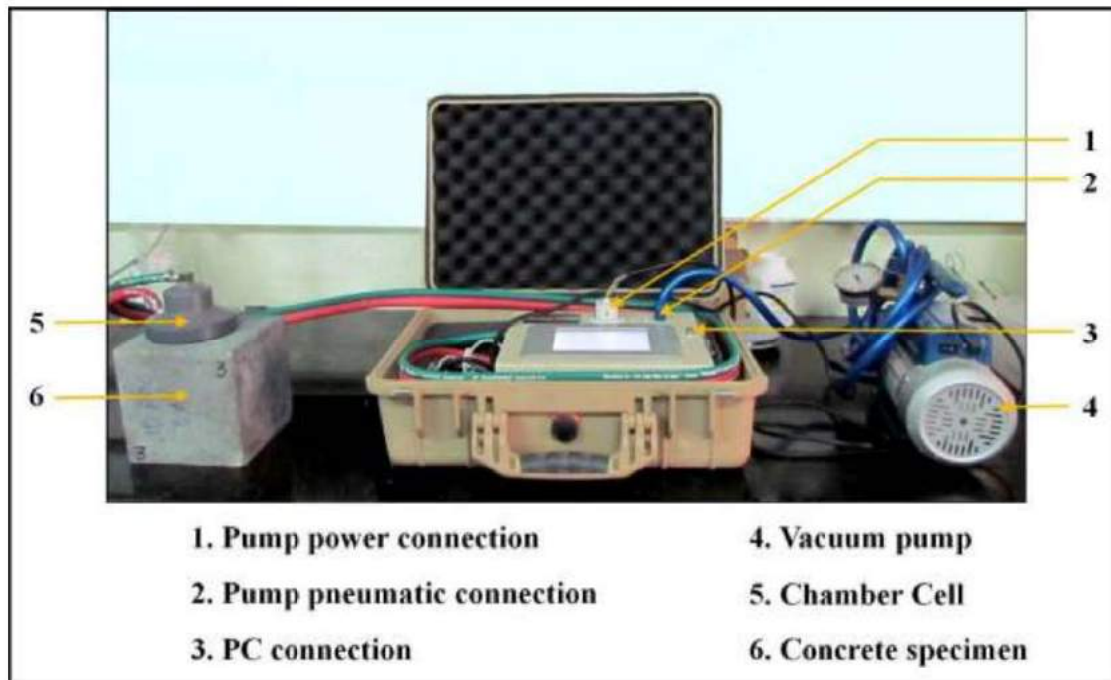


Figure 7.14: Torrent air permeability test setup

Due to this, the pressure in the inner chamber gradually increases with time. The instrument records the rise in the effective pressure at the end of the test, and converts it to the coefficient of air-permeability kT (10^{-16} m^2), which is directly reported by the instrument display.

7.2.5 Water based tests

The resistance to water penetration was studied by South African water sorptivity test and the water penetration test (DIN-1048 Part-5, 1994). For the DIN-1048 test, after 28 and 56 days of curing, the 150 mm cube specimens were transferred to an oven at 50°C for 7 days and the penetration test was conducted after this conditioning procedure (this is a deviation from the actual procedure, where the moist cured specimens is directly placed in the permeability apparatus without pre-conditioning; this was done in order to ensure a combination of initial sorption and penetration under pressure, in order to accentuate the differences between the concretes). The specimens were placed in the permeability cell, as shown in Figures 7.15 and 7.16, and the cover plate was seated on the surface of the specimen. A suitable rubber or neoprene gasket was provided at the bottom of the cover

plate to ensure proper contact between the specimen and the cover plate, as illustrated in Figure 7.15. A sealant was applied at the interface between the rubber gasket and specimen to prevent the leakage of water. Constant water pressure (0.5 N/mm^2) was maintained on the surface of the specimen (any surface other than the cast surface) for three days. Afterwards, the pressure was released and the specimens were immediately removed from the permeability cell. Specimens were split along the direction of water penetration, and the depth of penetration was measured within 5-10 minutes as described in the standard before drying of the specimen as shown in Figure 7.17. Average penetration depth of minimum three specimens is reported as the water penetration of concrete.

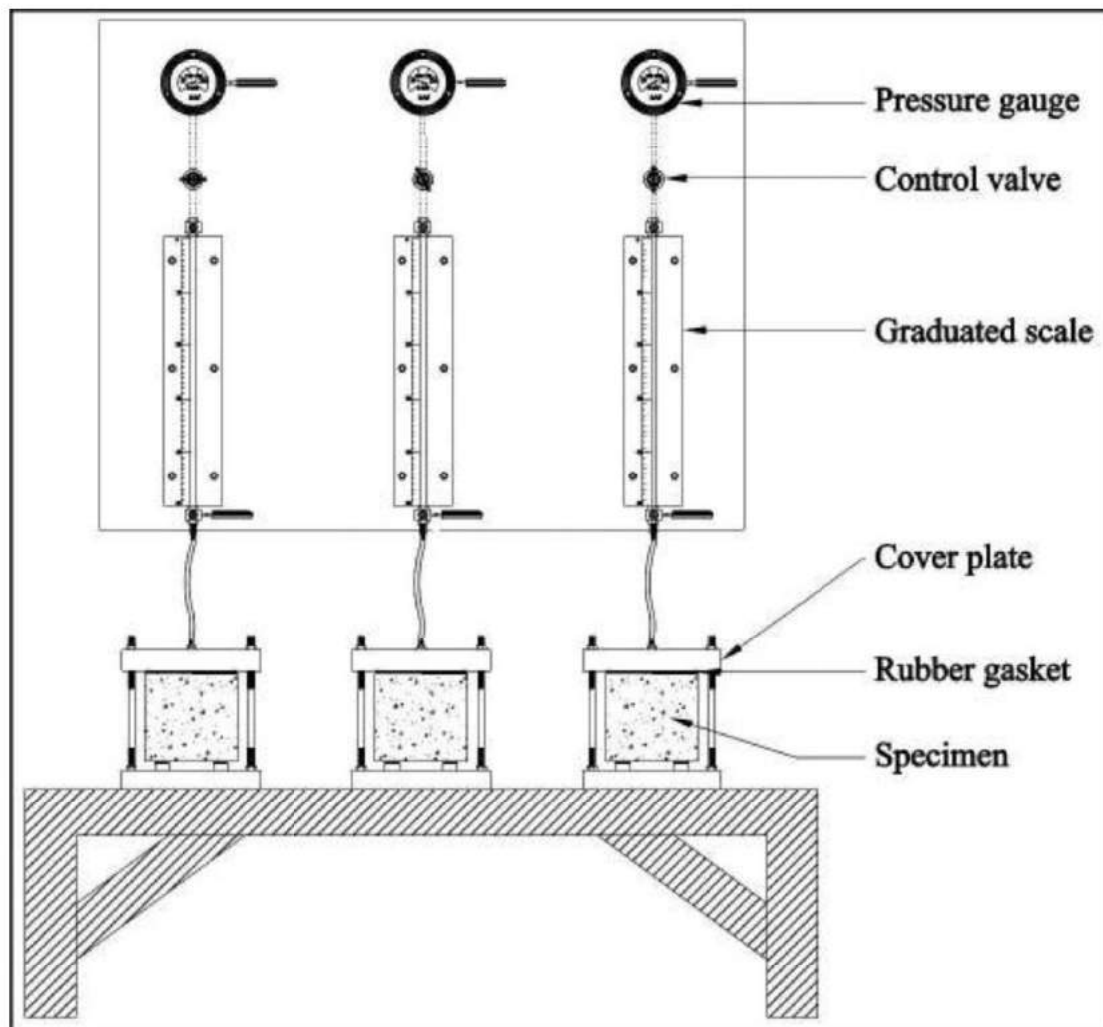


Figure 7.15: Schematic diagram of water permeability test apparatus



Figure 7.16: Placing of specimens in water permeability cell



Figure 7.17: Depth of water penetration

In the water sorptivity test, conditioned specimens were placed on wedges or rollers (placed at the bottom of a tray as shown in Figure 7.18a) and calcium hydroxide solution was poured into the tray up to a level of 2 mm above the bottom surface of the

specimens. Specimens were removed periodically for mass measurement, and the surface was slightly wiped with a moist paper towel to achieve saturated surface dry condition on the exposed face. The mass of the specimen was measured at 3, 5, 7, 9, 12, 16, 20 and 25 minutes on a balance with an accuracy of 0.01 g. After measurement, specimens were placed in the vacuum saturation tank. A similar saturation procedure to that mentioned in the RCPT test was followed and the vacuum saturated mass of each specimen was measured. A graph was plotted for mass gain (Mwt) against the square root of time, and the slope of the best fit line (F) was determined as shown in Figure 7.18b.

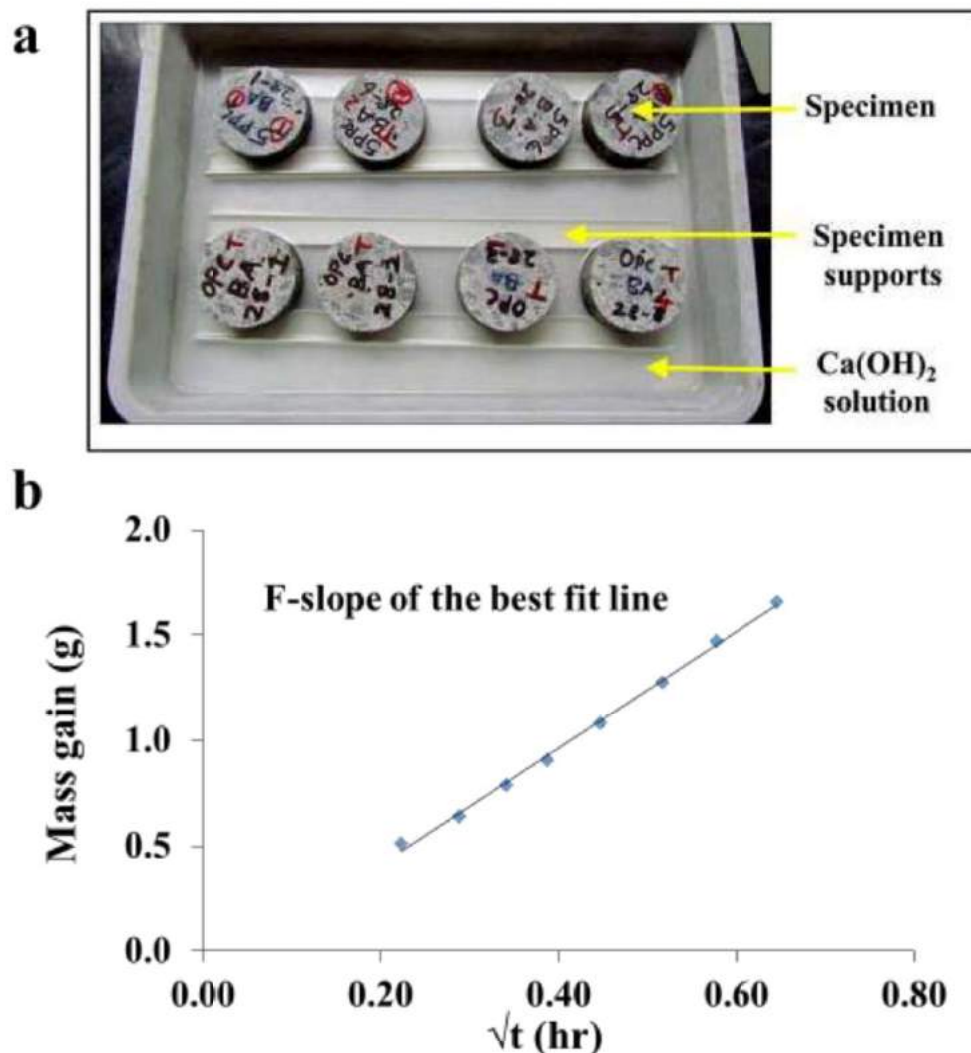


Figure 7.18: Water sorptivity test: a) Test set up using support as per DI manual (2003);
b) Graph for mass gain (Mwt) against the square root of time to determine slope

The sorptivity index was calculated as the average of the water sorptivity of at least three tested specimens in this study by using the following equation.

$$S = Fd / (M_{sv} - M_{so}) \quad (7.2)$$

Where

- d = Average specimen thickness in mm
- M_{sv} = Vacuum saturated mass of the specimen in g
- M_{so} = Dry mass of the specimen in g
- F = Measured slope of the best fit line (g/ $\sqrt{\text{hr}}$)

7.2.6 Electrical resistivity of concrete

The Wenner four-probe resistivity meter was used to measure the electrical resistivity of concrete specimens as per FM 5-578 (2004) guidelines. In this test, four equally spaced probes are diagonally placed on the saturated surface of concrete and alternating current is passed through two outer electrodes. The potential difference between two inner electrodes is measured as illustrated in Figure 7.19 and the corresponding resistivity of concrete is reported by the instrument. In this study, the 4-probe system was used to measure resistivity on four faces (not including cast face – see Figure 7.20) of a 150 mm cube specimen right after moist curing and the average resistivity is reported. Higher resistivity value indicates lower pore connectivity of the concrete.

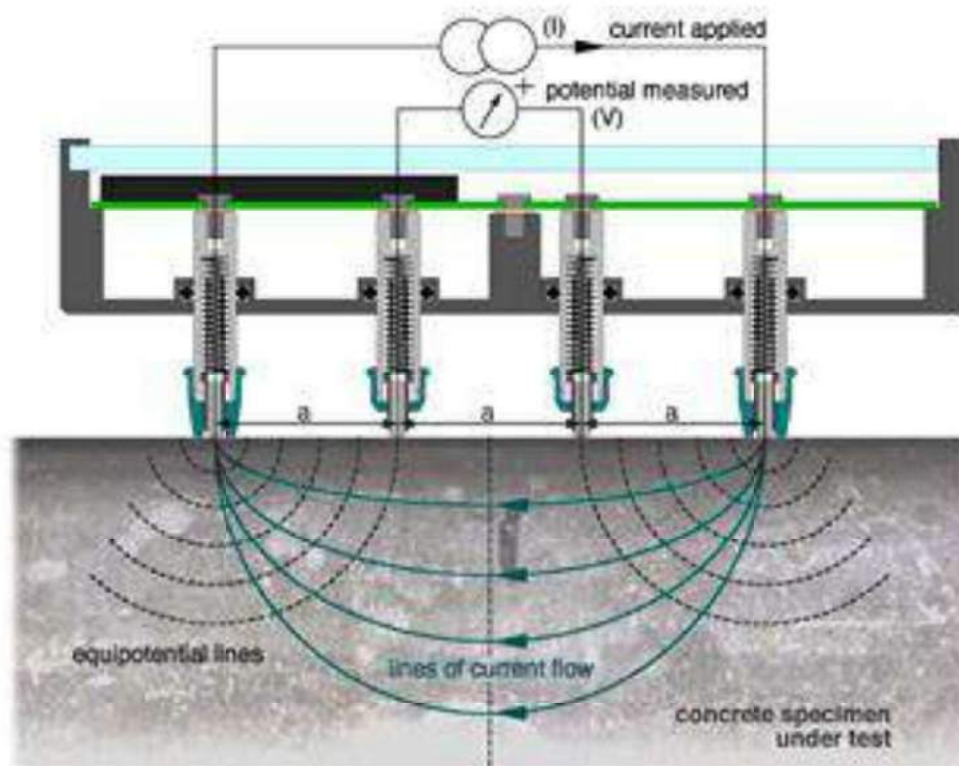


Figure 7.19: Schematic diagram of Wenner resistivity test (Resipod Proceq user manual, 2013)



Figure 7.20: Wenner resistivity test

7.2.7 Drying Shrinkage

Three numbers of 75 x 75 x 280 mm specimens were cast for each concrete. After 7 days of curing, the specimens were placed in a controlled drying environment (25 °C temperature and 65 % relative humidity). The initial length of the specimens and the corresponding length changes with respect to time (up to 90 days) due to drying shrinkage were measured using an extensometer (see Figure 7.21) as per guidelines (ACI 209.1R, 2005). The average strain in 4 specimens is reported for control and SCBA replaced concretes.

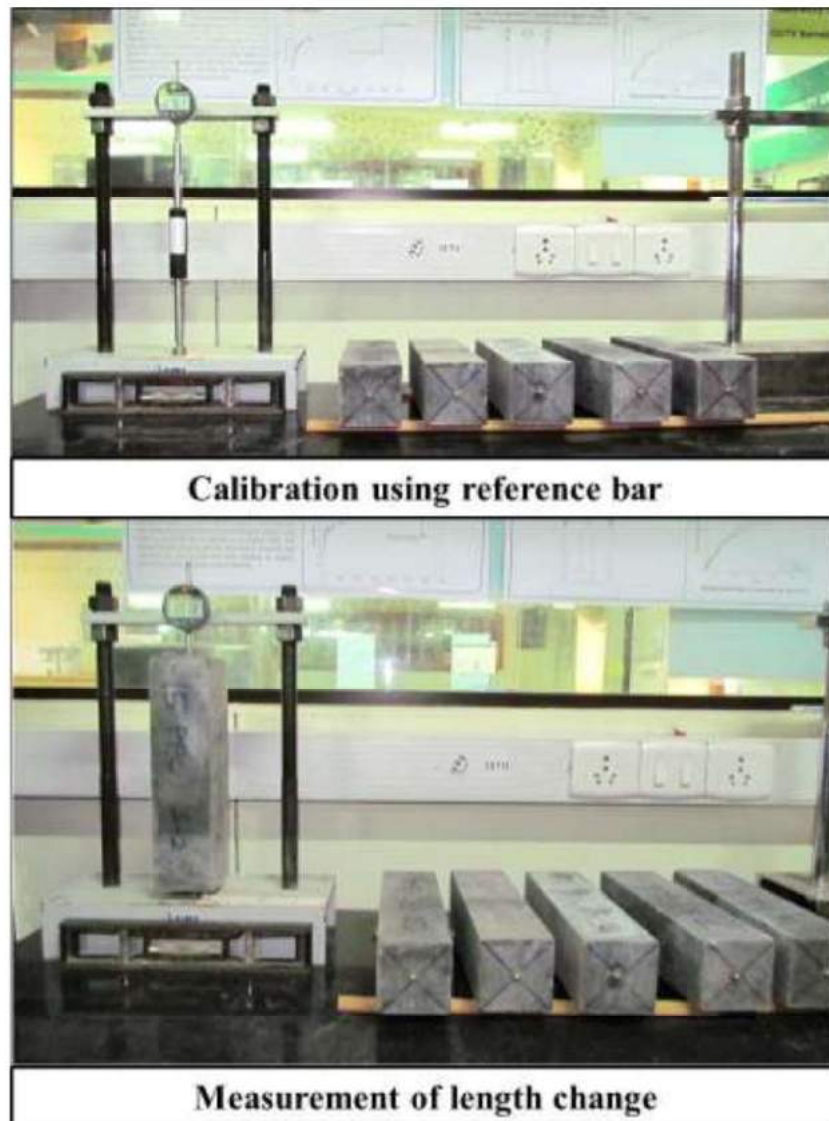


Figure 7.21: Drying shrinkage test set up

7.3 RESULTS AND DISCUSSION

7.3.1 Heat of hydration

Heat of hydration was measured for control concrete and 10 % and 20 % SCBA replaced concretes using an adiabatic calorimeter. The total heat curves are shown in Figure 7.22. Total heat liberated from the control sample was found to be higher (285 kJ/kg) up to 5 days of measurement as compared to 10 % SCBA replaced concrete (220 kJ/kg). Further marginal reduction was observed for 20 % replacement.

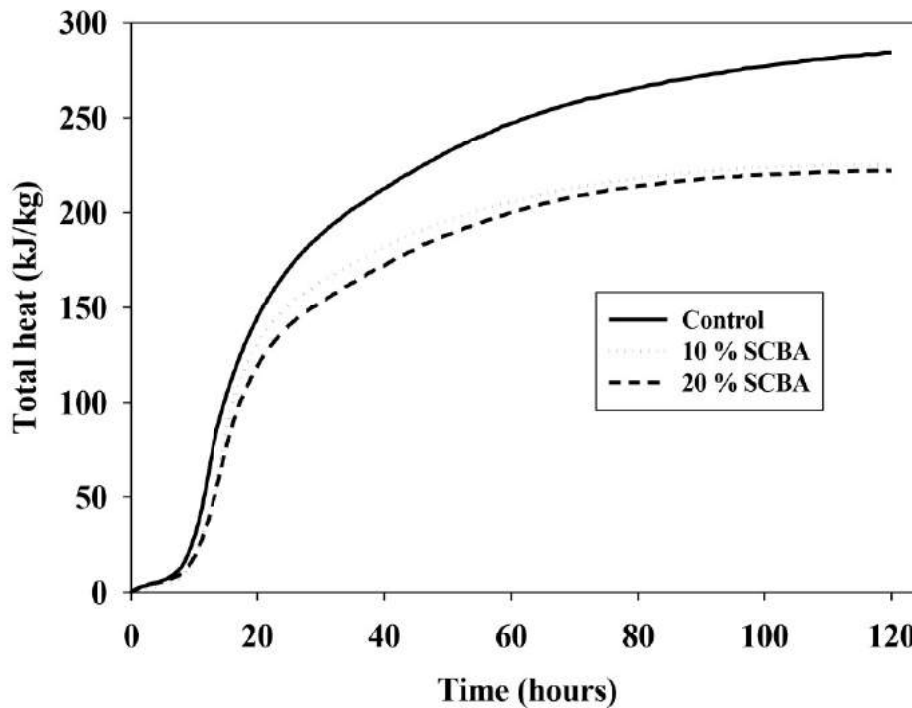


Figure 7.22: Comparison of total heat curves

A number of previous research studies have reported that specific surface of cement highly influences the rate of heat development in concrete (Graham et al., 2011; Ghiasvand et al., 2014). In this study, OPC and SCBA based Portland pozzolana cements were ground to same fineness ($300\text{--}310\text{ m}^2/\text{kg}$) and thus, the effect of fineness could be considered negligible with respect to heat of hydration. Therefore, the observed reduction in heat liberation is purely as a result of SCBA replacement.

In order to avoid the influence of the starting temperature, a maturity form of the heat evolution curve was used, as proposed by Ballim and Graham (2003). This method also normalizes the variations in time-temperature history for different concretes. The actual heat rate – time curves and the maturity heat rate – time curves for the different concretes are presented in Figures 7.23 and 7.24 respectively. The term t_{20} denotes the equivalent time of hydration at 20 °C. At the beginning, a brief period of high rate of heat liberation was observed for control and SCBA replaced samples due to the initial dissolution of ions and heat of wetting. Reduction in the rate of heat was detected after initial peak (corresponding to the dormant period) as shown in Figure 7.23. After this period, the main heat peak was observed – the position of the main peak was shifted to the right for the SCBA replaced concretes. Further, the peak heat rate was also reduced with increase in replacement of SCBA as shown in Figures. 7.23 and 7.24. This stage roughly corresponds to the final setting time of concrete and also the start of hardening. The heat rate results suitably correlate with setting time observations (setting time was increased with SCBA replacement) reported in Table 6.1 (Chapter 6).

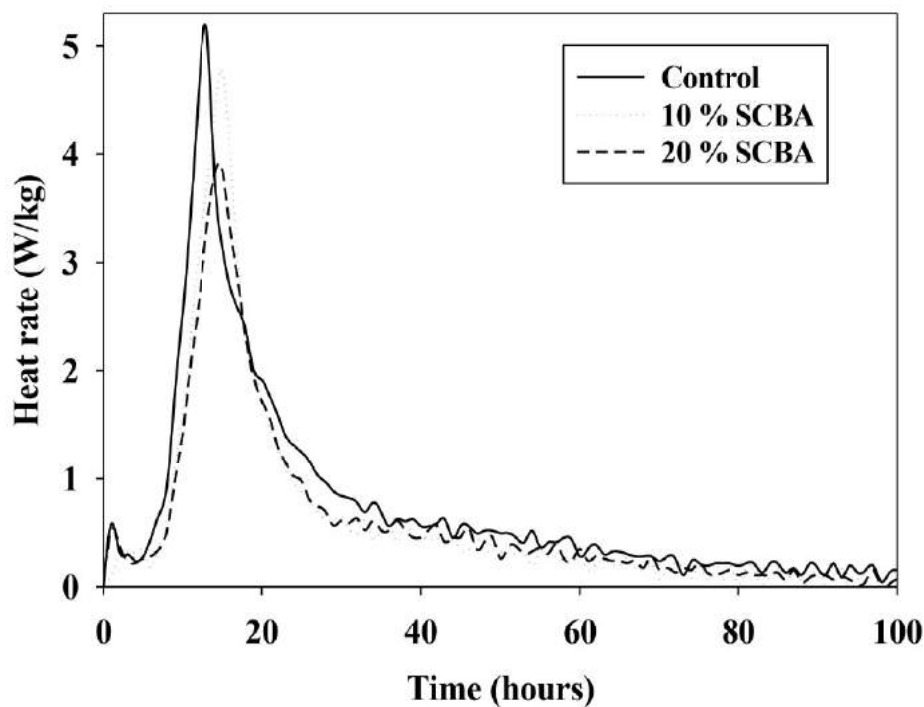


Figure 7.23: Comparison of heat of hydration rates for cements

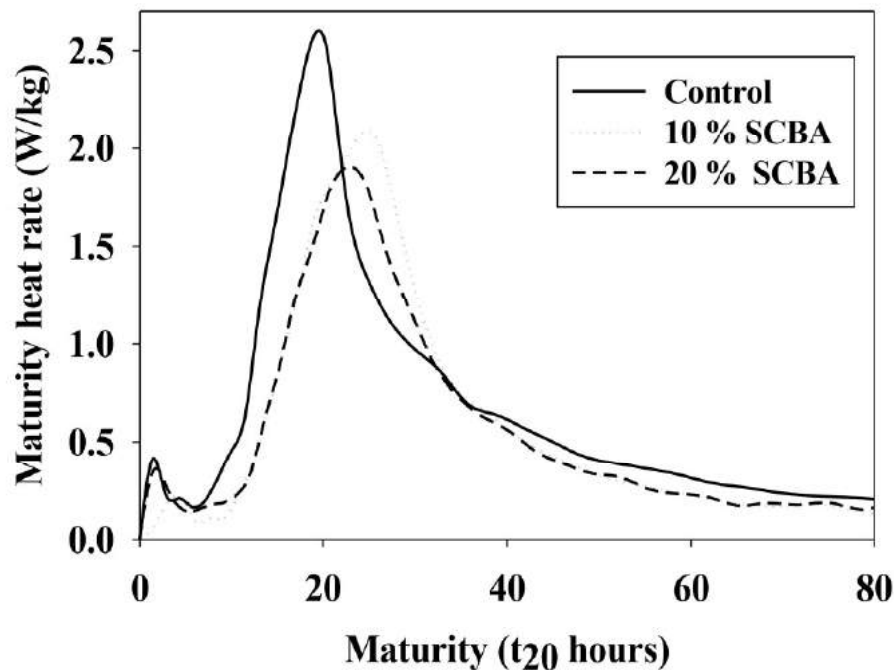


Figure 7.24: Comparison of maturity heat rates for cements

Chemical composition of the cement, primarily the C_3A , C_3S and gypsum contents significantly influence the heat evolution characteristics (Graham et al., 2011). Reduction in C_3A and C_3S due to replacement of cement with processed SCBA (because of dilution) is also another logical explanation for the reduction in the heat of hydration.

7.3.2 Compressive strength

Compressive strength of concrete for different bagasse ash blended cements was determined at 3, 28 and 56 days of curing. On the whole, the compressive strength results indicate that the same grade of concrete as with OPC can be produced with SCBA replacement up to 25%. Unlike the generally known problems of early age strength with fly ash concrete, the SCBA replaced concretes showed similar, if not marginally better, strength gain behavior compared to OPC concrete. In fact, the 3-day compressive strength for SCBA concretes was better than that of OPC concrete as depicted in Figure 7.25. Similar trends were seen after 28 and 56 days of curing also (with the exception of 25% SCBA concrete at 28 days).

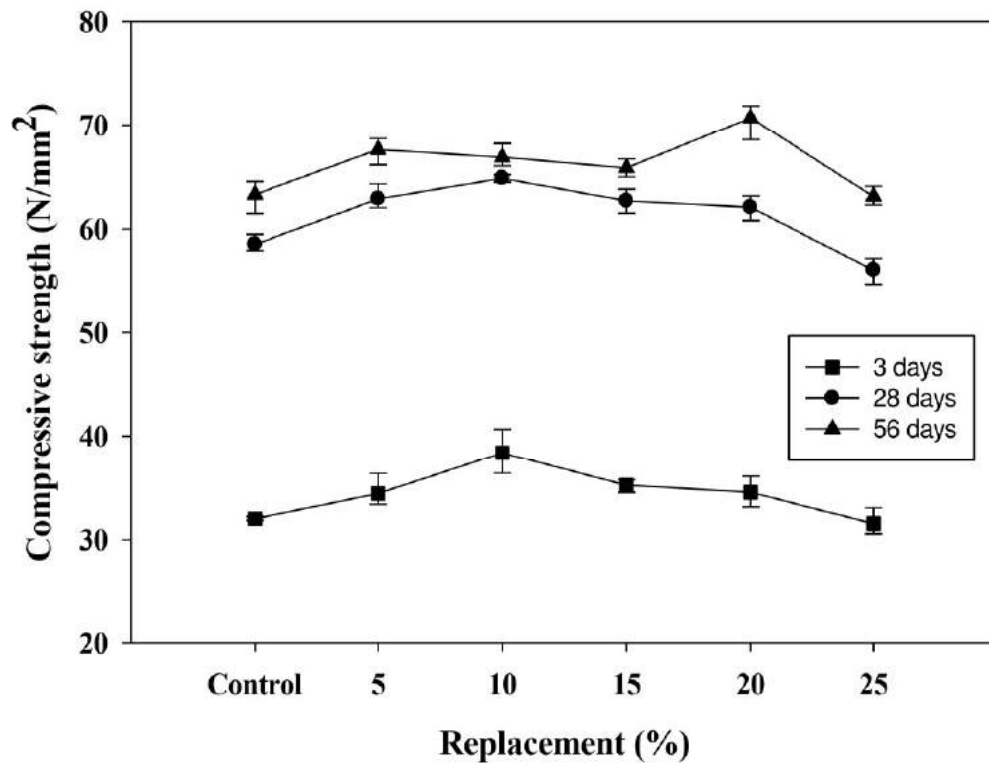


Figure 7.25: Compressive strength of concrete after 3, 28 and 56 days of curing

7.3.3 Chloride based tests

In the RCPT test, the total charge passed for control specimens during the 6-hour test period was 3060 and 2950 Coulombs at 28 and 56 days respectively. According to ASTM 1202-12 classification, control specimens had ‘moderate’ resistance against chloride ion penetration. Replacement of cement with bagasse ash considerably decreased the electrical conductance as illustrated in Figure 7.26. When compared to control specimens, the total charge passed was found to be reduced by 74 % and 83 % for 15 % and 25% SCBA replaced specimens respectively. SCBA replaced specimens showed significantly higher resistance than control specimens at 28 days as well as 56 days, and can be characterized as ‘very low’ permeability concretes as per guidelines. The significant reduction in charge passed can be attributed to a combination of many factors, the primary ones being: (a) lowering of pore solution conductivity, that is generally attributed to the use of supplementary cementing materials with reactive silica,

and (b) improvement in pore structure, or in other words, lowering of pore connectivity that results from the pozzolanic performance of SCBA.

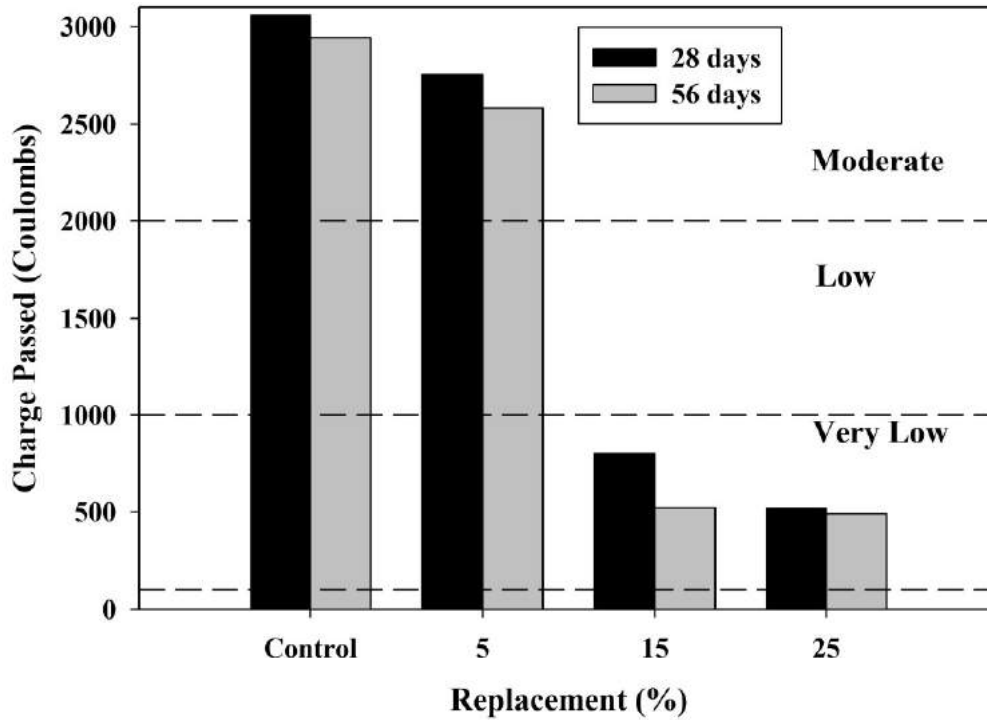


Figure 7.26: Total charge passed at 28 and 56 days of curing

Results of the chloride conductivity test, in terms of the chloride conductivity index (CCI) measured after 28 and 56 days of curing, are presented in Figure 7.27. Chloride conductivity indices of SCBA replaced concretes were lower than for control concrete. When compared to control, 32 % reduction in chloride conductivity index was observed for 25% SCBA replaced concrete at 28 days. In addition to this, a substantial reduction in chloride conductivity index was observed between 28 and 56 days for all the SCBA replacements because of the additional pozzolanic reaction. Reduction in CCI for 25 % SCBA replaced concrete was increased from 32 % to 54 % at 56 days. The notable reduction in the observed conductivity values for 15 % and 25 % SCBA replaced specimens compared to control specimen is a clear indication of the lesser permeability. Superior pozzolanic reactivity of the SCBA as well as enhancement in the pore structure because of pore refinement are responsible for higher resistance of SCBA replaced specimens against chloride ion penetration. Conductivity test results agreed well with the

observations from rapid chloride penetration test. In terms of the qualitative classifications suggested by Alexander et al. (1999) the 15 and 25% SCBA replaced concretes moved to the next higher category at 56 days.

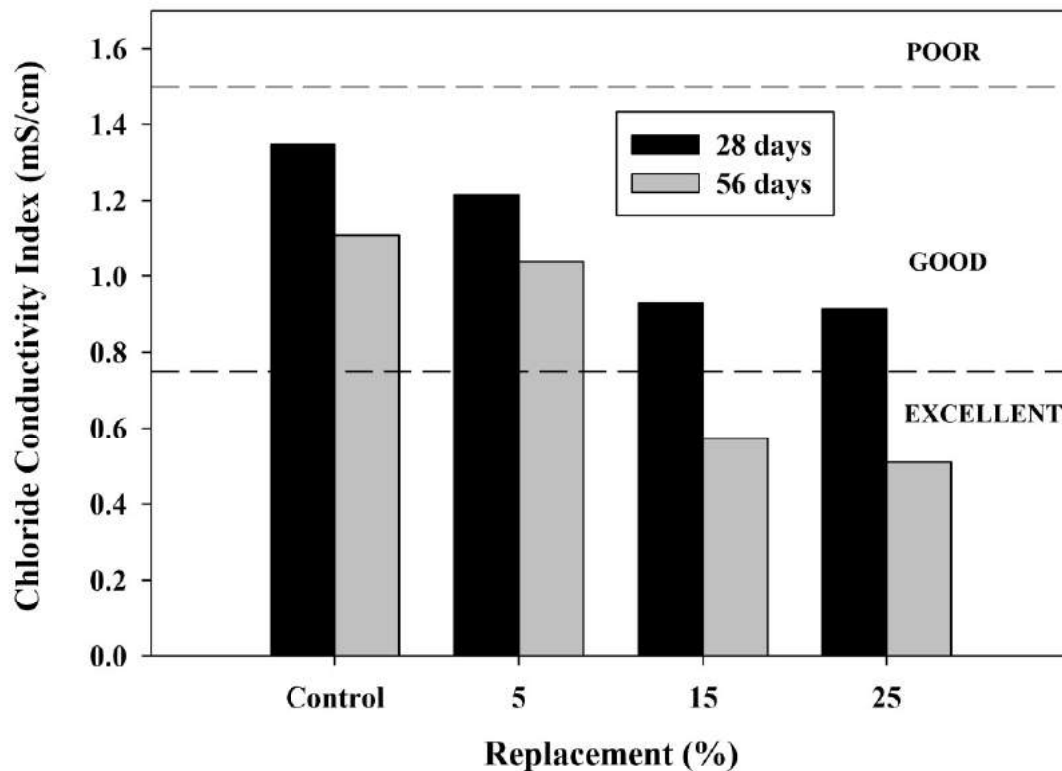


Figure 7.27: Chloride conductivity for concrete at 28 and 56 days of curing (qualitative classifications for concrete are also indicated)

7.3.4 Gas based tests

Results for oxygen permeability test are shown in Figure 7.28. As mentioned earlier, the oxygen permeability index (OPI) refers to the negative logarithm of the permeability coefficient – thus, higher OPI would indicate better concrete resistance against gas permeation. OPI values for control and 15%, 25 % SCBA replaced concretes were 10.0, 10.6 and 10.8 respectively after 56 days of curing. This significant increment in OPI value with the increase in SCBA replacement clearly indicates reduction in the permeability due to the pozzolanic performance of SCBA in concrete. As per the

qualitative classification suggested by Alexander et al. (1999) all concretes are in the ‘very good’ category.

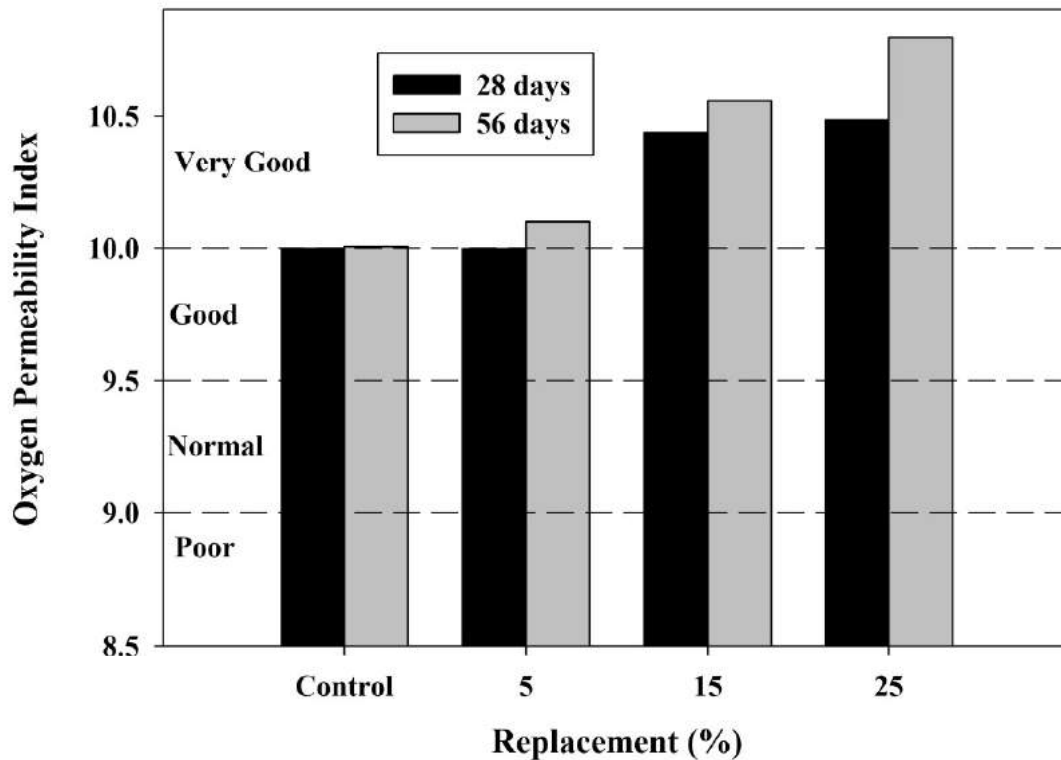


Figure 7.28: Oxygen permeability for concrete at 28 and 56 days of curing

In the Torrent test, if the specimen is more porous, a substantial rise in the effective pressure is observed in the inner chamber (Torrent Air permeability test user manual, 2010). As a result, the Torrent air permeability coefficient (kT) is higher. Oxygen permeability test is a gas permeability test that provides an indication about the degree of pore connectivity in the bulk concrete whereas Torrent air permeability test helps to assess the quality of cover concrete (DI manual, 2009). Coefficient of permeability for control concrete was $0.17 \times 10^{-16} \text{ m}^2$ at 28 days and it marginally reduced to 0.14×10^{-16} at 56 days as depicted in Figure 7.29. However, incorporation of SCBA led to significant reduction in the effective pressure for SCBA replaced concretes compared to control concrete at 28 as well as 56 days.

A considerable drop in the effective pressure represents greater improvement in the quality of cover concrete and also reduction in the permeability. Control specimens were categorized as ‘fair’ quality concrete as per qualitative classification recommended by standard SIA 162/1-2003. 5 % SCBA replaced concrete was also classified as ‘fair’ quality at 28 days. However, it moved to ‘very good’ range at 56 days due to additional pozzolanic reaction. Coefficient of permeability was further reduced to a greater extent for 15 % and 25 % SCBA replaced concretes as a result of enhancement in the quality of cover concrete. Test results from oxygen and Torrent air permeability tests clearly show the superior performance of SCBA replaced concretes compared to OPC concrete.

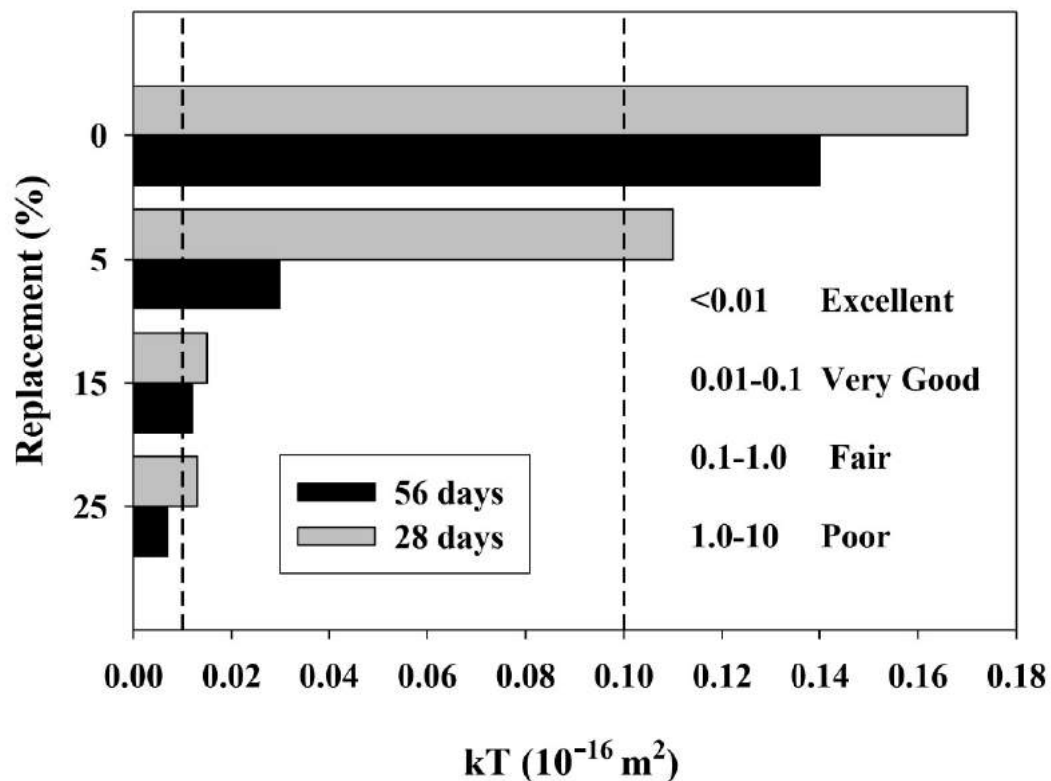


Figure 7.29: Torrent air permeability for concrete at 28 and 56 days of curing

7.3.5 Water based tests

Water sorptivity index was determined after 56 days of curing for control and SCBA replaced specimens. The sorptivity index indicates the resistance against movement of

water by capillary suction through the exposed surface of the concrete specimen, which is influenced by pore geometry of the concrete as well as curing duration. Unlike the results of the other permeability test methods, the trends with respect to sorptivity index (shown in Figure 7.30) for SCBA replaced concretes were not clear. While the 5% SCBA replaced concrete showed lower sorptivity compared to control concrete, the 15 and 25% SCBA replaced concretes indicated marginally higher sorptivity indices.

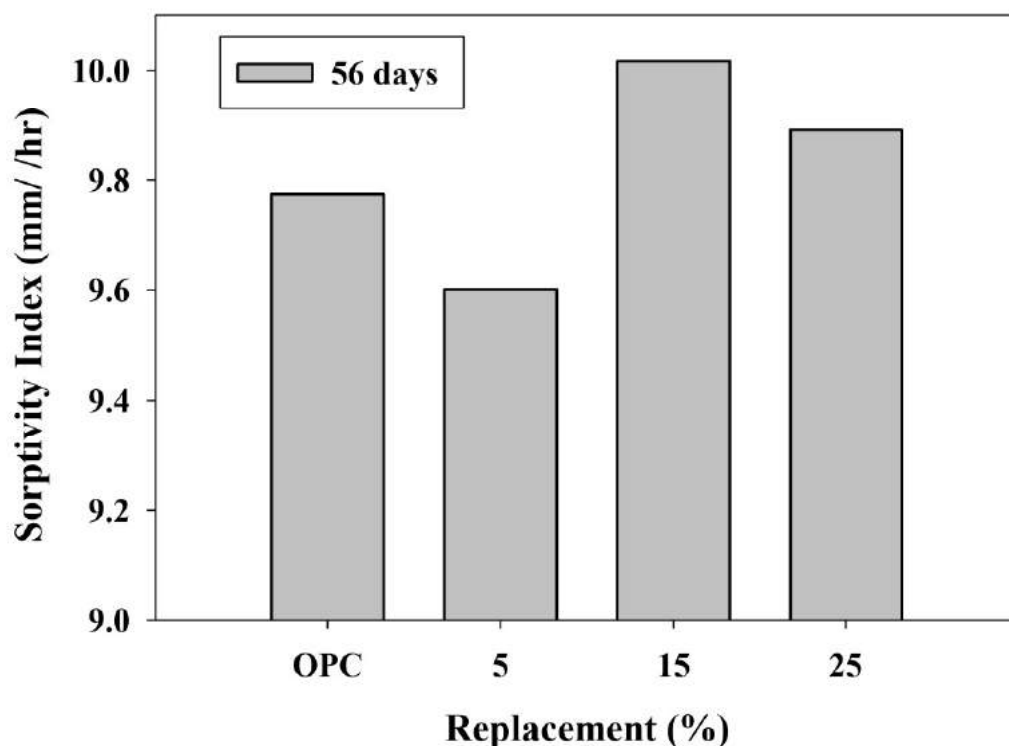


Figure 7.30: Sorptivity index for concrete at 56 days of curing

According to the classification suggested by Alexander et al. (1999), a wide range from less than 6 to greater than 15 exists for sorptivity index. In light of this, the variations seen in Figure 7.30 can be considered minor. Sorptivity index test is highly influenced by surface characteristics of specimen rather than the permeability (Alexander et al., 1999), which may account for the indifferent performance of the bagasse ash concretes. An additional explanation for the variation in the observed results is that the gain in mass in the sorptivity test is due to pore geometry and pore volume of the exposed surface, and may not be dependent on pore connectivity (Githachuri and Alexander,

2013). Because of this limitation in the sorptivity test, the performance of SCBA replaced concretes against water penetration was additionally evaluated by water permeability test as per DIN 1048-part 5 (1994) standard.

The water penetration depth was measured for control and SCBA replaced specimens in the DIN 1048 test after 28 and 56 days of curing. Average penetration depth for control concrete was 8.10 cm and 6.54 cm for 28 and 56 days cured specimens respectively. These higher than normal observed values can be attributed to the drying of the specimen at 50 °C for 7 days, which is a different way of conditioning than what is prescribed in the standard (where specimens removed from the moist room are directly tested). The conditioning method was followed in order to be consistent with the sorptivity test. Increase in SCBA replacement led to a reduction in water penetration, as depicted in Figure 7.31. When compared to control specimen, significant reduction (44%) was observed for 25 % SCBA replaced specimens at 28 days of curing. Penetration depth was further reduced to 74% for the same SCBA replacement after 56 days of curing. From the test results, it is evident that the use of SCBA significantly improves the resistance of concrete to water penetration.

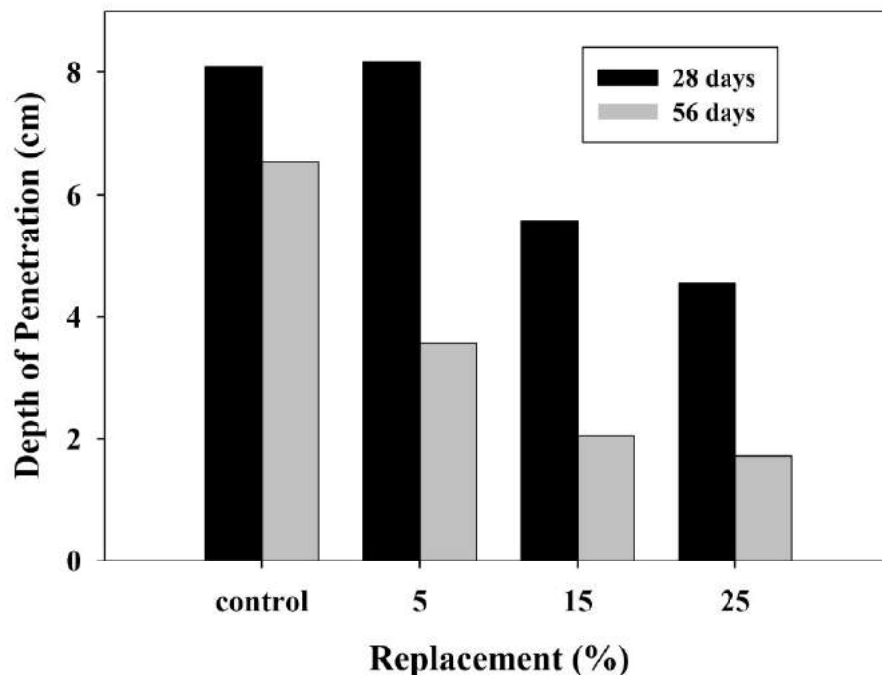


Figure 7.31: Water penetration depth for concrete at 28 and 56 days of curing

7.3.6 Electrical resistivity of concrete

Results of the Wenner resistivity test are described in Figure 7.32. Rupnow and Icengole (2011) have suggested that a strong correlation exists between surface resistivity and ion penetrability – higher resistivity implies lower penetrability. Resistivities of control and 5% SCBA replaced specimens were found to be in the ‘moderate risk’ category (as per the criteria suggested by Feliu et al., 1996) at 28 days as shown in Figure 7.32 (in this figure, the qualitative classifications represented as High, Moderate etc. are for the risk of corrosion). On the other hand, substantial increase in the surface resistivity was observed for 15 % and 25 % SCBA replaced specimens (26 k Ω -cm and 34 k Ω -cm respectively after 28 days of curing), and these two concretes fell in the ‘low risk’ category.

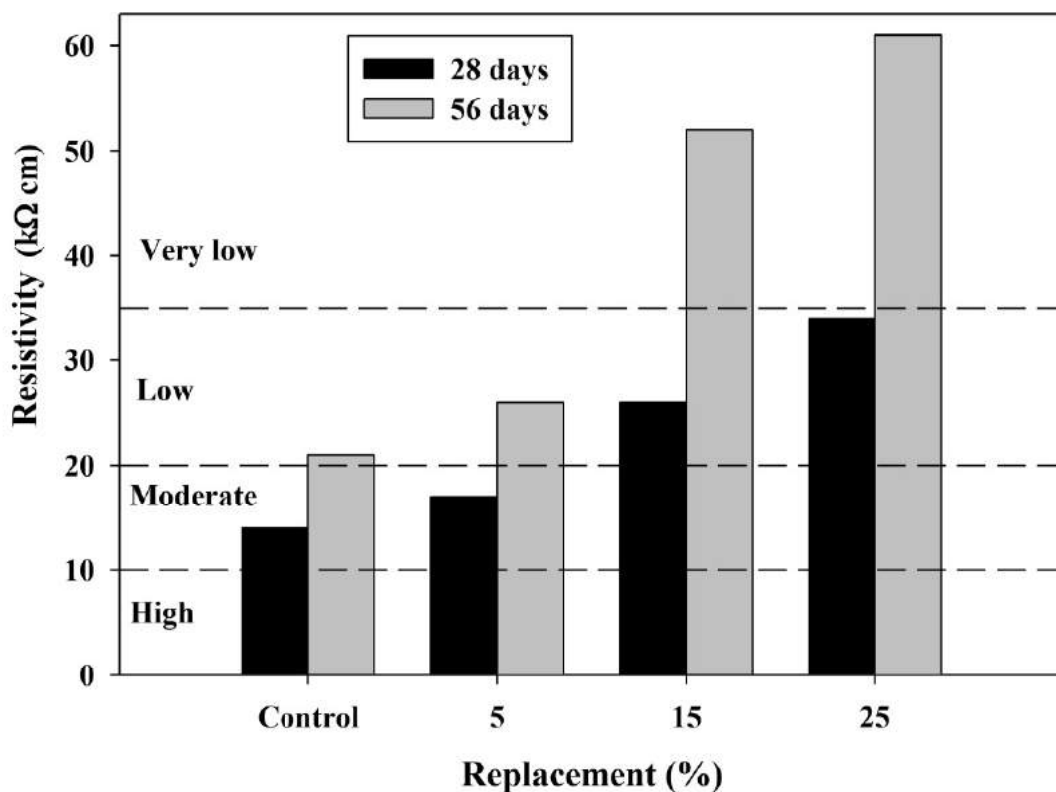


Figure 7.32: Resistivity for concrete at 28 and 56 days curing (qualitative classifications indicating corrosion risk based on Feliu et al. (2009) are also marked)

Higher surface resistivity was observed for all concretes at 56 days, but the enhancement in resistivity was significantly greater for the 15 and 25% SCBA replaced

concretes, which are again one qualitative category better. This is clearly an evidence for enhancement in the pore structure, reduction in the permeability of cover concrete as well as of the lowering of corrosion risk. 15 % and 25 % SCBA replaced concretes can be categorized as very low risk as per guidelines, as shown in Figure 7.32.

7.3.7 Drying Shrinkage

Length change due to drying shrinkage is presented in Figure 7.33. As expected, the rate of drying shrinkage was higher initially and marginally decreased with time. No significant differences were observed in the length change measurements between control and SCBA replaced concretes. Although small variations exist between different replacements, all the observed shrinkage strains are well below the limits recommended in the ACI 209 committee report (2005).

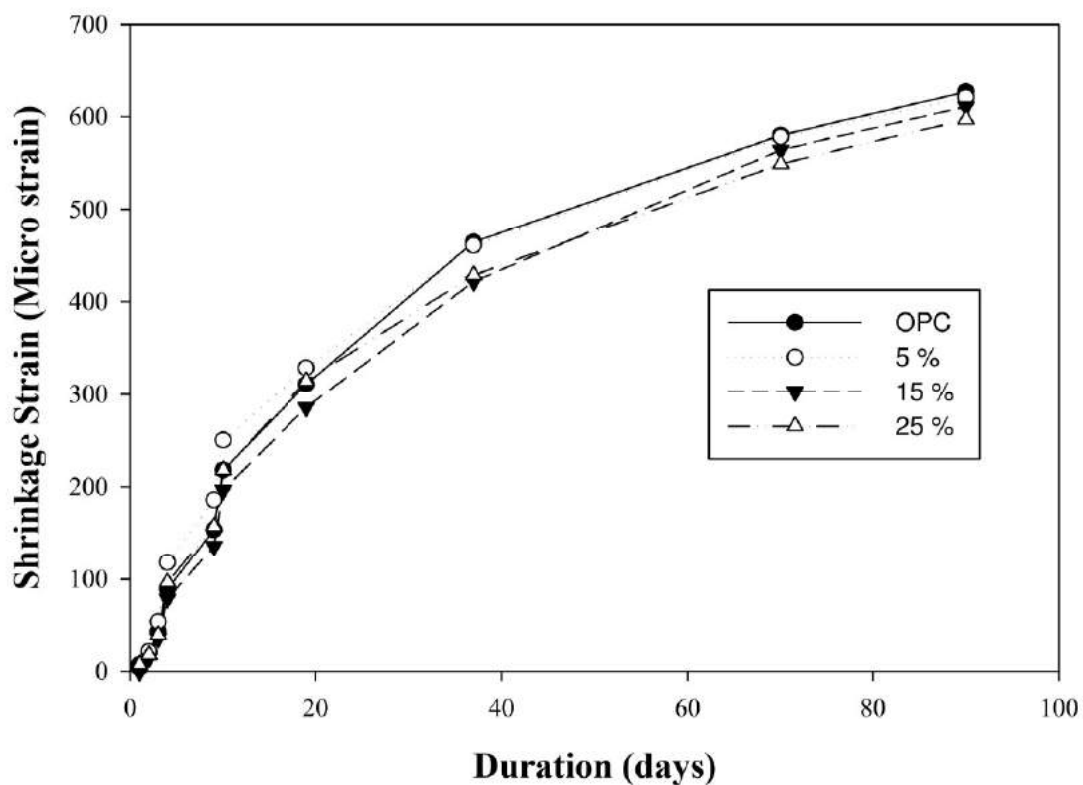


Figure 7.33: Drying shrinkage behaviour of concretes

7.4 SUMMARY

In this study, sugarcane bagasse ash (SCBA) based blended cements with five different levels of SCBA replacement were used to prepare concretes that were then subjected to a comprehensive evaluation of mechanical and durability properties (compressive strength, heat of hydration, drying shrinkage and durability characteristics). Concrete with bagasse ash replacement showed equal or marginally better strength performance compared to control concrete at different stages of curing. Additional long-term strength gain than control concrete due to pozzolanic reaction, significant reduction in permeability compared to control concrete by reason of pore refinement, lower heat of hydration than ordinary Portland cement and better long term properties were clearly observed in concretes with SCBA blended cements. The results clearly indicate that concrete of the same grade can be produced with up to 25% replacement of cement by SCBA.

CHAPTER 8

AVAILABILITY OF SUGARCANE BAGASSE ASH AND POTENTIAL FOR USE IN INDIAN CEMENT PLANTS

8.1 INTRODUCTION

The potential for application of any supplementary cementitious material significantly depends on the availability of the material and its pozzolanic characteristics. Because of high demand and rapid development in the construction sector, the consumption of Portland cement is increasing tremendously worldwide, and especially in India. The manufacturing process of cement needs a lot of raw materials from limited natural resources. Solid wastes from various by-products are used as blending material in the Portland pozzolana cement production to reduce cement content and achieve sustainable concrete. A number of alternative materials are available in enormous quantities in India and these materials have potential for use in cement production. A comprehensive estimation on the availability of sugarcane bagasse ash and its accessibility to the cement plants is imperative to achieve appropriate use of this material instead of disposal as waste. This chapter reports on a detailed systematic estimation of the availability of sugarcane bagasse ash in India. In addition to the quantification, accessibility of bagasse ash to Indian cement plants and comparison with accessibility of fly ash using ArcGIS analytical mapping tool are described in this chapter.

8.2 AVAILABILITY OF SUGARCANE BAGASSE ASH

The increased use of cogeneration systems in the sugar industries has led to an increase in generation of bagasse ash in India. It is important to estimate the extent of cultivation of sugarcane in India to quantify the exact availability of bagasse for cogeneration process. This is because sugarcane is crushed for different purposes such as sugar manufacturing, ethanol production etc. Therefore, a comprehensive background of the sugarcane

cultivation and generation of bagasse are presented in the following sections to estimate the availability of bagasse ash in India.

8.2.1 Contribution of India in world sugarcane production

India is the second largest producer of sugarcane in the world next to Brazil. India contributes 15% of the total sugarcane production in the world. Sugarcane cultivation in the world occupies an area of 20.42 million ha, accounting for a total production of 1333 million metric tons (FAO, 2003). The agricultural area in India under sugarcane cultivation spans about 4.175 million hectares with an average yield of 70 tonnes per hectare (<http://www.indianmirror.com/indian-industries/sugar.html>). Fifteen countries (Brazil, India, China, Cuba, Thailand, Pakistan, Mexico, South Africa, Columbia, Australia, United States of America, Philippines, Argentina, Myanmar, and Bangladesh) contribute to 86% of area and 87.1% of sugarcane production (NFCSE, 2011). World sugarcane production of major countries is illustrated in Figure 8.1 and production of sugarcane in three consecutive fiscal years (2008-2010) is shown in Figure 8.2.

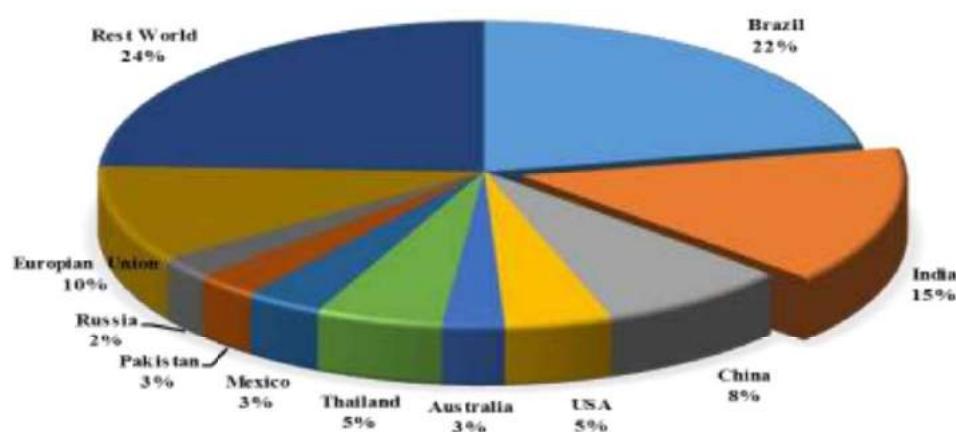


Figure 8.1: World sugarcane production

(Based on: http://www.vsisugar.com/india/statistics/international_sugar.html)

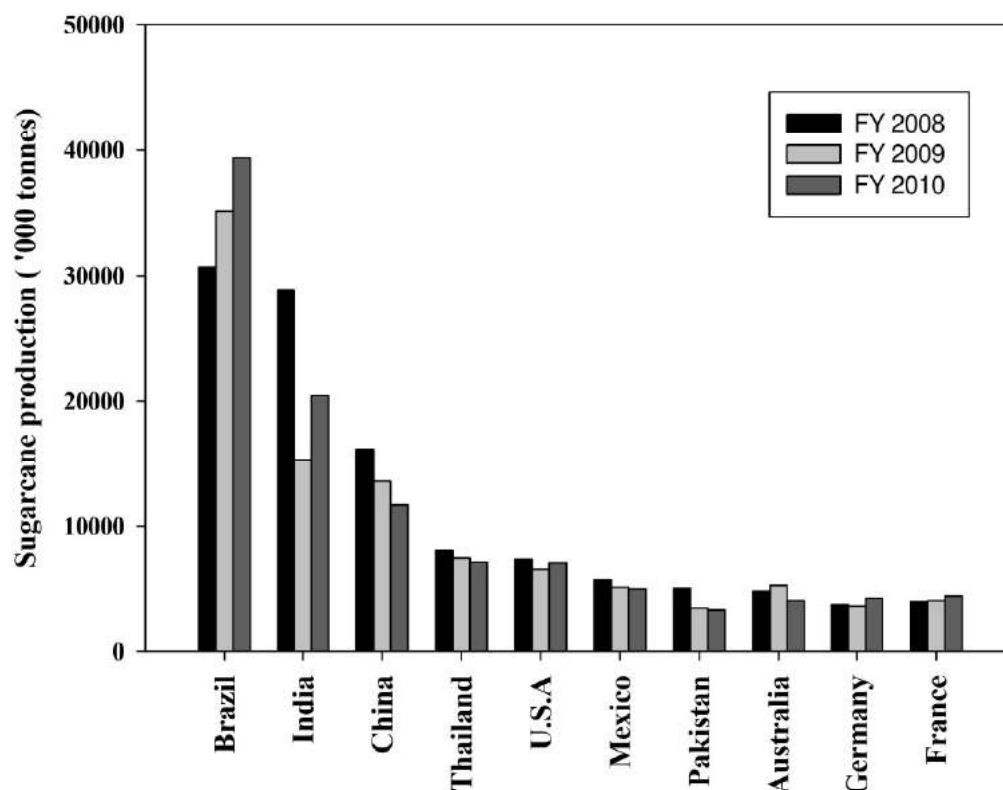


Figure 8.2: World sugarcane production in three consecutive fiscal years

The major sugarcane producing states in India are Uttar Pradesh, Karnataka, Maharashtra, Tamil Nadu, Gujarat, and Andhra Pradesh. These states contribute more than 85% of the total sugarcane production in India. Uttar Pradesh alone accounts for 41% of the total production. State wise sugarcane production in India is presented in Figure 8.3. The total production in India was about 340 MT in the year 2010-11, which was about 27% of the total sugarcane production in the world during the same period.

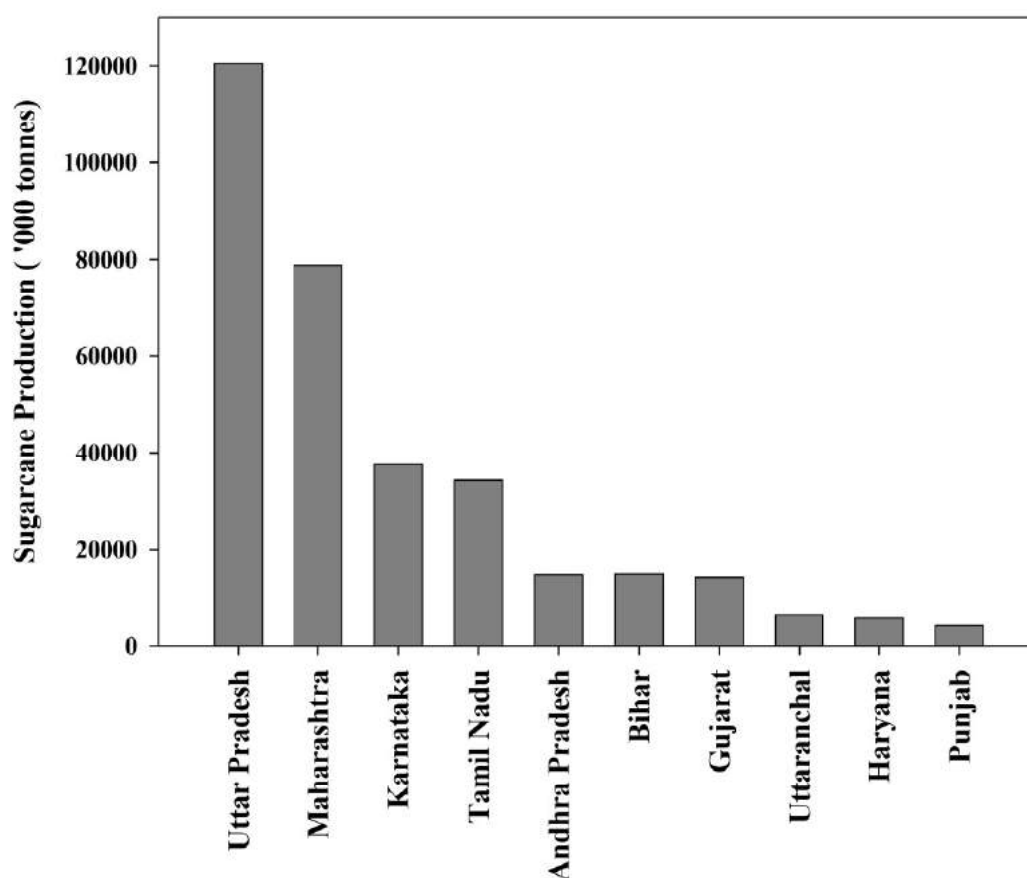


Figure 8.3: State wise sugarcane production in India (2010-11)

(Based on: Annual report on sugarcane cultivation, CACP, 2012)

Uttar Pradesh tops the list of sugarcane producing states with 76.85 MT production (2011-12). Maharashtra is the second leading producer with 54.5 MT production. In terms of yield per hectare, Tamil Nadu is the leading state with an average productivity of 108 tons/hectare followed by Karnataka (82.7 tons/hectare) in the year of 2008-2009 (Annual report on sugarcane cultivation, The commission for agricultural costs and prices (CACP), 2012).

Sugarcane production in India shows an increasing trend over the last 100 years both in terms of area under cultivation as well as productivity as shown in Figure 8.4. Over the last 8 decades - from 1930 to 2011 - the sugarcane production in the country increased by about 10 times (Report of Cooperative sugar, 2011)

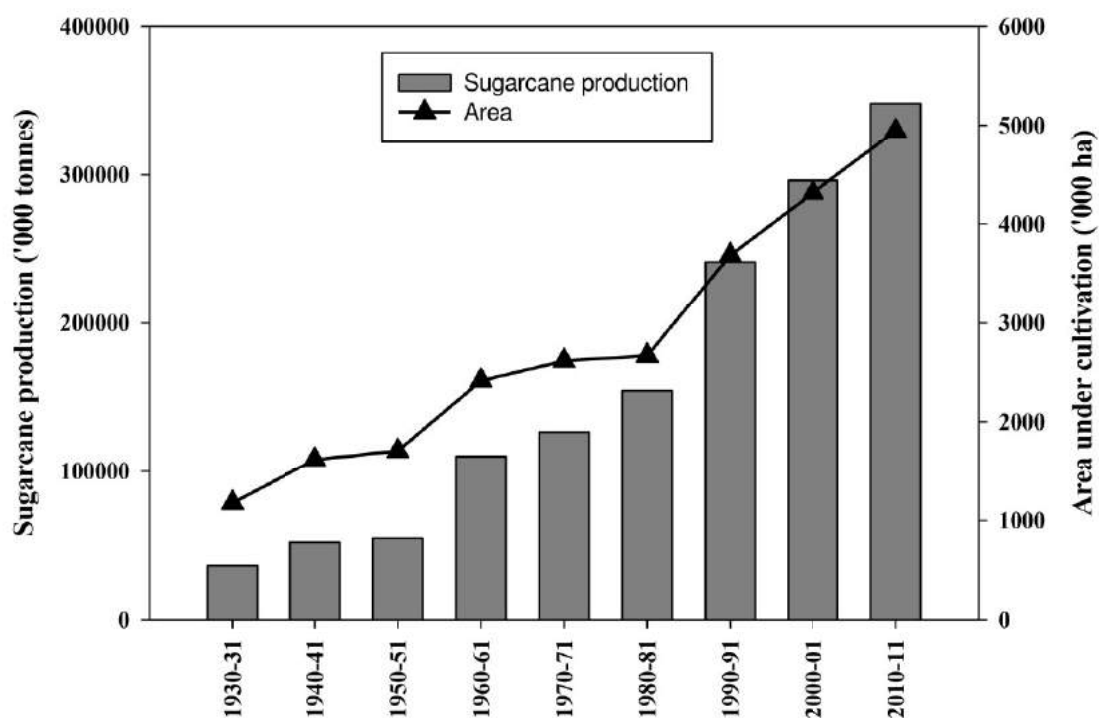


Figure 8.4: Trends of sugarcane production and area under cultivation in India

(Based on Report of Cooperative sugar, 2011)

In addition, the yield of sugarcane production increased from 33 tonnes/ha to 66 tonnes/ha. The yield nearly doubled over the last 50 years and production witnessed an increase by almost 8 times. The area under sugarcane cultivation showed an increase of about 2.5 times from the year 1950-51 to 2000-01 (Report of Cooperative sugar, 2011).

8.2.2 Availability of sugarcane bagasse in India

Sugarcane is crushed to extract the juice and after extraction, bagasse is separated to feed as fuel to the cogeneration boiler. As mentioned earlier, the crushing of sugarcane stalks produces 28-30% by weight of bagasse (Xiasun et al., 2003).

Generation of bagasse can be calculated from the total sugarcane production because almost the entire cultivated sugarcane is crushed for different purposes. However, availability of bagasse ash is only estimated based on the crushing capacity of sugar mills in this study to obtain the exact quantity of bagasse ash. Figure 8.5 illustrates sugarcane crushed as well as bagasse generated in India over the last 6 decades. Generation of bagasse was found to be increased steadily in India as a result of greater sugar production. The quantity of bagasse was calculated as the average value from the production in two consecutive fiscal years (2009-10 to 2010-11). The generation of sugarcane bagasse in the major sugarcane producing states is presented in Figure 8.6.

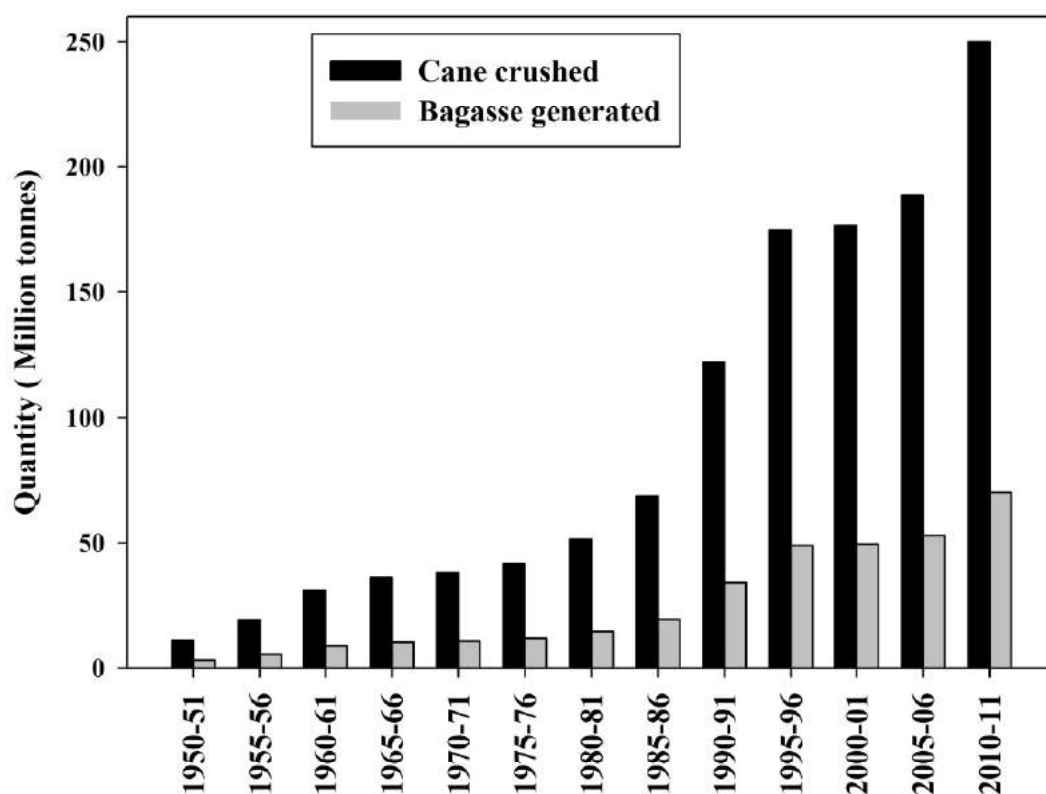


Figure 8.5: Sugarcane crushed and bagasse generated in India over the last 6 decades

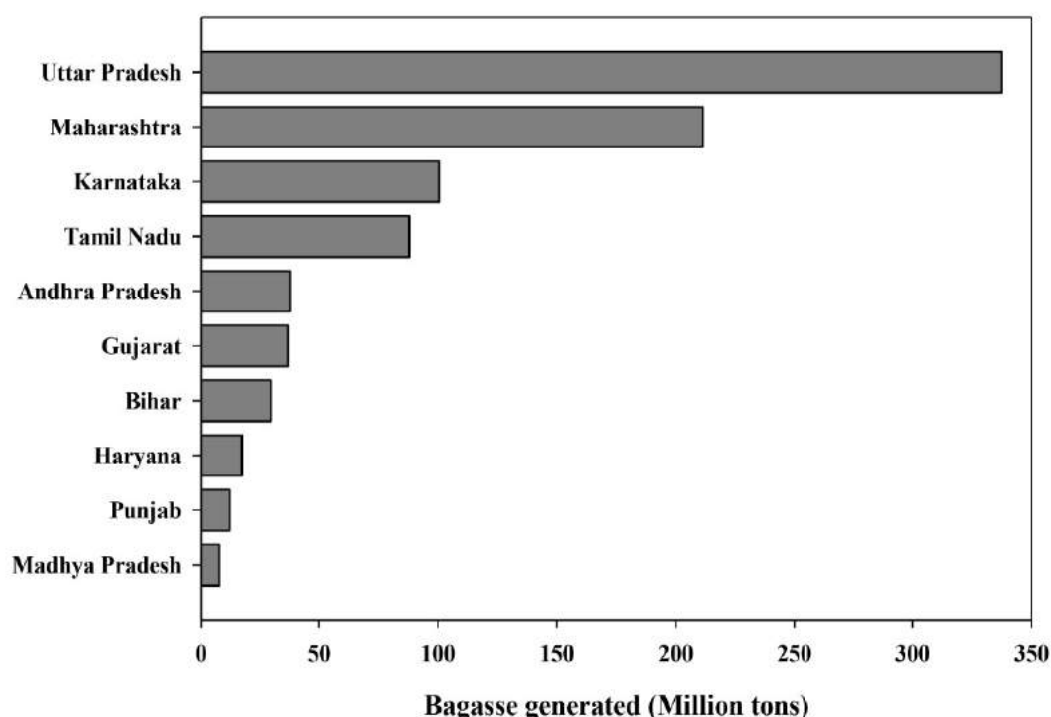


Figure 8.6: Generation of sugarcane bagasse in Indian states - Mean 2009-10 to 2010-11

Bagasse based co-generation makes a sugar mill self-sufficient in terms of the energy requirement. There are 566 operating sugar mills in India, out of which 219 have an installed modern cogeneration system (List of cane sugar factories and distilleries, 2011). In addition, bagasse is burnt as fuel in the remaining mills with conventional boiler system to produce low pressure steam for the production process of sugar. The total number of active sugar mills in the year 1950 was 139, and this number rose to 566 in 2011-2012, i.e. there was almost 5 times increase in the number due to increase in sugar production. Figure 8.7 shows the total number of sugar mills and number of sugar mills with modern co-generation plants in the chief sugarcane producing states of India.

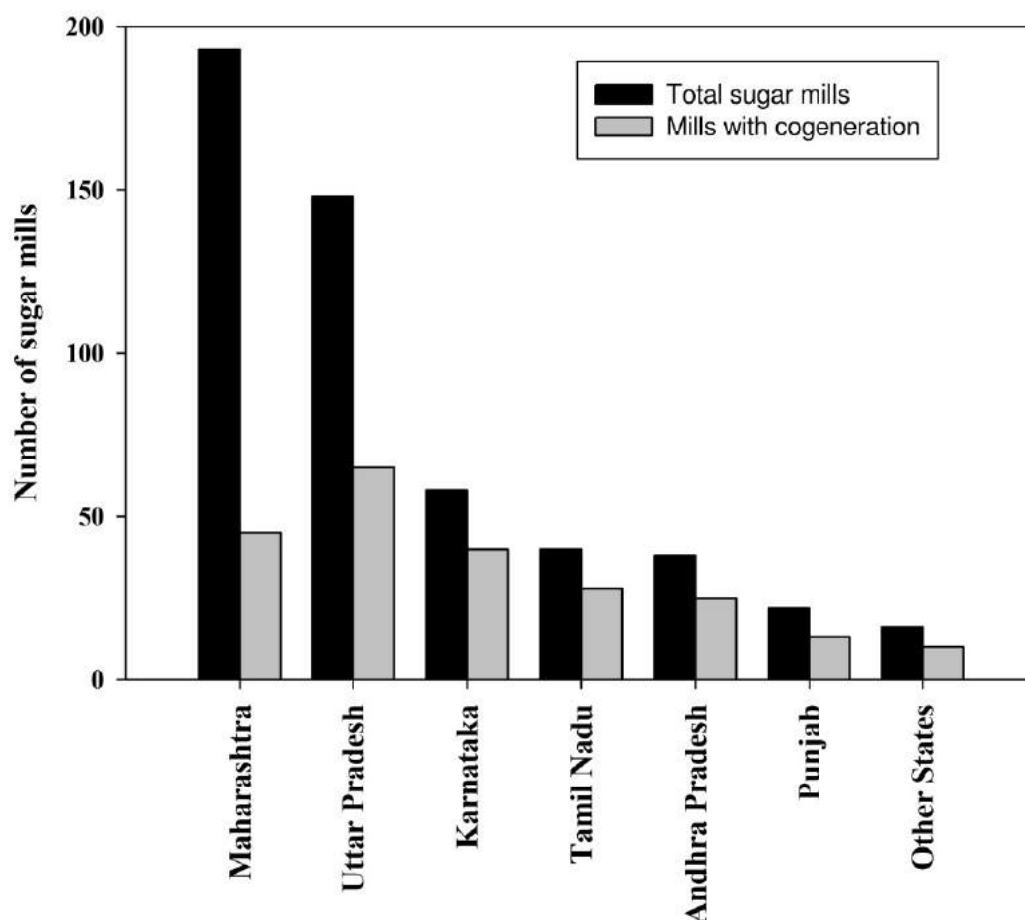


Figure 8.7: Total number of sugar mills with cogeneration plants

Bagasse based cogeneration plants began to develop in the sugar mills in 1990. Rapidly the co-generation process became popular and within 20 years more than 200 mills developed their own co-generation plants. Currently there are 220 sugar mills with an installed co-generation plant. The total power generation from 219 sugar mills having co-generation plants quantifies to 2636 MW (Solomon, 2011). Rapid implementation of modern cogeneration system in the country clearly indicates bagasse ash availability in India.

8.2.3 Availability of sugarcane bagasse ash in India

The fibrous ash is collected after the burning of bagasse in boilers during the cogeneration process. This fibrous waste material is found to have characteristics of a

supplementary cementitious material because it is rich in amorphous SiO_2 . 8-10% of the bagasse burned during the cogeneration process gets converted to bagasse ash (Goyal et al., 2010). Bagasse is burnt in the modern cogeneration boilers under controlled conditions at an optimum temperature and for an optimum time. One ton of cane produces energy of 1 MWh. Therefore, the production of 1 MWh of energy produces nearly 22-30 kg of bagasse ash (WADE Report, 2004). Thereby, quantifying the energy evolved from cogeneration process, the quantification of bagasse ash availability can be done. This section of this chapter aims in quantifying the availability of sugarcane bagasse ash in India.

In previous years, apart from cogeneration process, bagasse was used for several processes including as raw material in the manufacturing process of paper. At present, bagasse is completely used as fuel to the cogeneration boiler due to power scarcity as well as high economic revenue from the cogeneration system to the sugar mills. In addition to that, there have been a number of mandatory guidelines recommended to the sugar mills by power authority in India (CPRI) and state governments to promote biofuel utilization as well as tackle power shortage in the country.

Currently, all sugar mills that have cogeneration units completely utilize the bagasse generated during sugar production for the cogeneration process. From the cogeneration capacity of the plant and amount of bagasse burnt in cogeneration process, the total bagasse ash availability in the country is calculated to be 44220 tons/day. Uttar Pradesh is the leading producer of bagasse ash producing a quantity of 17160 tons/day. Maharashtra, Karnataka, Tamil Nadu, Andhra Pradesh etc. are the other major producers of bagasse ash.

Generally the operational season of sugar mills is about 200 days in a year (Natu, 2005). With this estimate, the total amount of bagasse ash generated annually in India amounts to be about 9 million tons, which is a large quantity to be disposed; this would be a critical concern for sugar industries due to lack of disposal land and environmental restrictions. Availability of bagasse ash is detailed state-wise in Table 8.1.

Table 8.1: Bagasse ash generation in sugar mills in states of India

Sl. No.	State	Number of sugar mills	Bagasse ash (tonnes/day)
1.	Andhra Pradesh	33	2195
2.	Bihar	9	896
3.	Gujarat	21	1624
4.	Chhattisgarh	1	60
5.	Haryana	15	1052
6.	Karnataka	56	4200
7.	Madhya Pradesh	9	453
8.	Maharashtra	192	10687
9.	Orissa	7	308
10.	Punjab	22	1290
11.	Tamil Nadu	40	3060
12.	Uttar Pradesh	143	17160
13.	Uttarakhand	10	997
14.	Other states	8	240
	Total	566	44222

Cogeneration process in the sugar industries in India is showing a consistent growth over the past decades. As stated earlier, 220 mills have modern cogeneration plants in India and new cogeneration plants are under construction in the remaining sugar mills. Because of economic benefits and self-sufficient energy generation, all the sugar industries are also expanding their available cogeneration capacity. Shortly, bagasse ash generation will reach large quantities and disposal will be a key issue in the sugar sector. For example, in the case of Tamil Nadu, there are 40 operational sugar mills in the state, 16 in co-operative sector, 3 in public sector and 21 in private sector. Out of these, 25 sugar factories have installed effective cogeneration power plants which are connected to high efficiency grids, and export the surplus power generated to the grid. Implementation of cogeneration process in remaining plants is striving towards completion. Increase in cogeneration trend in Tamil Nadu is depicted in Figure 8.8. Most of the sugar mills in the major states of sugar production in India are also under cogeneration plant implementation. Instead of disposal, the utilization of bagasse ash as pozzolanic material in concrete has to be promoted.

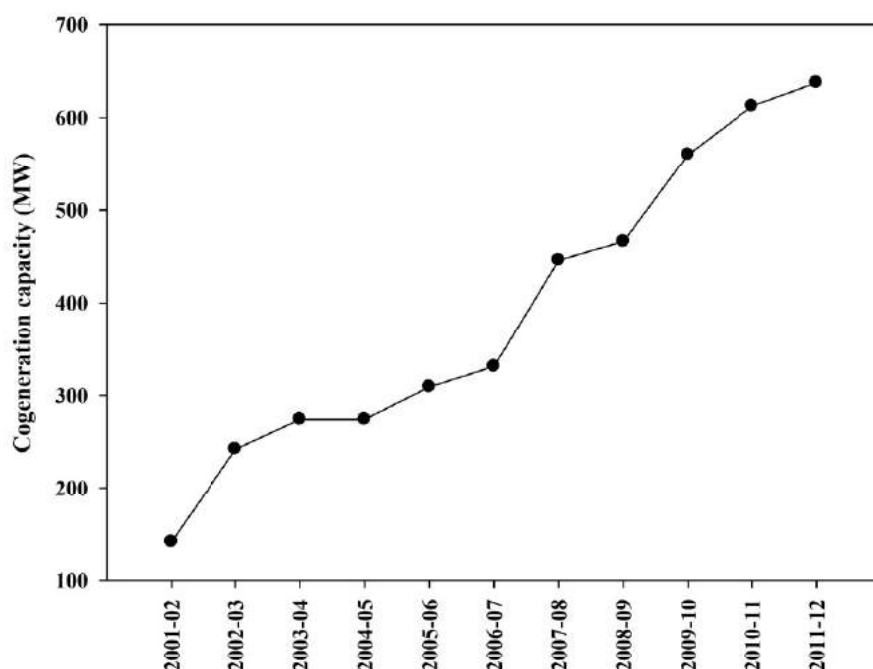


Figure 8.8: Trend in bagasse based cogeneration in Tamil Nadu
(Based on: Tamil Nadu electricity regulatory commission report, 2012)

8.3 AVAILABILITY MAPPING USING ArcGIS

At present, fly ash is mainly used as blending material for the production of Portland pozzolana cement in India. Although plentiful amount of fly ash is available for blended cement production, location of thermal plants due to availability of coal and variability in the characteristics of fly ash (highly depends on the properties of coal used for burning) are barriers for the cement manufacturers. Bagasse ash is available in abundant quantity in India and sugar mills are located around many cement plants due to the cultivation of sugarcane. In addition to that, the modern cogeneration system is well controlled with sophisticated instruments. Controlled process of burning of bagasse in the cogeneration boilers leads to uniform characteristics of the resultant bagasse ash. It is interested to note that an enormous quantity of bagasse ash is available adjacent to the cement plants compared to fly ash. To get a clear comparison of bagasse ash and fly ash accessibility to Indian cement plants, availability mapping was done using ArcGIS software.

8.3.1 Location of plants

According to the sugar technologist association of India (STAI, 2011) report, 566 sugar mills are available in India. For this study, the location of sugar mills was done using Google earth and the corresponding longitude as well as latitude were noted. Based on global cement magazine report (Edwards, 2013), India has 201 cement plants (inclusive of integrated cement plants and grinding units). In this study, only the major 137 integrated cement plants were considered for mapping. In accordance with Central Power Research Institute (CPRI, 2013) report, 88 coal based power plants were included in the mapping process to represent fly ash availability for comparison with bagasse ash. In a similar manner as for the sugar mills, longitude and latitude data of thermal plants as well as cement plants were collected. The plant locations were mapped by using ArcGIS. The locations of major cement plants, sugar mills and thermal plants in India are shown in Figures 8.9-8.11.

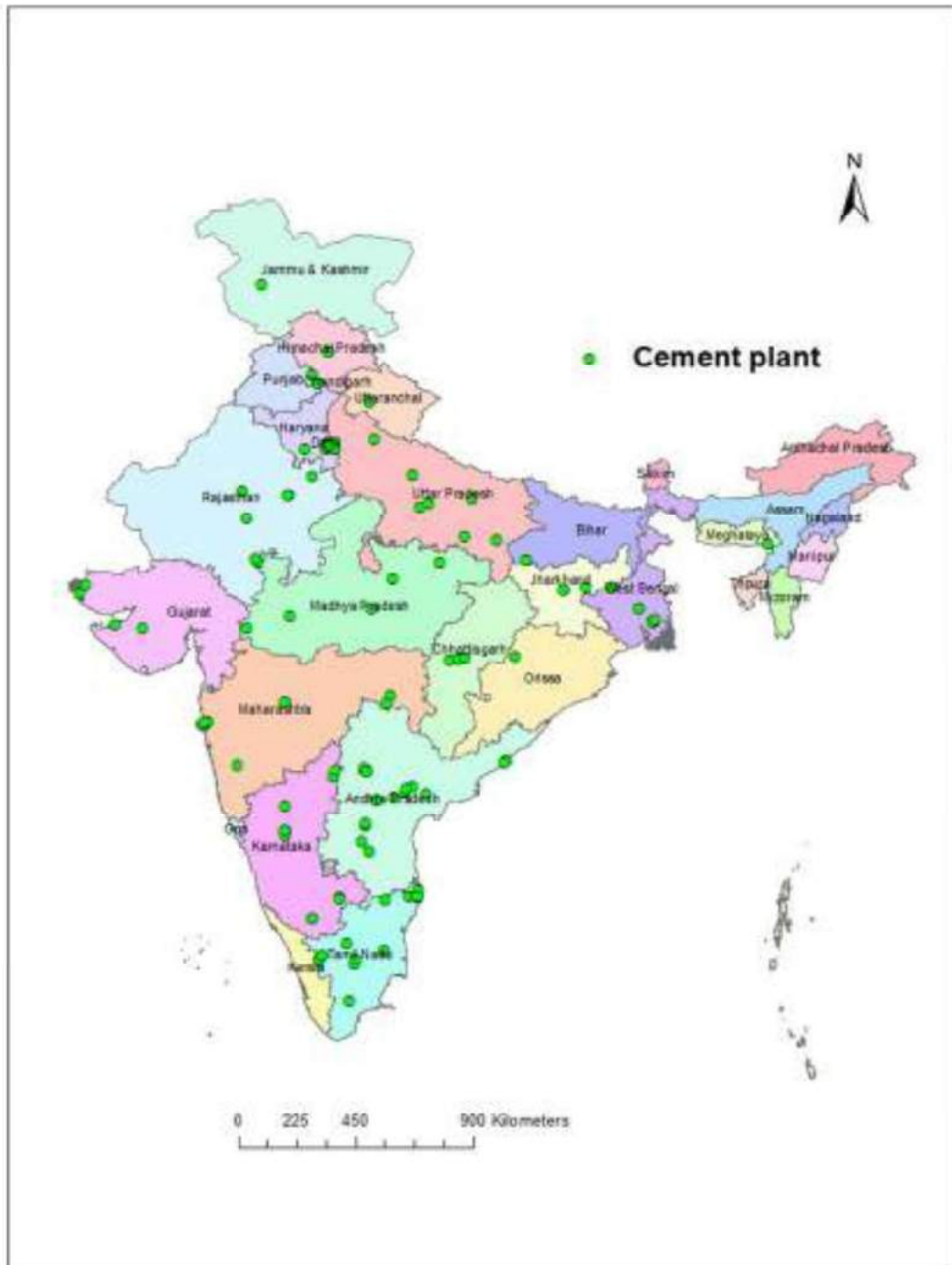


Figure 8.9: Location of cement plants in India

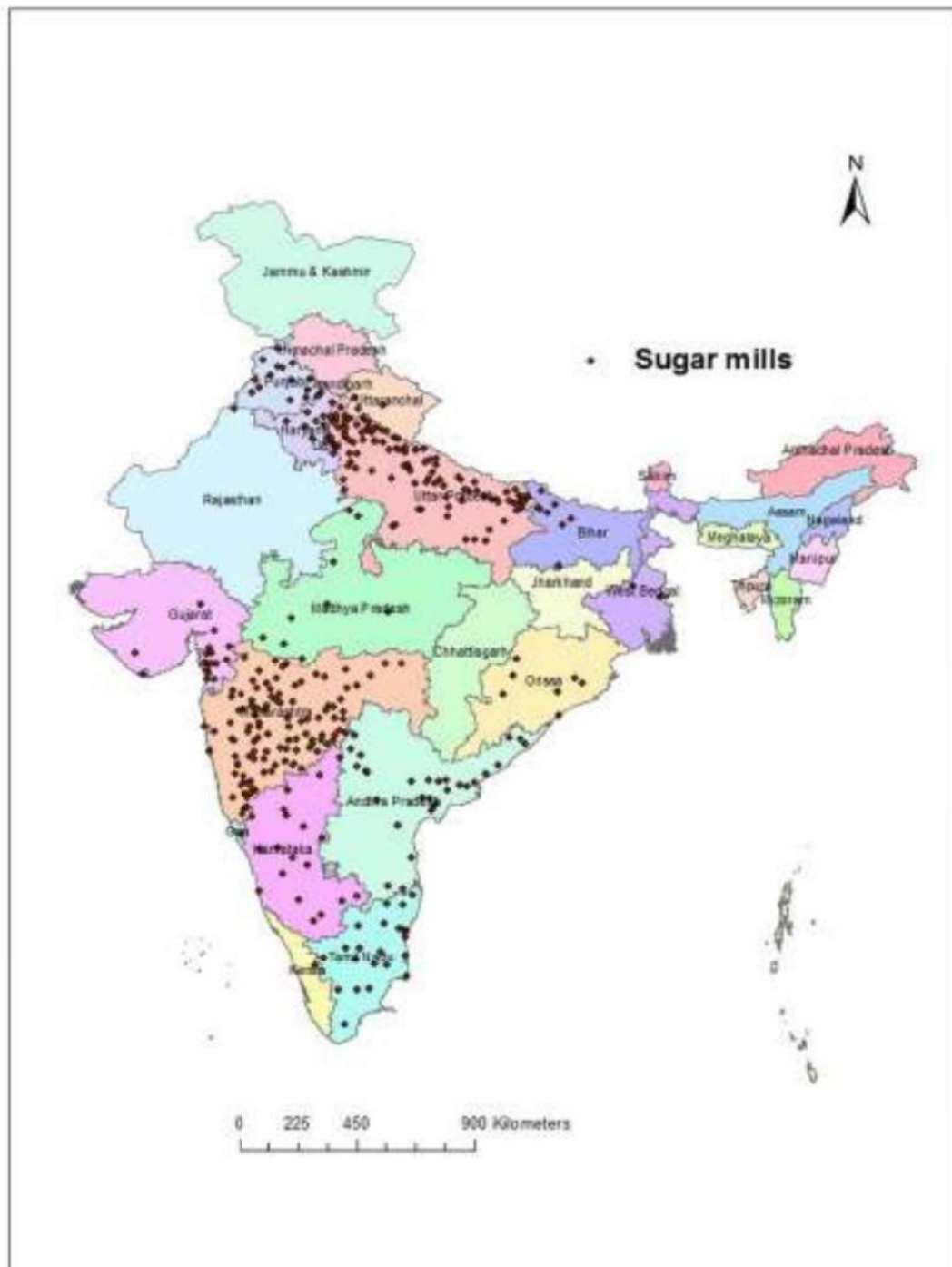


Figure 8.10: Location of sugar mills in India

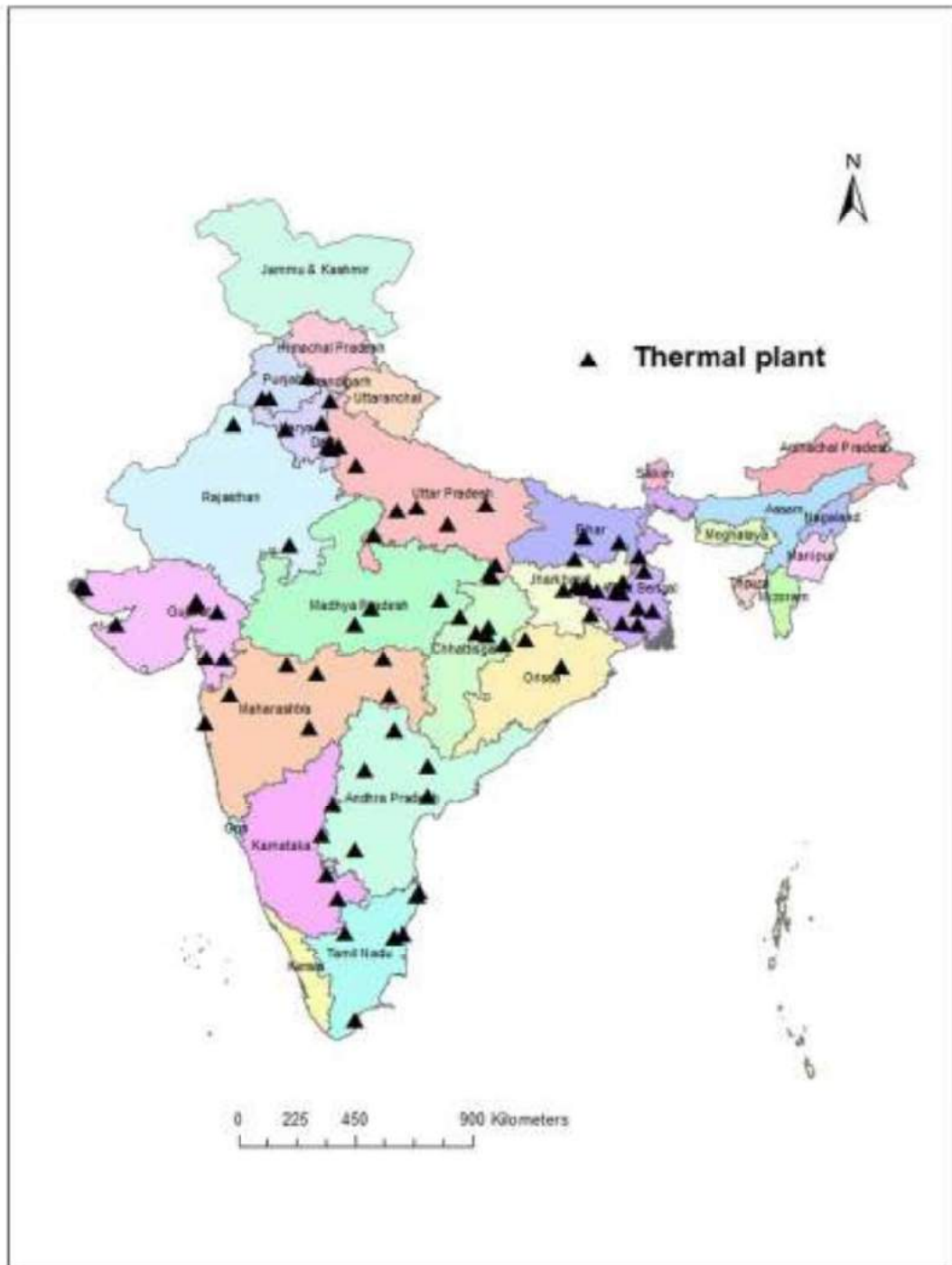


Figure 8.11: Location of thermal power plants in India

Figure 8.10 clearly shows the presence of sugar mills in all the parts of seven major states (Uttar Pradesh, Karnataka, Maharashtra, Tamil Nadu, Andhra Pradesh, Punjab and Haryana). On the other hand, only certain parts of Gujarat, Bihar, Orissa, Madhya Pradesh and West Bengal have sugar mills by reason of more sugarcane cultivation in specific areas. Figure 8.9 shows the presence of several cement plants in Uttar Pradesh, Tamil Nadu Karnataka, Maharashtra, Andhra Pradesh, and Haryana where bagasse ash is available in enormous quantities. On the contrary, the number of thermal power plants in these states (presented in Figure 8.11) is limited.

8.3.2 Availability mapping

The availability of bagasse ash was estimated based on the capacity of individual plant cogeneration system. The generation of bagasse ash from an individual plant was calculated and represented as the availability of bagasse ash on the same location (i.e. pointed on the same longitude and latitude in the map using ArcGIS). Instead of mapping the average value to the particular part of the state, this method attempts to understand the exact availability of alternative materials in a particular region. In a similar way, fly ash availability was marked in the map for comparison with bagasse ash. Figure 8.12 represents the availability of bagasse ash in India with seven classes (0-350 tonnes/day, each range marked with different colours) whereas availability of fly ash from individual thermal plants is illustrated in Figure 8.13 with five different ranges.

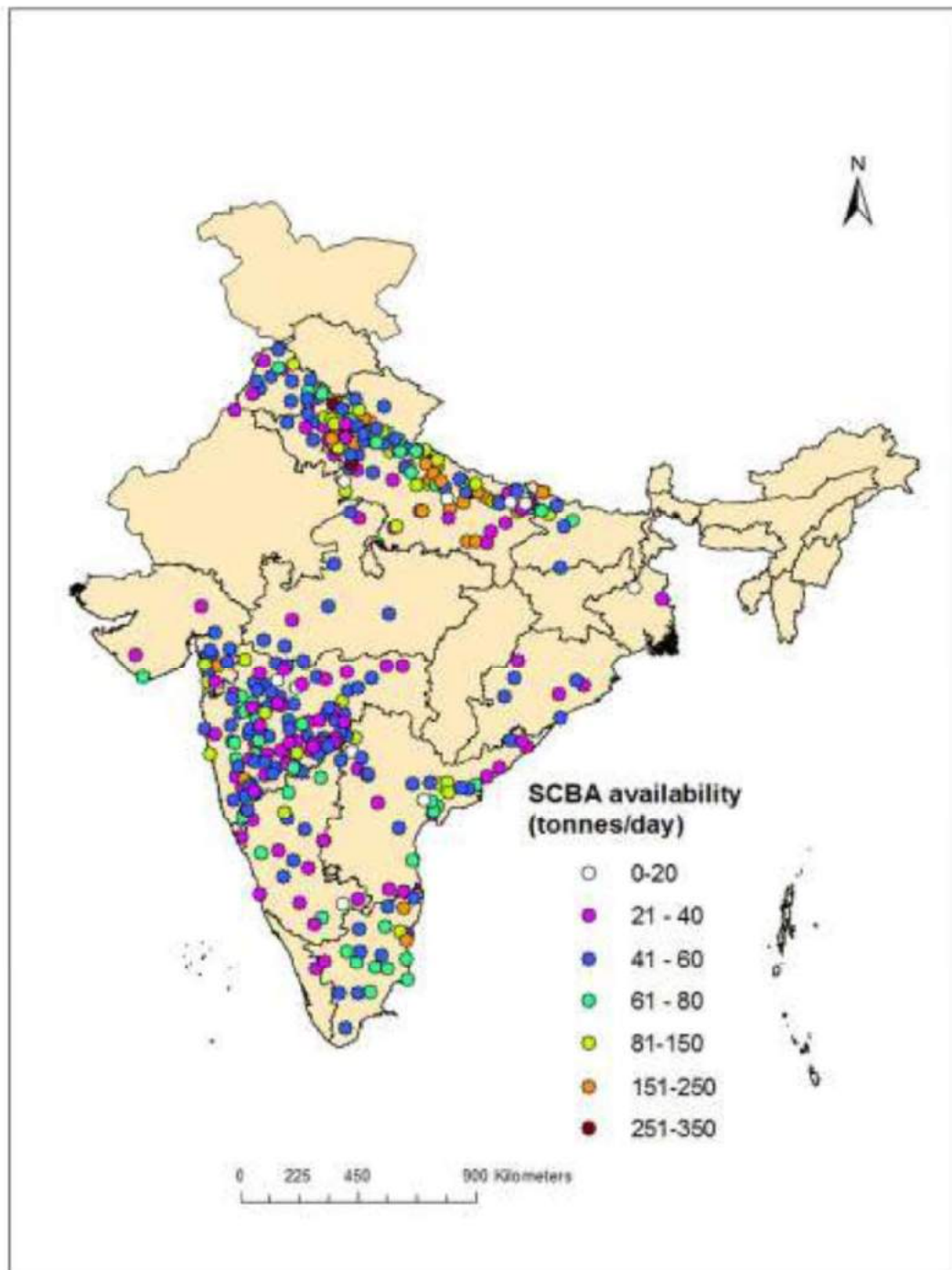


Figure 8.12: Availability of sugarcane bagasse ash in India

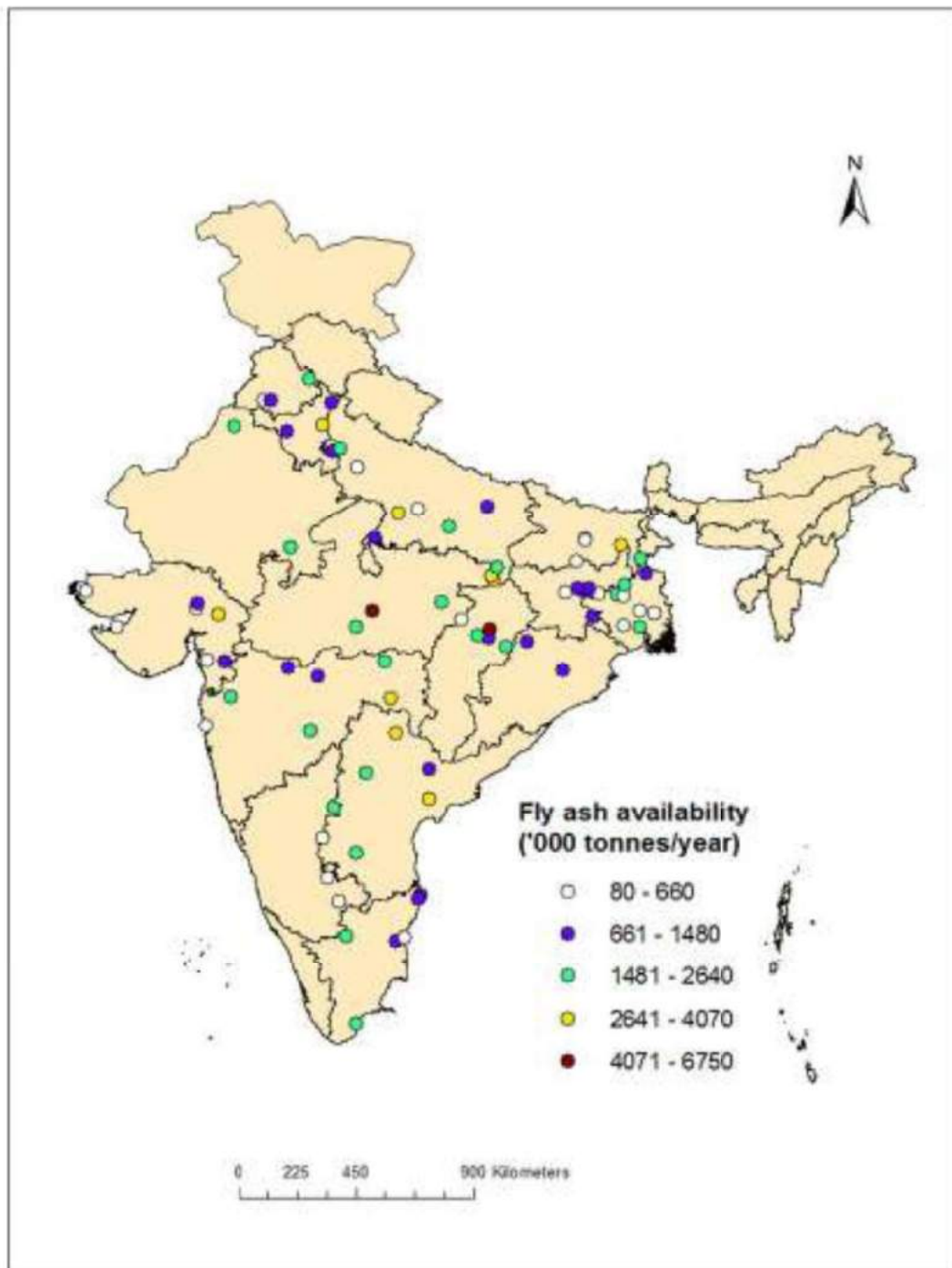


Figure 8.13: Availability of fly ash in India

The locations of cement plants are merged on the availability maps of bagasse ash and fly ash to reach a better understanding about the accessibility of these alternative materials to the cement manufacturers. It is interesting to note from Figures 8.14 and 8.15 that the accessibility of bagasse ash to the cement plants is better compared with fly ash. This is especially true in the major sugarcane producing states.

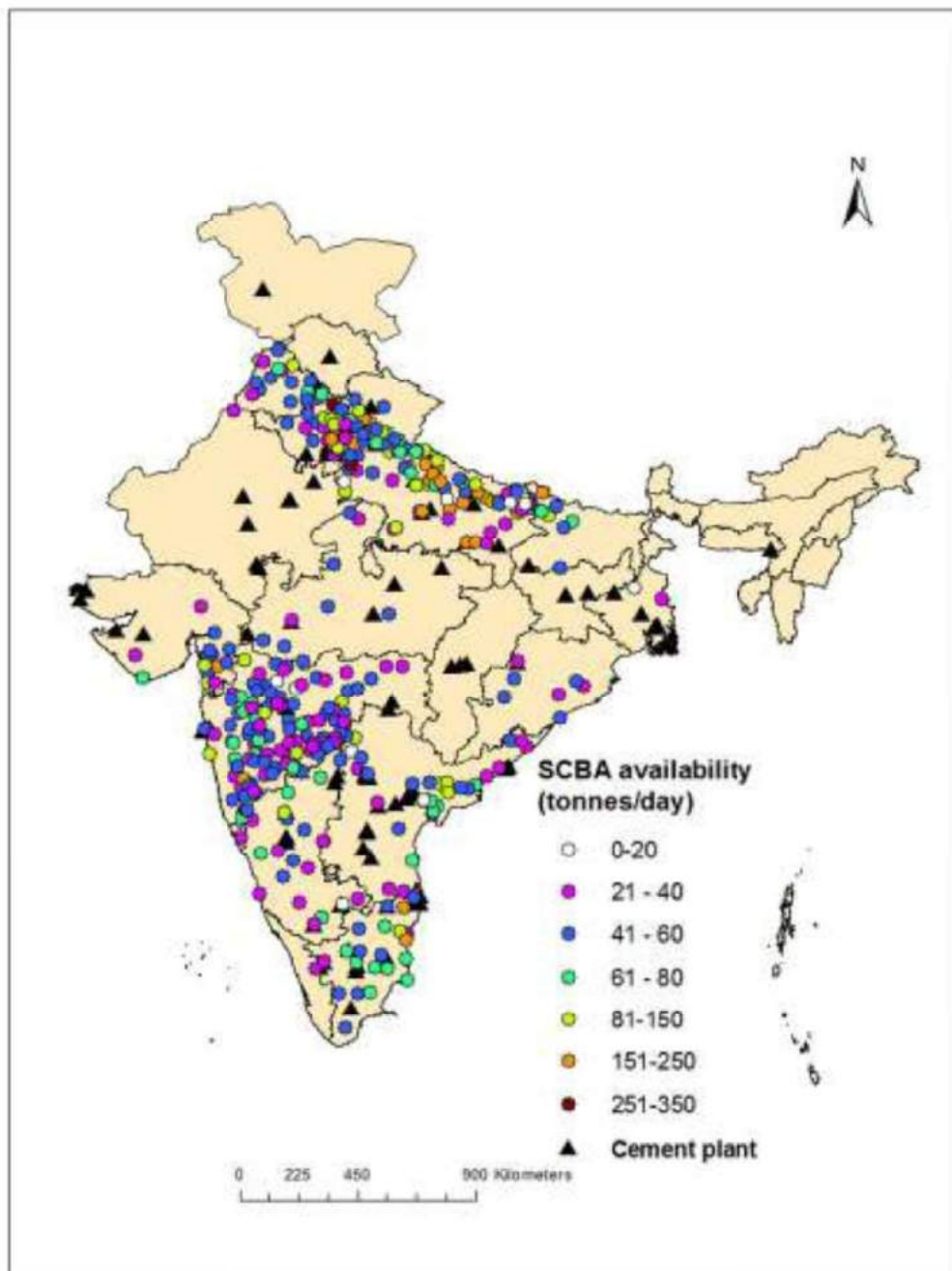


Figure 8.14: Location of cement plants on the availability map of sugarcane bagasse ash

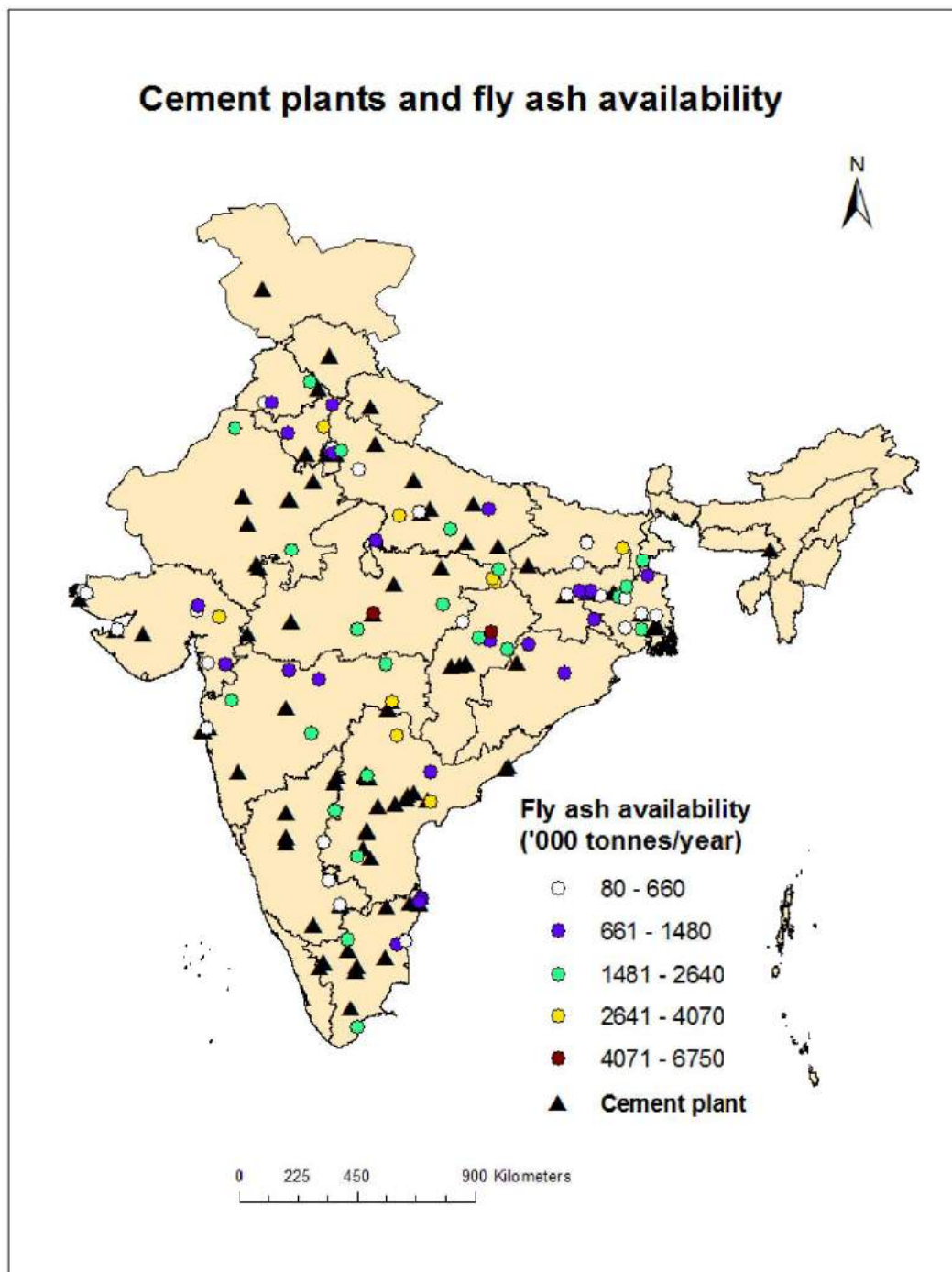


Figure 8.15: Location of cement plants on the availability map of fly ash

To enable a better understanding, the locations of cement plants, sugar mills and thermal plants were plotted on the same map to figure out the accessibility of bagasse ash and fly ash in a state-wise form. Figures 8.16-8.20 show presence of sugar mills and thermal plants along with cement plants for the major sugarcane producing states Tamil Nadu, Karnataka, Uttar Pradesh, Maharashtra, and Andhra Pradesh respectively. For example, in the case of Tamil Nadu, the central parts of the state have a number of cement plants and sugar mills close to each other as seen in Figure 8.16. In addition to that fly ash is not available in these regions, and needs to be transported over long distances, which affects its economy. Therefore, bagasse ash can be an excellent alternative source for blended cement production in the cement plants of the central part of Tamil Nadu. Similarly, Karnataka has a number of bagasse ash sources near to cement plants when compared to fly ash, as depicted in Figure 8.17. A quick glance of Figures 8.18 – 8.20 indicates a similar scenario in the other three states also.

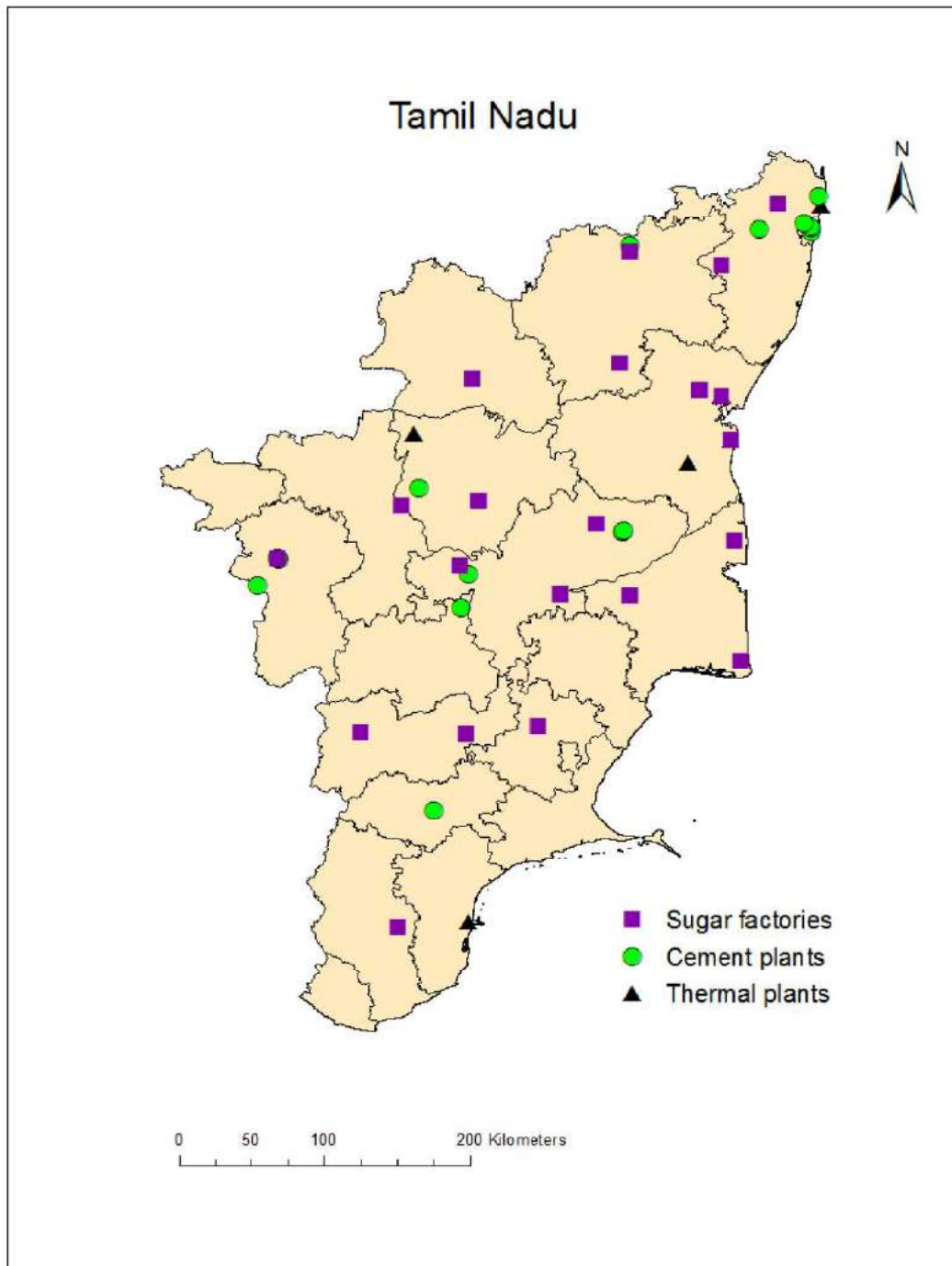


Figure 8.16: Location of sugar mills, cement and thermal plants in Tamil Nadu

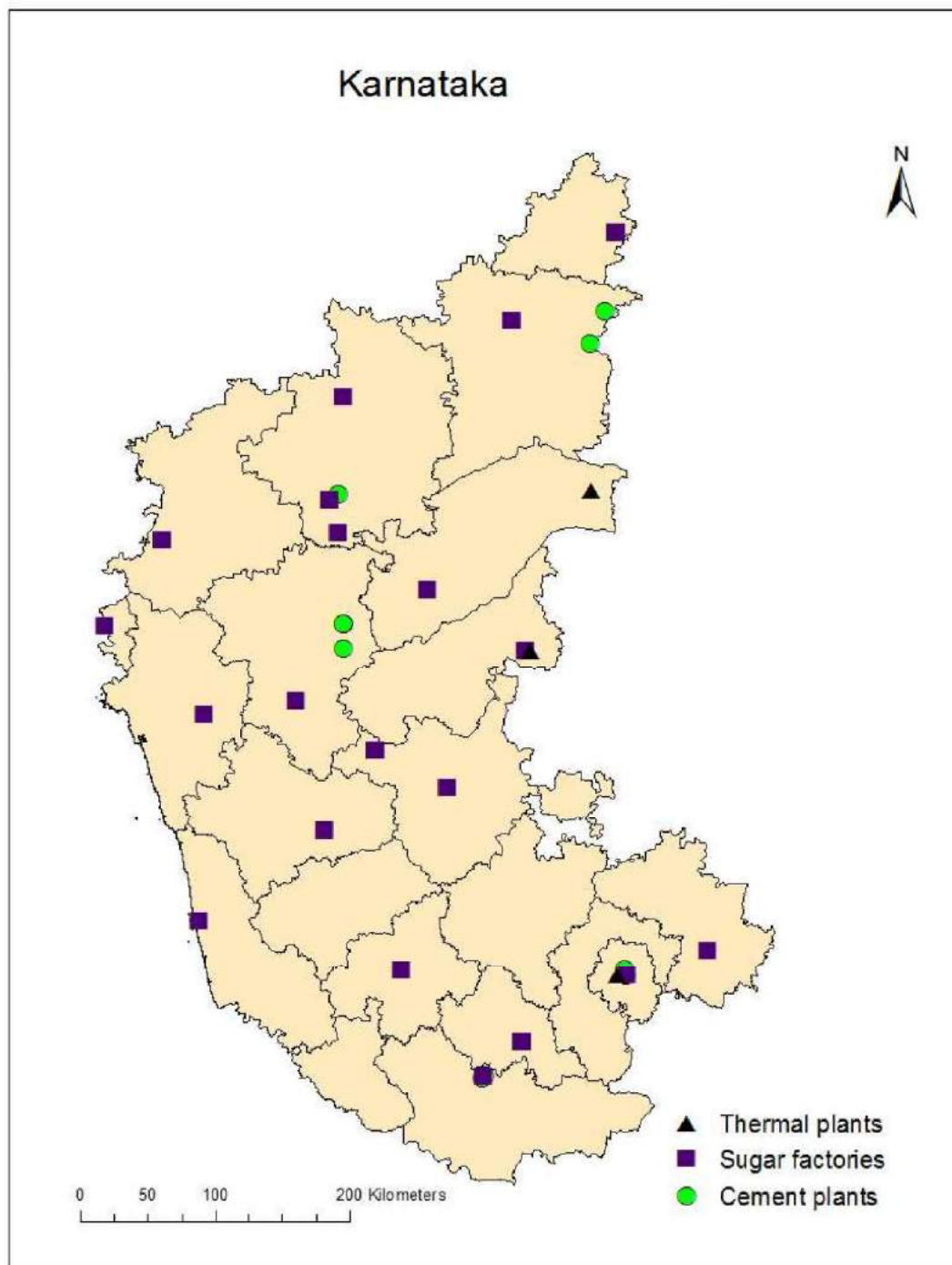


Figure 8.17: Location of sugar mills, cement and thermal plants in Karnataka

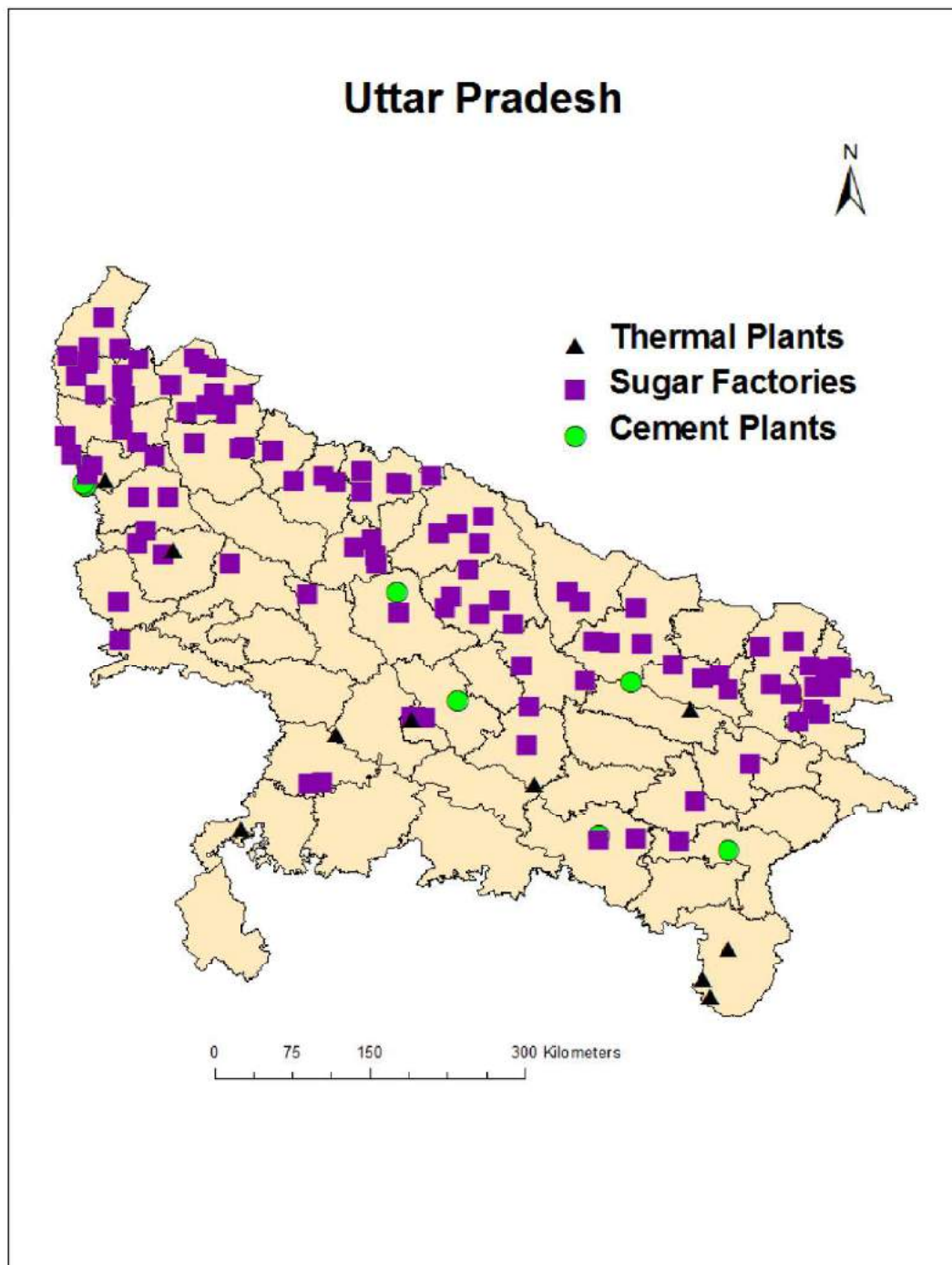


Figure 8.18: Location of sugar mills, cement and thermal plants in Uttar Pradesh

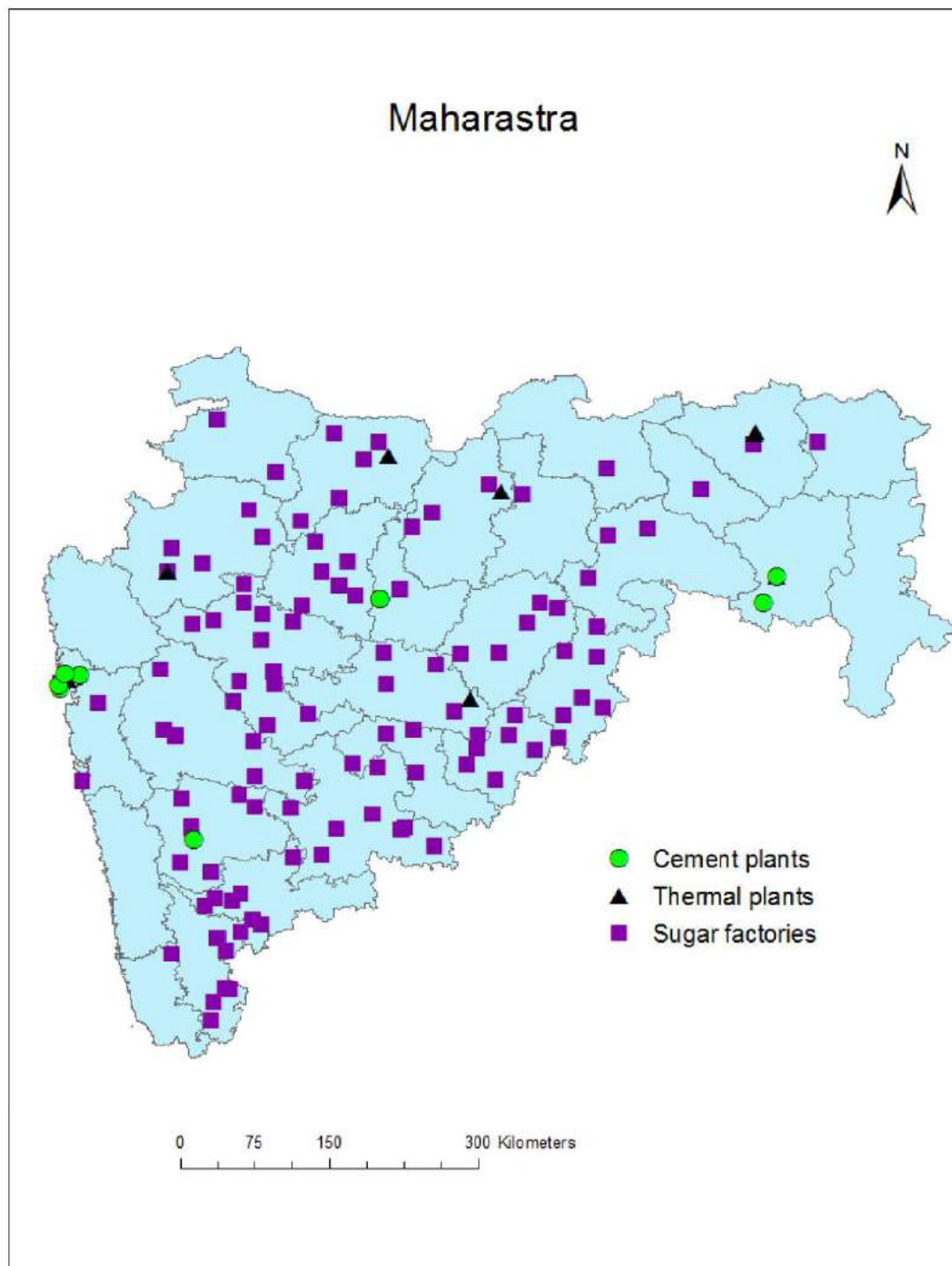


Figure 8.19: Location of sugar mills, cement and thermal plants in Maharashtra

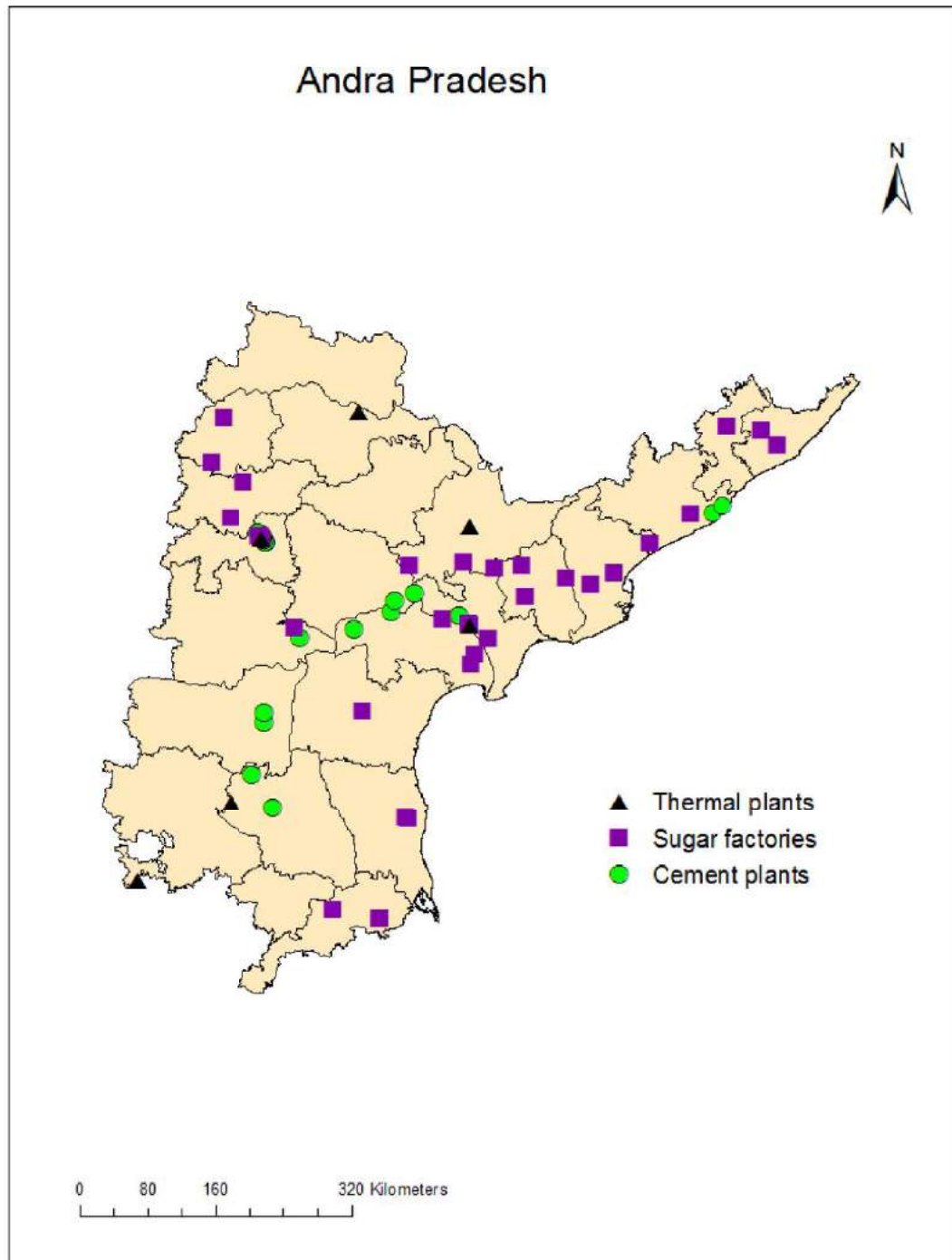


Figure 8.20: Location of sugar mills, cement and thermal plants in Andra Pradesh

The current research study has shown that bagasse ash has a good pozzolanic performance and can be used as a suitable alternative material in concrete. In addition, the abundant availability of bagasse ash close to the cement plants reduces the transportation cost significantly when compared with fly ash, enabling economic benefits to the cement manufacturers.

Although bagasse ash has potential for use as pozzolanic material to produce high quality durable concrete, it is directly disposed as waste material to the nearest land which causes severe environmental pollution. Due to the black colour of bagasse ash, it contaminates water sources in the disposal area. In addition, presence of light weight particles in the raw bagasse ash causes severe air pollution. Disposal of bagasse ash has become a severe problem in India because of rapid implementation of a number of new cogeneration plants and significant expansion in the capacity of available plants. This mapping study clearly indicates the availability of rich sources of bagasse ash in India with good accessibility to the cement plants, which would make it possible to achieve both economic and environmental benefits.

8.4 SUMMARY

Availability of sugarcane bagasse ash in India was estimated based on current cogeneration capacity of sugar mills and elaborately presented in this chapter. Rapid implementation of cogeneration system in the sugar mills as well as expansion of existing capacity are responsible for the generation of enormous quantities of bagasse ash in India. Availability mapping of bagasse ash in India was reported and compared with availability of fly ash from thermal plants in this chapter. In addition, accessibility of bagasse ash and fly ash to the Indian cement plants, particularly in the major sugarcane producing states, was clearly illustrated with the help of a mapping tool. From this study, it was clearly found that bagasse ash is available in plentiful quantities adjacent to the cement plants with better accessibility than fly ash. Disposal of this ash is found to be a critical issue for sugar industries due to environmental constraints and land requirement. Utilization of bagasse ash as supplementary cementitious material in the blended cement production strives to achieve durable as well as sustainable concrete and can tackle the disposal problem significantly.

CHAPTER 9

CONCLUSIONS AND RECOMMENDATIONS FOR FURTHER STUDY

9.1 INTRODUCTION

The present study contributed to improve the comprehensive understanding of pozzolanic characteristics of sugarcane bagasse ash and its performance in concrete as a cementitious blending material. Based on the results of the present study, proper characterization strategy and suitable processing methodology were suggested to use bagasse ash in a large scale for the production of bagasse ash based Portland pozzolana cement, instead of disposal. The salient conclusions drawn out from the different phases of present research study are summarized in this chapter. Major contributions from the present study and recommendations for further research are described in the later part of the chapter.

9.2 SPECIFIC CONCLUSIONS

Specific conclusions on characterization of sugarcane bagasse ash, microstructure of sugarcane bagasse ash, influence of processing on pozzolanic activity, admixture compatibility, performance evaluation of SCBA based blended cements and availability mapping are presented in the following sections.

9.2.1 Characterization of sugarcane bagasse ash

- The sample of sugarcane bagasse ash used in this study had significantly large reactive silica content (more than 70%) in its oxide composition and showed the potential to be used as supplementary cementitious material in concrete.
- The sample of raw bagasse ash consisted of different types of particles. Most of the particles of raw bagasse ash were completely burnt fine particles. In addition to fine

particles, two different types of fibrous unburnt particles were observed in the raw bagasse ash, namely coarse fibrous unburnt particles and fine fibrous unburnt particles. Structure and size of these fibrous particles were entirely different from the burnt fine particles.

- Raw bagasse ash collected for this study showed lesser pozzolanic activity index than minimum requirement as per standard (75%) due to the presence of fibrous particles. Raw bagasse ash cannot be directly used as pozzolanic material and needs some processing to enhance the activity index, in order to classify as supplementary cementitious material.
- After numerous trials, complete removal of coarse and fine fibrous unburnt particles from raw bagasse was achieved by sieving through 300 μm sieve.
- Loss on ignition of raw sugarcane bagasse ash was high due to the presence of large carbon content in the fibrous unburnt particles. Removal of these fibrous unburnt particles reduced loss on ignition to acceptable limits.
- In the strength activity test, water requirement of the sieved bagasse ash mortar was lesser than raw bagasse ash mortar to obtain the same flow. This shows that removal of the fibrous carbon particles also improves workability of the mortar.
- Different test methods were used in this study to evaluate pozzolanic activity of different particles present in the raw bagasse ash. These included the conventional strength activity index test, lime reactivity test, electrical conductivity test, Frattini test, and lime saturation test. Results from all tests indicated superior pozzolanic activity for the fine burnt particles of bagasse ash, and poor activity for the fibrous particles.
- Removal of coarse fibrous carbon particles from raw bagasse ash by sieving improved its pozzolanic activity from 69 % to 79%. Sieved bagasse ash can thus be used as pozzolanic material because of better pozzolanic performance and workability as well as lower value of loss on ignition.
- Frattini test and electrical conductivity method were suggested to be more reliable for the evaluation of pozzolanic activity of supplementary cementitious materials because of the issues associated with the strength based tests.

9.2.2 Microstructure of sugarcane bagasse ash

- Prismatic, spherical, irregular, and fibrous particles were observed in the microstructure of raw bagasse ash, which was studied by scanning electron microscopy.
- Most of the detected particles in the micrograph of raw bagasse ash were irregular particles. Significant amount of Si (50 %) was found to be present in irregular particles by EDS analysis.
- Spherical particles that were observed in the microstructure are formed due to the melting of particles at high temperature. Elemental compositions of spherical particles were entirely different from irregular and fibrous particles. Prismatic particles were observed in the micrograph of raw bagasse ash and these particles had well-defined structures. Higher amount of Si (47%) was observed in the elemental composition of prismatic particles.
- Layered cellular structure with scattered epidermal layers was observed in the micrograph of coarse fibrous particles. Epidermal layers were found to be randomly oriented on the surface of cellular structure. In addition, presence of dumbbell-shaped particles was seen on the epidermal layer. The coarse fibrous particles were found to have large amount of carbon in their elemental composition and not silica.
- Fine fibrous unburnt particles had completely different microstructure compared to coarse fibrous unburnt particles. A well-ordered intercellular structure with channels was observed in the cell wall of fine fibrous particles. Carbon was observed as primary element (more than 80 %) along with insignificant amount of silica content (lesser than 2%) in the observed phases of fine fibrous particles by EDS analysis.
- A number of pits were found to be present on the cell walls of coarse and fine fibrous particles due to incomplete burning of plant fibres during the cogeneration process.

9.2.3 Influence of processing on pozzolanic performance

- The influence of burning of raw bagasse ash was investigated by controlled burning at temperatures of 600, 700, 800, and 900 °C. This process was found to influence the

pozzolanic activity of bagasse ash. Pozzolanic activity of the burnt sample was higher than raw bagasse ash sample up to a temperature of 800 °C. Burnt bagasse ash at 700 °C showed maximum pozzolanic activity.

- After 900 °C burning, changes in colour (from extreme black to white) and particle size were observed. A number of white particles were found to be present in the burnt samples at 800 °C. Samples burnt at 900 °C and above had entirely white particles.
- At higher temperatures, crystallization of cristobalite was detected by XRD, and this led to a reduction in pozzolanic activity. More number of well-defined prismatic particles – which were cristobalite particles – was detected in the micrograph of white particles and these particles were found to be rich in Si (more than 50 %). Presence of similar particles was detected (although in small amounts) in the micrograph of raw bagasse ash. During cogeneration process, bagasse particles which were present near to the flame may have experienced higher temperatures than the average temperature of the boiler, and may have led to the formation of prismatic particles in raw bagasse ash.
- The influence of fineness was studied by grinding the raw bagasse ash to different sizes ranging from 210 – 45 µm. Pozzolanic activity of the raw bagasse ash sample was found to be more than ground material up to 75 µm fineness. During grinding process, coarse and fine fibrous carbon particles were ground to a greater degree as compared to the silica, and caused reduction in strength.
- As per the minimum index requirement of 75%, the results showed that bagasse ash ground to less than 53 µm can be classified as a supplementary cementitious material.
- Burnt bagasse ash at 700 °C had higher pozzolanic activity index than sieved sample. Additional grinding of these samples to cement fineness resulted in only a minor increase in pozzolanic activity. On the other hand, the pozzolanic activity of the sieved and ground (SG) sample was significantly higher than the burnt and ground (BG) sample. The continued presence of fibrous particles in the burnt and ground (BG) sample resulted in lower pozzolanic activity than SG sample, in which case the fibrous particles had been effectively removed by the sieving process.

- Comparing the different processing methods, sieving through 300 μm and grinding to cement fineness (300 m^2/kg) was suggested as the best processing method for sugarcane bagasse ash because of maximum pozzolanic activity, low value of loss on ignition, and minimum processing energy inputs compared to other processing methods.

9.2.4 Admixture compatibility

- The saturation dosage of both types of superplasticizers was increased with increase in bagasse ash replacement.
- Relative fluidity of bagasse ash based cement paste was decreased compared to the control paste for the same water-binder ratio and superplasticizer dosage. The powder volume was increased with bagasse ash replacement due to its low relative density and this led to the reduction in relative fluidity.
- Mini-slump spread was increased with increase in superplasticizer dosage. Nevertheless, after saturation dosage only minimal change in the average spread was observed. Saturation dosage was clearly detectable in the flow curve of Marsh cone test because of substantial drop in flow time at all dosages before saturation dosage. Observations from Marsh cone test agreed well with mini slump test results.
- Cellular structure of fibrous particles and irregular shape of fine burnt particles were observed in the SEM micrograph of raw bagasse ash. The irregular structure of burnt silica particle which was present in the processed bagasse ash was a reason for the reduction in relative fluidity of SCBA based cement paste compared to control paste.
- Sugarcane bagasse ash based cements were found to be compatible with polycarboxylic ether based superplasticizer and not compatible with suphonated naphthalene based superplasticizer.

9.2.5 Performance evaluation of SCBA based blended cements

- Specific gravity of blended cements was found to be decreased with increase in replacement of bagasse ash due to low relative density of processed bagasse ash.

Similar fineness was observed for ordinary Portland cement and bagasse ash blended cements because of the well-controlled production process. Even though initial and final setting times were increased with increase in bagasse ash replacement, the experimental values were found to be within the permissible limits.

- Silica content was found to be increased with increase in bagasse ash replacement in the oxide composition of blended cements. Due to higher K_2O content present in the bagasse ash, increase in K_2O was clearly observed for blended cements.
- Concrete with bagasse ash replacement showed equal or marginally better strength performance compared to control concrete, even at 3 days. The results clearly indicate that concrete of the same grade can be produced with up to 25% replacement of cement by SCBA.
- Heat of hydration of concrete containing SCBA based cements with 10 and 20% replacement was studied using adiabatic calorimetry. The total heat as well as the peak heat rate of bagasse ash blended concrete was found to be lesser than the control mix.
- Durability performance of SCBA based Portland pozzolana cements was investigated by six different methods. Blended cements were ground to similar fineness as OPC to completely exclude filler effect. Observed reduction in permeability with increase in SCBA replacements is purely from pozzolanic performance of SCBA.
- The oxygen permeability test showed only marginal increase in oxygen permeability index for SCBA blended cements. However, remarkable reduction in air permeability was observed for SCBA replaced specimens compared to control concrete in Torrent air permeability test.
- Durability performance of concrete with SCBA based cements against chloride and water penetration was investigated. Resistance of concrete against chloride and water penetration significantly increased with increase in bagasse ash replacement.
- Although water sorptivity test showed a marginal deviation in the result, significant reduction in the water penetration was observed under an applied pressure.

- Prominent reduction in permeability of concrete with increase in SCBA replacements is due to superior pozzolanic performance of SCBA as well as enhancement in the pore structure as a result of pore refinement.
- Surface resistivity of SCBA replaced concretes was found to be higher compared to control concrete due to excellent pozzolanic performance of SCBA as well as improvement in the quality of concrete.
- Drying shrinkage behaviour of SCBA replaced concretes was similar to that of OPC concrete.
- The results of the comprehensive evaluation of mechanical and durability characteristics suggest that sugarcane bagasse ash can be used as cement replacement in blends up to 25% to produce good quality concrete.

9.2.6 Availability mapping of sugarcane bagasse ash

- Sugarcane bagasse ash is generated in large quantities (44220 tonnes/day) in India. Disposal of bagasse ash is a critical issue for sugar industries due to environmental constraints and land requirement. Rapid implementation of new modern cogeneration plants and expansion of cogeneration capacity of existing plants in sugar industries are further expected to increase bagasse ash generation significantly in India.
- From a systematic mapping of the availability of bagasse ash vis a vis the availability of fly ash for cement manufacture, it was clearly observed that bagasse ash is more accessible to the cement plants when compared with fly ash, especially in the major sugarcane producing states. Because of superior pozzolanic performance and good accessibility, bagasse ash is suggested as an excellent alternative cementitious blending material to the cement plants.

9.3 MAJOR CONTRIBUTIONS FROM THE STUDY

Proper characterization scheme of sugarcane bagasse ash for use as an alternative supplementary cementitious material and comprehensive understanding of its pozzolanic performance are the important contributions from the present study. Based on the

observations from detailed material characterization and processing study, a suitable processing methodology was developed to produce bagasse ash based blending material with superior pozzolanic activity and minimum level of processing energy to enable potential use of the material in large scale. The suggested methodology is a fruitful outcome of the present study and is achieved based on systematic and scientific experimental investigations. A number of alternative cementitious materials are locally available in enormous quantities and this methodology can be directly adopted to characterize the pozzolanic performance of any new cementitious material. In addition, bagasse ash based Portland pozzolana cements were produced based on the suggested methodology and performance evaluation was carried out in cement, cement paste, mortar and concrete to validate the defined methodology. Availability mapping of bagasse ash in India was elaborately described in the study. Availability maps illustrate exact details on the better accessibility of the bagasse ash to Indian cement plants and compared with accessibility of fly ash. This will help to identify the appropriate available sources of bagasse ash adjacent to the cement plants and promote the use of bagasse ash in the blended cement production to a greater extent, especially in areas with limited fly ash availability. The understanding of the multi-component nature of potential pozzolanic materials as well as of the influence of different processing techniques would help to improve the level of utilization of such materials.

9.4 RECOMMENDATIONS FOR FURTHER STUDY

The present study describes the suitability of bagasse ash as an alternative cementitious material. This study specifically concentrated on basic material characterization, evaluation of pozzolanic activity and its performance evaluation in concrete. Further research in this specialized problem may lead to better understanding of performance of bagasse ash in concrete. In this context, following studies are highly recommended for further research:

- Bagasse ash was collected from a single source and used throughout the study for characterization and performance evaluation. The characterization scheme can be

further examined for different sources of bagasse ash to ensure the pozzolanic characteristics of bagasse ash.

- Performance evaluation of bagasse ash in concrete was investigated in the present study for a particular grade of concrete with constant water to binder ratio and cementitious content. Performance evaluation, especially durability performance, can be further investigated for different grades of concrete with wide ranges of water to binder ratio and cementitious content.
- Performance evaluation of bagasse ash in concrete can be extended to understand others properties such as sulfate resistance, creep, alkali silica reaction, different types of shrinkage and corrosion resistance.
- A number of activation methods are available such as chemico-mechanical activation, ultrafine grinding to enhance the pozzolanic performance of supplementary cementitious materials. Refinement in processing techniques can be studied to increase pozzolanic activity of bagasse ash.
- Better understanding of rheology of paste and concrete with SCBA blends needs to be achieved to work towards increased levels of replacement.
- Performance evaluation for bagasse based ternary blends is highly recommended to understand the interaction of bagasse ash with other cementitious materials as well as promote the utilization of such blends in the modern high strength concrete.

REFERENCES

ACI 209.1R-05 (2005) Factors affecting shrinkage and creep of hardened concrete. American Concrete Institute. United States.

Agullo, L., B.C. Toralles, R. Gettu, and A. Aguado (1999) Fluidity of cement pastes with mineral admixtures and superplasticizer- A study based on the Marsh cone test. *Materials and structures*, 32, 479-485.

Alexander, M.G., Y. Ballim, and J.R. Mackechnie (1999) Guide to the use of durability indexes for achieving durability in concrete structures. Achieving durable and economic concrete construction in the South African context. Research Monograph, 2, 5-11.

Alonso, M.M., M. Palacios, and F. Puertas (2013) Compatibility between polycarboxylate-based admixtures and blended-cement pastes. *Cement and Concrete Composites*, 35, 151–162.

Alonso, M.M., M. Palacios, F. Puertas, A.G. Torre, and M.A.G. Aranda (2007) Effect of polycarboxylate admixture structure on cement paste rheology. *Construction and Building Materials*, 57, 65–81.

Andersen, P.J., D.M. Roy, and J.M. Gaidis (1987) Effect of adsorption of superplasticizers on the surface of cement. *Cement and Concrete Research*, 17, 805-813.

Aquino, W., D.A. Lange, and J. Olek (2001) The influence of metakaolin and silica fume on the chemistry of alkali-silica reaction products. *Cement and Concrete Composites*, 23, 485–493.

Asbridge, A.H., C.L. Page, and M.M. Page (2002) Effects of metakaolin, water/binder ratio and interfacial transition zones on the microhardness of cement mortars. *Cement and Concrete Research*, 32, 1365-1369.

ASTM C 109-11b (2011) Standard test method for compressive strength of hydraulic cement mortars using 50 mm cube specimens. American Society for Testing and Materials, West Conshohocken, United States.

ASTM C430-08 (2008) Standard test method for fineness of hydraulic cement by the 45- μm (No. 325) sieve. American Society for Testing and Materials, West Conshohocken, United States.

ASTM C1202-12 (2012) Standard test method for electrical indication of concrete's ability to resist chloride ion penetration. American Society for Testing and Materials, West Conshohocken, United States.

ASTM C1240-12 (2012) Standard specification for silica fume used in cementitious mixtures. American Society for Testing and Materials, West Conshohocken, United States.

ASTM C1437-07 (2007) Standard test method for flow of hydraulic cement mortar. American Society for Testing and Materials, West Conshohocken, United States.

ASTM C150/C150M-12 (2013) Standard specification for Portland cement. American Society for Testing and Materials, West Conshohocken, United States.

ASTM C1709-11 (2011) Standard guide for evaluation of alternative supplementary cementitious materials (ASCM) for use in concrete. American Society for Testing and Materials, West Conshohocken, United States.

ASTM C204 (2011) Standard test methods for fineness of hydraulic cement by air-permeability apparatus. American Society for Testing and Materials, West Conshohocken, United States.

ASTM C219-13a (2013) Standard terminology relating to hydraulic cement. American Society for Testing and Materials, West Conshohocken, United States.

ASTM C311-11b (2011) Standard test methods for sampling and testing fly Ash or natural pozzolans for use in Portland-cement concrete. American Society for Testing and Materials, West Conshohocken, United States.

ASTM C494/C494M (2013) Standard specification for chemical admixtures for concrete. American Society for Testing and Materials, West Conshohocken, United States.

ASTM C618-12a (2012) Standard specification for coal fly ash and raw or calcined natural pozzolan for use in Concrete. American Society for Testing and Materials, West Conshohocken, United States.

ASTM C989/C989M-13 (2013) Standard specification for slag cement for use in concrete and mortars. American Society for Testing and Materials, West Conshohocken, United States.

Aitcin, P.C. High performance concrete, E & FN Spon, London, 1998.

Awal, A.S.M. and I.A. Shehu (2013) Evaluation of heat of hydration of concrete containing high volume palm oil fuel ash. *Fuel*, 105, 728–731.

Badogiannis, E. and S. Tsivilis (2009) Exploitation of poor Greek kaolins: Durability of metakaolin concrete. *Cement and Concrete Composites*, 31, 128–133.

Bai, J. and S. Wild (2002) Investigation of the temperature change and heat evolution of mortars incorporating PFA and Metakaolin. *Cement and Concrete Composites*, 24(2), 201–209.

Ballim, Y. and P.C. Graham (2003) A maturity approach to the rate of heat evolution in concrete. *Magazine of Concrete Research*, 55, 249-256.

Batra, V.S., S. Urbonaite, and G. Svensson (2008) Characterization of unburned carbon in bagasse fly ash. *Fuel*, 87, 2972-2976.

Bensted, J. and P. Barnes *Structure and performance of cement*, Spon Press, New York, 2000.

Blezard, R. History of calcareous cements. pp. 1–19. In **P.C. Hewlett** (ed.) *Lea's Chemistry of Cement and Concrete*. Arnold, London, 1998.

Bonen, D. and S.L. Sarkar (1995) The superplasticizers adsorption capacity of cement paste, pore solution composition, and parameters affecting flow loss. *Cement and Concrete Research*, 25, 1423-1434.

Breugel, V.K. Prediction of temperature development in hardening concrete. pp 52-75. In **R. Springenschmid** (ed.) *Prevention of Thermal Cracking in Concrete at Early Ages*. E & FN Spon, London, 1998.

Brindley, G.W. and M. Nakahira (1958) A new concept of the transformation sequence of kaolinite to mullite. *Nature*, 181, 1333–1334.

BS EN 196-5 (2005). Method of testing cement. Pozzolanicity test for pozzolanic cement. British Standard. United Kingdom.

Cabrera, J.G. and C. Plowman (1987) Hydration and microstructure of high fly ash content concrete. Conference on concrete dams, London.

Camoes, A. (2005) Influence of mineral admixtures in the fresh behaviour of superplasticized concrete mixes. Proceedings of International Conference on Concrete for Structures, Coimbra, July, 1-8.

Cement Manufacturers Association (CMA). 52nd Annual Report 2012-13, Cement Manufacturers Association, New Delhi, India, 2013.

Cetin, E., B. Moghtaderi, R. Gupta, and T.F. Well (2004) Influence of pyrolysis conditions on the structure and gasification reactivity of biomass chars. *Fuel*, 83, 2139–2150.

Changling, H., M. Emil, and O. Bjame (1994) Thermal stability and pozzolanic activity of calcined kaolin. *Applied Clay Science*, 9, 165–187.

Chao, L., S. Henghu, and L. Longtu (2010) A review: The comparison between alkali-activated slag (Si + Ca) and metakaolin (Si + Al) cements. *Cement and Concrete Research*, 40, 1341–1349.

Chopra, S.K., S.C. Ahluwalia, and S. Laxmi (1981) Technology and manufacture of rice husk masonry cement. Proceeding of ESCAP/RCTT Third Workshop on Rice Husk Ash Cements. New Delhi, November.

Chusilp, N., J. Chai, and K. Kraiwood (2009) Utilization of bagasse ash as a pozzolanic material in concrete. *Construction and Building Materials*, 23, 3352–3358.

Coleman, N.J. (1996) Metakaolin as a cement extender. PhD Thesis, University of Aston. United Kingdom.

Colleparidi, M. (1998) Admixtures used to enhance placing characteristics of concrete. *Cement and Concrete Composites*, 20, 103-112.

Cordeiro, G.C., R.D. Filho, L.M. Tavarase, and E.M. Fairbairn (2008) Pozzolanic activity and filler effect of sugar cane bagasse ash in Portland cement and lime mortars. *Cement and Concrete Composites*, 30 (5), 410-418.

Cordeiro, G.C., R.D. Filho, L.M. Tavarase, and E.M. Fairbairn (2009) Effect of calcination temperature on the pozzolanic activity of sugar cane bagasse ash. *Construction and Building Materials*, 23, 3301–3303.

Cordeiro, G.C., R.D. Filho, L.M. Tavarase, and E.M. Fairbairn (2009) Ultrafine grinding of sugar cane bagasse ash for application as pozzolanic admixture in concrete. *Cement and Concrete Research*, 39, 110-115.

Cordeiro, G.C., R.D. Filho, L.M. Tavarase, E.M. Fairbairn, and S. Hempel (2011) Influence of particle size and specific surface area on the pozzolanic activity of residual rice husk ash. *Cement and Concrete Composites*, 33, 529–534.

Darwin, D. and J. Browning (2008) Multiple corrosion protection systems for reinforced concrete bridge components: An update. *Proceedings of National concrete bridge conference*, St. Louis, Missouri, 16-21.

DIN 1048 Part 5 (1994) Testing of hardened concrete. German Institute for Standardization. Berlin, Germany.

Dodson, V.H. and T.D. Hayden (1989) Another look at the Portland cement/chemical admixture incompatibility problem. *Cement, Concrete and Aggregates*, 11, 52-56.

Donatello, S., M. Tyrer, and C.R. Cheeseman (2010) Comparison of test methods to assess pozzolanic activity. *Cement and Concrete Composites*, 32, 121–127.

Duan, P., Z. Shui, W. Chen, and C. Shen (2013) Enhancing microstructure and durability of concrete from ground granulated blast furnace slag and metakaolin as

cement replacement materials. *Journals of materials research and technology*, 2(1), 52-59.

Durability Index Testing Procedure Manual (2009) Concrete durability index testing, South Africa.

Duval, R. and E.H. Kadri (1998) Influence of silica fume on workability and compression strength of high performance concrete. *Cement and Concrete Research*, 28, 533–547.

Edwards, P. The incredible Indian cement industry. pp. 47-55. In *Global cement magazine*, Pro Global Media Limited, Surrey, United Kingdom, 2013.

Feliu, S., C. Andrade, J.A. Gonzdlez, and C. Alonso (1996) A new method for in-situ measurement of electrical resistivity of reinforced concrete. *Materials and Structures*, 29, 362-365.

Ferraris, C.F., K.H. Obla, and R. Hill (2001) The influence of mineral admixtures on the rheology of cement paste and concrete. *Cement and Concrete Research*, 31, 245-255.

FM 5-578 (2004) Florida method of test for concrete resistivity as an electrical indicator of its permeability. Florida department of transportation. United States.

Food and Agriculture Organization of the United Nations (FAO). Proceedings of Thirty-second conference of FAO. Food and Agriculture Organization of the United Nations, Rome, December, 2003.

Frias, M., M.I. Sanchez de Rojas, and J. Cabrera (2000) The effect that the pozzolanic reaction of metakaolin has on the heat evolution in metakaolin-cement mortars. *Cement and Concrete Research*, 30(2), 209–216.

Frias, M., V. Ernesto, and S. Holmer (2011) Brazilian sugar cane bagasse ashes from the cogeneration industry as active pozzolans for cement manufacture. *Cement and Concrete Composites*, 33, 490–496.

Gambhir, M.L. *Concrete Technology: Theory and Practice*, Tata McGraw Hill publishing company limited, New Delhi, India, 2013.

Ganesan, K., M. Rajagopal, and Thangavel (2007) Evaluation of bagasse ash as supplementary cementitious material. *Cement and Concrete Composites*, 29, 515-524.

Ghiasvand, E., A.A. Ramezaniapour, and A.M. Ramezaniapour (2014) Effect of grinding method and particle size distribution on the properties of Portland-pozzolan cement. *Construction and Building Materials*, 53, 547–554.

Gibbon, G.J., Y. Ballim, and G.R.H. Grieve (1997) A low-cost, computer controlled adiabatic calorimeter for determining the heat of hydration of concrete. *Journal of Testing and Evaluation*, 5(2), 261–266.

Githachuri, K. and M.G. Alexander (2013) Durability performance potential and strength of blended Portland limestone cement concrete. *Cement and Concrete Composites*, 39, 115–21.

Goyal, A., H. Kunio, O. Hidehiko, and A. Muhammad (2010) Processing of Sugarcane Bagasse ash and Reactivity of Ash-blended Cement Mortar. *Transactions of The Japanese Society of Irrigation, Drainage and Rural Engineering*, 77, 243-251.

Graham, P.C., Y. Ballim, and J.B. Kazirukanyo (2011) Effectiveness of the fineness of two South African Portland cements for controlling early-age temperature development in concrete, *The Journal of the South African institution of civil Engineering*, 53, 39–45.

Hallal, A., E.H. Kadri, K. Ezziane, A. Kadri, and H. Khelafi (2010) Combined effect of mineral admixtures with superplasticizers on the fluidity of the blended cement paste. *Construction and Building Materials*, 24, 1418–1423.

Hamad, M.A. and I.A. Khattab (1981) Effect of the combustion process on the structure of rice hull silica. *Thermochimica Acta*, 48, 343–349.

Horsakulthai, V., S. Phiuvanna, and W. Kaenbud (2011) Investigation on the corrosion resistance of bagasse-rice husk-wood ash blended cement concrete by impressed voltage. *Construction and Building Materials*, 25, 54–60.

Hasanbeigi, A., C.F. Chen, and L. Price (2012) Organizations, programs and resources for energy efficiency and productivity in the cement industry. Institute for Industrial Productivity, Washington, United states.

IS 12269 (2008) Specification for 53 grade ordinary Portland cement. Bureau of Indian Standards, New Delhi, India.

IS 1489 Part 1 (2005) Portland pozzolana cement Specification - Fly ash based. Bureau of Indian Standards, New Delhi, India.

IS 1727-1967 (2004) Methods of test for pozzolanic materials. Bureau of Indian Standards, New Delhi, India.

IS 2386 Part 1 (2007) Methods of test for aggregates for concrete - Particle size and shape. Determination of density. Bureau of Indian Standards, New Delhi, India.

IS 2386 Part 3 (2007) Methods of test for aggregates for concrete - Part 3: Specific gravity, density, voids, absorption and bulking. Bureau of Indian Standards, New Delhi, India.

IS 383 (2007) Specification for coarse and fine aggregates from natural sources for concrete. Bureau of Indian Standards, New Delhi, India.

IS 4031 Part 3 (2005) Methods of physical tests for hydraulic cement. Determination of soundness. Bureau of Indian Standards, New Delhi, India.

IS 4031 Part 4 (2005) Methods of physical tests for hydraulic cement. Determination of consistency of standard cement paste. Bureau of Indian Standards, New Delhi, India.

IS 4031 Part 5 (2005) Methods of physical tests for hydraulic cement. Determination of initial and final setting times. Bureau of Indian Standards, New Delhi, India.

IS 4031 Part 11 (2005) Methods of physical tests for hydraulic cement. Determination of density. Bureau of Indian Standards, New Delhi, India.

IS 8112 (2005) 43 Grade ordinary Portland cement - specifications. Bureau of Indian Standards, New Delhi, India.

Jayashree, C. (2009) Study of cement-superplasticizer interaction and its implications for concrete performance. PhD thesis. Indian Institute of Technology Madras, India.

Jayasree, C. and R. Gettu (2008) Experimental study of the flow behaviour of superplasticized cement paste. *Materials and Structures*, 41, 1581-1593.

Jiang, S., B.G. Kim, and P.C. Aitcin (1999) Importance of adequate soluble alkali content to ensure cement/superplasticizer compatibility. *Cement and Concrete Research*, 29, 71-78.

Jolicœur, C. and M.A. Simard (1998) Chemical admixture-cement interaction: Phenomenology and physico-chemical concepts. *Cement and Concrete Composites*, 20, 87-101.

Kamiya, K., A. Oka, H. Nasu, and T. Hashimoto (2000) Comparative study of structure of silica gels from different sources. *Journal of Sol-Gel Science and Technology*, 19, 495–499.

Kantro, D.L. (1980) Influence of water-reducing admixtures on properties of cement paste-A miniature slump test. *Cement concrete and Aggregates*, 2, 95-102.

Khatib, J.M. and R.M. Clay (2003) Absorption characteristics of metakaolin concrete. *Cement and Concrete Research*, 34, 19–29.

Kiattikomol, K., C. Jaturapittakul, S. Songpiriyakij, and S. Chutubitim (2001) A study of ground coarse fly ashes with different fineness from various sources as pozzolanic material. *Cement and Concrete Composites*, 23, 335-343.

Kjeldsen, A.M., R.J. Flatt, and L. Bergstrom (2006) Relating the molecular structure of comb-type superplasticizers to the compression rheology of MgO suspensions. *Cement and Concrete Research*, 36, 1231–1239.

Krishna, R.N. (1996) Dispersing action of superplasticizers with different grades of cements and fly ash. *American Concrete Institute materials journal*, 93, 351-355.

Krishnan, K.A. and T.S. Anirudhan (2002) Removal of mercury (II) from aqueous solutions and chlor-alkali industry effluent by steam activated and sulphurised activated carbons prepared from bagasse pith: kinetics and equilibrium studies. *Journal of hazardous materials*, 92, 161–183.

Kroehong, W., T. Sinsiri, and C. Jaturapitakkul (2011) Effect of Palm Oil Fuel Ash Fineness on Packing Effect and Pozzolanic Reaction of Blended Cement Paste. *Procedia Engineering*, 14, 361–369.

Lasserre, P. Globalisation Cement Industry, Global Strategic Management Mini Cases Series (GSMMCS), Palgrave Macmillan, New York, 2007.

Luxan, M.P., F. Madruga, and J. Saavedra (1989) Rapid evaluation of pozzolanic activity of natural products by conductivity measurement. *Cement and Concrete Research*, 19, 63-68.

Mackenzie, R.C. Differential thermal analysis, Academic Press, London, 1970.

Magarotto, R., I. Torresan, and N. Zeminian (2003) Influence of molecular weight of polycarboxylate ether superplasticizers on the rheological properties of fresh cement paste, mortar and concrete. *Proceedings of International Congress on the Chemistry of Cement*, Durban, South Africa, 514-526.

Mailvaganam, N.P. (1999) Chemical admixtures in concrete- Side effects and compatibility problems. *The Indian Concrete Journal*, 73, 367-374.

McCarter, W.J. and D. Tran (1996) Monitoring pozzolanic activity by direct activation with calcium hydroxide. *Construction and Building Materials*, 10(3), 179-184.

Mehta, P.K. and P.J.M. Monteiro *Concrete Microstructure, Properties, and Materials*, The McGraw-Hill Companies, United States, 2006.

Mollah, M.Y.A., P. Palta, T.R. Hess, R.K. Vempati, and D.L. Cocke (1995) Chemical and physical effect of sodium lignosulphonate superplasticizer on the hydration of Portland cement and solidification/ stabilization consequences. *Cement and Concrete Research*, 25, 671-682.

Montakarntiwong, K., N. Chusilp, W. Tangchirapat, and C. Jaturapitakkul (2013) Strength and heat evolution of concretes containing bagasse ash from thermal power plants in sugar industry. *Materials and Design*, 49, 414-420.

Morales, E.V., E.V. Cocina, M. Frias, S.F. Santos, and H. Savastano (2009) Effects of calcining conditions on the microstructure of sugar cane waste ashes (SCWA): Influence in the pozzolanic activation. *Cement and Concrete Composites*, 31, 22-28.

Morat, M. and C. Comel (1983) Hydration reaction and hardening of calcined clays and related minerals: Influence of calcinations process of kaolinite on mechanical strength of hardened metakaolinite. *Cement Concrete Research*, 13, 631–637.

Moropoulou, A., E. Bakolas, and Aggelakopoulou (2004) Evaluation of pozzolanic activity of natural and artificial pozzolans by thermal analysis. *Thermochimica Acta*, 420, 135–140.

Mostafa, N.Y. and P.W. Brown (2005) Heat of hydration of high reactive pozzolans in blended cements: Isothermal conduction calorimetry. *Thermochimica Acta*, 435, 162–167.

Naik, T.R. Maturity functions for concrete cured during winter conditions. pp. 107-117. In **Naik, T.R. (ed.)**, Temperature effects on concrete. ASTM STP 858, American Society for Testing Materials. West Conshohocken, United States, 1985.

Nair, D.G., A. Fraaij, A.A.K. Klaassen, and A.P.M. Kentgens (2008) A structural investigation relating to the pozzolanic activity of rice husk ashes. *Cement and Concrete Research*, 38, 861–869.

National Federation of Cooperative Sugar Factories (NFCSF). Annual Report on Cooperative sugar, National Federation of Cooperative Sugar Factories Limited, 43 (4). New Delhi, India, 2011.

Natu, S.C. (2005) Cogeneration India Actions-Activities-News. Cogeneration Association of India, Newsletter, 2, 1-12.

Nehdi, M. and M.A. Rahman (2007) Estimating rheological properties of cement pastes using various rheological models for different test geometry, gap and surface friction. *Cement and Concrete Research*, 34, 1993–2007.

Neville, A.M. Properties of concrete, Pearson education limited, United Kingdom, 2011.

Newman, J. and B.S. Choo Advanced Concrete Technology - Part 1 Constituent Materials. Butterworth-Heinemann. An imprint of Elsevier, United Kingdom, 2003.

Nkinamubanzi, P.C. and P.C. Aitcin (2004) Cement and superplasticizer combinations: Compatibility and Robustness. Cement Concrete and Aggregates, 26, 1-8.

NT BUILD 356 (1989) Concrete, repairing materials and protective coating: embedded steel method, chloride permeability, NORDTEST, Espoo, Finland.

Otieno, M., H. Beushausen, and M. Alexander (2014) Effect of chemical composition of slag on chloride penetration resistance of concrete. Cement and Concrete Composites, 46, 56–64.

Palacios, M., F. Puertas, P. Bowen, and Y.F. Houst (2009) Effect of PCs superplasticizers on the rheological properties and hydration process of slag-blended cement pastes. Journal of materials science, 44, 2714–2723.

Pan, S.C., D. Tseng, C.C. Lee, and C. Lee (2003) Influence of the fineness of sewage sludge ash on the mortar properties. Cement and Concrete Research, 33, 1749–1754.

Pappua, A. and M. Saxenaa (2007) Solid wastes generation in India and their recycling potential in building materials. Journals of Building and Environment, 42, 2311–2320.

Park, C.K., M.H. Noh, and T.H. Park (2005) Rheological properties of cementitious materials containing mineral admixtures. Cement and Concrete Research, 35, 842–849.

Paya, J., M.V. Borrachero, J. Monzo, E.P. Mora, and F. Amahjour (2001) Enhanced conductivity measurement techniques for evaluation of fly ash pozzolanic activity. Cement and Concrete Research, 31, 41-49.

Paya, J., J. Monzo, M.V. Borrachero, L.D. Pinzon, and L.M. Ordonez (2002) Sugarcane bagasse ash (SCBA): studies on its properties for reusing in concrete production. *Journal of Chemical technology and Biotechnology*, 77, 321-325.

Prasath, G. and M. Santhanam (2013) Experimental investigations on heat evolution during hydration of cementitious materials in concrete using adiabatic calorimetry. *The Indian Concrete Journal*, 87(6), 19-28.

Puertas, F., M.M. Alonso, and T. Vazquez (2005) Effect of polycarboxylate admixtures on Portland cement paste setting and rheological behaviour. *Materials and structures*, 55, 61–73.

Quero, V.G.J., F.M.L. Martinez, P.M. Garcia, C.G. Tiburcio, and J.C.G. Nava (2013) Influence of sugar-cane bagasse ash and fly ash on the rheological behaviour of cement pastes and mortars. *Construction and Building Materials*, 40, 691–701.

Ramachandran, V.S. Concrete admixtures handbook - Properties, Science and Technology, Standard publishers, New Delhi, India, 2002.

Rashad, A.M. (2013) Metakaolin as cementitious material: History, scours, production and composition – A comprehensive overview. *Construction and Building Materials*, 41, 303–318.

Resipod Proceq user manual (2013) Surface resistivity measurement. Schwerzenbach, Switzerland.

Ridi, F., E. Fratini, P. Luciani, F. Winnefeld, and P. Baglioni (2011) Hydration kinetics of tricalcium silicate by calorimetric methods. *Journal of Colloid and Interface Science*, 364, 118–124.

Roncero, J., S. Valls, and R. Gettu (2002) Study of the influence of superplasticizers on the hydration of cement paste using nuclear magnetic resonance and X-ray diffraction techniques. *Cement and Concrete Research*, 22, 103-108.

Rupnow, T.D. and P.J. Icenogle Evaluation of Surface resistivity measurements as an alternative to the Rapid chloride permeability test for quality assurance and acceptance. Report No. FHWA/LA.11/479. July, 2011.

Sahmaran, M., H.A. Christianto, and I.O. Yaman (2006) The effect of chemical admixtures and mineral additives on the properties of self-compacting mortars. *Cement and Concrete Composites*, 28, 432–440.

Sakai, E., K. Yamada, and A. Ohta (2003) Molecular structure and dispersion–adsorption mechanism of comb-type superplasticizers used in Japan. *Journal of Advanced Concrete Technology*, 1, 16-25.

Sanz, J., A. Madani, J.M. Serratos, J.S. Moya, and S. Aza (1988) Aluminum-27 and silicon-29 magic-angle spinning nuclear magnetic resonance study of the kaolinite–mullite transformation. *American Ceramic Society*, 71, 418–421.

Schindler, A. and B.F. McCullough (2002) Importance of concrete temperature control during concrete pavement construction in hot weather conditions. *Journal of Transportation Research board*, 1813, 3-10.

Shekarchi, M., A. Bonakdar, M. Bakhshi, A. Mirdamadi, B. Mobasher (2010) Transport properties in metakaolin blended concrete. *Construction and Building Materials*, 24, 2217–2223.

SIA 162/1-E (2003) Non-destructive site air-permeability Test. *Concrete Construction – Complementary specifications*. Swiss Standard Method.

Singh, N.B., V.D. Singh, and S. Rai (2000) Hydration of bagasse ash-blended Portland cement. *Cement and Concrete Research*, 30, 1485-1488.

Snelson, D.G., S. Wild, and M.O. Farrel (2008) Heat of hydration of Portland Cement–Metakaolin–Fly ash (PC–MK–PFA) blends. *Cement and Concrete Research*, 38, 832–840.

Solomon, S. (2011) Sugarcane By-Products Based Industries in India, *Sugar Tech*, December, 13(4), 408–416.

Somna, R., C. Jaturapitakkul, P. Rattanachu, and W.Chalee (2012) Effect of ground bagasse ash on mechanical and durability properties of recycled aggregate concrete. *Materials and Design*, 36, 597–603.

Souza, A.E., S.R. Teixeira, G.T.A. Santos, F.B. Costa, and E. Longo (2011) Reuse of sugarcane bagasse ash (SCBA) to produce ceramic materials. *Journal of Environmental Management*, 92, 2774-2780.

Sugar Technologist association of India (STAI). List of cane sugar factories and distilleries, Kanpur, India, 2009.

Tamil Nadu electricity regulatory commission (TNERC). Comprehensive tariff order for bagasse based cogeneration plants, Internal report: (Ref No.7-2012/dated 31-07–2012), Tamil Nadu electricity regulatory commission, Chennai, 2012.

Taylor, H .F. W. (2nd edition) *Cement Chemistry*, Thomas Telford Publishing, London, 1997.

The Commission for Agricultural Costs and Prices (CACP). Annual report on sugarcane cultivation, New Delhi, India, 2012.

Torrent Air permeability test user manual. Measures the air-permeability of the cover concrete and other porous materials. Materials Advanced Services, Argentina, 2010.

Torresan, I. and R. Khurana (1998) New superplasticizers based on melamine polymer. Proceedings of Fourth CANMET International Conference, ACI international, Japan, 235-253.

Turanli, L., B. Uzal, and F. Bektas (2005) Effect of large amounts of natural pozzolan addition on properties of blended cements. Cement and Concrete Research, 35, 1106–1111.

United States Geological Survey (USGS), Mineral Commodity Summaries 2011, Reston, Virginia, January, 2011.

Vikan, H., H. Justnes, F. Winnefeld, and R. Figi (2007) Correlating cement characteristics with rheology of paste. Cement and Concrete Research, 37, 1502-1511.

Vanoss, H.G. US and World cement Production 2008 and 2009. Mineral commodity summaries, United States Geological Survey (USGS), January, 2012.

Walters, G.V. and T.R. Jones (1991) Effect of metakaolin on ASR in concrete manufactured with reactive aggregates. Proceeding of International conference on durability of concrete, American Concrete Institute, 2, 941–947.

Wang, C.H. and W.H. Dilger Prediction of temperature distribution in hardening concrete. pp 21-28. In **R. Springenschmid** (ed.) Prevention of Thermal Cracking in Concrete at Early Ages. E & FN Spon, London, 1998.

World Alliance for Decentralized Energy (WADE). Bagasse cogeneration - Global review and potential, Scotland, 2004.

World Business Council for Sustainable Development (WBCSD)/International Energy Agency (IEA), Technology Roadmap Low-Carbon Technology for the Indian Cement Industry. IEA publication, Paris, 2013.

World Energy Council. Efficient Use of Energy Utilizing High Technology: An Assessment of Energy Use in Industry and Buildings. London, 1995.

Worrell, E., P. Lynn, M. Nathan, H. Chris, and O.M. Leticia (2001) Carbon dioxide emissions from the global cement industry. *Annual Review of Energy and Environment Resources*, 26, 303–29.

XiaSun, J., F.X. Sun, R.C. Sun, P. Fowler, and M. Baird (2003) In homogeneities in the Chemical Structure of Sugarcane Bagasse Lignin. *Journal of Agricultural and Food Chemistry*, 51 (23), 6719–6725.

Zhang, M.H. and V.M. Malhotra (1996) High-performance concrete incorporating rice husk ash as a supplementary cementing material. *American Concrete Institute materials journal*, 93(6), 629–636.

Zhang, M.H., K. Sisomphon, T. Siong, and D.J. Sun (2010) Effect of superplasticizers on workability retention and initial setting time of cement pastes. *Construction and Building Materials*, 24, 1700–1707.

Zhang, Y., W. Sun, and S. Liu (2002) Study on the hydration heat of binder paste in high-performance concrete. *Cement and Concrete Research*, 32, 1483–1488.

LIST OF PAPERS ON THE BASIS OF THIS THESIS

REFEREED JOURNALS

1. **Bahurudeen, A., A.V. Marckson, A. Kishore, and M. Santhanam** (2014) Development of sugarcane bagasse ash based Portland pozzolana cement and evaluation of compatibility with superplasticizers. *Construction and Building Materials* 68 (2014) 465–475.
2. **Bahurudeen, A. and Manu Santhanam** Influence of different processing methods on the pozzolanic performance of sugarcane bagasse ash. *Cement and Concrete composites*. (Under Review)
3. **Bahurudeen, A., K. Deepak, D.V. Gokul, and Manu Santhanam** Performance evaluation of sugarcane bagasse ash based Portland pozzolana cement in concrete. *Cement and Concrete composites*. (Under Review)
4. **Bahurudeen, A., K.S. Vaisakh, and Manu Santhanam** Sugarcane bagasse ash as supplementary cementitious material: Availability and potential for use in concrete”, *The Indian Concrete Journal* (Under Review)

PRESENTATIONS IN INTERNATIONAL CONFERENCES

1. **Bahurudeen, A. and M. Santhanam** (2014) Performance evaluation of sugarcane bagasse ash-based cement for durable concrete. *Proceedings of 4th International conference on the Durability of concrete structures*. Purdue University, West Lafayette, United States, 275-281.
2. **Bahurudeen, A. and M. Santhanam** (2013) Characterisation of sugarcane bagasse ash as supplementary cementitious material in concrete. *Proceedings of UKIERI concrete congress- Innovations in concrete construction*, NIT Jalandhar, India, March, 181-185.
3. **Bahurudeen, A. and M. Santhanam** (2014) Sugarcane bagasse ash- An alternative supplementary cementitious material. *Proceedings of International Conference on Advances in civil engineering and chemistry of innovative materials*, SRM University, India, March, 837-842.

DOCTORAL COMMITTEE

CHAIR PERSON

Dr. A. Meher Prasad
Professor and Head
Department of Civil Engineering

GUIDE

Dr. Manu Santhanam
Professor
Department of Civil Engineering

MEMBERS

Dr. Ravindra Gettu
Professor
Department of Civil Engineering

Dr. Radhakrishna G Pillai
Assistant Professor
Department of Civil Engineering

Dr. Gandham Phanikumar
Associate Professor
Metallurgical and Materials Engineering

Dr. S. Sankaran
Associate Professor
Metallurgical and Materials Engineering

CURRICULUM VITAE

Name : Bahurudeen A.

Date of birth : 02 - 07 - 1986

Educational qualifications

2008 **Bachelor of Engineering (B.E.)**

Institution : Alagappa Chettiar College of
Engineering and Technology,

Anna University

Karaikudi

Tamil Nadu, India

Specialization : Civil Engineering

2010 **Master of Engineering (M.E.)**

Institution : College of Engineering Guindy

Anna University

Chennai

Tamil Nadu, India

Specialization : Structural Engineering

Doctor of Philosophy (Ph.D.)

Institution : Indian Institute of Technology Madras

Chennai, India

Specialization : Concrete Technology

Civil Engineering